

# For Reference

NOT TO BE TAKEN FROM THIS ROOM

Ex libris  
UNIVERSITATIS  
ALBERTAENSIS













THE UNIVERSITY OF ALBERTA

RELEASE FORM

NAME OF AUTHOR            GORDON PUTZ  
TITLE OF THESIS           RIVER MIXING AND MICROORGANISM SURVIVAL,  
                              SLAVE RIVER, N.W.T.  
DEGREE FOR WHICH THESIS WAS PRESENTED   MASTER OF SCIENCE  
YEAR THIS DEGREE GRANTED        1983

Permission is hereby granted to THE UNIVERSITY OF ALBERTA LIBRARY to reproduce single copies of this thesis and to lend or sell such copies for private, scholarly or scientific research purposes only.

The author reserves other publication rights, and neither the thesis nor extensive extracts from it may be printed or otherwise reproduced without the author's written permission.



THE UNIVERSITY OF ALBERTA

RIVER MIXING AND MICROORGANISM SURVIVAL, SLAVE RIVER, N.W.T.

by



GORDON PUTZ

A THESIS

SUBMITTED TO THE FACULTY OF GRADUATE STUDIES AND RESEARCH  
IN PARTIAL FULFILMENT OF THE REQUIREMENTS FOR THE DEGREE  
OF MASTER OF SCIENCE

IN

ENVIRONMENTAL ENGINEERING

DEPARTMENT OF CIVIL ENGINEERING

EDMONTON, ALBERTA

SPRING, 1983





THE UNIVERSITY OF ALBERTA  
FACULTY OF GRADUATE STUDIES AND RESEARCH

The undersigned certify that they have read, and  
recommend to the Faculty of Graduate Studies and Research,  
for acceptance, a thesis entitled RIVER MIXING AND  
MICROORGANISM SURVIVAL, SLAVE RIVER, N.W.T.  
submitted by GORDON PUTZ  
in partial fulfilment of the requirements for the degree of  
MASTER OF SCIENCE  
in ENVIRONMENTAL ENGINEERING.



## Abstract

The study reported herein involved investigations of the transverse mixing and microorganism survival within the Slave River downstream of Fort Smith, N.W.T. The Fort Smith wastewater treatment and disposal system consists of a three cell lagoon system, followed by a continuous discharge to the Slave River through a submerged near-shore outfall.

The study included field bacteriological sampling and tracer tests under open water and ice covered conditions. The purpose of the tracer tests was to provide an accurate measurement of the wastewater mixing (the dilution and distribution) within the river. The tracer data serves as a reference against which the time-dependent survival of microorganisms may be assessed.

The mixing studies were conducted using continuous injection of Rhodamine WT fluorescent dye and sampling at several selected cross sections over a 40 km reach of the river. The tracer tests indicated the mixing in the upper portion of the study reach was considerably lower than expected from test results on other natural streams and modelling using reach-averaged geometry, velocity and transverse mixing coefficient would prove unsatisfactory. However, a numerical modelling scheme using local parameters was found satisfactory and used to find local values of the transverse mixing coefficient.





Bacteriological sampling and analysis for total and fecal coliforms were conducted for each sampling station. After accounting for the physical mixing the limited data indicated a barely discernable microorganism die-off rate within the study reach under ice cover conditions. During the summer the high efficiency of treatment within the lagoon system reduced indicator concentrations in the river to levels which prevented any evaluation of the die-off rate. The numerical model for the mixing was adapted to allow prediction of the concentration of microorganisms within the wastewater plume for various decay rates.



## Acknowledgements

The basic funding for this project was provided by the Department of Local Government, Government of the Northwest Territories under the supervision of V. Christensen. B. Doulton provided liason with this Department and participated in field work. The microbiology work was supervised by J. Bell, Environment Protection Service, Edmonton. In addition the assistance of the following persons in field and laboratory studies is gratefully acknowledged: C. O'Brien, J. McComiskey, T. Lalonde, J. Greer, D. Caverson, B. George, I. Jollife, and K. Oberoi. D. Dragon, Town Superintendent for Fort Smith, made the Engineering facilities of the town available, and the Fort Smith office of Water Survey of Canada, under A. Wilson, provided much appreciated advice and assistance with field procedures.

The author would also like to thank the following: T. Casey for the use of his textformatting subroutines used in thesis production, Dr. D. W. Smith and Dr. R. Gerard for their suggestions and guidance, and finally S. Putz for typing the original manuscript and her continuous support, patience and encouragement.



## Table of Contents

Chapter		Page
I.	INTRODUCTION .....	1
II.	LITERATURE REVIEW .....	7
	A. Transverse Mixing .....	7
	Introduction .....	7
	Early Laboratory Studies .....	13
	Field Studies .....	20
	B. Microbial Self-Purification .....	38
	Ohio River Study .....	38
	Other Investigations .....	43
	Sample Integrity .....	60
	C. Health Implications .....	61
III.	OBJECTIVES .....	64
IV.	FIELD STUDIES .....	66
	A. Introduction .....	66
	B. Surveys .....	70
	Winter Tests .....	70
	Summer Tests .....	92
	Supplementary Data .....	94
	C. Tracer Methods .....	96
	Injection and Sampling .....	96
	Sample Analysis and Results .....	103
	D. Bacteriological Methods .....	109
	Sampling .....	109
	Laboratory Analysis and Results .....	139
V.	MATHEMATICAL ANALYSIS OF FIELD RESULTS .....	145





A. Tracer Analysis .....	145
B. Microorganism Decay Analysis .....	154
VI. COMPUTER MODELLING .....	166
A. Tracer Modelling .....	166
July 1980 and March 1981 Tests .....	166
Dimensionless Transverse Mixing Coefficient .....	167
March 1980 Test .....	193
B. Microorganism Modelling .....	194
VII. DISCUSSION .....	206
A. Transverse Mixing .....	206
B. Microorganism Decay .....	217
C. Dimensionless Curves .....	218
D. Comparison of Results to Other Studies .....	220
VIII. CONCLUSIONS .....	228
BIBLIOGRAPHY .....	231
APPENDIX I Derivation of the Pollutant Conservation Equation .....	237
APPENDIX II Derivation of Mixing Equations for Wide Prismatic Channels .....	241
Basic Equation .....	241
Transverse Mixing Zone .....	245
Longitudinal Dispersion .....	247
Mixing Regions .....	248
APPENDIX III Velocity Estimates and Flow Distributions .....	249
APPENDIX IV Dye Adsorption Studies .....	253
APPENDIX V Indicator Bacteria Data .....	260



APPENDIX VI Numerical Solution Method, Conservative Tracers .....	271
APPENDIX VII Numerical Solution Method, Non-Conservative Pollutants .....	284





## List of Tables

Table	Page
2.1 Comparative Incidence of Several Diseases -adapted from Hrudey and Raniga (1980).....	62
4.1 Tracer Injection Data.....	99
4.2 Tracer Recoveries.....	108
4.3 Bacteriological Sample Time Information for Winter Tests.....	140
4.4 Effluent Parameters.....	143
5.1 Calculation of Reach-Averaged $E_z$ .....	152
5.2 Calculation of Dimensionless $E_z$ .....	153
5.3 Dimensionless $E_z$ from Other Investigations.....	155
5.4 t Test at 13.0 km and 27.8 km.....	163
5.5 Near Left Bank Concentrations.....	163
5.6 Microorganism Recovery.....	165
6.1 Numerical Solution and Plume Characteristics July 1980.....	188
6.2 Numerical Solution and Plume Characteristics March 1980.....	189
6.3 Iterative Solution for March 1980 Mixing.....	202
6.4 Ratio of Measured Microbial Concentrations to Time-Dependent Decay Curves....	205
7.1 Dimensionless Mixing Coefficient versus Plume-Region Aspect Ratio.....	213
7.2 Decay Coefficients from Other Investigators.....	224
IV-1 Dye Adsorption Analysis.....	255
V-1 Coliform Counts March 1980.....	261
V-2 Coliform Counts July 1980.....	263
V-3 Coliform Counts March 1981.....	266



Table		Page
V-4	Estimated Flow Times March 1981.....	270
VI-1	Comparison of Analytical and Numerical Solutions for a constant $D$ .....	283



## List of Figures

Figure	Page
2.1	Typical Velocity Gradients in a Natural Stream.....8
2.2	Mixing Due to Differential Advection.....8
2.3	Time Dependent Mixing with Differential Advection -adapted from Beltaos (1979).....10
2.4	Transverse Coordinate Transformation.....26
2.5	Dimensionless Mixing Coefficient versus Aspect Ratio -adapted from Lau and Krishnappan (1981).....34
2.6	Coliform Decay Curves Formulated from Early Studies -data from Phelps (1944), Kittrell and Kochtitzky (1947).....44
2.7	Several More Recent Coliform Decay Studies -adapted from Kittrell and Furfari (1963).....50
2.8	Fecal Coliform Composite Decay Curves -adapted from Ballentine and Kittrell (1968).....51
2.9	Fecal Coliform Ratio versus Flow Time -adapted from Ballentine and Kittrell (1968).....52
2.10	<i>E. coli</i> Mortality versus Water Temperature -adapted from McFeters and Stuart (1972).....57
4.1	Study Location Map -adapted from Smith and Gerard (1981).....67
4.2	Profile of the Lagoon Outfall -adapted from Smith and Gerard (1981).....67
4.3	Cross Section Geometry and Flow Distribution March 1980 .....75
4.4	Cross Section Geometry and Flow Distribution July 1980 and March 1981.....83
4.5	Floats and Anchoring Apparatus.....95
4.6	Slave River Discharge at Fort Fitzgerald -data from Water Survey of Canada.....97



Figure	Page
4.7	Illustration of Variation in Tracer Concentration with Time and Distance following a Finite Duration Constant Rate Injection -from Smith and Gerard (1981).....100
4.8	Weir Apparatus for Tracer Injection -from Smith and Gerard (1981).....100
4.9	Sampling Rods -from Smith and Gerard (1981).....105
4.10	Dimensionless Tracer and Microorganism Concentrations March 1980.....110
4.11	Dimensionless Tracer and Microorganism Concentrations July 1980.....118
4.12	Dimensionless Tracer and Microorganism Concentrations March 1981.....127
5.1	Change in Variance of Best Fit Tracer Distributions with Distance from the Outfall.....147
5.2	Selected Distributions for Microorganism Decay Analysis.....157
6.1	Computer Modelling of Normalized Tracer Distributions July 1980.....168
6.2	Computer Modelling of Normalized Tracer Distributions March 1981.....177
6.3	Dimensionless Mixing Coefficient versus Distance.192
6.4	March 1980 Computer Modelling.....195
7.1	Apparent Increase in Bacterial Population due to Improper Consideration of Mixing.....207
7.2	Dimensionless Mixing Coefficient versus Lateral Distance from the Left Bank March 1981.....210
7.3	Dimensionless Mixing Coefficient versus Lateral Distance from the Left Bank July 1980.....211
7.4	Dimensionless Mixing Coefficient versus Aspect Ratio.....215





Figure		Page
7.5	Tanana River Studies -data from Gordon (1972) and Davenport, Sparrow, and Gordon (1976).....	223
7.6	Other Ice Condition Decay Studies -data from Ballentine and Kittrell (1968).....	225
I-1	Pollutant Flux In and Out of a Fluid Element in Cartesian Coordinates.....	238
II-1	Coordinate System.....	242
III-1	Velocity-Depth Correlation.....	251
IV-1	Dye Adsorption Analysis.....	256
IV-2	Adsorption Isotherm for Sample Containers.....	258
V-1	Background Concentrations March 1981.....	268
VI-1	Grid System Used in the Numerical Scheme.....	273
VI-2	Program Flow Chart.....	278



## List of Plates

Plate		Page
4.1	Slave River looking downstream over Bell Rock.....	68
4.2	Aerial view of Fort Smith.....	68
4.3	Fort Smith lagoon system.....	69
4.4	Winter River Travel.....	72
4.5	Drilling Sampling Holes.....	74
4.6	Winter Velocity Measurement.....	93
4.7	Summer River Transportation.....	93
4.8	Constant Head Weir.....	101
4.9	Pump Apparatus for Tracer Injection.....	101
4.10	Winter Injection Tent.....	102
4.11	Winter Sampling.....	104
4.12	Fluorometer.....	104
4.13	Bacteriological Sampling.....	138



## List of Symbols

$a$	resistance equation exponent
$a_0, b_0, d_0, f_0, n$	microorganism decay empirical coefficients
$a, b, d, g, m$	finite difference weighting coefficients
$A$	area, $m^2$
$b, m$	adsorption isotherm constants
$\bar{b}$	half-plume width defined as the lateral distance between maximum $c'$ and 0.5 maximum $c'$ , $m$
$c$	measured tracer concentration, ppb
$c^\infty$	fully mixed tracer concentration, ppb
$c'$	dimensionless tracer concentration
$c_0$	injection solution tracer concentration, ppb or %
$\bar{c}$	average tracer concentration component, ppb
$c'$	fluctuating tracer concentration, ppb
$\Delta c$	change in tracer concentration due to adsorption, ppb
$c'[R], c'[L]$	dimensionless tracer concentrations at the right and left banks
$C_s$	Dimensionless Chezy roughness coefficient
$C$	Dimensionless concentration scale
$D_z$	transverse diffusion factor representing average velocity, depth and mixing coefficient, $m^5/s^2$
$D, F$	numerical solution variable coefficients, $1/m$
$e$	base of the natural logarithms
$E_z$	transverse mixing coefficient, $m^2/s$
$f$	friction factor
$g$	acceleration due to gravity, $m^2/s$



$h$	local depth, m
$\bar{h}$	plume region average depth, m
$H$	mean channel depth, m
$k$	microbial decay coefficient, $1/d$
$K_s$	light extinction coefficient, $1/m$
$K$	constant diffusion coefficient, $m^2/s$
$\ell$	general length scale, m
$L$	average daily surface solar radiation, langelys/hr
$L$	longitudinal length scale, m
$M$	total solute mass, Kg
$N$	measured bacteria concentration, per 100mL
$N_0$	initial bacteria concentration, per 100mL
$N'$	dimensionless bacteria concentration
$P$	percentage of maximum bacteria concentration
$q$	cumulative discharge, $m^3/s$
$q_j, p_j, r_j$	numerical solution matrix coefficients, $1/m$
$Q$	total channel discharge, $1/m$
$Q_n$	diffusive flux, $m/s$
$Q_0$	tracer injection flow, $m^3/s$ or $mL/s$
$r$	hydraulic radius, m
$\bar{r}$	plume region average hydraulic radius, m
$R$	mean channel hydraulic radius, m
$S$	total energy gradient, approximated by slope of the water surface in uniform flow, $m/m$
$S_n$	sinuosity
$S$	numerical solution forcing vector, $1/m$
$t$	time, sec





$T$	temperature, °C
$u, v, w$	velocity components, Cartesian coordinates, m/s
$\bar{u}, \bar{v}, \bar{w}$	mean velocity components, Cartesian coordinates, m/s
$u', v', w'$	fluctuating velocity components, Cartesian coordinates, m/s
$U^*$	average plume region shear velocity, m/s
$V$	mean channel velocity, m/s
$V^*$	mean channel shear velocity, m/s
$W$	mean channel width, m
$x, y, z$	Cartesian coordinates, m
$\alpha, \gamma, \lambda$	numerical solution variable coefficients, 1/m
$\beta$	a constant
$\delta$	transverse length scale, m
$\epsilon$	turbulent diffusion coefficient, m <sup>2</sup> /s
$\eta$	dimensionless cumulative discharge
$\theta/2, \omega/2$	finite difference weighting coefficients
$\mu$	first moment of measured concentration distribution with respect to the LB using the dimensionless transverse cumulative flow coordinate
$\rho$	mass density, Kg/m <sup>3</sup>
$\sigma_z^2$	variance of measured concentration distributions with respect to transverse distance, m <sup>2</sup>
$\sigma^2$	variance of measured concentration distributions with respect to dimensionless cumulative flow
$\tau_0$	boundary shear stress, Kg/ms <sup>2</sup>
$\phi$	molecular diffusion coefficient, m <sup>2</sup> /s
$\psi$	shape-velocity factor



## I. INTRODUCTION

Natural stream capability for self-purification of microbial contaminants originating from wastewater discharges has long been recognized, but the process is inadequately understood. Wastewater microbial concentrations generally decrease downstream of an effluent outfall due to two distinct processes:

- a. the decay process, which is a time dependent die-off of microorganisms within the effluent plume, and
- b. the mixing process, which is the reduction in microorganism concentrations due to dilution within the stream.

Die-off of effluent microorganisms occurs due to adverse environmental conditions and predation by other microbes within the receiving stream. Die-off rates tend to be much higher in the summer than during winter months. The longest microbial persistence is believed to occur under ice cover conditions in cold northern rivers. The cold water temperature retards predation and respiration, while the ice sheet eliminates the lethal effects of sunlight. Low flow conditions, which reduce the receiving stream's dilution capacity, are generally concurrent with ice cover conditions. Thus, the reduction in river microbial concentrations, already retarded by longer persistence time, is further reduced by decreased dilution capacity.



Enteric pathogenic microorganisms are usually more difficult to isolate and enumerate than fecal indicator bacteria and therefore die-off studies have been conducted using the fecal indicators to simplify analysis. Laboratory studies have been less than totally successful in simulating the stream decay process, often giving confusing results. The limited success in the laboratory requires the decay process be studied in the field to gain a better understanding of the process.

Field studies may be conducted by two methods:

- a. utilizing membrane chamber apparatus, or
- b. actual bacteriological stream sampling downstream of an effluent outfall.

The membrane chamber method uses a submerged vessel with walls permeable to stream water but impenetrable by microorganisms. The chamber, dosed with a known initial population, is anchored at a desired location within the stream and samples for enumeration withdrawn at selected time intervals. The enclosed microorganisms are exposed to the physical environmental factors of the stream such as temperature, pH, and nutrient concentration due to the free exchange of fluid through the permeable walls. However, they are not influenced by stream organism predation or stream mixing because microorganisms can not move through the membrane walls. Therefore, the actual natural purification process is not completely simulated.





Bacteriological sampling downstream of effluent outfalls is the best method of studying the natural purification process but requires extensive sampling and river surveys. Sections are located downstream of the effluent source and samples for enumeration taken at selected points across the stream width. The initial numbers of microorganisms must be evaluated by determining the raw effluent concentration and flow. The microorganisms are close to neutrally buoyant and move with the stream currents. Downstream of the outfall they are mixed with the receiving water as the effluent plume spreads across the stream and simultaneously die-off as a function of time. Reductions in microorganism concentration due to dilution or mixing effects, within regions where effluent has only partially mixed with stream, must be quantified before an accurate evaluation of the time dependent decay process is possible.

Often when wastes are discharged to natural streams complete mixing of the effluent across the stream is assumed a short distance downstream of the outfall. The microorganism concentration decreases beyond this distance are then attributed to the time dependent decay process. However, the region preceding complete mixing in the stream may be of significant length in which case the two-dimensional<sup>1</sup> nature of the mixing in this zone must be

-----  
<sup>1</sup> Two-dimensional meaning there are significant concentration gradients in both the streamwise and transverse (across the stream) directions.





considered before die-off can be accurately assessed. The transverse (two-dimensional) mixing is of prime importance when considering bank discharges into wide natural channels where complete mixing may not occur for a hundred or more river widths downstream of an outfall.

Mixing of the effluent within the stream occurs due to dispersion by differential advection and diffusion. Diffusion is movement of pollutant from areas of high concentration towards areas of lower concentration as a result of random motion. In streams the random motion is predominantly caused by turbulence, a property of the fluid flow. Dispersion by differential advection is caused by significant vertical and transverse velocity gradients within natural streams and occurs in conjunction with diffusion. For example, as pollutant diffuses from an area of high concentration and low streamwise velocity, to an area of lower concentration and higher streamwise velocity, the difference in velocity of the predominant fluid motion will cause the pollutant to be dispersed in the streamwise or longitudinal direction.

Transverse mixing may be described by a differential mass balance equation for a conservative tracer. Solutions to the equation require a prior knowledge of the transverse mixing coefficient, an empirical parameter, which is a measure of the rate at which an effluent plume will spread across the receiving stream. Predictions of the transverse mixing coefficient have limited accuracy unless derived



from a field tracer study of the mixing along the stream reach of interest for existing flow conditions.

Clearly the most reliable means to study microbial self-purification of streams is through field bacteriological sampling in conjunction with a tracer study of the reach of interest to define the mixing with no decay.

Large streams often serve as major sources for water supply systems. Microbial purification by water treatment and disinfection provides a safeguard against the transmission of water-borne diseases from contaminated raw water to the consumer. However, most rivers are used for other purposes such as fishing and recreation which bring individuals into contact with the untreated raw water and the risk of infection. In addition casual consumption of raw water (consumption with no disinfection) presents a health risk common to northern rivers due to established native life-style and unfamiliarity with the possible consequences. Natural purification represents a barrier to serious outbreaks of water-borne disease as a result of these additional water uses. A better understanding of the die-off process, the relationship between indicator and pathogenic microorganism numbers, and the tolerable levels of indicators is required to aid in the formulation of satisfactory water quality-water use policies.

The large dilution capacity of many northern rivers and the relatively long distances between isolated



settlements utilizing the stream as a water source should be considered in establishing water quality and waste treatment regulations. An improved understanding of the rates of natural purification and therefore a better knowledge of the stream's feasible capacity to assimilate wastes may allow inter-community distances to be safely utilized for reduction in microorganism concentrations. A strategy combining natural purification and simple wastewater treatment facilities (such as grit removal, primary treatment, etc.) to maintain acceptable receiving water quality would generally prove most economic, allowing construction of more sophisticated facilities to be delayed until projected water usage and wastewater production warrant them.





## II. LITERATURE REVIEW

### A. Transverse Mixing

#### Introduction

A soluble pollutant discharged into a stream will be diluted simultaneously by the processes of diffusion and mixing due to differential advection. Beltaos (1979) presented the following concise description of the mixing process in streams.

Diffusion is movement of a solute within the stream due to random motion in the presence of concentration gradients. The solute mass moves from areas of high concentration to areas of lower concentration. The random motion may be molecular, a property of the fluid, or turbulent, a property of the fluid flow.

Mixing due to differential advection is caused by mean velocity gradients. Most natural streams have significant vertical and lateral velocity gradients as shown in Figure 2.1. Differential advection mixing occurs in conjunction with diffusion as illustrated in Figure 2.2. Diffusion will cause solute flux in the direction of lowest concentration, which for example may be at the water surface or streambed. The high velocity of the main fluid body will cause particles moving upward to increase in velocity while those moving downward will decrease in velocity. The result is a pollutant spread in the streamwise (longitudinal)





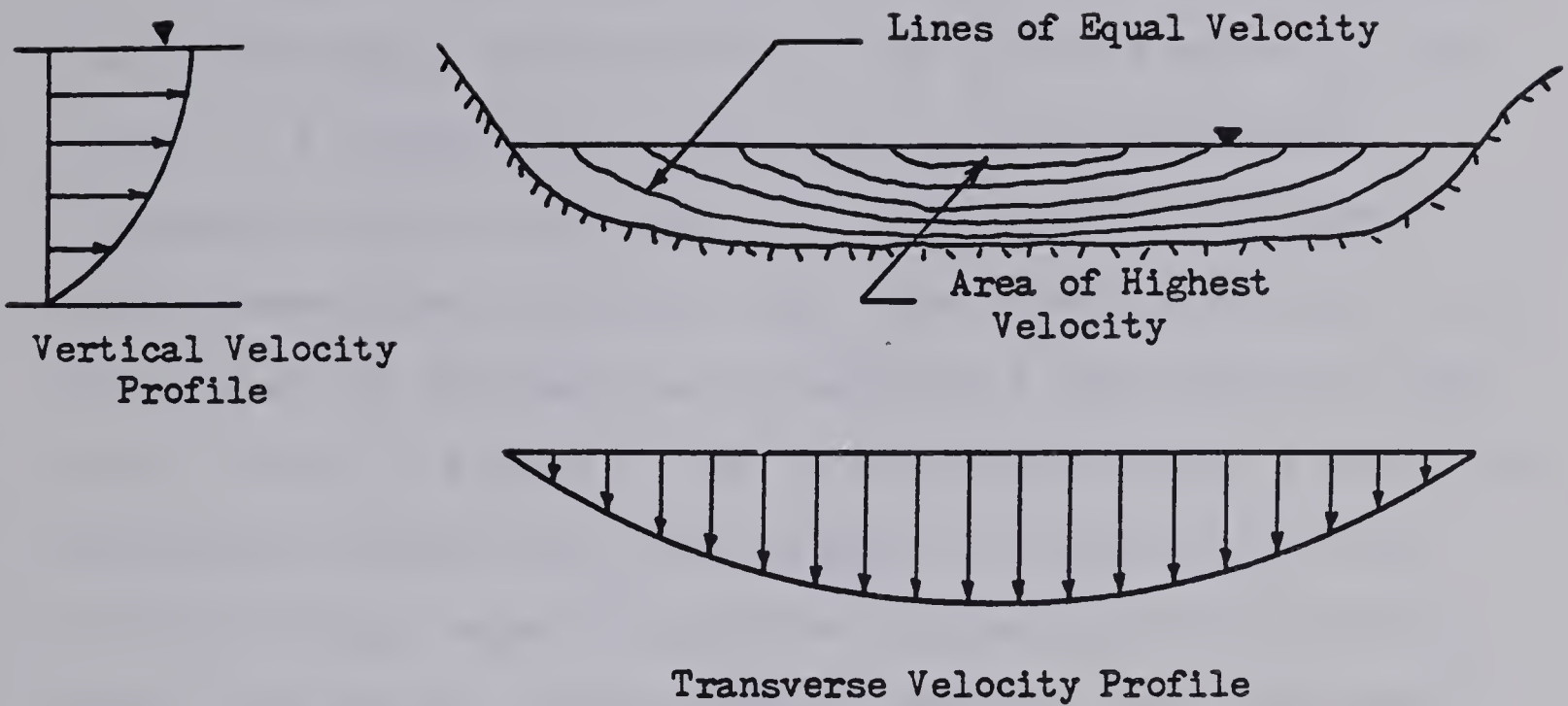


Figure 2.1 Typical Velocity Gradients in a Natural Stream

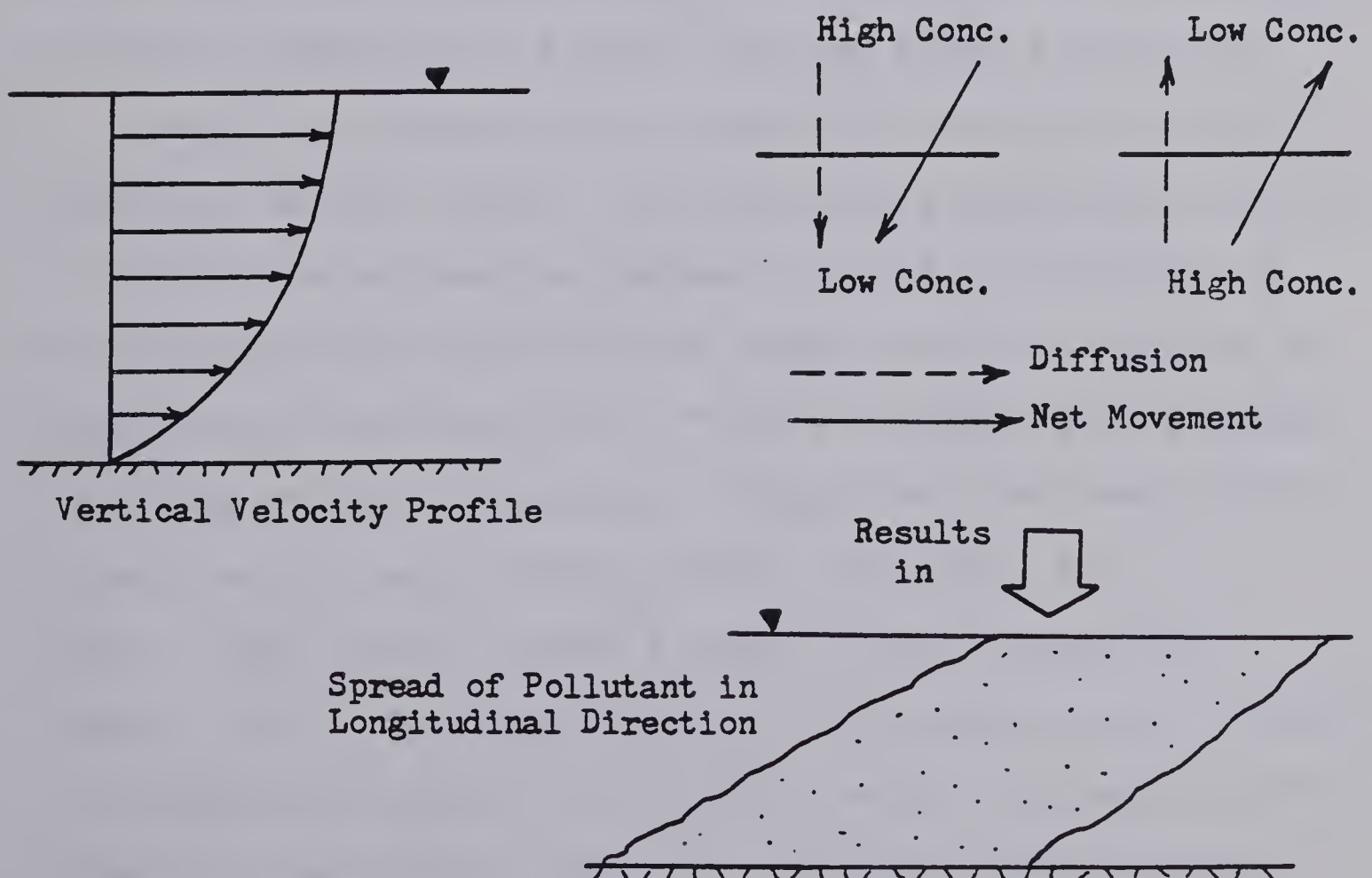


Figure 2.2 Mixing Due to Differential Advection



direction. Similar results occur due to lateral (transverse) velocity gradients.

Beltaos (1979) described the interaction of diffusion and differential advection with the aid of Figure 2.3. At time  $t = 0$  a quantity of pollutant is instantaneously released into the main flow of a stream. The pollutant moves downstream with the local flow velocity mixing in all directions by diffusion and remaining a near uniform cloud until time  $t_1$ . Beyond  $t_1$ , the diffusing pollutant eventually encounters velocities significantly different than the original local velocity and the boundaries of the cloud begin to spread by differential advection. The pollutant cloud appears as a horseshoe shape at time  $t_2$ , elongated in the longitudinal direction. The longitudinal spread has been increased by differential advection and the transverse diffusion enhanced as a result of the plume stretching.

Beyond  $t_2$ , the pollutant cloud will continue to mix, reach the banks, reflect, and eventually approach a uniform concentration across the channel. Beyond the distance at which uniform concentration is established the problem is essentially one dimensional. This one-dimensional process, generally called longitudinal dispersion, has been studied extensively by many investigators ( examples are Elder (1959) Glover (1964) Fischer (1967a) Sayre and Chang (1968)). However, Beltaos (1979) points out, at least for idealized channels, the mixing length increases as the square of the channel width and therefore the practical



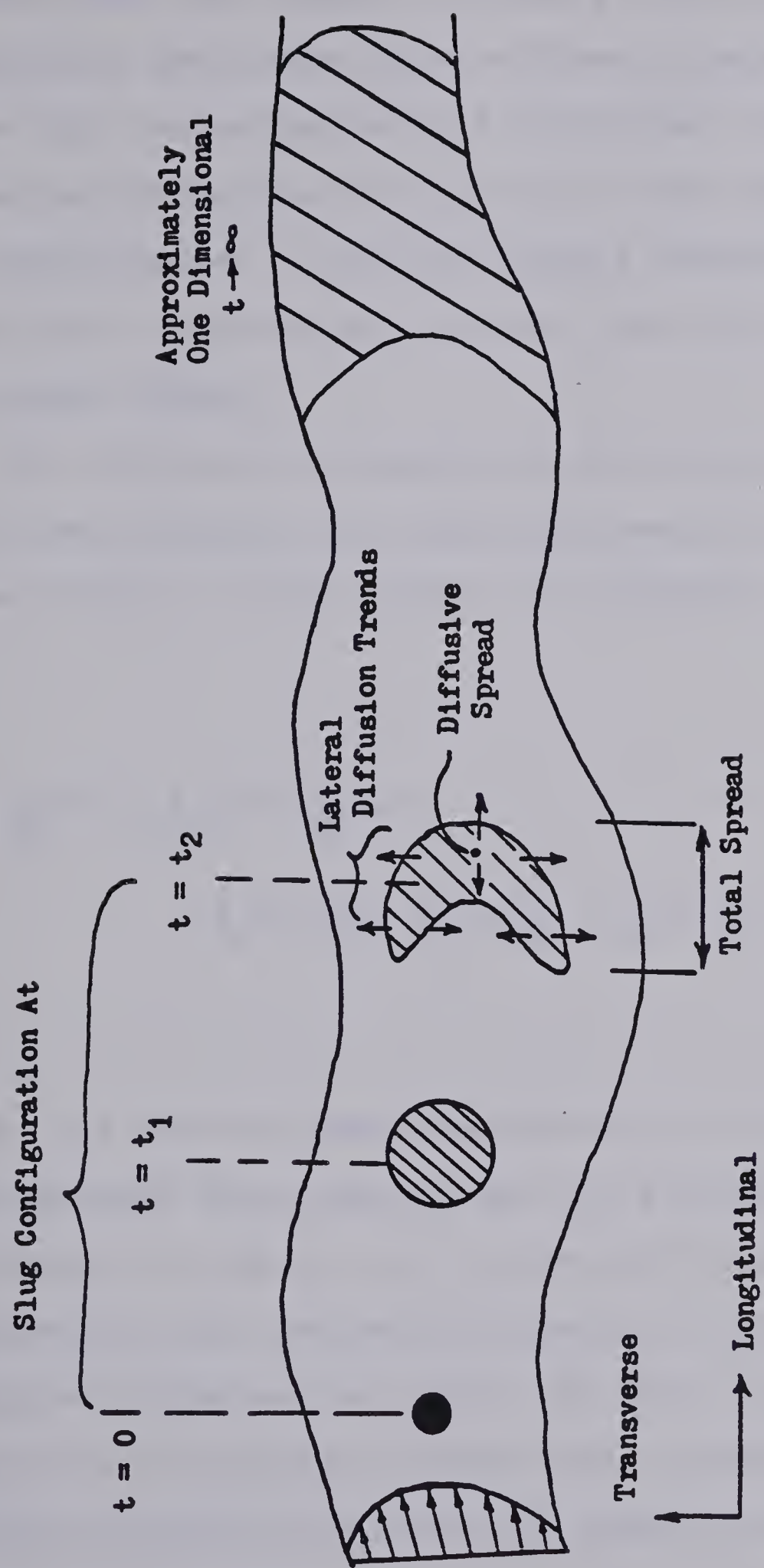


Figure 2.3 Time Dependent Mixing with Differential Advection  
 -adapted from Beltaos (1979)





value of longitudinal dispersion theory may be limited by channel size. The region of primary interest is often immediately downstream of an effluent discharge in the zone where high concentrations and significant transverse concentration gradients will exist. This region prior to the establishment of uniform lateral concentrations is called the transverse mixing zone, and its length termed the mixing length.

The differential equation describing mixing is derived from a mass balance of a neutrally buoyant conservative tracer within a fluid element (see Appendix I):

$$\frac{\partial c}{\partial t} + \frac{\partial}{\partial x}(uc) + \frac{\partial}{\partial y}(vc) + \frac{\partial}{\partial z}(wc) = \frac{\partial}{\partial x}(\epsilon_x \frac{\partial c}{\partial x}) + \frac{\partial}{\partial y}(\epsilon_y \frac{\partial c}{\partial y}) + \frac{\partial}{\partial z}(\epsilon_z \frac{\partial c}{\partial z}) \quad (2.1)$$

where  $c$  is time-averaged concentration,  $u, v, w$  are time-averaged velocities in the  $x, y, z$  directions indicated in Figure I-1, and  $\epsilon_x, \epsilon_y, \epsilon_z$  are coefficients of diffusion representing the combined influence of turbulent and molecular random motion within the fluid. In deriving Equation 2.1 turbulent diffusion was expressed in the form of Fick's gradient law, which is commonly used to describe molecular diffusion.





Simplified differential equations describing mixing beyond the mixing length, and within the transverse mixing zone may be derived by depth-averaging Equation 2.1 and making order of magnitude approximations. Details of these derivations are given in Appendix II. The resulting equations are:

$$\frac{\partial c}{\partial t} + u \frac{\partial c}{\partial x} = \frac{\partial}{\partial x} (E_x \frac{\partial c}{\partial x}) \quad (2.2)$$

which describes longitudinal dispersion, or mixing beyond the mixing length, and

$$h \frac{\partial c}{\partial t} + hu \frac{\partial c}{\partial x} = \frac{\partial}{\partial z} (hE_z \frac{\partial c}{\partial z}) \quad (2.3)$$

which describes mixing within the transverse mixing length or zone. The diffusion coefficients have been replaced by new parameters,  $E_x$  and  $E_z$ , called mixing coefficients. The mixing coefficients incorporate dispersional effects due to secondary circulations into Equation 2.2 and 2.3 on the assumption they are dependent upon lateral concentration gradients.

An intermediate zone will exist in which the longitudinal and transverse diffusion terms will be of the same magnitude and therefore must both be considered. Many early investigations into longitudinal mixing involved this



intermediate zone and provided the original interest in transverse diffusion.

### Early Laboratory Studies

Adolph Fick was one of the earliest investigators of the diffusion process.<sup>1</sup> In 1855 Fick proposed an expression describing molecular diffusion, although at the time the actual physics of the process was not understood. Fick stated, analogous to Fourier's law of heat flow, that solute mass flux in a given direction is proportional to the gradient of solute concentration in that direction (see Equation I-2).

The following classical diffusion equation may be derived by considering conservation of solute mass, diffusive flux (ie. the right hand side of Equation 2.1) and a constant diffusion coefficient

$$\frac{\partial c}{\partial t} = K \left( \frac{\partial^2 c}{\partial x^2} + \frac{\partial^2 c}{\partial y^2} + \frac{\partial^2 c}{\partial z^2} \right) \quad (2.4)$$

where K is the diffusion coefficient. The fundamental solution to Equation 2.4 (which describes both diffusion and heat flow) is the Gaussian distribution. For example, the solution to the one-dimensional form of Equation 2.4 is

---

<sup>1</sup> A concise description of the early development of diffusion theory is given by Fischer et al. (1979) whose major points are briefly outlined here.



$$c(x,t) = (M/\sqrt{4\pi Kt}) \exp(-x^2/4Kt) \quad (2.5)$$

where  $M$  is the total mass of solute and  $t$  is the time elapsed from a point source injection. The fundamental solution can be extended to more complex problems by using image sources to account for reflecting boundaries and a moving reference frame to account for advective solute flux in laminar flow.

Random walk statistical theory, which describes the probable distribution of solute resulting from random collisions of molecules (molecular diffusion), was developed following Fick's hypothesis. Random walk theory indicates that after an initial number of individual movements or time periods the distribution of solute molecules will closely approximate the Gaussian distribution, thus implying the validity of Fick's law and equation 2.4.

G.I. Taylor extended diffusion theory to turbulent flows. Taylor's work suggested that after an initial time period the diffusion process may be described by a turbulent diffusion equation, in which turbulent diffusive flux is described by Fick's law with turbulent diffusion coefficients. Turbulent diffusion is analogous to molecular diffusion but is the result of a distinctly different physical process. Molecular diffusion, as noted above, is the result of molecular collisions, while turbulent diffusion results from the much larger scale random motion





of "fluid packages" or "eddies" characteristic of turbulent flow.

Taylor's work also showed that after an initial time period the turbulent diffusion coefficient is the product of a length scale and the intensity of the turbulence, the length scale being a measure of the size of the eddies created by the turbulence.

Taylor (1954) extended his work on turbulent diffusion to shear flows (i.e. flows in which significant velocity gradients exist) by analysing solute diffusion in pipe flow. He showed the problem reduced to a section-averaged one dimensional equation similar to Equation 2.2. The mixing coefficient is generally called the longitudinal dispersion coefficient and accounts for mixing due to differential advection and streamwise diffusion. Calculation of the longitudinal dispersion coefficient requires a knowledge of the vertical diffusion or, in Taylor's work the radial diffusion, across the velocity profile. Taylor obtained a value for the radial diffusion coefficient using the 'Reynold's analogy' that solute mass and momentum diffusion are equal in magnitude. The momentum flux through a surface is equal to the shear stress at the surface,  $\tau$ , divided by the fluid density,  $\rho$  and is equivalent to the solute diffusion flux  $Q_n$ . Therefore

$$\epsilon_y = \tau / (\rho \partial u / \partial y) = Q_n / (\partial c / \partial y) \quad (2.6)$$





where  $\epsilon_y$  is the vertical diffusion coefficient and  $\partial u / \partial y$  is the vertical velocity profile (for Taylor's analysis  $y$  is in the radial direction). Hence,  $\epsilon_y$  may be calculated using Equation 2.6 provided the distribution of velocity and shear stress are known.

Elder (1959) applied Taylor's results to uniform flow in an infinitely wide open channel and determined the longitudinal dispersion coefficient. Elder calculated the vertical diffusion coefficient using Equation 2.6 and the logarithmic velocity profile given by

$$u = \bar{u} + u' = \bar{u} + \frac{V^*}{\kappa} (1 + \ln(y/h)) \quad (2.7)$$

where  $\bar{u}$  is the depth-averaged velocity,  $u'$  the deviation from the average velocity,  $h$  the total depth,  $y$  the distance from the bed,  $\kappa$  von Karman's constant generally taken as 0.4 and  $V^*$  the shear velocity. The shear velocity is a convenient method of expressing the magnitude of the boundary shear stress  $\tau_0$  and is given by

$$V^* = \sqrt{\tau_0 / \rho} = \sqrt{gRS} \quad (\text{for open channels}) \quad (2.8)$$

where  $R$  is the mean channel hydraulic radius,  $S$  the slope of the energy line and  $g$  the gravitational constant. The distribution of shear stress across the flow may be derived from a force balance and is given by



$$\tau = \tau_0(1-(y/h)) \quad (2.9)$$

Using Equations 2.6, 2.7 and 2.9 the following expression for the vertical diffusion coefficient may be derived

$$\epsilon_y = \kappa(y/h)(1-y/h)hV^* \quad (2.10)$$

Integrating over the depth of flow Elder predicted the depth-averaged vertical diffusion coefficient as

$$\overline{\epsilon_y} = 0.067hV^* \quad (2.11)$$

While investigating longitudinal dispersion in a wide rectangular flume experiment Elder (1959) also observed the lateral (transverse) concentration distributions resulting from a point source slug injection of tracer. Elder noted the distributions closely matched the Gaussian distribution (the fundamental solution to the classical diffusion equation) and proposed an empirical expression for the depth-averaged transverse turbulent diffusion coefficient in the same form as Equation 2.11, i.e.

$$\epsilon_z = \beta HV^* \quad (2.12)$$

where  $H$  is the mean channel depth and  $\beta$  a constant. An empirical expression is necessary because no theoretical relationship exists to predict the transverse diffusion of



momentum. Fitting the best Gaussian curve to his experimental results Elder gave the value of  $\beta$  as 0.23. Elder noted this value was much larger than for vertical diffusion.

Recalling Taylor's earlier work, Equation 2.12 indicates the length scale of turbulence may be characterized by the depth of flow and the intensity of turbulence by the shear velocity.

The close approximation of transverse concentration distributions, for wide rectangular channels, to a Gaussian relationship allows the transverse diffusion coefficient to be calculated from experimental data. Sayre and Chang (1968) determined a constant transverse diffusion coefficient,  $K_z$ , for a number of continuous (i.e.  $\partial c / \partial t = 0$ ) point source experiments in a rectangular flume using the relationship:

$$K_z = \frac{V}{2} \frac{d\sigma_z^2}{dx} \quad (2.13)$$

where  $V$  is the mean channel velocity,  $x$  the distance from the tracer injection point, and  $\sigma_z^2$  the variance of the measured transverse concentration distributions. The diffusion coefficient  $K_z$  in Equation 2.13 represents a constant  $\epsilon_z$ , considered independent of position in the flow. The relationship applies for the region between the establishment of a uniform vertical concentration and the distance at which reflections of the tracer plume from the





side walls begin to distort the Gaussian distribution. This method of analysis and those similar to it are generally termed the method of moments.

The major conclusions of Sayre and Chang (1968) relating to transverse diffusion for uniform flow in rectangular flumes were:

- a. The transverse diffusion process downstream of a continuous point source can be represented by a two-dimensional Fickian dispersion equation provided uniform concentration in the vertical has been established,
- b. The confining effects of sidewalls can be accounted for by treating them as reflecting barriers, and,
- c. The average value of  $\beta$  in Elder's relationship was 0.17 for the flow conditions used in their experiments.

Flume studies of transverse diffusion have been conducted by other investigators. Yotsukura and Cobb (1972), in a brief review of the results of these studies, indicated the value of  $\beta$  for the Elder relationship may range from 0.11 to 0.26.

Equation 2.1 may be simplified using the following assumptions:

- a. negligible vertical and transverse velocities (ie.  $v \approx 0$ ,  $w \approx 0$ ),
- b. streamwise velocity,  $u$ , is constant independent of position, and,





- c. the diffusion coefficients are constants  
independent of position

Applying these simplifications Equation 2.1 reduces to

$$\frac{\partial c}{\partial t} + V \frac{\partial c}{\partial x} = K_x \frac{\partial^2 c}{\partial x^2} + K_y \frac{\partial^2 c}{\partial y^2} + K_z \frac{\partial^2 c}{\partial z^2} \quad (2.14)$$

which describes three-dimensional mixing in uniform flow of constant streamwise velocity  $V$  and constant diffusion coefficients  $K_x$ ,  $K_y$ , and  $K_z$ . Sayre and Chang (1968) developed an analytical solution to Equation 2.14, but the solution has extremely limited application in natural streams due to the simplifications involved.

### Field Studies

The first field investigations of transverse diffusion were reported by Glover (1964) and Fischer (1967b). Glover measured the transverse concentration distributions of short lived radioisotopes, downstream of a continuous point source of power plant effluent, along a short reach of the Columbia River. He reported a value for  $\beta$  of 0.72. Fischer conducted tracer studies along a straight portion of an earth canal. He reported a value for  $\beta$  of 0.24 for continuous point source discharges located at midstream and at the bank.

Fischer (1967b) used a modification of the method of moments in his analysis. He calculated the variance of the transverse distribution of tracer mass flux rather than



concentration passing a measured section. This implicitly includes the effects of local depth and velocity in the calculation. He also adjusted the variance for minor changes in channel width. In discussing his results Fischer proposed a physical explanation for the large values of transverse diffusion coefficient measured in comparison to that which can be theoretically predicted for vertical diffusion. Fischer stated:

"the scale of turbulence, or 'eddy size', is partially dependent on the proximity of normal boundaries and is more restricted in the vertical. Thus, although the turbulent motion is originally excited by the presence of boundary shear, the large scale movements which produce the maximum mixing are more effective in the transverse direction."

Despite this observation, many investigators continue to use a vertical length scale such as  $H$  to characterize eddy size.

Yotsukura, Fischer and Sayre (1970) recognized that transverse mixing in natural channels may be greatly enhanced due to the influence of secondary currents. Secondary currents may be created by variable bed shear, channel irregularities or bends within the stream. Increased mass transfer due to secondary currents could explain the high value of  $\beta$  reported by Glover (1964) for the Columbia River. Yotsukura et al. (1970) conducted a



steady-state transverse mixing investigation along a gently curved reach of the Missouri River downstream of a mid-channel tracer injection. A numerical simulation of the mixing was used to find the transverse mixing coefficient by fitting solution distributions to the measured tracer concentrations. The explicit finite difference scheme they utilized was based upon a stream tube concept and accounted for varying channel depth and velocity. The mass transfer between stream tubes was assumed to be entirely diffusive, incorporating any secondary current effects into the diffusion term. They considered the numerical scheme superior to the method of moments for analysis of transverse mixing in natural streams because Equation 2.13 was derived for infinitely wide channels with uniform depth and velocity.

The numerical solution gave an overall best fit to the measured distributions with a reach-averaged  $\beta$  of 0.6. However, a sensitivity analysis indicated the transverse mixing coefficient could vary as much as 100 percent along the reach without appreciably altering the solution. Yotsukura et al. (1970) concluded that  $\beta$  for large meandering channels would generally be larger and more variable than results obtained for small straight channels.

Holley, Siemans and Abraham (1972) investigated the effects of secondary currents, channel geometry and local velocity, which are generally lumped into the diffusion coefficient, in an effort to distinguish which mechanisms





the coefficient should represent. In particular they considered the effects of transverse variation of depth, streamwise velocity, the diffusion coefficient itself and the presence of transverse velocities.

Holley et al. worked with an implicit finite difference model which gave solutions to Equation 2.3. They first looked at the influence of local depth by considering a trapezoidal and rectangular channel with equivalent mean velocity and depth.' The solution obtained for a continuous bank injection of tracer indicated the equivalent rectangular section seriously underestimated the concentration along the injection bank. The discrepancy decreased with increasing distance from the outfall. Analysis of the solution distributions for the trapezoidal channel, using the method of moments, resulted in a larger transverse diffusion coefficient than input to their model.

Holley et al. proposed the following empirical expressions for the transverse diffusion coefficient to investigate the effects of lateral variation in local streamwise velocity and the coefficient itself:

$$\epsilon_z = \beta u h \quad (2.15)$$

where  $u$  is the local streamwise velocity,  $h$  the local depth,  $\beta$  a constant, and

-----  
' Predicting  $\epsilon_z$  with Elder's expression using section mean  $V^*$  and  $H$  essentially assumes an idealized rectangular channel.





$$\epsilon_z = \beta u H$$

(2.16)

where  $H$  is the mean channel depth. The value of  $u$  was calculated from an assumed parabolic transverse velocity distribution used for purposes of the simulation. Numerical solutions for continuous side injection into a trapezoidal channel, using  $\epsilon_z$  predicted by Equations 2.15 and 2.16, were compared to that using Equation 2.12. The distributions obtained using Equation 2.16 were equivalent to those of Equation 2.12 with only minor differences in the peak concentration. However, the distributions obtained using Equation 2.15 had extremely high bank concentrations in comparison to those of Equation 2.12. This discrepancy decreased with distance from the source, similar to the influence of local depth.

Holley et al. showed the transverse velocity,  $w$ , generally assumed zero, may be calculated using the expression:

$$w = -\frac{1}{h} \frac{\partial}{\partial x} \int_s^z u h \, dz \quad (2.17)$$

where  $s$  is the transverse location of the streamline passing through the pollutant source. Using typical data from the IJssel River in The Netherlands they demonstrated that the transverse velocity term dropped in deriving Equation 2.3' may easily be of the same magnitude as the

---

<sup>1</sup> See Appendix II



transverse diffusion term. The correct formulation of Equation 2.3 under such conditions would be

$$h \frac{\partial c}{\partial t} + hu \frac{\partial c}{\partial x} + hw \frac{\partial c}{\partial z} = \frac{\partial}{\partial z} (hE_z \frac{\partial c}{\partial z}) \quad (2.18)$$

In conclusion Holley et al. formulated a more general method of moments analysis using the transverse distribution of tracer flux (similar to Fischer 1967b) which effectively considers local depth and velocity. Their change in variance expression also included a term accounting for any significant transverse velocity.

The effects of local stream geometry, variable streamwise velocity, and the presence of transverse velocity, considered within the moment analysis of Holley et al. (1972) and Fischer (1967b), may more easily be accounted for using a transverse coordinate transformation introduced by Yotsukura and Cobb (1972). The new transverse coordinate is defined as the cumulative flow,  $q$ , given by

$$q(z) = \int_0^z uh \, dz \quad (2.19)$$

where  $z = 0$  represents the left bank as shown in Figure 2.4 and  $u$  is the mean velocity in the direction of flow. At the right bank  $z = W$ , the total stream width and  $q = Q$ , the total stream discharge. Equation 2.19 indicates a line of constant  $q$  represents a depth-averaged streamline and hence two adjacent lines of constant  $q$  define a streamtube.



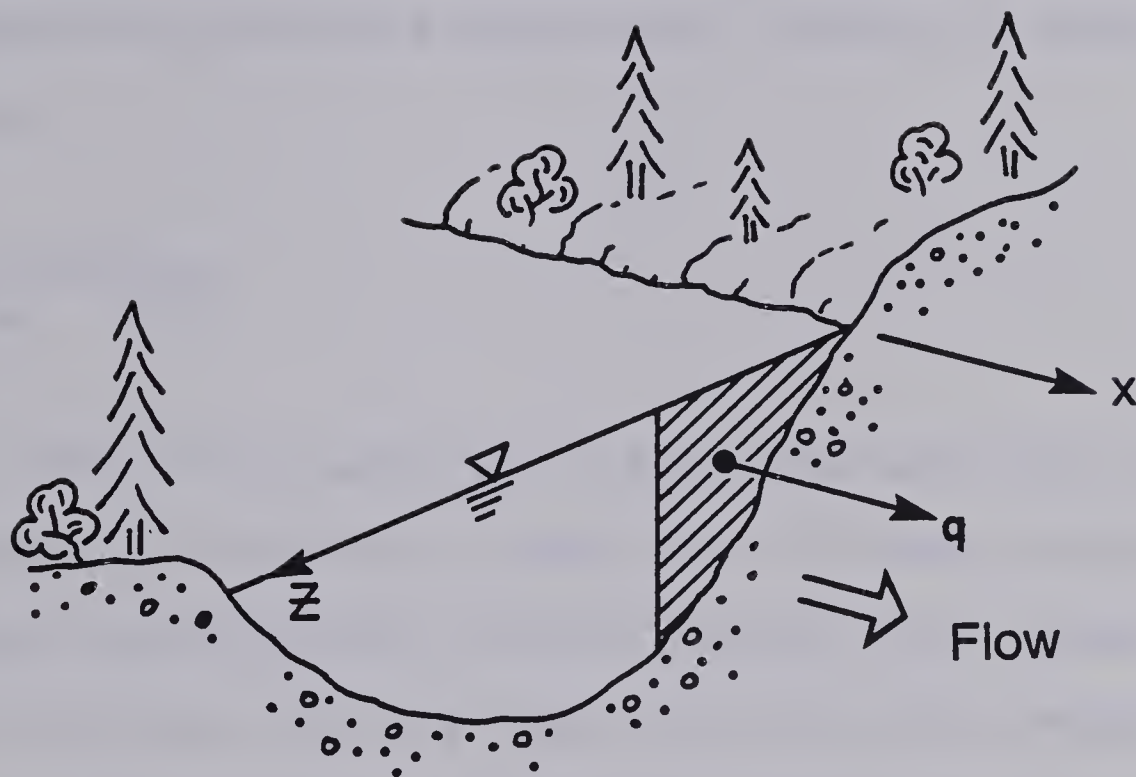


Figure 2.4 Transverse Coordinate Transformation





Important features of the 'q' transformation are:

- a. there is no average flow across a line of constant  $q$  and therefore no transverse advection, and
- b. the plan view of a natural stream of variable width is transformed into a simple rectilinear form of constant width.

Yotsukura and Cobb (1972) introduced the 'q' transformation into the steady-state version of Equation 2.3 giving

$$\frac{\partial c}{\partial x} = \frac{\partial}{\partial q} (uh^2 E_z \frac{\partial c}{\partial q}) \quad (2.20)$$

Although  $uh^2 E_z$  will vary with  $q$  Yotsukura and Cobb showed that numerical solutions to Equation 2.20 were relatively insensitive to variations in the term for mid-stream region tracer injections. On this basis they proposed replacing  $uh^2 E_z$  with a constant flow-averaged parameter,  $D_z$ , given by

$$D_z = \frac{1}{Q} \int_0^Q uh^2 E_z dq \quad (2.21)$$

Introducing  $D_z$  and non-dimensionalizing  $c$  and  $q$  gives

$$\frac{\partial c'}{\partial x} = \frac{D_z}{Q^2} \frac{\partial^2 c'}{\partial \eta^2} \quad (2.22)$$

where the dimensionless transverse coordinate,  $\eta$ , and dimensionless concentration  $c'$  are given by





$$\eta = q/Q \quad (2.23)$$

$$c' = c/c_{\infty} \quad (2.24)$$

where the fully mixed river concentration  $c_{\infty} = c_0 Q_0 / Q$ ,  $Q_0$  being the tracer injection discharge of concentration  $c_0$ .

Yotsukura and Cobb (1972) developed analytical solutions to Equation 2.20 for point and line sources of conservative tracer, accounting for boundary reflections using the method of images. The solutions were verified using a field study conducted on the South River and previous test results of Fischer (1967b) and Yotsukura, Fischer and Sayre (1970). Analytical solutions were fitted to measured data using trial values of  $E_z$ . The calculated distributions and mixing coefficients were generally in good agreement with those measured or predicted for relatively straight shallow reaches of natural streams.

The cumulative discharge concept was further refined by Yotsukura and Sayre (1976) by introducing an orthogonal curvilinear coordinate system. The longitudinal coordinate surfaces in this system follow the bends of the natural stream and denote streamlines at any transverse location. Discrepancies in distances along coordinate surfaces are accounted for by introducing metric (scaling) coefficients into the transformed version of Equation 2.3. For gently



meandering channels, without abrupt flow constrictions or expansions the metric coefficients approach unity and the curvilinear system reduces to Cartesian coordinates.

Yotsukura and Sayre (1976) concluded the new coordinate system could better approximate the effects of secondary currents caused by bends or channel irregularities.

Beltaos (1979) adapted the analysis of Sayre and Chang (1968) to the 'q' transformation and the situation where the pollutant has spread to the banks. The relation equivalent to Equation 2.13 is

$$\frac{d\sigma^2}{dx} = \frac{2D_z}{Q^2} (1 - (1-\mu)c'[R] - \mu c'[L]) \quad (2.25)$$

where  $\sigma^2$  is the variance of the  $c'$ - $\eta$  distribution at any section,  $\mu$  is the first moment with respect to the left bank ( $\eta=0$ ) and  $c'[R]$  and  $c'[L]$  are the right and left bank dimensionless concentrations. Integrating Equation 2.25 with respect to  $x$  gives

$$\begin{aligned} \sigma^2 &= \frac{2D_z}{Q^2} \int_0^x (1 - (1-\mu)c'[R] - \mu c'[L]) dx \\ &= \frac{2D_z}{Q^2} I \end{aligned} \quad (2.26)$$

A plot of  $\sigma^2$  versus  $I$ , calculated from measured concentration distributions, should therefore give a linear plot through the origin. The mixing coefficient may then be



calculated from the slope of the best fit line to the plot using a rearranged form of Equation 2.21 given by Beltaos (1979,1980) as

$$E_z = D_z / \psi V H^2 \quad (2.27)$$

where  $\psi$  is a reach-averaged 'shape-velocity factor' given by

$$\psi = \int_0^1 \left[ \frac{h}{H} \right]^3 \left[ \frac{u}{V} \right]^2 d \left[ \frac{z}{W} \right] \quad (2.28)$$

This shape factor may be determined for each section from measured channel geometry and measured or estimated velocities.

An excellent review of transverse mixing theory, past investigations, applications, field procedures and results is presented by Beltaos (1979,1980). The value of  $E_z/HV^*$  for the studies of natural streams reported ranged from 0.18 to 7.20. Some of the field investigations described utilize the concept of dosage to derive a value of transverse mixing coefficient from a slug injection of tracer (time dependent mixing). Dosage is defined as the time integral of depth-average concentration at a given location downstream of a slug injection, ie.

$$\theta = \int_0^{\infty} c \, dt \quad (2.29)$$







where  $\theta$  is the dosage. Beltaos (1975) showed that the variation of dosage downstream of a slug injection is analogous to that of concentration downstream of a steady-state injection.

Although the transverse mixing coefficient may be determined from tracer tests uncertainty remains as to the best method of predicting its magnitude from channel and flow characteristics. The following form of the empirical expression defining the transverse mixing (diffusion) coefficient, first proposed by Elder (1959), is generally accepted.

$$E_z = \beta \ell V^* \quad (2.30)$$

However, some debate remains as to the most appropriate parameter to use as a length scale,  $\ell$ , in the relationship. Most investigators have used a vertical length scale such as  $H$ , as proposed by Elder, or  $R$ . As noted earlier Fischer (1967b) recognized the length scale of turbulence is restricted by boundaries in the vertical direction and thus in large natural channels the mixing due to larger scale lateral eddies is very significant. Wide variations in the values of dimensionless mixing coefficients, even for straight rectangular channels, are reported in the literature. Lau and Krishnappan (1977), in an attempt to explain these variations, used dimensional analysis to identify the functional relationship for the dimensionless



mixing coefficient in a straight rectangular channel

$$E_z/\omega V^* = \text{func}(f, W/H) \quad (2.31)$$

where  $f$  is the friction factor (bed shear) and  $W/H$  the width to depth ratio (aspect ratio) of the channel. Lau and Krishnappan's analysis of straight rectangular flume experiments indicated the dominant mechanism involved in transverse mixing is lateral secondary circulation (created by variable bed shear) which may be characterized by aspect ratio. Considering secondary circulation the dominant mechanism they suggest the product  $HV^*$ , which characterizes the magnitude and vertical scale of turbulence created by the boundary shear, is undesirable as a scaling factor for  $E_z$ . They consider  $WV$  or  $WV^*$ , which characterize the magnitude and lateral scale of turbulence, to be more appropriate. A plot of  $E_z/WV^*$  versus  $W/H$  formed a near single curve, with only minor influence of friction factor. In comparison a plot of  $E_z/HV^*$  versus  $W/H$  had considerable scatter. Lau and Krishnappan therefore suggest that non-dimensionalizing  $E_z$  with  $WV^*$  is the best method.

In a similar study of natural stream data Lau and Krishnappan (1981) identified secondary circulation due to stream curvature' as a third major mechanism contributing

-----  
' The pronounced effect of stream curvature on the magnitude and variability of the transverse mixing coefficient has been studied by several investigators. A summary of studies on this subject is presented by Beltaos (1979).





to transverse mixing. Considering the variability of river bend occurrence, shape, and radius Lau and Krishnappan considered channel sinuosity<sup>1</sup>,  $S_n$ , a rough measure of channel curvature more appropriate than a rigid measure such as bend radius. The functional relationship for dimensionless coefficient in natural channels may therefore be expressed as

$$E_z/WV^* = \text{func}(f, W/H, S_n) \quad (2.32)$$

Following their method of analysis for rectangular laboratory channels, values of  $E_z/WV^*$  versus  $W/H$  were plotted for reported results of transverse mixing tests in natural channels. This plot is reproduced in Figure 2.5. Only tests which determined  $E_z$  with a separate consideration of transverse velocities, either using a generalized method of moments analysis as presented by Holley et al. (1972) or the streamtube model of Yotsukura and Cobb (1972), were considered.

Streams of estimated sinuosity near 1.0 plotted on a single curve slightly above the laboratory results for straight rectangular channels. This would be expected due to the larger secondary currents present in the natural streams. Lau and Krishnappan again noted the boundary friction factor appeared to have little influence in

-----  
<sup>1</sup> Sinuosity is defined as the ratio of thalweg length and down valley distance, the thalweg being the line of peak flow intensity along the channel length.



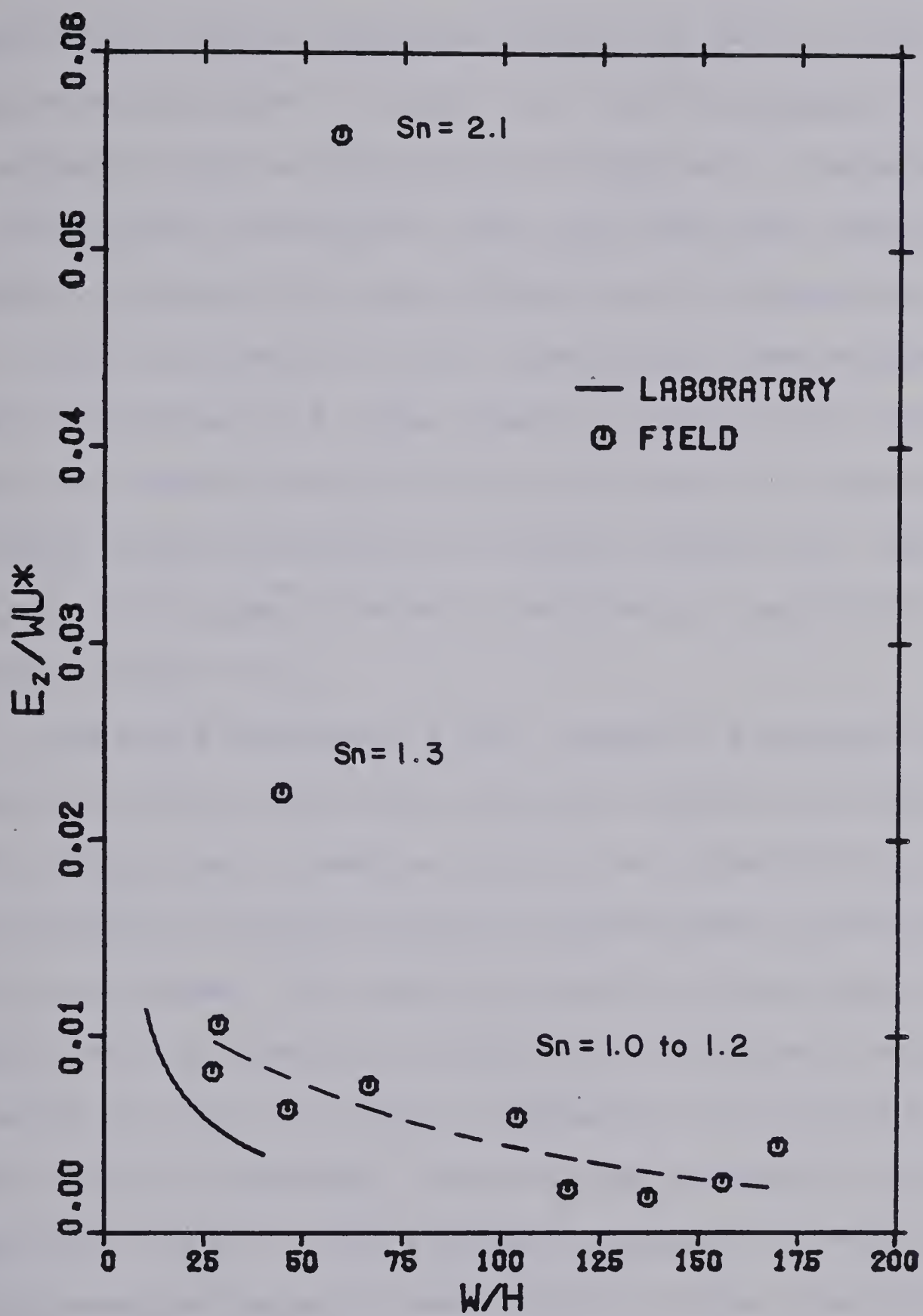


Figure 2.5 Dimensionless Mixing Coefficient versus Aspect Ratio  
—adapted from Lau and Krishnappan (1981)





comparison to  $S_n$  or  $W/H$ . Two points of larger value of  $S_n$  plotted well above the curve defined by points of  $S_n$  approximately equal to unity. Lau and Krishnappan concluded a parameter such as sinuosity is important in determining  $E_z$  for natural streams but felt more data was required before any empirical relationship may be formulated.

Smith and Gerard (1981) essentially demonstrated the same dependence of  $E_z$  upon channel curvature by listing measured dimensionless mixing coefficients for natural streams ranked according to stream irregularity. The streams with higher channel irregularity consistently had higher values of  $E_z$ .

Lau and Krishnappan (1981) recently presented an implicit finite difference numerical modelling scheme utilizing the streamtube concept and specifically suited to analysis of steady-state two-dimensional transverse mixing problems.<sup>1</sup> The model was used to investigate the sensitivity of numerical solutions to different averaging schemes for the term  $uh^2E_z$  of Equation 2.20. Solutions for five different schemes, including the assumption of the applicability of a flow-averaged constant  $D_z$ , were obtained using measured geometry and velocity of the Grand River. A comparison of the numerical solutions obtained for a side injection to the measured concentration distributions indicated the most accurate simulations could be obtained

-----

<sup>1</sup> The modelling scheme of Lau and Krishnappan (1981) first proposed by Stone and Brian (1963) was adapted for use in the study described in the following chapters. Details of the modelling scheme are given in Appendix VI.



using local values of  $uh^2$  and a constant  $E_z$  at each section, although  $E_z$  could vary from section to section along the reach.

Lau and Krishnappan (1981) noted their study results were not in agreement with Yotsukura and Cobb (1972) who suggested the transverse variation in  $uh^2E_z$  had little effect upon numerical solutions. Lau and Krishnappan concluded a constant term may only be satisfactory for central stream region injections where local values of  $uh^2E_z$  would be closely approximated by the flow-averaged value given by Equation 2.21. Maximum concentration gradients for central region injections coincide with an area of small variation in  $uh^2E_z$ . Near the banks large variations in  $uh^2E_z$  occur and local values would be poorly represented by a flow-averaged value. Maximum concentration gradients for side injections occur within this area of poor representation of  $uh^2E_z$  causing significant solution errors.

The possibility of this type of error was first recognized and demonstrated by Holley, Siemons, and Abraham (1972). Recently Smith and Gerard (1981) found the analysis of a shore attached effluent plume occupying less than 20 percent of the channel flow of an extremely wide river indicated a value of mixing coefficient inconsistent with previously published data. The discrepancy was believed to be due to the assumption that a constant  $uh^2E_z$  term accurately represented the small plume region.



The effects of an ice cover on transverse mixing was investigated by Engmann and Kellerhals (1974). They suggested stream mixing capacity (ie.  $E_z$ ) is reduced under an ice cover, but the dimensionless coefficient,  $E_z/RV^*$ , remains relatively constant. Other ice covered mixing studies reported by Beltaos (1979, 1980) also indicated  $E_z$  is reduced, however the value of  $E_z/RV^*$  was inconsistent and was as much as two and one-half times those for open water tests in the same reach. Beltaos (1979) suggested the decreased mixing capacity may be due to a reduction in the transverse velocities associated with the helical motion at stream bends. Considering the results of Lau and Krishnappan the reduced mixing capacity is apparently the result of the increased aspect ratio under an ice cover which, among other things, could be expected to reduce the transverse velocities at bends as suggested by Beltaos. However with present knowledge the effect of an ice cover on the value of dimensionless  $E_z$  must be considered rather indefinite.

Although understanding of the transverse mixing process has improved substantially since Elder's first open channel experiments, extrapolation of field results from one location to another remains difficult. Numerical or analytical predictions based upon estimated coefficients may be adequate as first order approximations, however, uncertainty as to the actual value of transverse mixing coefficient requires tracer tests for accurate assessments







of plume characteristics. Beltaos (1979) suggests at least two to three tests are required to define the variation of transverse mixing coefficient and mixing capacity over the range of flow conditions along the stream reach of interest.

## **B. Microbial Self-Purification**

### **Ohio River Study**

Probably the first comprehensive study of natural stream purification was conducted on the Ohio River by the United States Public Health Service. The study included hydrometric surveys, pollution source identification and chemical and bacteriological water quality studies. Frost and Streeter (1924) described the results of the three year bacteriological self-purification portion of the study.

Frost and Streeter demonstrated the existence of natural bacterial self-purification within the Ohio by a simple analysis of the conservation of numbers of organisms present within the river. Although self-purification is easy to identify they point out the natural process is difficult to study because a river reach free from tributary dilution effects or additional bacterial pollution sources is required for sampling. A reach of the Ohio River downstream of Cincinnati, which was relatively free from interferences, with the majority of effluent continuously discharged along a single bank, was chosen for



analysis. Preliminary observations by Frost and Streeter indicated die-off of total coliforms<sup>1</sup> could be broadly grouped into the following two seasonal periods

- a. a 'summer period', April to November, representing water temperatures of 8° to 27° C, and
- b. a 'winter period', December to March, representing water temperatures of about 1.5° to 4.7° C in which a notable reduction in die-off rate was evident.

They also found the maximum section-averaged coliform count generally occurred downstream of the effluent source and proposed several possible explanations:

- a. coliforms actually reproduce in the river,
- b. disintegration of clumped bacteria masses allows correct enumeration counts downstream of the source, or
- c. sampling errors due to incomplete mixing of the effluent causes an apparent increase in numbers.

Frost and Streeter observed a slow, but progressive lateral spread of the effluent plume within their study reach. Sampling at various depths confirmed that mixing occurred rapidly in the vertical, however, they speculated large sampling errors could occur in section means due to incomplete transverse mixing. The sampling cross section areas had each been divided into thirds, each of which were represented by a single sampling point located at its centre. Frost and Streeter recognized that until the edge

-----

<sup>1</sup> Coliform content was actually reported as concentration of *B. coli* according to the test methods of that period.



of the effluent plume extended fully across an area represented by one of the sampling points, the mean coliform count for that area, measured at the point, would underestimate the actual count. They concluded from this:

- a. sampling errors in the upper portion of the study reach would generally underestimate the section-mean coliform count, and
- b. the magnitude of this error would decrease with distance as the mixing becomes more uniform.

Uncertain of the reliability of data in the upper portion of the reach Frost and Streeter decided to analyse their data based upon two separate approaches:

- a. accept the data as correct and observe the coliform changes as a function of flow time from the effluent source, and
- b. discount the increase in coliform count as sampling error and only observe the coliform changes as a function of flow time from the point of maximum mean-sectional count.

Analysis based upon the first approach indicated a peak concentration occurring about 10 to 15 hours of flow time downstream of the effluent source under summer conditions. The peak was followed by a rapid decrease in coliform count with increasing flow time. The winter data was more variable but indicated the same general trend. Frost and Streeter attempted to model the coliform population using the relationship





$$P = \frac{b_0}{1 + (d_0 t + f_0)e^{a_0 t}} \quad (2.33)$$

where  $P$  is percentage of the maximum coliform count,  $t$  is the flow time from the source, and  $a_0$ ,  $b_0$ ,  $d_0$  and  $f_0$  are empirical constants. Fitting a curve to the measured data using Equation 2.29 gave only moderate success. Considering the uncertainty of the mechanism creating the peak or in fact its actual existence modelling of this form was not pursued further.

Analysis based upon the second approach indicated the coliform die-off following the peak could be modelled using a relationship of the form

$$P = a_0 e^{-k_1 t} + b_0 e^{-k_2 t} \quad (2.34)$$

where  $P$  and  $t$  have the same definition as for Equation 2.33,  $a_0$  and  $b_0$  are empirical coefficients, and  $k_1$  and  $k_2$  are decay coefficients for base  $e$  logarithms. Equation 2.34 is simply an extension of the single term first order reaction proposed by Chick (1908, 1910) to describe bacterial die-off under unfavourable environmental conditions. Chick's Law may be stated as:

$$N = N_0 e^{-kt} \quad (2.35)$$

where  $N$  is the bacterial concentration after time  $t$ ,  $N_0$  the initial microorganism concentration at  $t = 0$ , and  $k$ , the





decay coefficient for natural logarithms.

Frost and Streeter formulated Equation 2.34 with two terms after observing the shape of  $\log P$  versus  $t$  plots which consisted of an initial declining linear region, a transition zone and a final declining linear region. They suspected the shape of the curve was due to the presence of two dominant strains of coliforms each with a different decay coefficient.

The coefficients  $a_0$  and  $b_0$  represent the estimated initial proportion of each coliform strain composing the total coliform population. The relationship could be expressed as a series of exponential terms, each representing a distinct coliform strains, however, such complexity was not necessary considering the two phase appearance of the decay curves. Frost and Streeter also indicated the decline in decay rate, after some initial period, may be a function of the bacterial concentration itself in which case the extended die-off would have to be described by an equation of different form.

The average die-off of total coliforms during the summer period was satisfactorily modelled by Equation 2.34 using  $a_0 = 99.51$ ,  $k_1 = 1.08/\text{day}$ ,  $b_0 = 0.49$ , and  $k_2 = 0.134/\text{day}$ . The winter data was quite variable and indicated a slight increase in coliform concentrations for higher river stage. Frost and Streeter felt this was the result of sampling errors and omitted several sections from their analysis. Declining curves were sketched for the



winter data but no attempt was made to mathematically fit a curve due to the uncertainty associated with the points. Phelps (1944) later estimated the winter coefficients for Equation 2.34 using Frost and Streeter's data as  $a_0 = 97.0$ ,  $k_1 = 1.17/\text{day}$ ,  $b_0 = 3.0$  and  $k_2 = 0.06/\text{day}$ . The value of  $k_2$  for winter conditions compared to the summer indicates coliforms tend to persist much longer for cold water conditions. The curves formulated using Equation 2.34 are shown in Figure 2.6.

Frost and Streeter cautioned that the above formulation for summer data and the curve for winter data would not represent all rivers in general or even the Ohio under all conditions. They speculated that in some situations Equation 2.34 may consist of a series of first order terms each representing an individual coliform strain. A subsequent investigation of a reach of the Ohio above Cincinnati indicated a much slower rate of coliform decline. However, Frost and Streeter did not consider this unusual because the effluent source was some distance upstream of the reach and the coliform population would have been in the latter stages of decline during sampling.

### Other Investigations

Hoskins (1925) presented the results of bacterial self-purification studies of the Upper and Lower Illinois River which indicated the same general trends as the Ohio River study. Hoskins made no mathematical formulation of



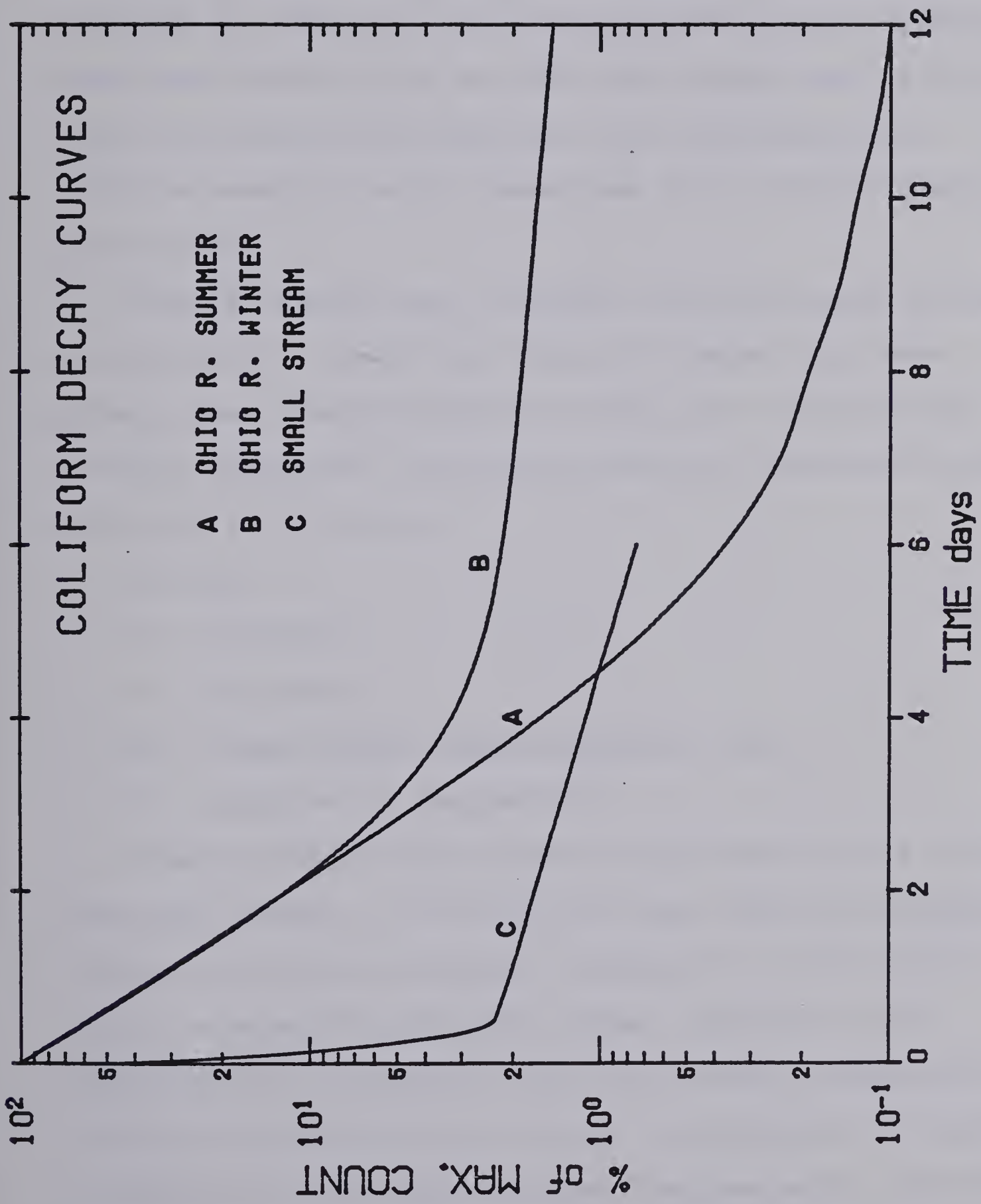


Figure 2.6 Coliform Decay Curves from Early Studies  
 -data from Phelps (1944), Kittrell and Kochtitzky (1947)





the die-off curves but noted that if actual average bacterial counts in the river were plotted against flow time the results for the Ohio and Illinois were in good agreement. Hoskins also made the important observation that although raw effluent coliform concentrations are generally a minimum during winter periods the reduced rate of die-off within the receiving stream may cause maximum yearly coliform counts to occur downstream of an outfall during this period.

Several factors may influence coliform growth or death rate within a stream. The effects of temperature have already been demonstrated by the Ohio and Illinois River studies. Additional contributing factors cited by Kittrell and Furfari (1963) are:

- a. pH,
- b. turbidity,
- c. nutrients,
- d. stream channel characteristics, and
- e. predation by zooplankton.

The optimum pH for growth of coliforms is well within the normal range of 6.7 to 8.3 for most natural streams and therefore pH is generally not considered a significant factor in determining die-off rates. Streeter (1934) speculated that turbidity could contribute to a decline in coliform concentration as a result of adsorption of cells to particle surfaces and subsequent sedimentation. Nutrients for coliform growth are abundant in sewage effluent,



however, dilution within the receiving stream may reduce nutrient concentrations to limiting levels causing die-off due to starvation.

Kittrell and Kochtitzky (1947) investigated natural purification in a small, shallow, turbulent stream and compared the results to the Ohio River summer period. They found coliform bacteria declined much more rapidly in the small stream than in the larger and deeper Ohio River. A best fit curve to their data (see Figure 2.6) was given in the form of Equation 2.34 with  $a_0 = 97.5$ ,  $k_1 = 15.2/\text{day}$ ,  $b_0 = 2.5$  and  $k_2 = 0.20/\text{day}$ . Kittrell and Furfari (1963) felt this extremely high purification rate may be due to the presence of shallow riffle areas with bed attached biological growth containing coliform predator species. Increased exposure to sunlight due to shallow water depth may also contribute significantly.

Predation of coliforms by zooplankton, especially protozoa, was established as a major contributor to coliform death rates in sewage effluent by Purdy and Butterfield (1918). Predation is generally believed to be the major factor in bacterial self-purification of streams. The predator-prey relationship of protozoa and coliforms is also closely associated with the question of coliform growth within natural streams following discharge (often termed aftergrowth) and will be further discussed below.

Early attempts had been made during the Ohio River study to investigate coliform die-off in laboratory batch



tests. However, it was discovered coliforms initially increased in numbers in laboratory containers even if samples were taken from portions of the river reach where coliforms were declining. Butterfield (1933) conducted a number of jar tests on polluted Ohio River water and effluent samples under varying environmental conditions. His objective was to determine what factors cause or modify the characteristic growth-death curve observed by Frost and Streeter (1924). Butterfield's results indicated temperature and removal of sediments had pronounced effects upon the time to and magnitude of peak coliform concentration and subsequent death rate in the jar tests. He concluded changes in environmental conditions existing in the river at the time of sampling could allow temporary coliform growth within the samples. He further speculated the peak in coliform numbers would increase with the extent of the disturbance.

With this conclusion in mind Hoskins and Butterfield (1933) investigated the effect of dilution of polluted water on changes in coliform population. An increase in section-average coliform count of the Illinois River below its confluence with the unpolluted Kankakee River was cited as an indication that dilution temporarily caused conditions favourable for coliform growth. Jar tests of varying dilutions of sewage effluent and Illinois River samples were conducted and indicated increasing dilution ratio corresponded to higher peak concentrations. Hoskins





and Butterfield concluded the dilution temporarily disrupted the predator-prey relationship between protozoa and coliforms, apparently reducing coliform concentrations to a level limiting to protozoa growth. Rapid regeneration allow the coliforms to reproduce to a peak concentration before the slower responding protozoa increase in numbers. As the protozoa population increases coliforms decline due to predation and subsequently both populations continue to decline as nutrients become limiting.

Hoskins and Butterfield's explanation appears convincing but has not been universally accepted.

Phelps (1944) stated:

"It is hardly to be believed that there is actual multiplication of intestinal organisms in the streams themselves, although this possibility cannot, with present knowledge, be entirely eliminated."

Regarding jar tests it seems unlikely that an instantaneous complete mix batch test can adequately simulate the continuous and progressive dilution which occurs in a natural stream. Additionally jar tests can not account for coliform consuming zooplankton which may be encountered along the stream as identified by Kittrell and Furfari (1963). Without the total elimination of sampling errors due to inaccurate consideration of dilution, clumping of bacteria and variability of enumeration data it is unlikely the question of coliform aftergrowth will ever





be conclusively resolved.

After the work of Kittrell and Kochtitzky (1947) there is a marked lack of literature on bacterial self-purification of natural streams until Kittrell and Furfari (1963) presented an excellent review of all the early investigations. Kittrell and Furfari also included the results of several more recent studies for which the declining phases are shown in Figure 2.7. The results shown are in general agreement with those reported for the Ohio and Illinois Rivers.

Methods to enumerate coliform bacteria of strictly fecal origin were introduced in the 1960's. Ballentine and Kittrell (1968) reported the results of numerous short duration bacterial self-purification studies which included data for both total and fecal coliforms. They pointed out a drawback of total coliforms as an indicator of fecal contamination was the common occurrence of coliform group members in the natural environment. High densities of total coliforms in aquatic environments may not be solely the result of effluent discharges. Ballentine and Kittrell prepared composite decay curves for fecal coliforms under winter and summer conditions using 15° C water temperature as the dividing criteria. The curves are shown in Figure 2.8 and indicate die-off of fecal coliforms under winter conditions is significantly less than during the summer as was observed earlier for total coliforms. A plot of the ratio of fecal coliforms to total coliforms is shown in



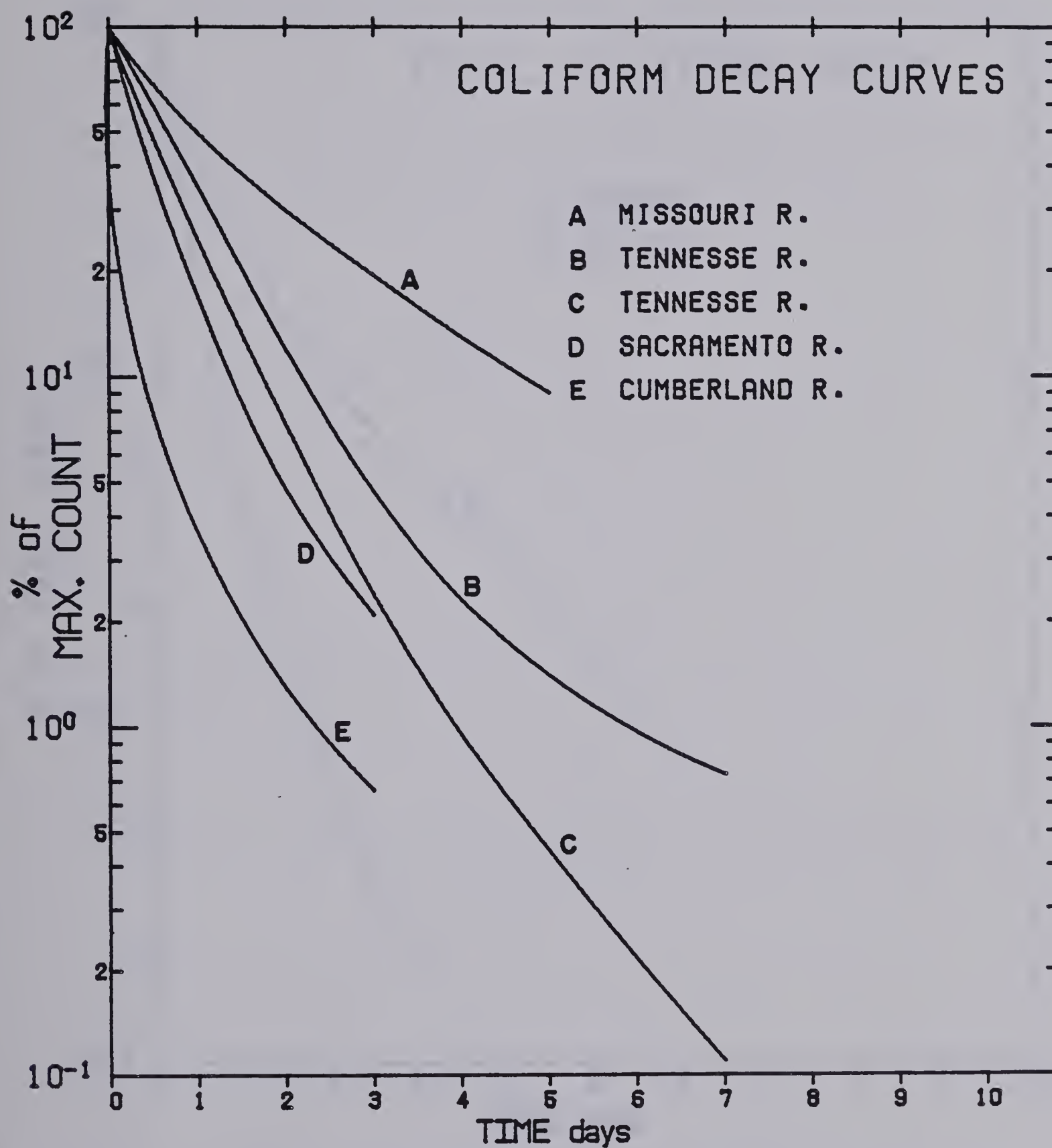


Figure 2.7 Several More Recent Coliform Decay Studies  
-adapted from Kittrell and Furfari (1963)



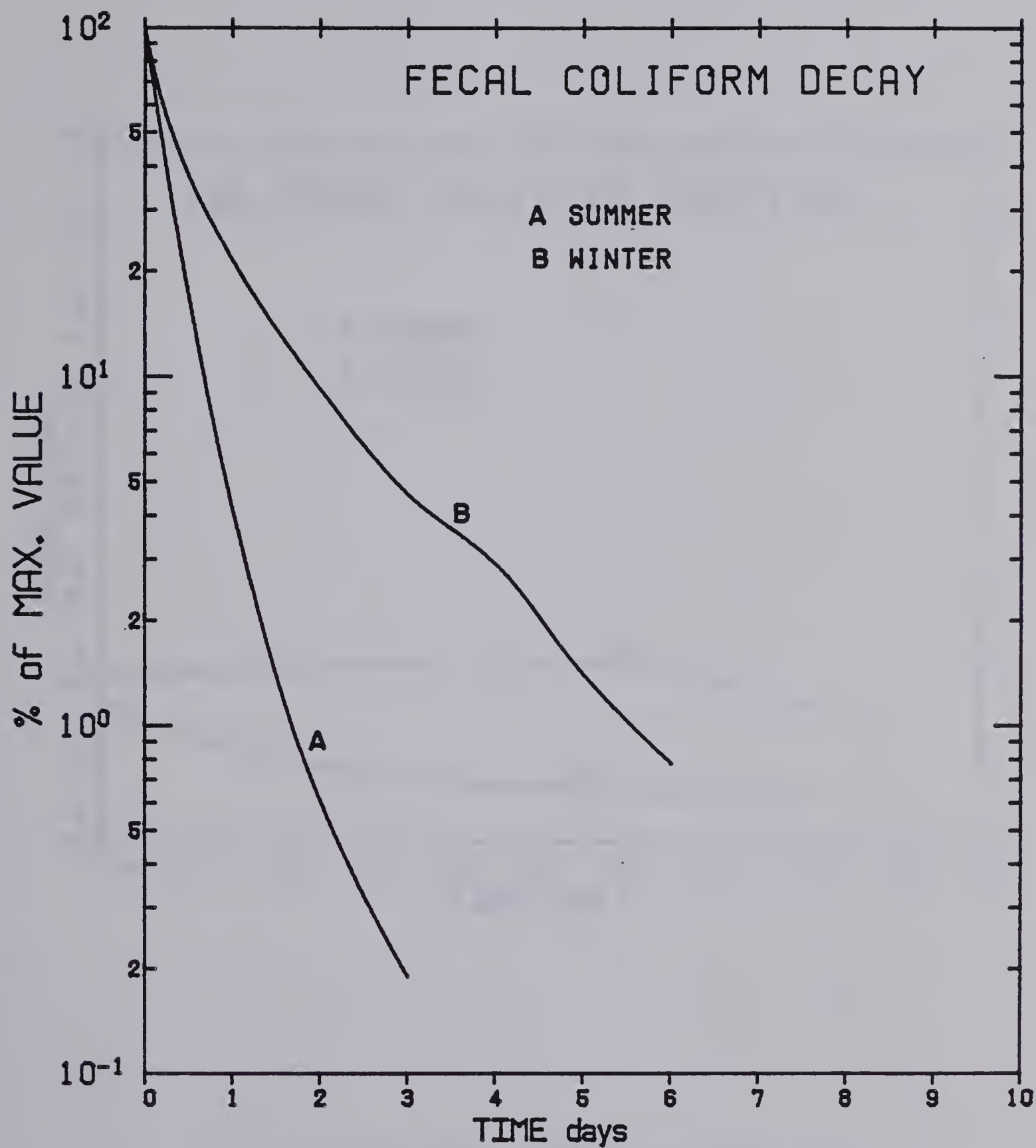


Figure 2.8 Fecal Coliform Composite Decay Curves  
-adapted from Ballentine and Kittrell (1968)





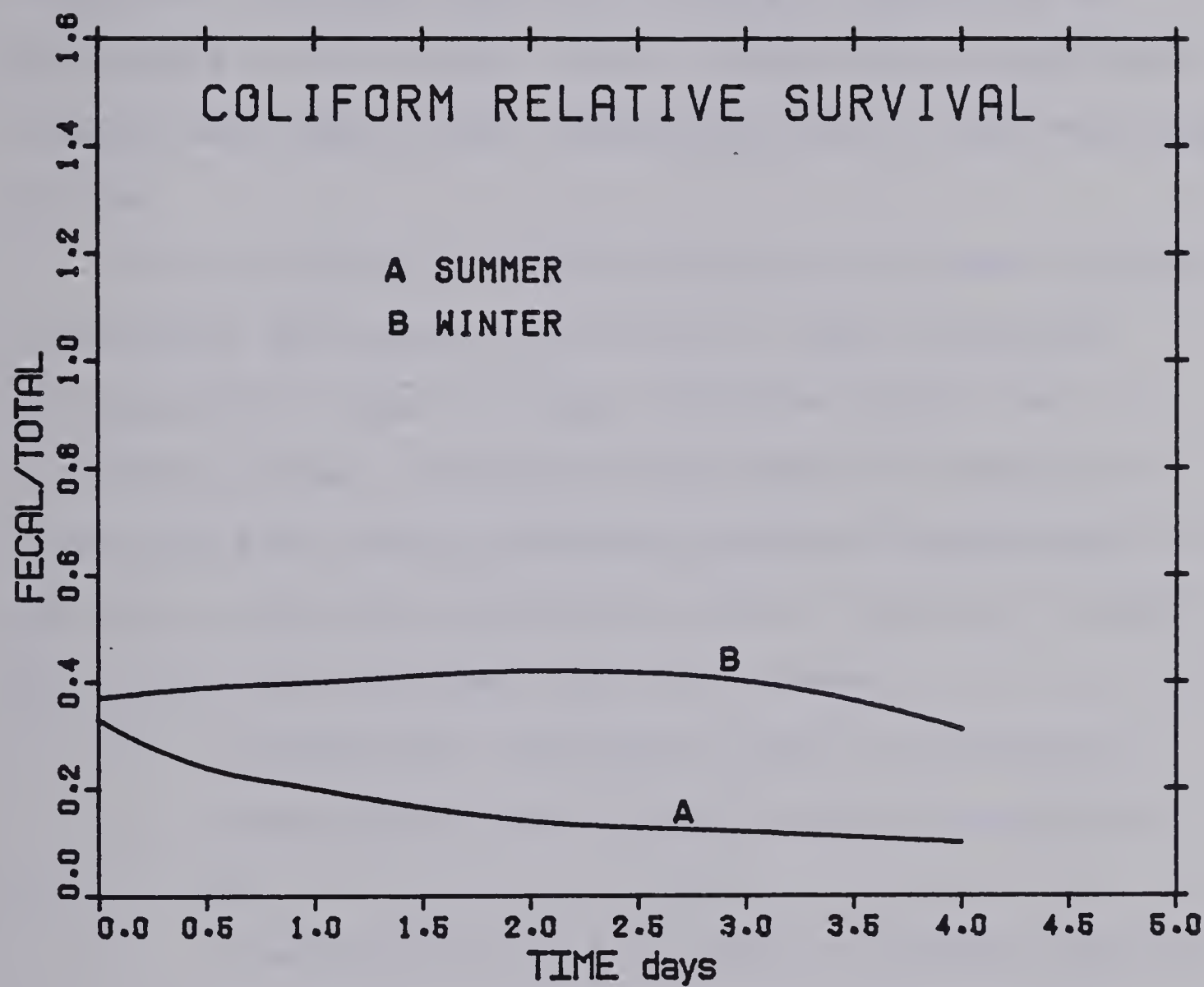


Figure 2.9 Fecal Coliform Ratio versus Flow Time  
-adapted from Ballentine and Kittrell (1968)



Figure 2.9 which indicates fecal coliforms generally tend to die-away faster than total coliforms. Ballentine and Kittrell speculated this was due to specific nutritional requirements in comparison to other coliforms. They also noted that although fecal coliforms are assumed to be indicators of very recent fecal contamination significant numbers may remain after extended periods in the receiving stream.

It is interesting to note only one of eleven surveys reported by Ballentine and Kittrell (1968) indicated aftergrowth of total or fecal coliforms within the receiving stream. A study with the specific objective of identifying any fecal coliform aftergrowth downstream of an effluent source was conducted by Deaner and Kerri (1969). The study was significant for two reasons:

- a. no significant regrowth of fecal coliforms was evident within the 5 hours of flow time sampled, and
- b. a fluorescent tracer was used to identify suitable locations for truly representative sampling within a reach where mixing was incomplete, thus, substantially eliminating many of the sampling errors.

Deaner and Kerri (1969) recommended the use of tracer studies as general practice for all bacteriological sampling programs as a means of obtaining more representative samples.



As discussed previously Frost and Streeter (1924) formulated expressions to model coliform populations within the Ohio River. Equation 2.33 describes the entire curve including regrowth while Equation 2.34 describes only the declining limb from the peak concentration. Streeter (1934) formulated an exponential expression similar to Equation 2.34 which describes the entire curve:

$$N = (N_0 - a_0)e^{-k_1 t^n} ((a_0 - b_0)e^{-k_2 t} + b_0 e^{-k_3 t}) \quad (2.36)$$

where  $a_0$  and  $b_0$  are constants representing the ordinate intercepts of the linear portions of the declining phase of the curve and  $n$  is a constant defining the sharpness of the peak of the curve. Equation 2.36 is written for two major fractions of the coliform population but may be expanded further to include several fractions.

Fair and Geyer (1956) proposed the following expression for the declining phase

$$N = N_0 (1 + n f_0 t)^{-1/n} \quad (2.37)$$

where  $n$  and  $f_0$  are empirical coefficients.

Velz (1970) suggested that the decline of the dominant species fraction was of the most significance in practical applications of self-purification and proposed the process could be satisfactorily represented using Chick's Law (Equation 2.35). Velz fitted straight lines to the initial





decline of coliforms reported in the studies of Frost and Streeter (1924), Hoskins (1925), Kittrell and Furfari (1963) and several other unreported studies. The decay coefficient  $k$  (for natural logarithms) ranged from 0.60 to 1.06/day for winter tests and from 1.15 to 2.21/day for summer tests.

Mahlock (1974) compared several deterministic and statistical models for predicting fecal and total coliform concentrations downstream of a continuous effluent source. Results of the comparative analysis for the river studied indicated the total coliform population may be successfully modelled using Chick's Law, while the fecal coliforms were more successfully modelled using a statistical scheme. Mahlock presumed a statistical scheme using environmental parameters was more successful in modelling fecal coliforms since they are more susceptible to environmental changes. Although statistical schemes may be superior for modelling fecal coliforms Mahlock points out deterministic schemes such as Chick's Law are at present preferred for prediction purposes since they are easier to implement, not requiring a large data base of independent environmental parameters.

An alternative method of studying microbial survival is with the use of membrane filter chambers. The chamber allows the free exchange of stream water and nutrients through its membrane sidewalls but prevents movement of microbes in or out of the system. Survival studies using membrane filter chambers are satisfactory for





investigations of the effects of environmental factors such as temperature, pH, nutrient levels or predation within an isolated mixed culture. They can not however simulate the effects of predation by zooplankton within the receiving stream or the progressive dilution due to mixing.

McFeters and Stuart (1972) investigated the survival of *E. coli* in natural water in the field and laboratory using membrane filter chambers. In particular they studied the effects of temperature and pH in the laboratory using a continuous flow through apparatus. Optimum survival occurred in the range of pH 6 to 8. The dramatic effect of temperature is shown in Figure 2.10 where the half-life is the time to 50% reduction in population. The sharp increase in survival below 15° C offers support to the reduced death rates observed during winter periods in stream surveys. Considering the retarding effect of reduced temperature on biological activity, presumably predation at lower temperatures will be reduced and temperature itself will become the most important factor effecting coliform survival in cold waters.

Membrane filter chambers have also been used to investigate the short and long term survival of coliforms compared to pathogenic organisms in natural waters. Studies of this type have been reported by McFeters, Bissonnette, Jezeski, Thomson and Stuart (1974) and Dutka and Kwan (1980).



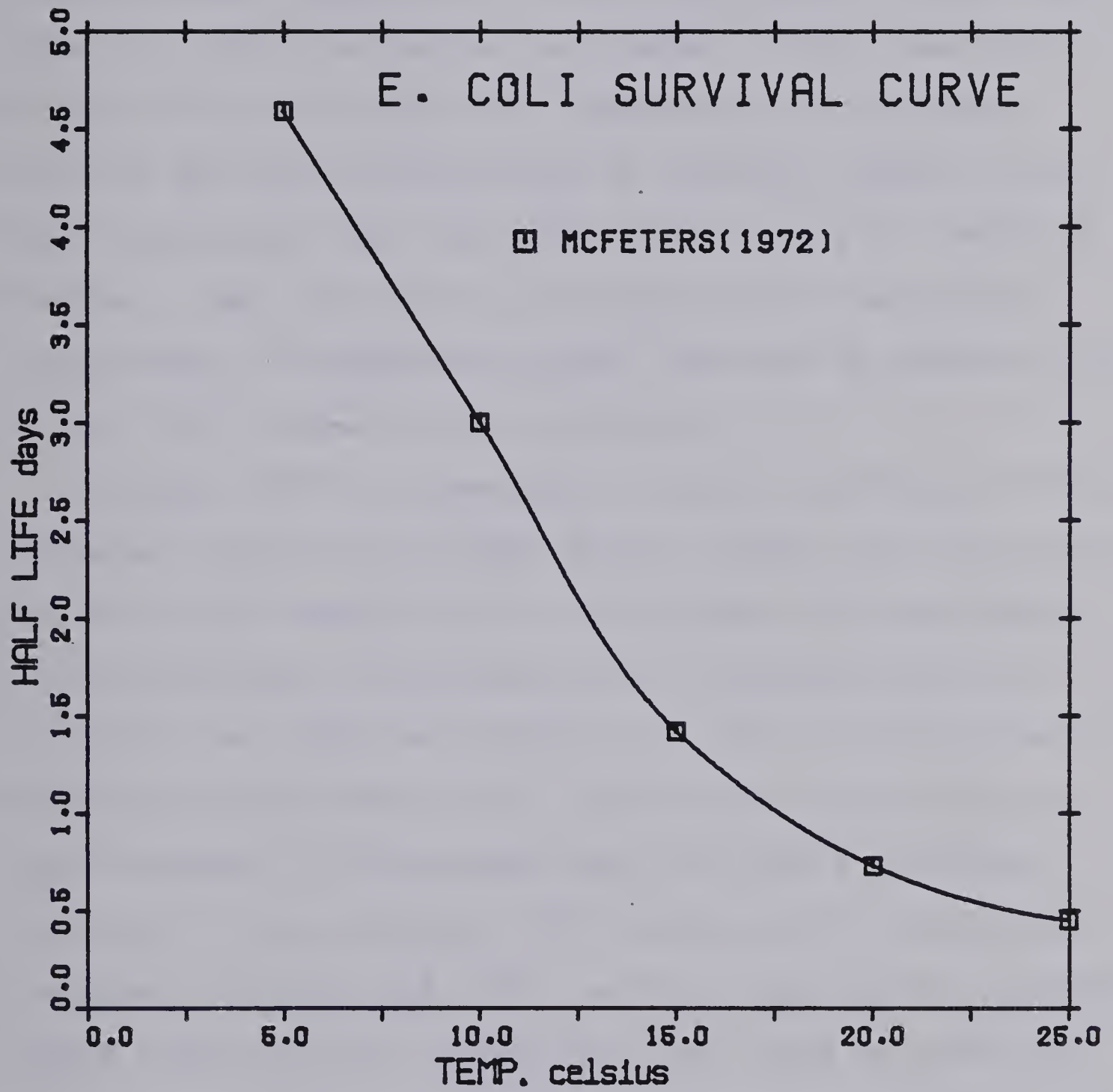


Figure 2.10 *E. coli* Mortality versus Water Temperature  
-adapted from McFeters and Stuart (1972)



The effect of water temperature on coliform survival studies in the field has been demonstrated by arbitrarily dividing surveys into summer or winter periods based upon a dividing water temperature. Frost and Streeter (1924) used about 5° C while Ballentine and Furfari (1968) used 15° C. Gordon (1972) postulated cold temperature microorganism survival may be more pronounced in northern regions, where water temperature may only exceed 15° C for a few weeks of the year, than indicated by extrapolation of decay data from surveys in temperate regions. The work of McFeters and Stuart (1972) supports this hypothesis.

Gordon (1972) and Davenport, Sparrow and Gordon (1976) conducted tests on the Tanana River, Alaska, with ice cover and 0° C water temperature to investigate low temperature coliform survival. The studies were conducted along an isolated river reach equivalent to 7 days of travel time downstream of the Chena River confluence. Sewage effluent from Fairbanks is discharged into the Chena a few miles upstream of the confluence. The results of the two studies are shown in Figure 7.5. Both surveys found higher coliform counts remaining after seven days than would be predicted using decay information from more temperate regions.

Recently Smith and Gerard (1981), in a preliminary study of the Slave River downstream of Fort Smith, N.W.T., reported no significant die-off of indicator organisms was evident within the 18 hours of travel time sampled.





The long persistence of indicator organisms demonstrated by these recent surveys emphasize the concern over the transmission of disease in northern regions. Work by Dahling and Safferman (1979) in conjunction with the Tanana River tests has shown that indicator organisms were not adequate as a consistent quantitative measure of enteric virus concentration in the receiving water. However, they concluded the persistence of fecal coliforms was a definite indication of a risk of viral contamination.

Mancini (1978) derived an empirical relationship to allow prediction of coliform mortality rates on the basis of water temperature, exposure to sunlight and percentage of sea water content. The equation was formulated from previously reported laboratory and field studies for the slope of the initial portion of the declining limb of the decay curve. A simplified version of the equation for fresh water may be expressed as

$$k = 1.84(1.07)^{T-20} + \frac{L}{K_s H} (1 - e^{-K_s H}) \quad (2.38)$$

where  $k$  is the decay coefficient (  $1/d$  ) of Chick's Law for natural logarithms,  $T$  is the water temperature in degrees Celcius,  $L$  is the average daily surface solar radiation in langleys/hr,  $K_s$  is the light extinction coefficient and  $H$  is the completely mixed depth of water. Mancini cautions that Equation 2.38 is only satisfactory for initial



estimates of coliform mortality due to the large scatter of data used in its formulation. Additionally the lethal effects of sunlight have been solely based on data from salt water and have not been verified for fresh water.

### Sample Integrity

An important consideration in all bacteriological surveys is the storage and handling of samples where analysis can not proceed immediately. **Standard Methods** recommends a maximum holding temperature of 10° C and analysis within 8 hours of sampling. Davenport and Gordon (1978) investigated the effects of holding temperature and storage time upon the coliform concentration of primary effluent samples with an original temperature of 9.5° to 10° C. Samples were held at <1°, 5° and 10° C with analysis conducted at 0, 2, 4, 6 and 8 hours. Their results suggest a holding temperature of 5° C or less with analysis within 8 hours is desirable to provide an adequate measure of the original coliform count. Samples held at less than 1° C showed some decreases after 6 hours while those held at 10° C increased in concentration. These results are in good agreement with the minimum growth temperature of *E. coli* of 7.5° to 7.8° C reported by Shaw, Marr and Ingraham (1971) and the increased survival at lower temperatures reported by McFeters and Stuart (1972).



### C. Health Implications

The high occurrence of diseases, which may be transmitted through the water environment, is of great concern in northern Canada. Hrudehy and Raniga (1980) demonstrated the seriousness of the problem with the comparison of disease occurrence in the Northwest Territories, Alberta and Canada as a whole shown in Table 2.1. The high occurrences of these selected diseases in the Northwest Territories can not be proven to be directly attributable to water supply and wastewater disposal, but the figures of Table 2.1 provide very strong circumstantial evidence of a connection.

Martin (1980), in a report on public health in the Northwest Territories, identified several contributing factors in the spread of disease among native populations:

- a. poor personal hygiene due to limited readily available potable water,
- b. casual water consumption due to custom or distinct preference for unchlorinated water, and
- c. lack of knowledge of the causes and methods of transmission of disease.

The serious implications of the long persistence of microorganisms in northern waters is clearly evident when considered in view of the already high disease incidence and other factors contributing to disease transmission. Knowledge and understanding of the long term survival of enteric bacteria and viruses is required for safe





Table 2.1 Comparative Incidence of Several Diseases  
-adapted from Hruvey and Raniga (1980)

Disease	Region	Incidence per 100,000 Population					Ratio to 5 Year National Average
		1975	1976	1977	1978	1979	
Typhoid	Canada	0.58	0.91	0.38	0.45	0.44	N.C.
	Alberta	0.22	-	0.05	0.31	0.20	N.C.
	N.W.T.	-	-	2.3*	2.3*	2.3*	N.C.
Salmonellosis	Canada	12.9	11.9	16.4	28.9	30.4	1.00
	Alberta	14.2	9.7	14.3	43.8	37.1	1.19
	N.W.T.	43.7	18.8	30.0	59.6	97.2	2.48
Shigellosis (Bacillary Dysentery)	Canada	9.7	7.0	5.0	5.0	5.6	1.00
	Alberta	17.7	26.8	13.0	9.4	7.5	2.30
	N.W.T.	1081	479	291	142	396	73.9
Hepatitis Type A	Canada	17.5	15.6	17.9	11.6	6.8	1.00
	Alberta	30.3	29.3	50.5	26.6	13.6	2.17
	N.W.T.	425	418	520	61.9	37.0	21.1
Population thousands	Canada	22 697.1	22 997.1	23 257.6	23 482.5	23 671.5	-
	Alberta	1 778.3	1 838.0	1 896.4	1 952.1	2 008.9	-
	N.W.T.	41.2	42.6	43.3	43.6	43.2	-

\* single case only  
N.C. = not calculated





utilization of receiving streams for waste disposal and the prevention of further outbreaks of water borne disease as development of the north progresses. In this regard microbiological standards for effluent and receiving waters have been incorporated into the recently established **Guidelines for Municipal Type Wastewater Discharges in the Northwest Territories 1981** set by the Northwest Territories Waterboard.



### III. OBJECTIVES

Previous investigations of microbial self-purification have indicated cold climatic conditions generally give the longest periods of indicator bacteria persistence. Northern rivers are ice covered for a significant portion of the year and generally have lower water temperature than rivers in more temperate regions. The characteristics of low water temperature, and isolation from sunlight during ice cover are therefore believed to lengthen microbial persistence in northern rivers. These characteristics, combined with reduced dilution capacity due to concurrent low winter flows, decrease the rate of decline of microbial concentrations. The resultant higher microbial concentrations present an increased risk of disease transmission downstream of effluent outfalls.

The basic objective of this study was to investigate the persistence of indicator bacteria under varying flow and climatic conditions in a northern river. The study includes comprehensive field investigations of river mixing in conjunction with field bacteriological sampling programs under winter ice covered and summer conditions. From these studies the die-off of indicator bacteria can be evaluated, as discussed earlier.

A subsidiary objective was the establishment, with the aid of the field data, of a mixing model for prediction of conservative tracer concentrations downstream of outfalls. Finally, the mixing model was adapted to a non-conservative



parameter (microorganisms) by incorporating a decay term into the numerical scheme.





## IV. FIELD STUDIES

### A. Introduction

An examination of the effluent mixing and microorganism decay characteristics of the Slave River downstream of Fort Smith, Northwest Territories under ice covered and summer conditions was the task of the study described herein. The river reach of interest and its location are shown in Figure 4.1. An aerial view of a portion of this reach, looking downstream over Bell Rock, is shown in Plate 4.1.

Fort Smith, which has a population of approximately 2400, is located on the west bank of the Slave River immediately downstream of the Rapids of the Drowned, the last of a series of rapids stretching upstream for 29 km to Fort Fitzgerald (see Plate 4.2). Domestic sewage from the town is collected and treated in the three cell lagoon system shown in Plate 4.3. The system has a design retention time of about 90 days. Effluent from the lagoon system is continuously discharged to the Slave River through a 350 m long, 250 mm diameter insulated polyethylene pipeline leading to a submerged bank outfall as shown in Figure 4.2.

The mixing characteristics of the river were determined by injecting a conservative tracer at a constant rate into the effluent and measuring the variations in its steady-state concentration downstream of the outfall. The



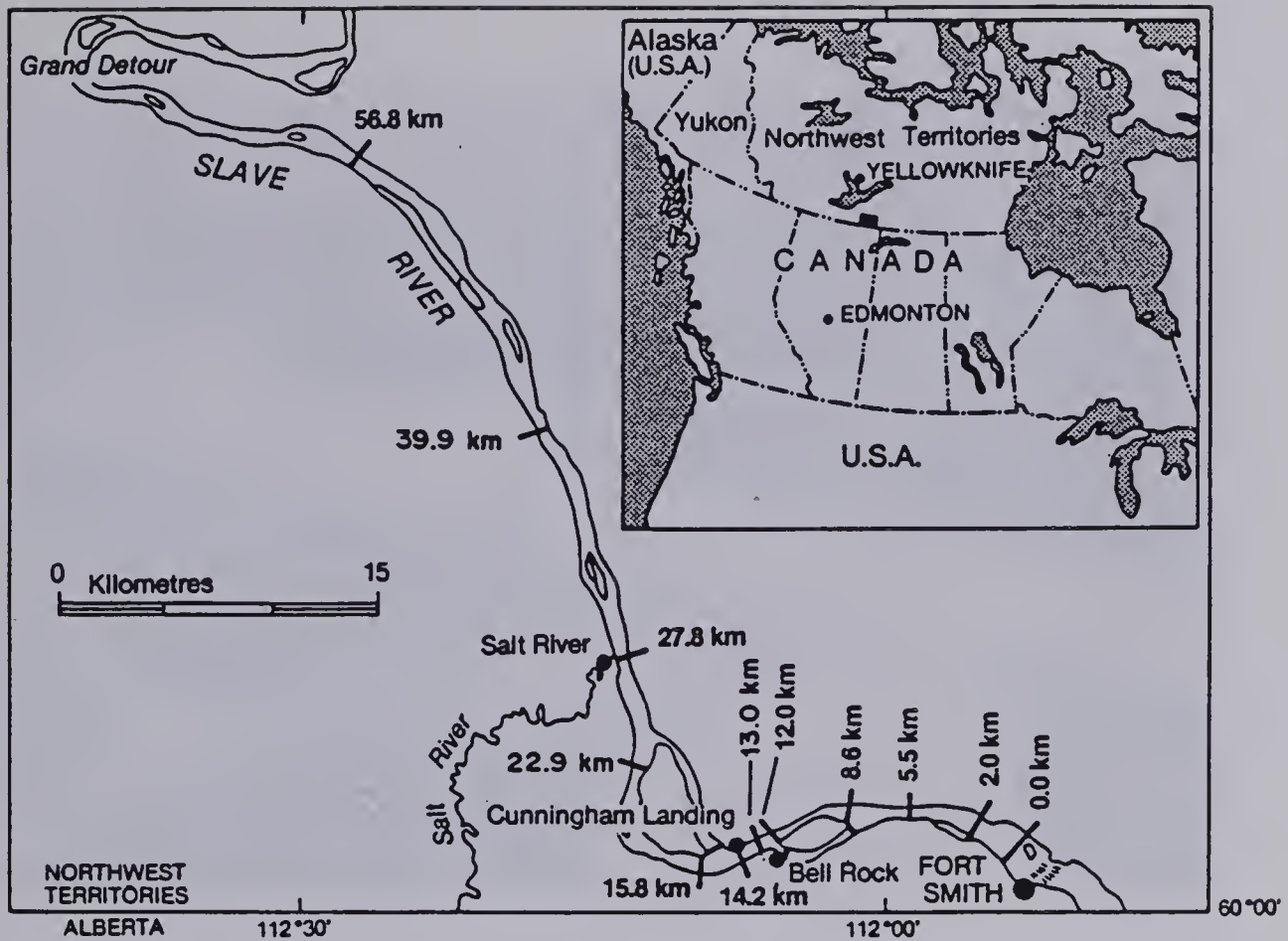


Figure 4.1 Study Location Map  
-adapted from Smith and Gerard (1981)

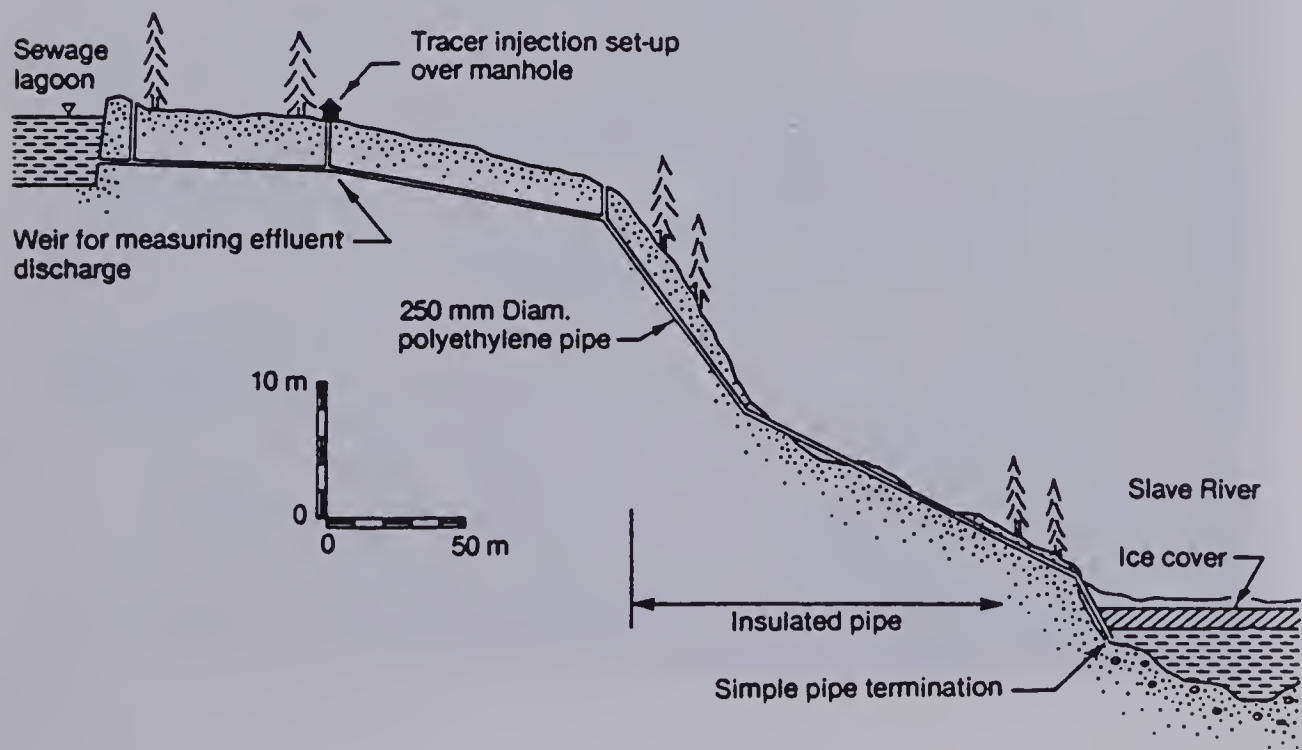


Figure 4.2 Profile of the Lagoon Outfall  
-adapted from Smith and Gerard (1981)





Plate 4.1 Slave River looking downstream over Bell Rock



Plate 4.2 Aerial View of Fort Smith







Plate 4.3 Fort Smith Lagoon System





measured concentration distributions of the conservative tracer represent the effects of physical dilution with no decay. Indicator bacteria concentrations measured at the same sampling locations allowed decreases in number due to decay alone to be isolated when compared to the conservative tracer concentrations.

The first field studies were carried out in March 1980 under ice cover conditions. These were followed by summer studies in July 1980. The results of the March 1980 study were reported by Smith and Gerard (1981). This initial study indicated the rate of spread of the effluent plume in the upper portion of the river reach was much smaller than would be expected. Additionally, die-off of indicator bacteria was not discernable over the entire study reach corresponding to an average residence time of approximately 18 hours following effluent discharge to the river. Because these results were somewhat anomalous and based upon a limited amount of data, ice cover studies were repeated in March 1981 with a more intensive sampling program.

## **B. Surveys**

### **Winter Tests**

Field tests and surveys were carried out during ice cover conditions over the periods of March 17-22, 1980 and



March 15-22, 1981. The spring test periods were chosen to coincide with an interval representative of minimum river flow and sufficiently early in the year to ensure safe ice conditions, yet with a reasonable number of daylight hours for working.

Limited access to the river along the reach, the distances between sections, and time constraints imposed by the sampling and survey program, required the use of several two man teams. Travel along the river reach was predominantly by snowmobile and sled (see Plate 4.4), but several of the most distant sections required sampling by aircraft.

Planning of the initial test of March 1980 was based upon preliminary estimates of the effluent plume characteristics derived from limited information on stream geometry and an estimate of river discharge. Sampling holes were located at each section to attempt to adequately define the transverse concentration profile. The number of holes and their spacing was based upon the estimated plume characteristics and manpower and time considerations.

Unfortunately the lack of detailed information on stream geometry and uncertainty as to the offshore location of the effluent outfall caused several of the sections to have less than satisfactory hole locations. With the benefit of the spring and summer surveys of 1980 the sampling holes for the March 1981 test could be located to provide a much better definition of the tracer





Plate 4.4 Winter River Travel





concentration distributions. In addition several new sections were sampled and surveyed. The location of the sampling sections within the river reach are shown in Figure 4.1.

The sampling holes were drilled using 200 mm diameter power ice augers (see Plate 4.5). Each hole was initially located by estimation and then, after it was drilled, its exact transverse location was measured.

Cross section geometry was determined by measuring the depth to the bottom of the ice and the river bed at each hole. The entire section geometry was measured at each sampling site in March 1980. These are shown in Figure 4.3. The section geometry within the expected plume region only was measured during the March 1981 test; the remainder of the section was determined from the summer 1980 surveys with allowance for stage difference and an average ice cover. These sections are a much more detailed measure of the section geometry than the March 1980 survey and are shown in Figure 4.4.

An estimated depth-averaged velocity distribution within the plume region at each section was required for interpretation of the river mixing characteristics and travel times. Time and manpower constraints prevented taking velocity measurements at each section. Instead velocity measurements at selected cross sections were used to define the relation between depth and depth-averaged velocity for the reach and this relationship used to





Plate 4.5 Drilling Sample Holes



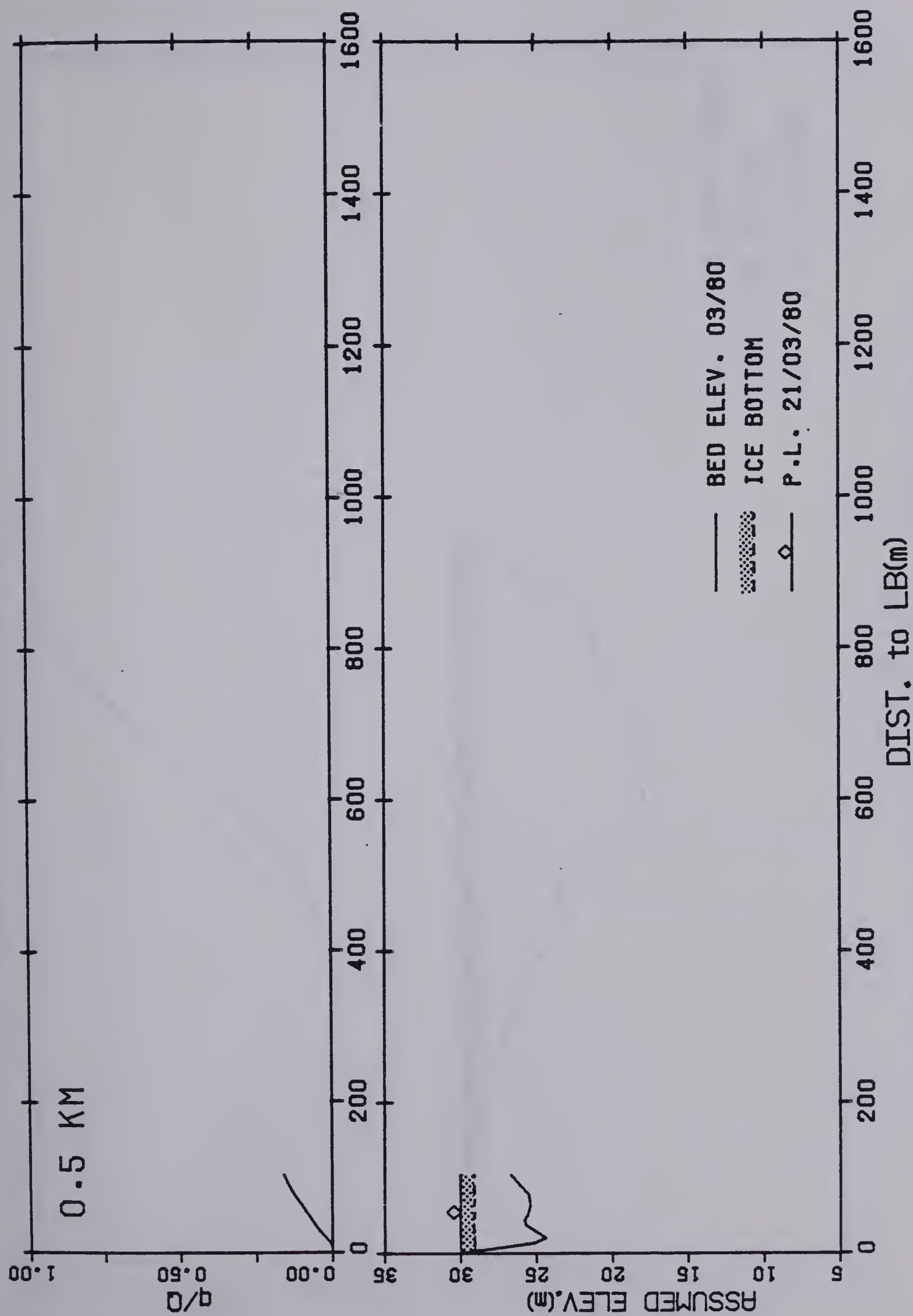


Figure 4.3(a) Cross Section Geometry and Flow Distribution March 1980



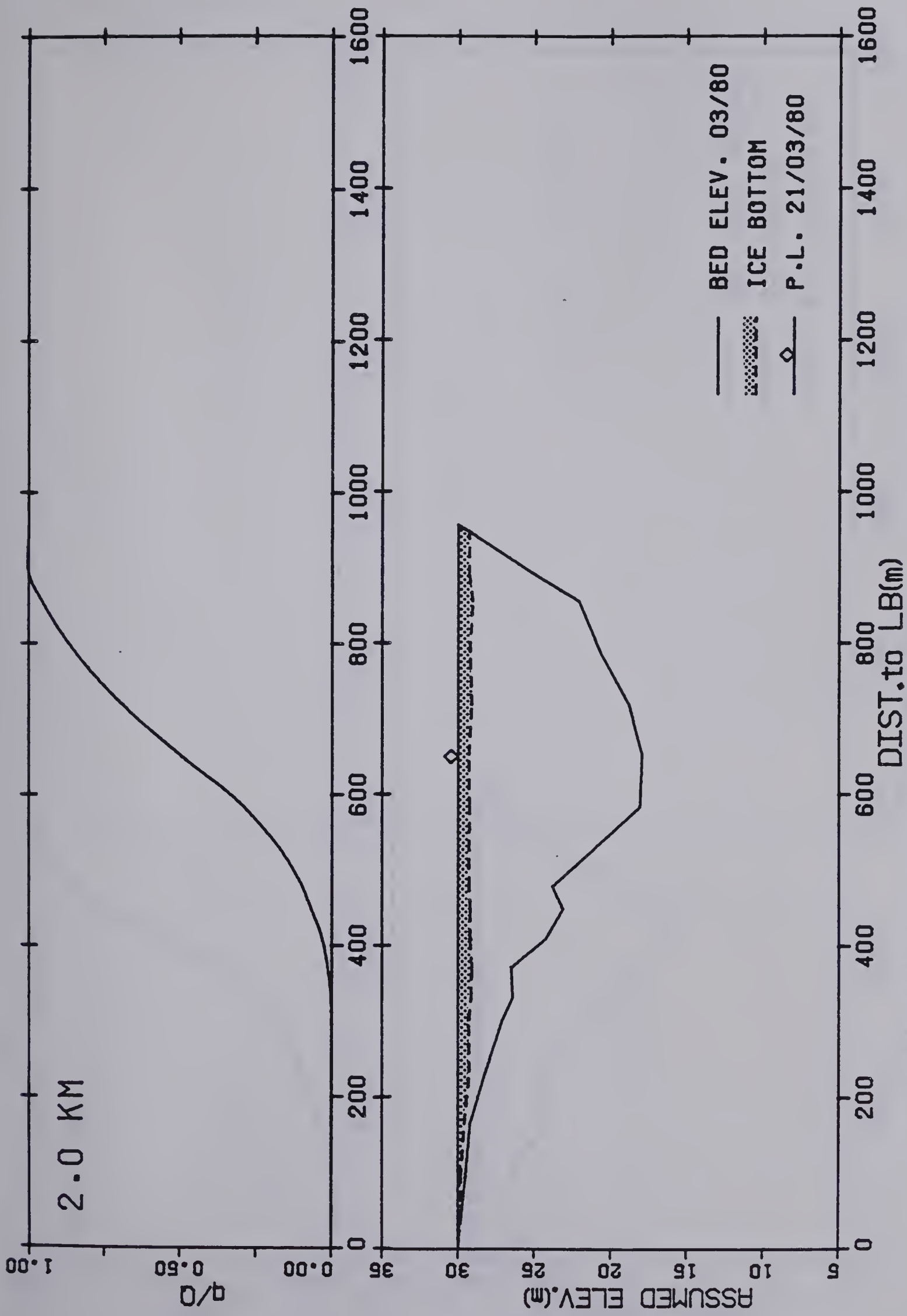


Figure 4.3(b) Cross Section Geometry and Flow Distribution March 1980





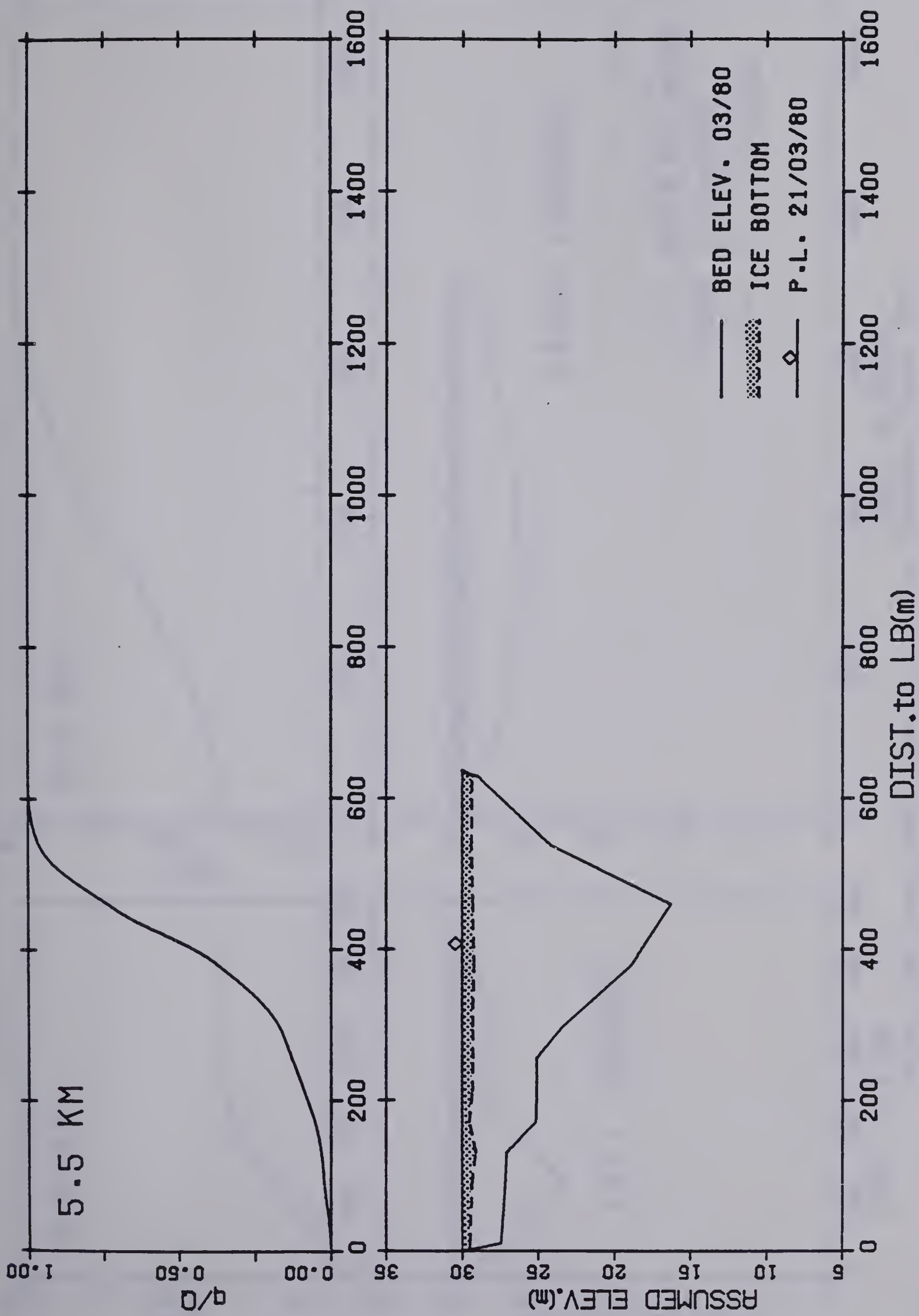


Figure 4.3(c) Cross Section Geometry and Flow Distribution March 1980



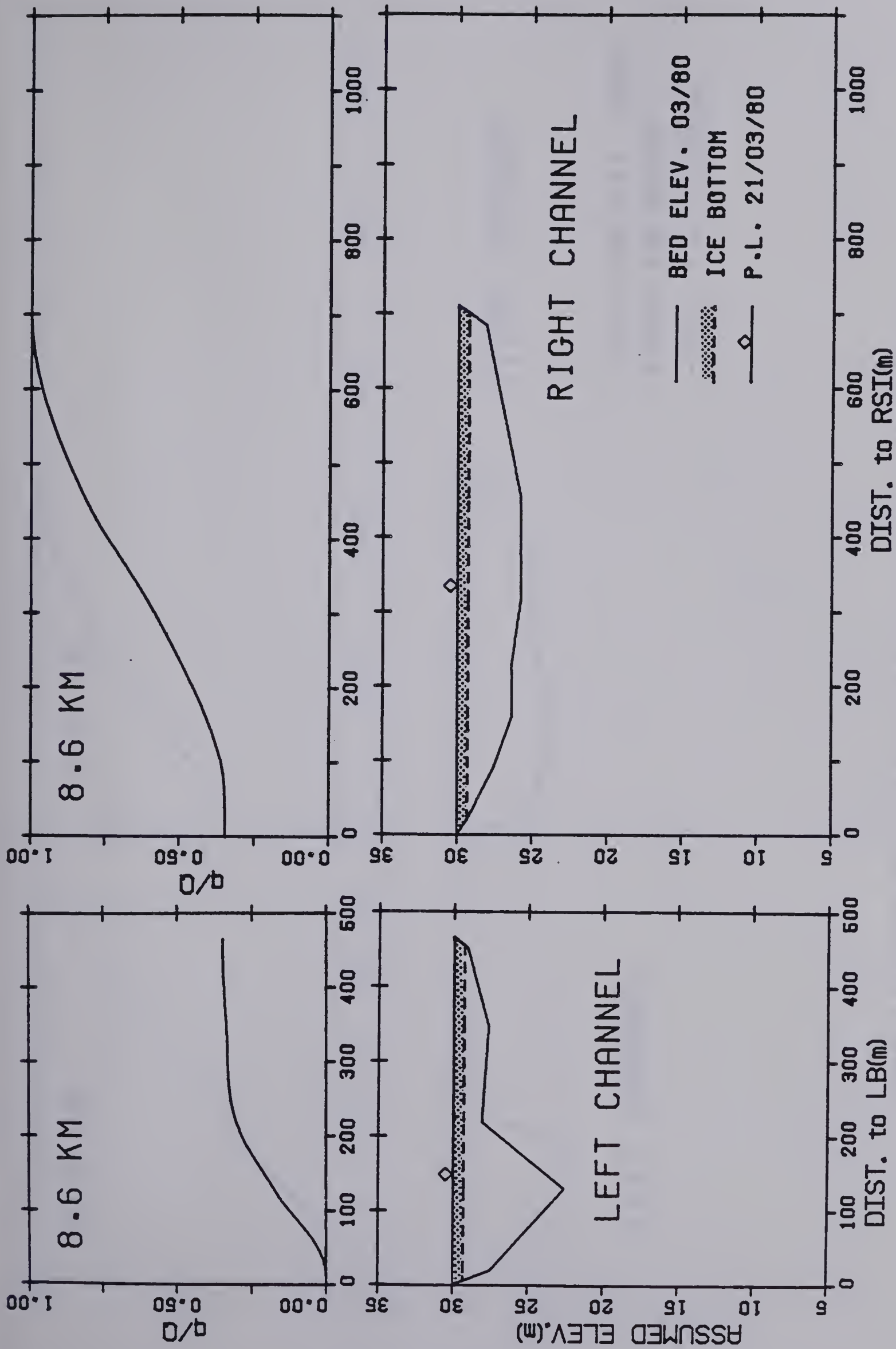


Figure 4.3(d) Cross Section Geometry and Flow Distribution March 1980



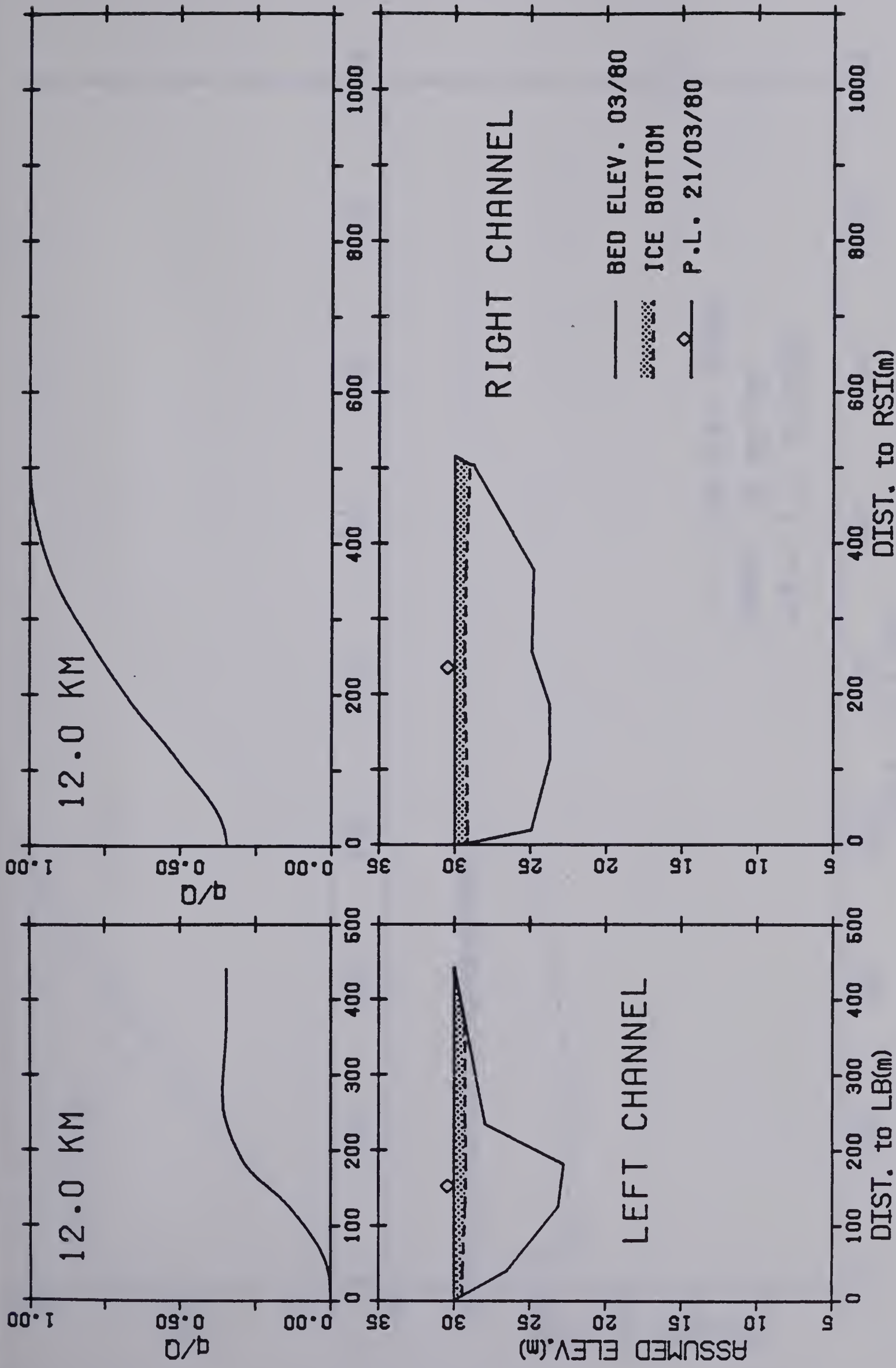


Figure 4.3(e) Cross Section Geometry and Flow Distribution March 1980





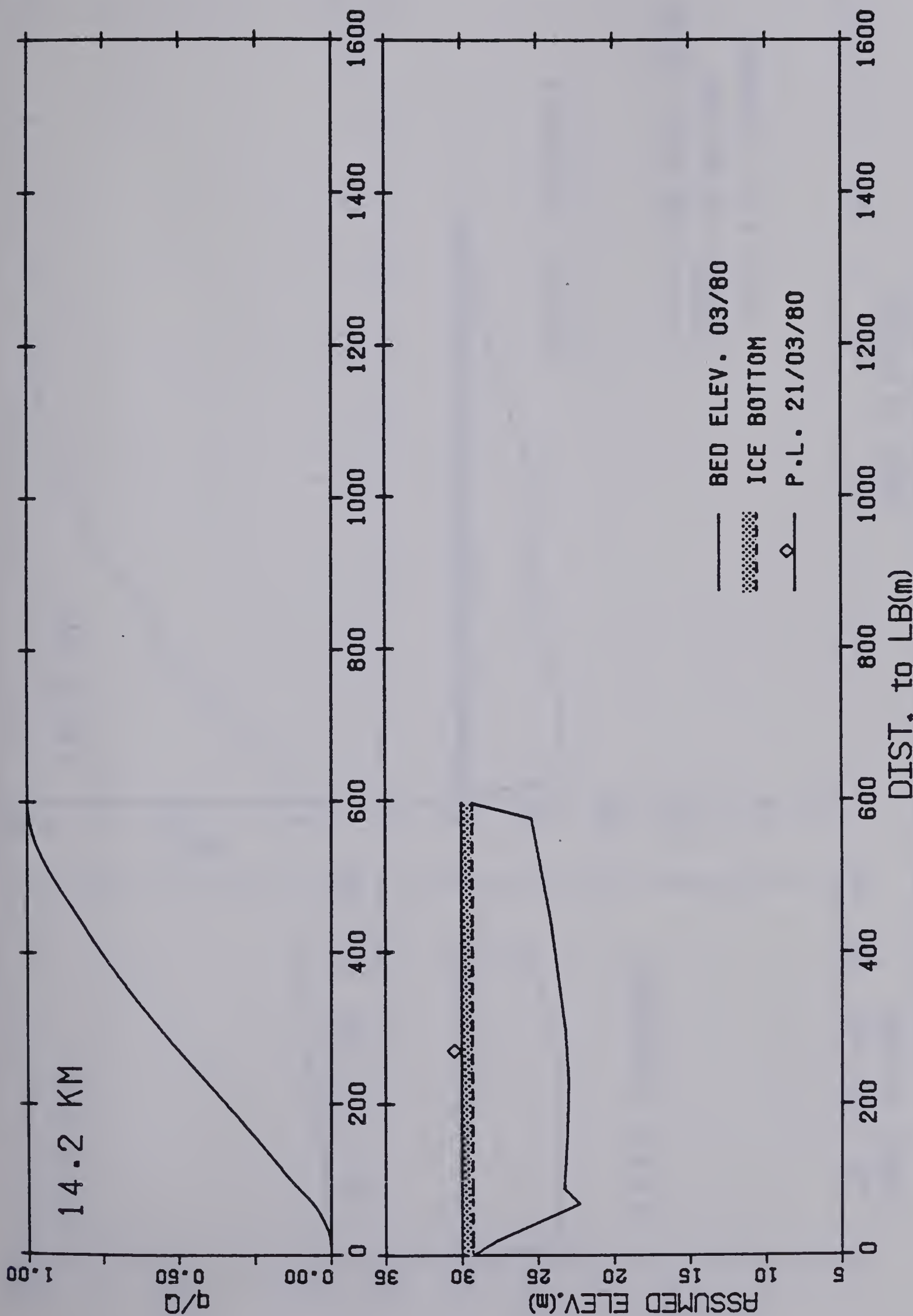


Figure 4.3(f) Cross Section Geometry and Flow Distribution March 1980



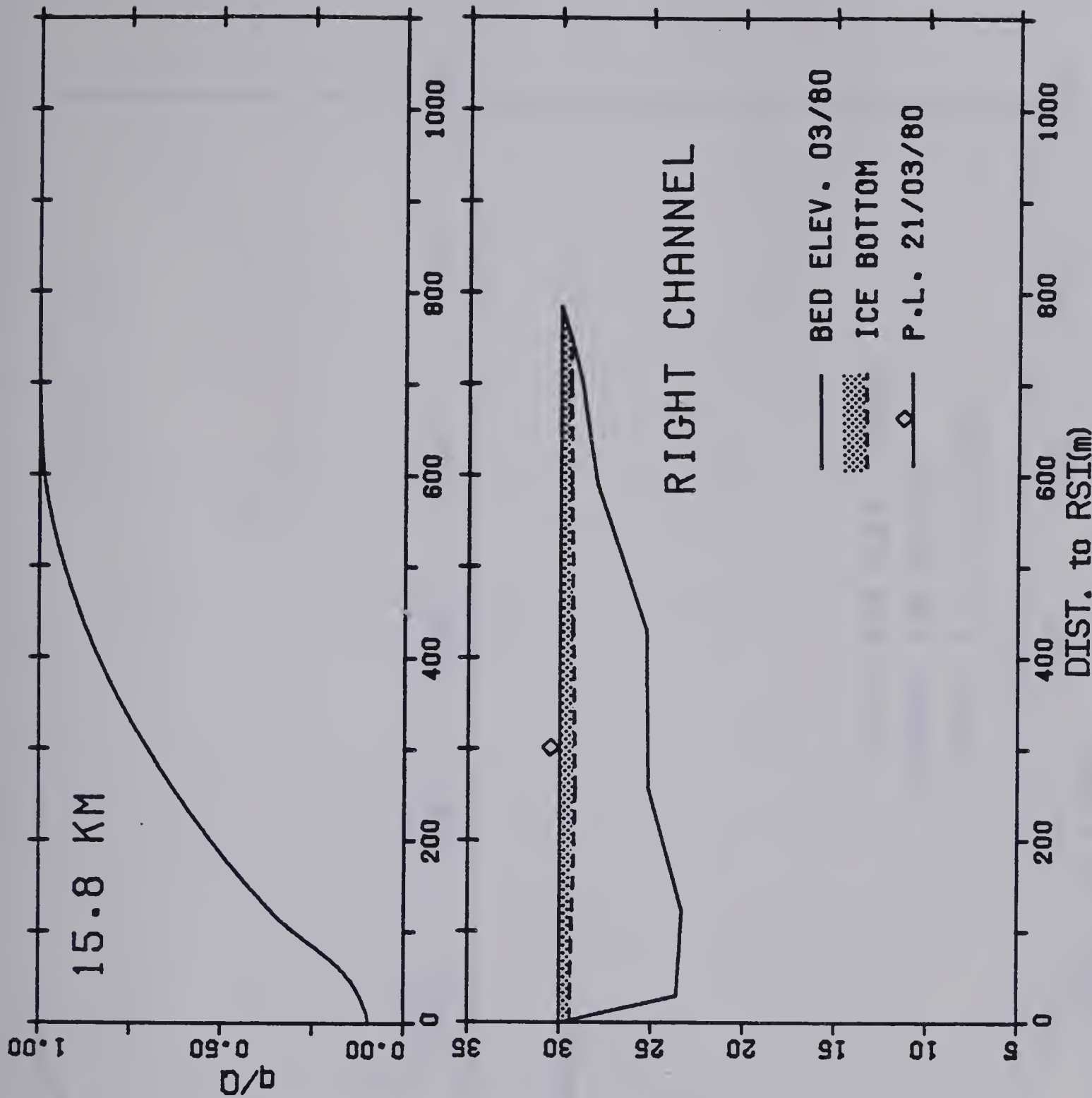
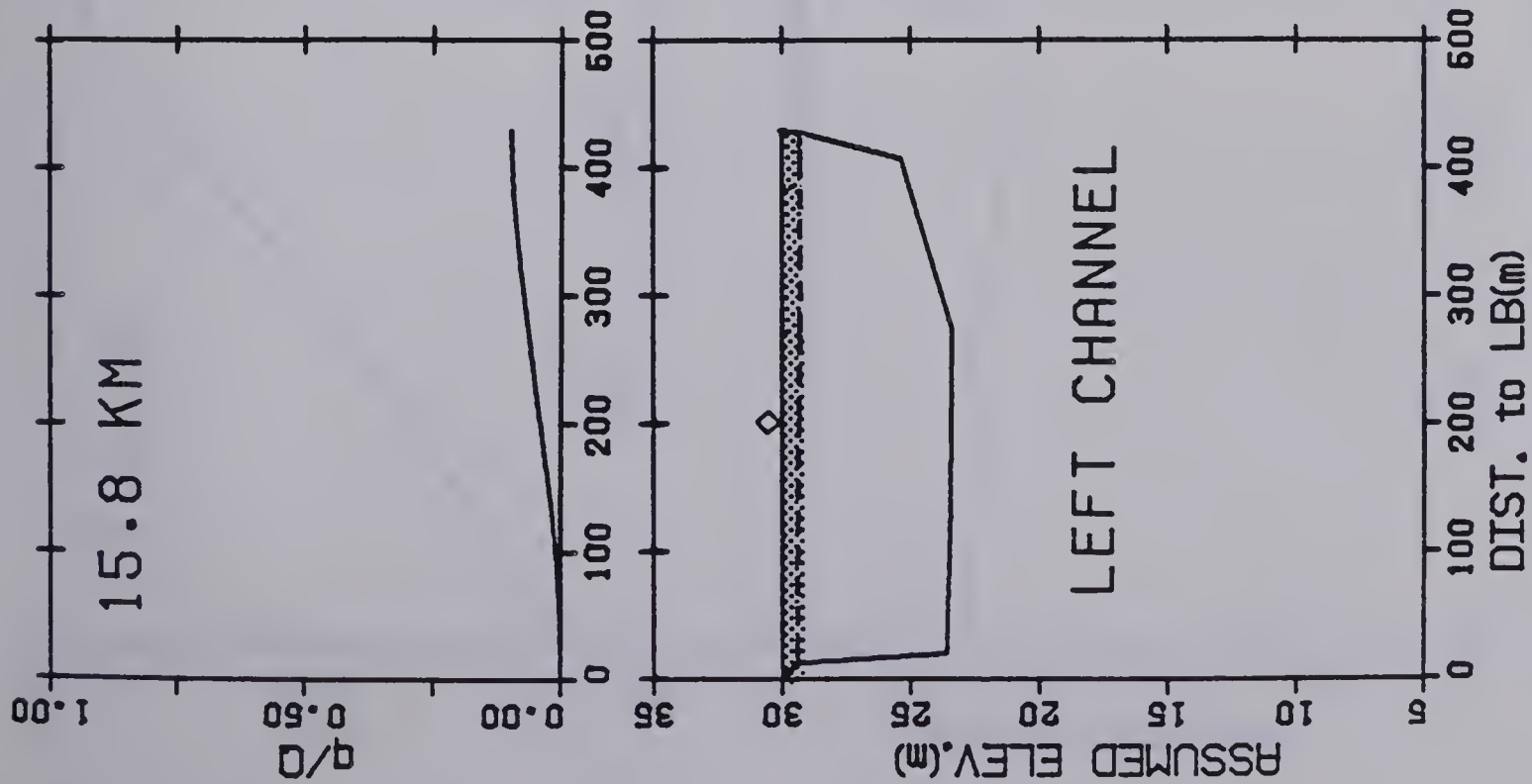


Figure 4.3(g) Cross Section Geometry and Flow Distribution March 1980



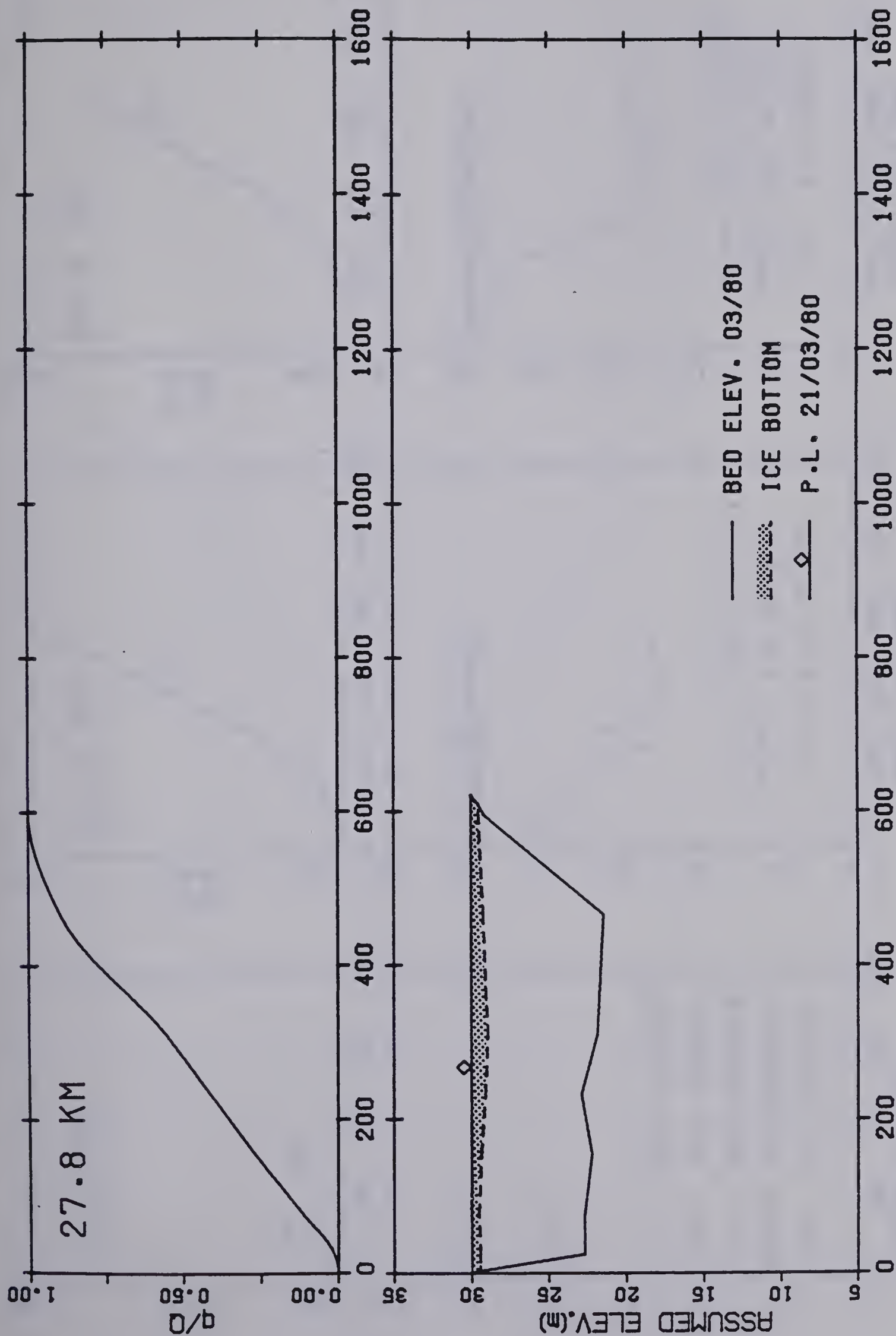


Figure 4.3(h) Cross Section Geometry and Flow Distribution March 1980



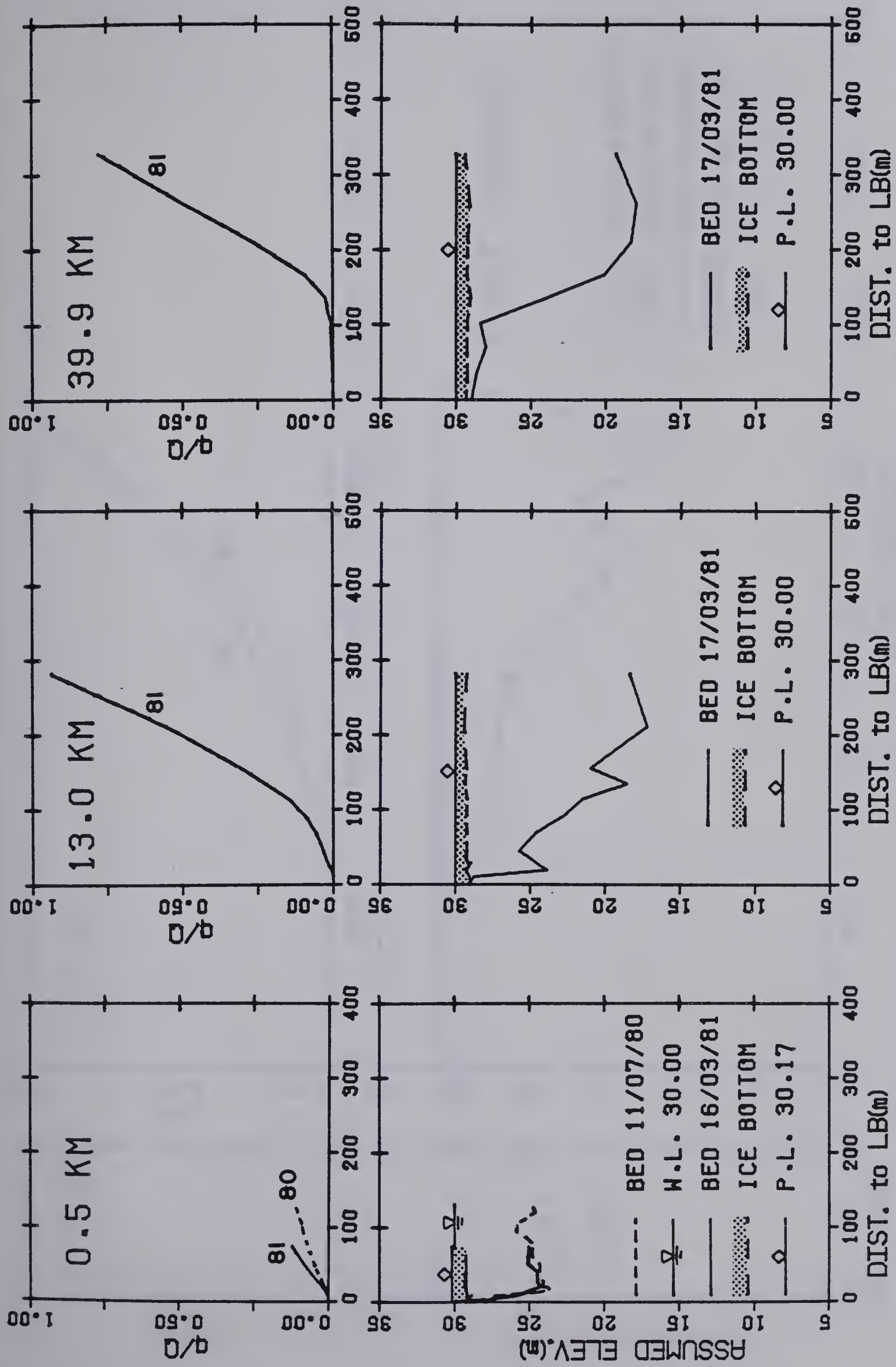


Figure 4.4(a) Cross Section Geometry and Flow Distribution July 1980 and March 1981





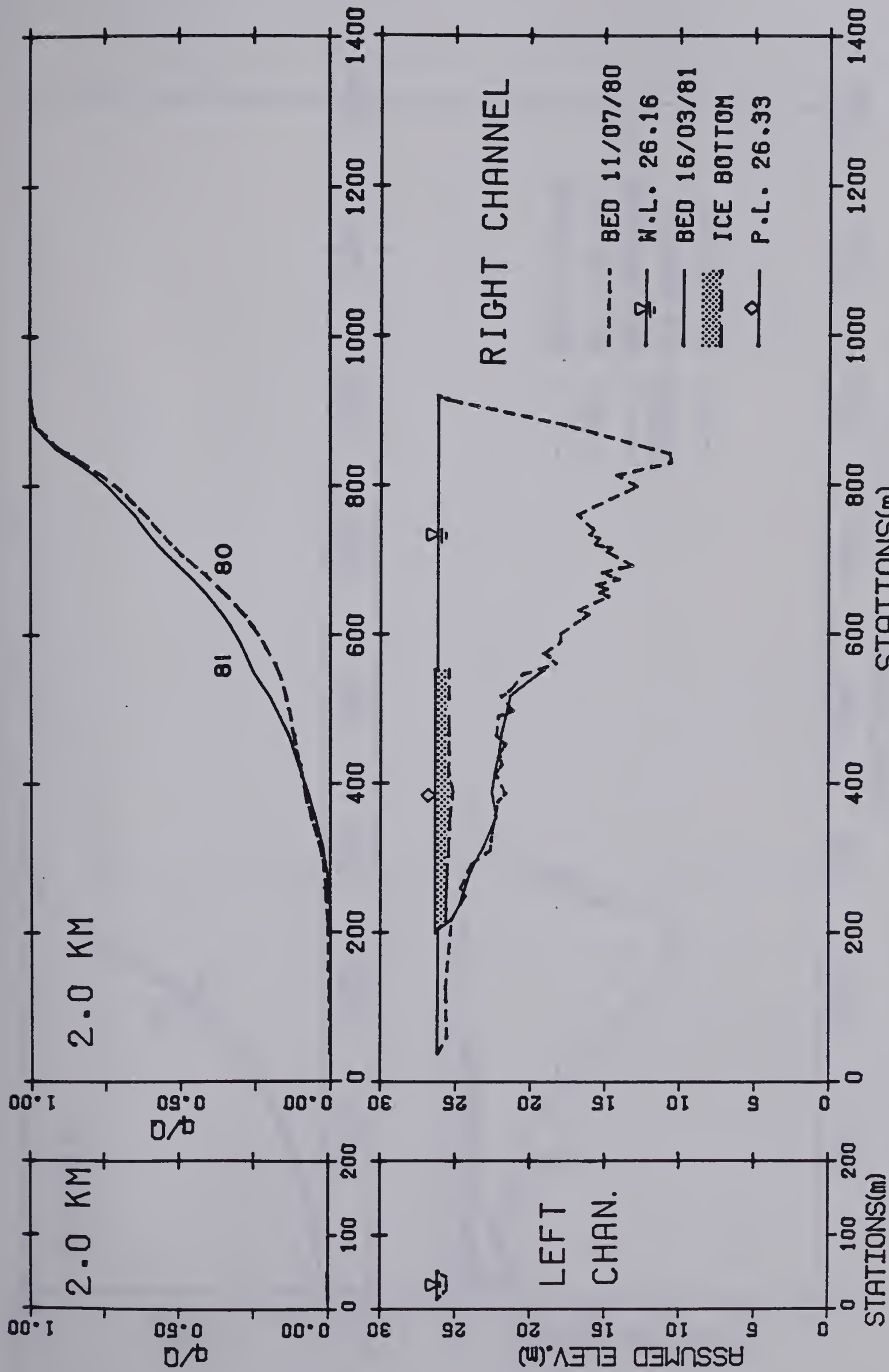


Figure 4.4(b) Cross Section Geometry and Flow Distribution July 1980 and March 1981



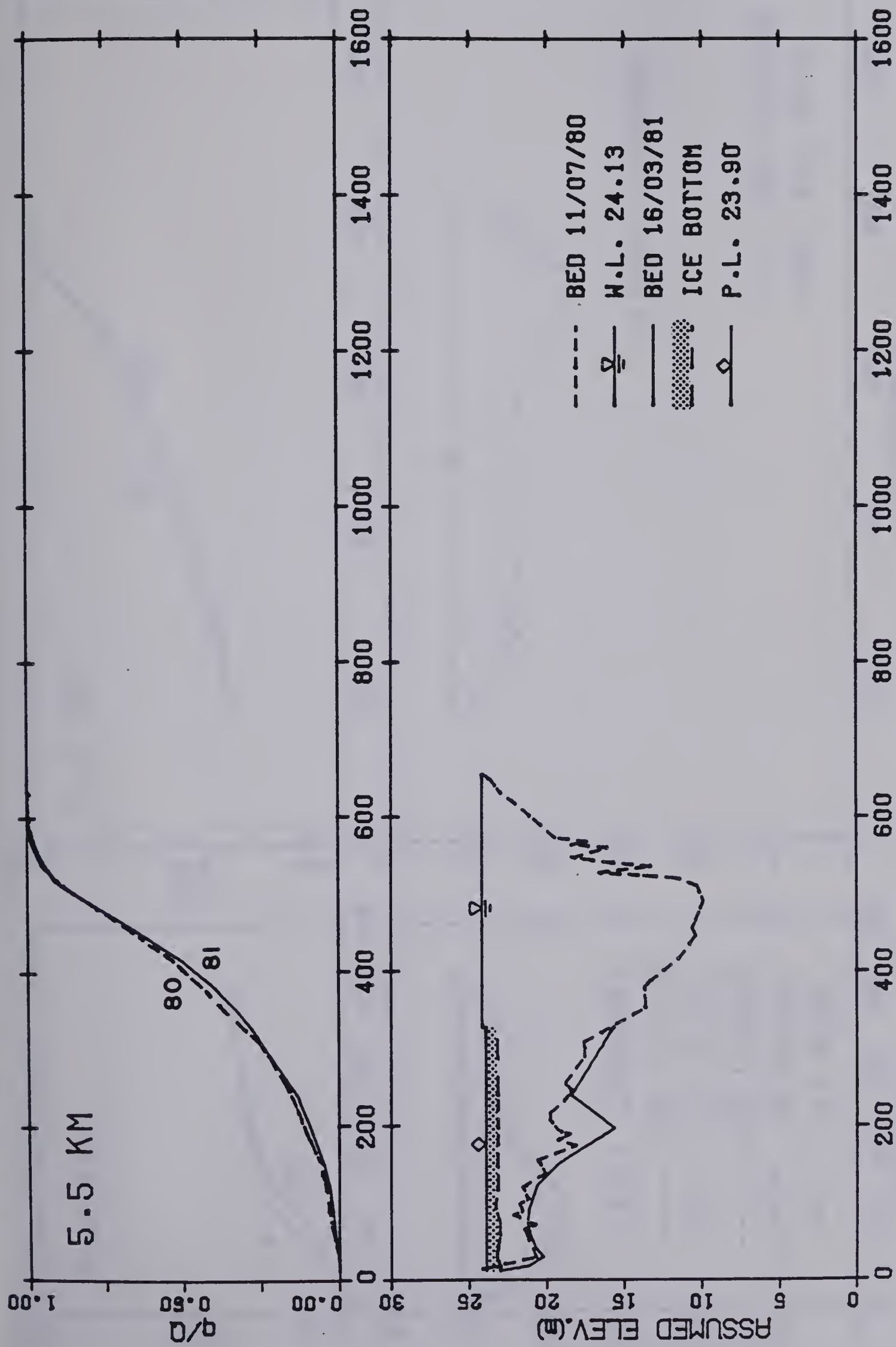


Figure 4.4(c) Cross Section Geometry and Flow Distribution July 1980 and March 1981



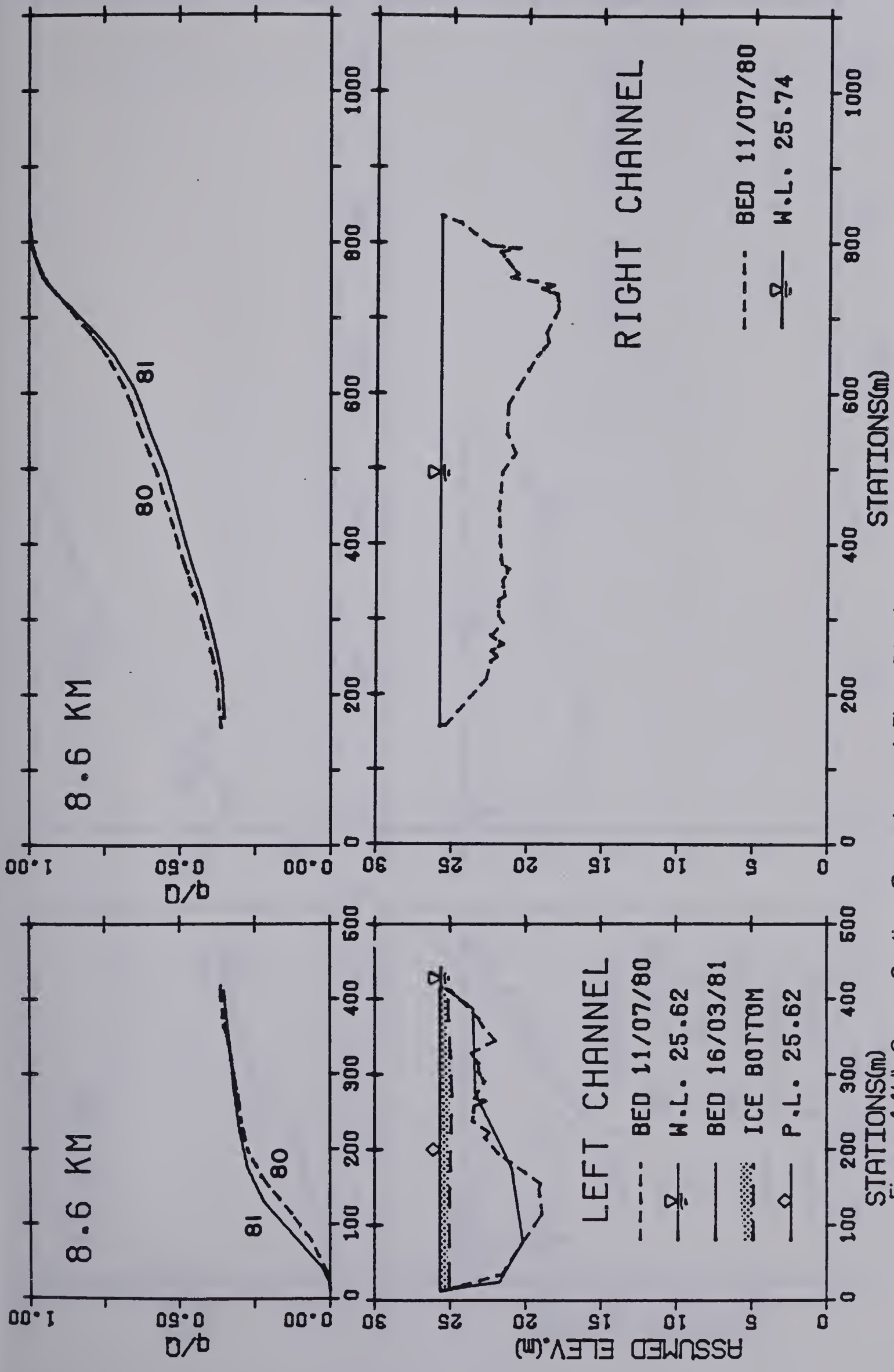


Figure 4.4(d) Cross Section Geometry and Flow Distribution July 1980 and March 1981





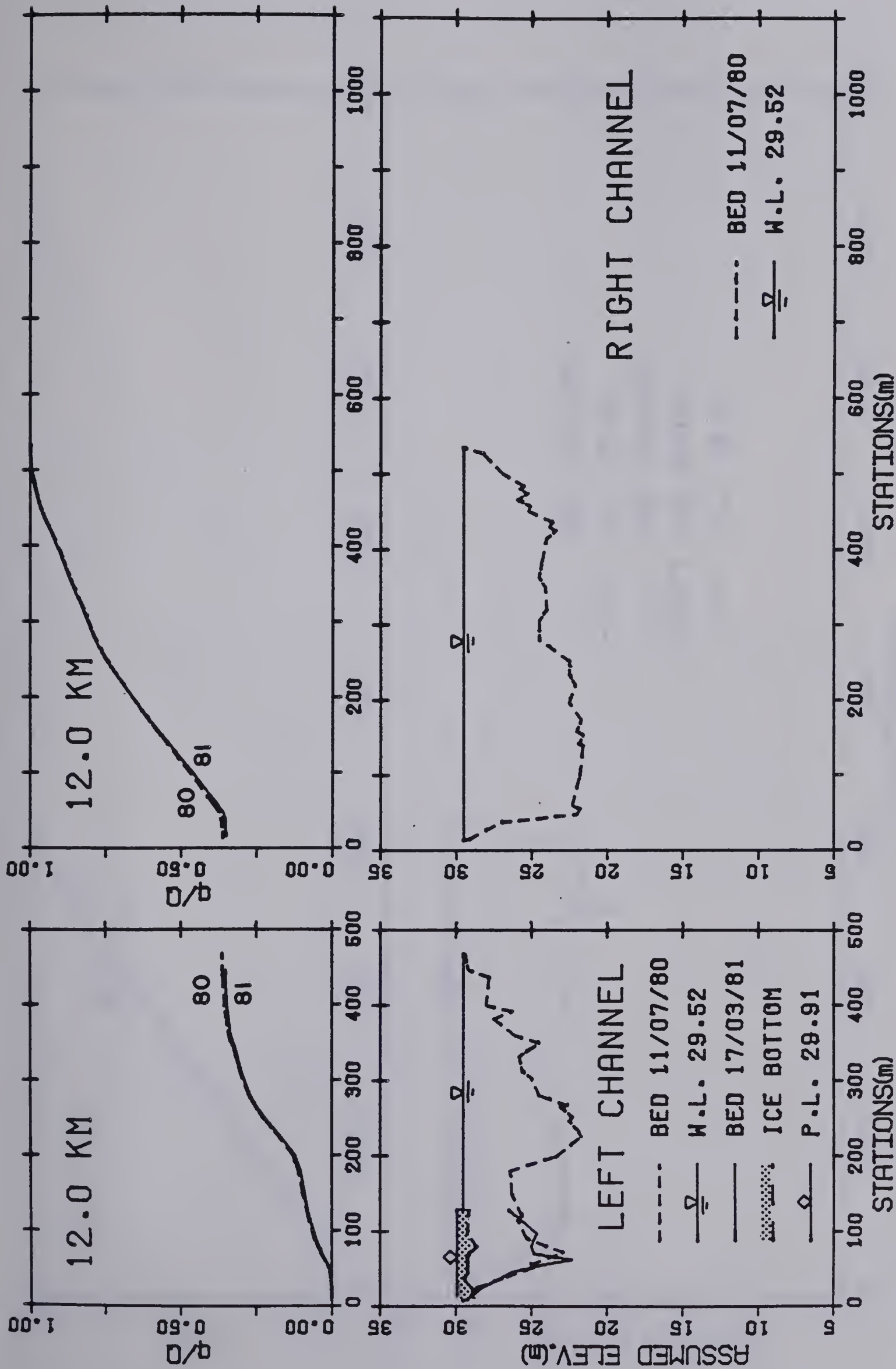


Figure 4.4(e) Cross Section Geometry and Flow Distribution July 1980 and March 1981



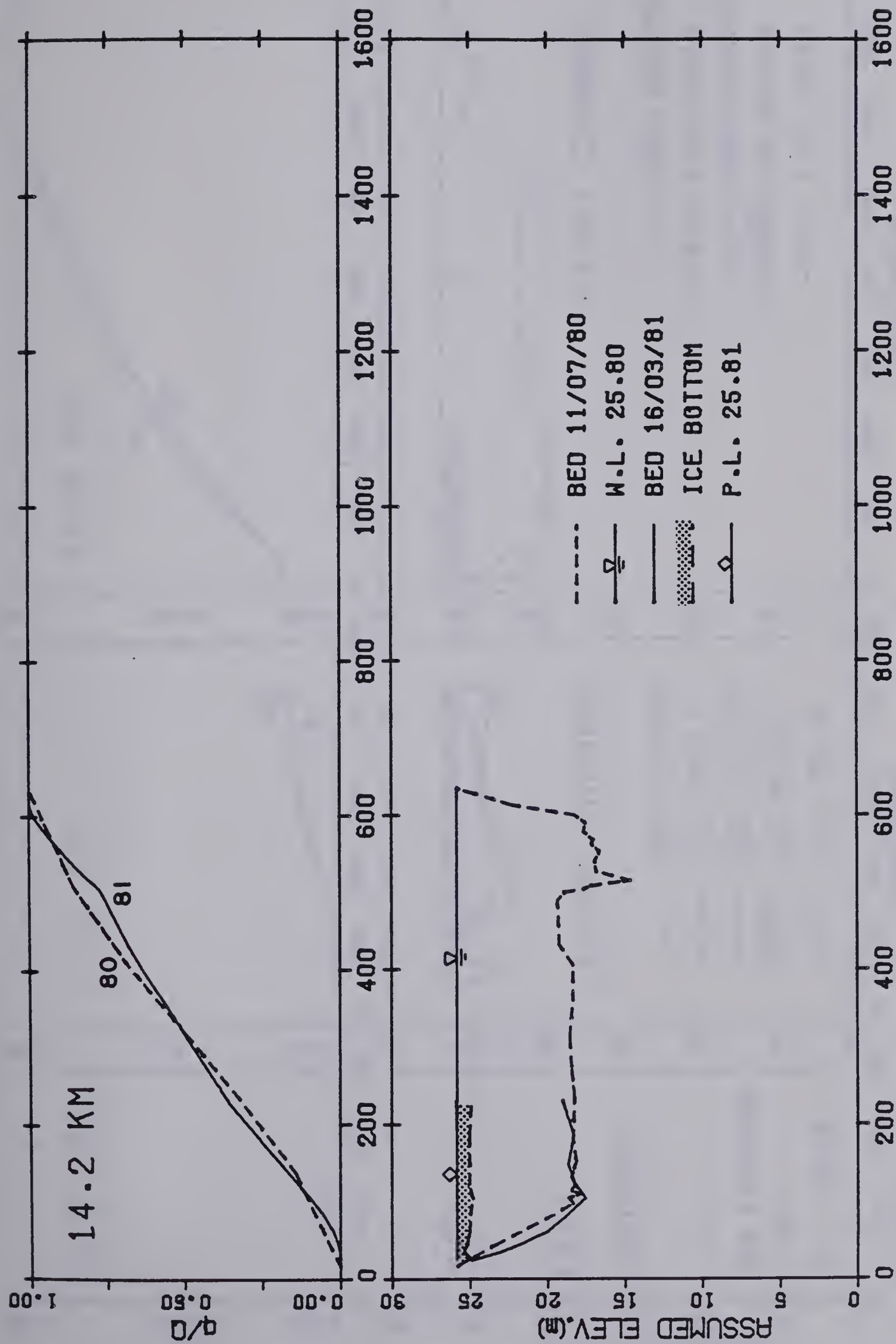


Figure 4.4(f) Cross Section Geometry and Flow Distribution July 1980 and March 1981



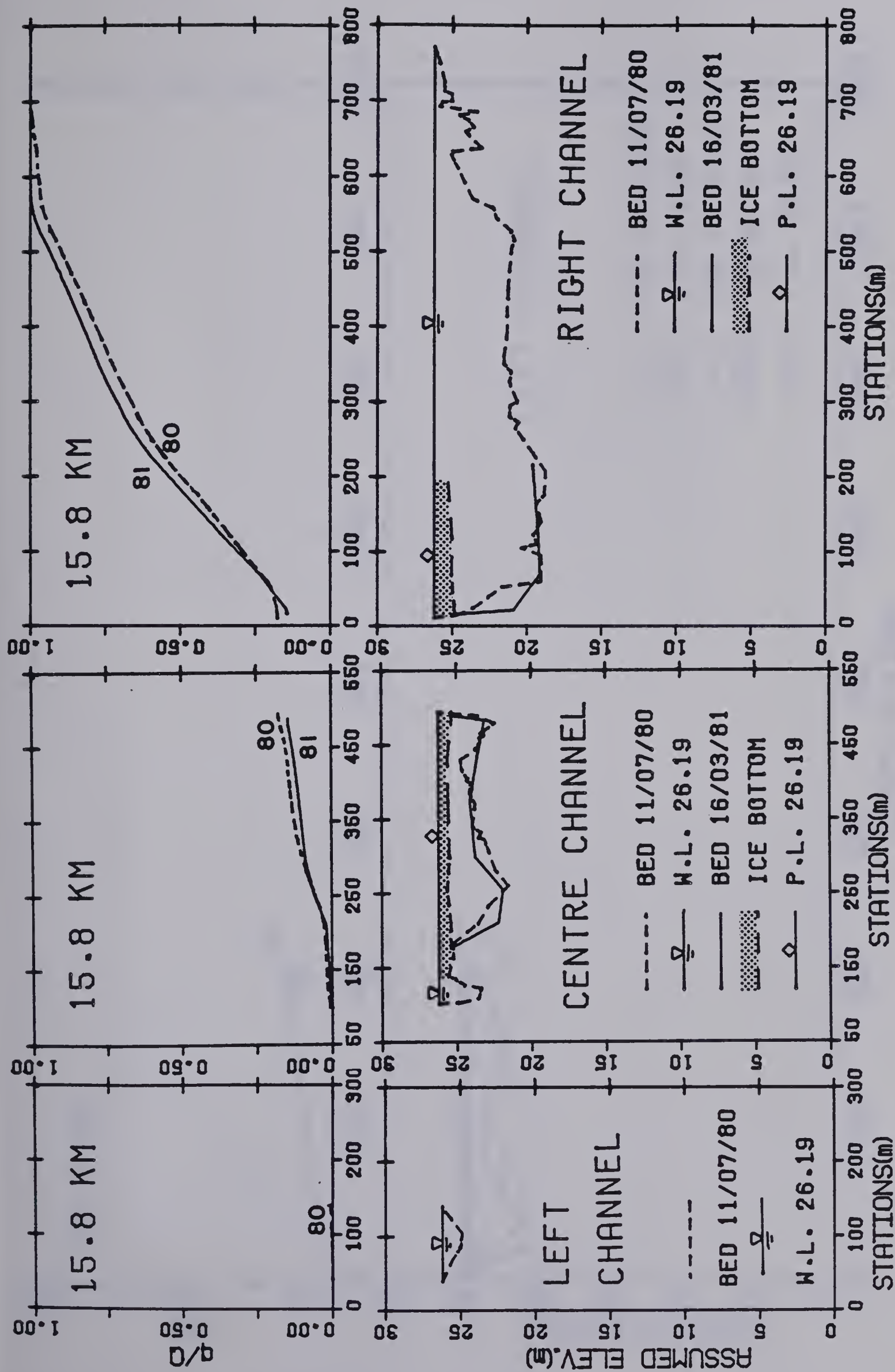


Figure 4.4(g) Cross Section Geometry and Flow Distribution July 1980 and March 1981





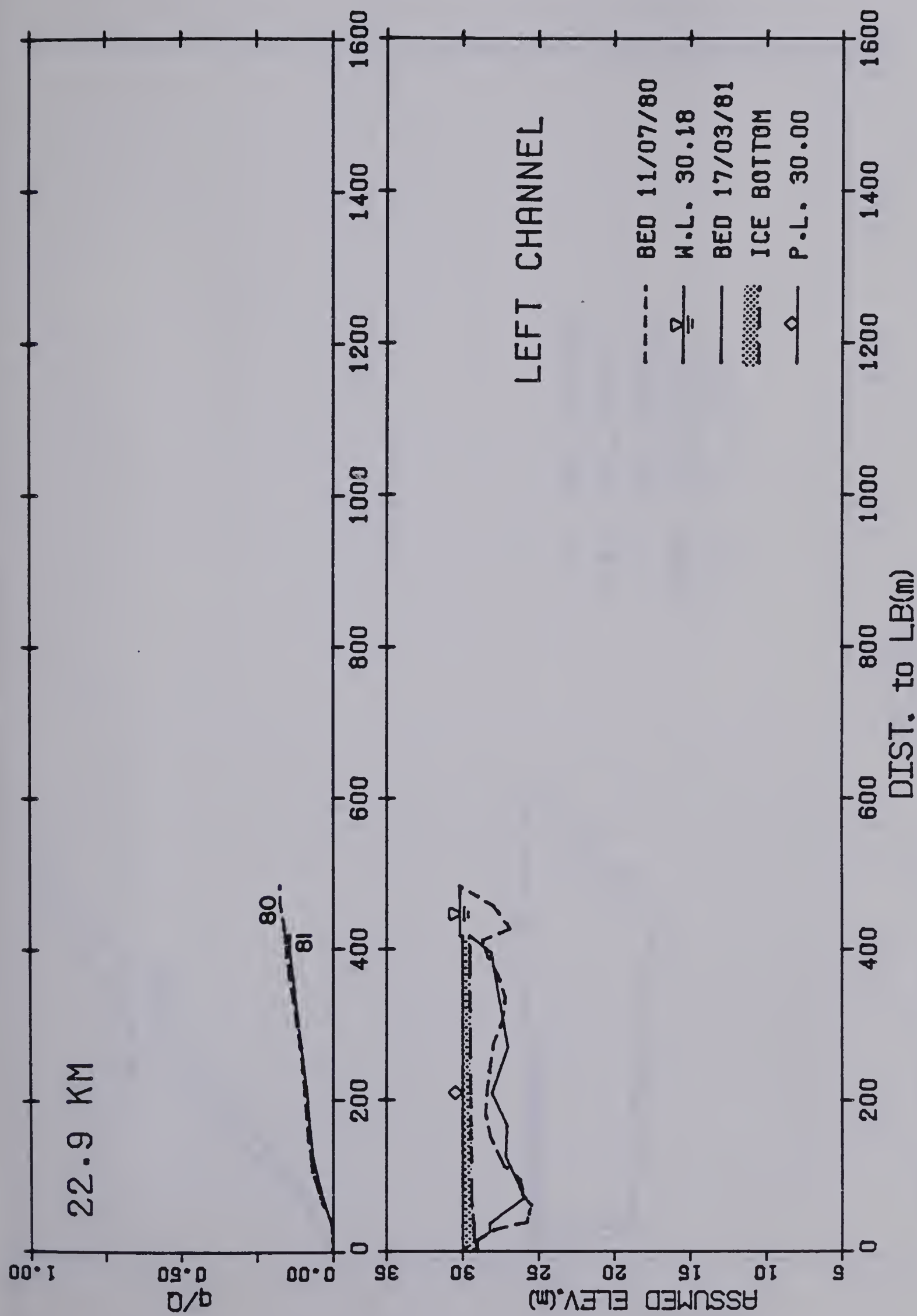


Figure 4.4(h) Cross Section Geometry and Flow Distribution July 1980 and March 1981





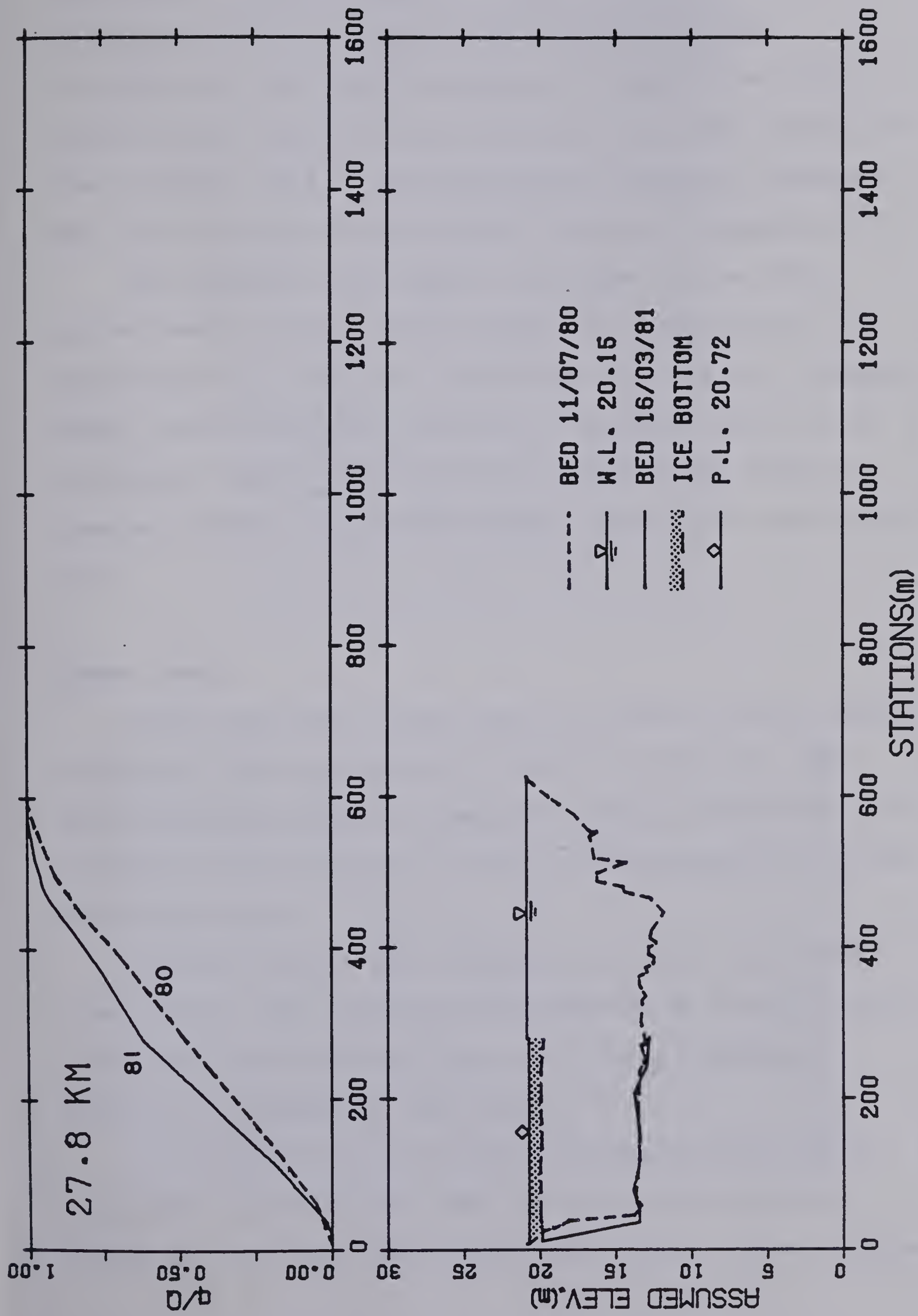


Figure 4.4(ii) Cross Section Geometry and Flow Distribution July 1980 and March 1981



synthesize depth-averaged velocity distributions at unmeasured sections. The synthesized and measured distributions were used to prepare the cumulative flow distributions shown in Figures 4.3 and 4.4. The details of the procedure used in the synthesis of velocity estimates and the flow distribution curves is given in Appendix III.

The velocity measurements were made with a Price current meter, using a Water Survey of Canada winter rig consisting of a 'hot box' containing a hand winch, propane heater (which prevents freezing of the meter when out of the water) and a special circular weight which could be lowered through the 200 mm diameter auger holes (see Plate 4.6).

### Summer Tests

Field tests and surveys were carried out during summer conditions over the period of June 23 to July 12, 1980. Peak discharge conditions generally occur in mid-June and therefore this test period would be representative of high flow conditions.

Section surveys were conducted by three man survey crews. Small open aluminum boats powered by outboard motors were used for travelling along the river, sounding of sections, and sampling (see Plate 4.7).

Cross section locations were basically identical to the winter tests. Actual sampling sites and transverse distances from shore were established using floats anchored





Plate 4.6 Winter Velocity Measurement



Plate 4.7 Summer River Transportation







to the river bed (see Figure 4.5). The floats were first spaced on a transverse line across the section by estimation and later their distances from shore determined by triangulation. The channel widths were precisely measured using a laser electronic distance measuring device.

Cross section geometry was determined by sonic sounding of the river bed using the floats as transverse reference points. Bank surveys were conducted and temporary bench marks established at the majority of the cross sections. The measured section geometries are shown in Figure 4.4.

Velocity measurements were made at selected sections and as for the winter tests estimates made at unmeasured sites using a relationship between depth and depth-averaged velocity. Cumulative flow curves prepared from these measurements and estimates are shown in Figure 4.4.

The summer velocity measurements were made with a Price current meter suspended from a 'bridge frame' hand winch secured over the bow of the survey boat. The anchored floats at each section were used as transverse reference points during the metering procedure.

### Supplementary Data

The average distances downstream of the effluent outfall shown in Figure 4.1 were determined by locating the sections on air photos and navigation chart coverage of the



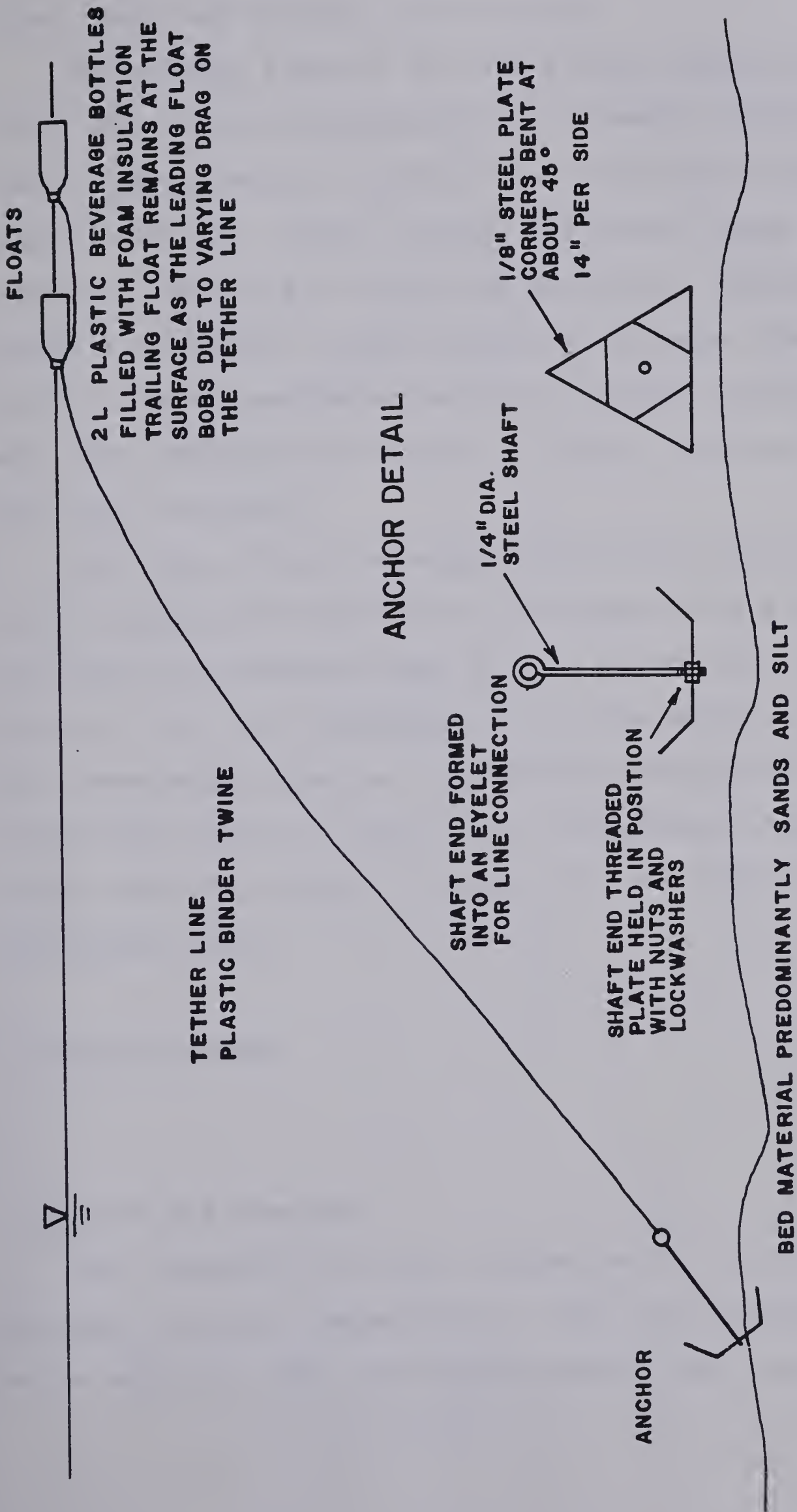


Figure 4.5 Floats and Anchoring Apparatus



river reach and scaling the distances.

The average slope of the Slave River between Fort Smith (downstream of Rapids of the Drowned) and Great Slave Lake is approximately  $0.046 \times 10^{-3}$  m/m (Northwest Hydraulic Consultants Ltd. (1980)). Summer and winter gauge height readings, between Fort Smith and Bell Rock, referenced to geodetic elevation, ( data from field surveys, Shawinigan Stanley (1980), and Water Survey of Canada ) closely agreed with this average and a value of  $0.05 \times 10^{-3}$  m/m was chosen for use in analysis.

The Slave River discharge is monitored continuously at Fort Fitzgerald by Water Survey of Canada. The discharge at Fort Smith was taken as that at Fort Fitzgerald one day earlier. The river discharges during the sampling periods were reasonably steady as indicated by the partial hydrographs shown in Figure 4.6. The average discharge values used for analysis of each test are indicated on the hydrograph plots.

### C. Tracer Methods

#### Injection and Sampling

The conservative tracer Rhodamine WT, a fluorescent dye that is easily detectable at very low concentrations, while being non-toxic and biodegradable, was chosen for the





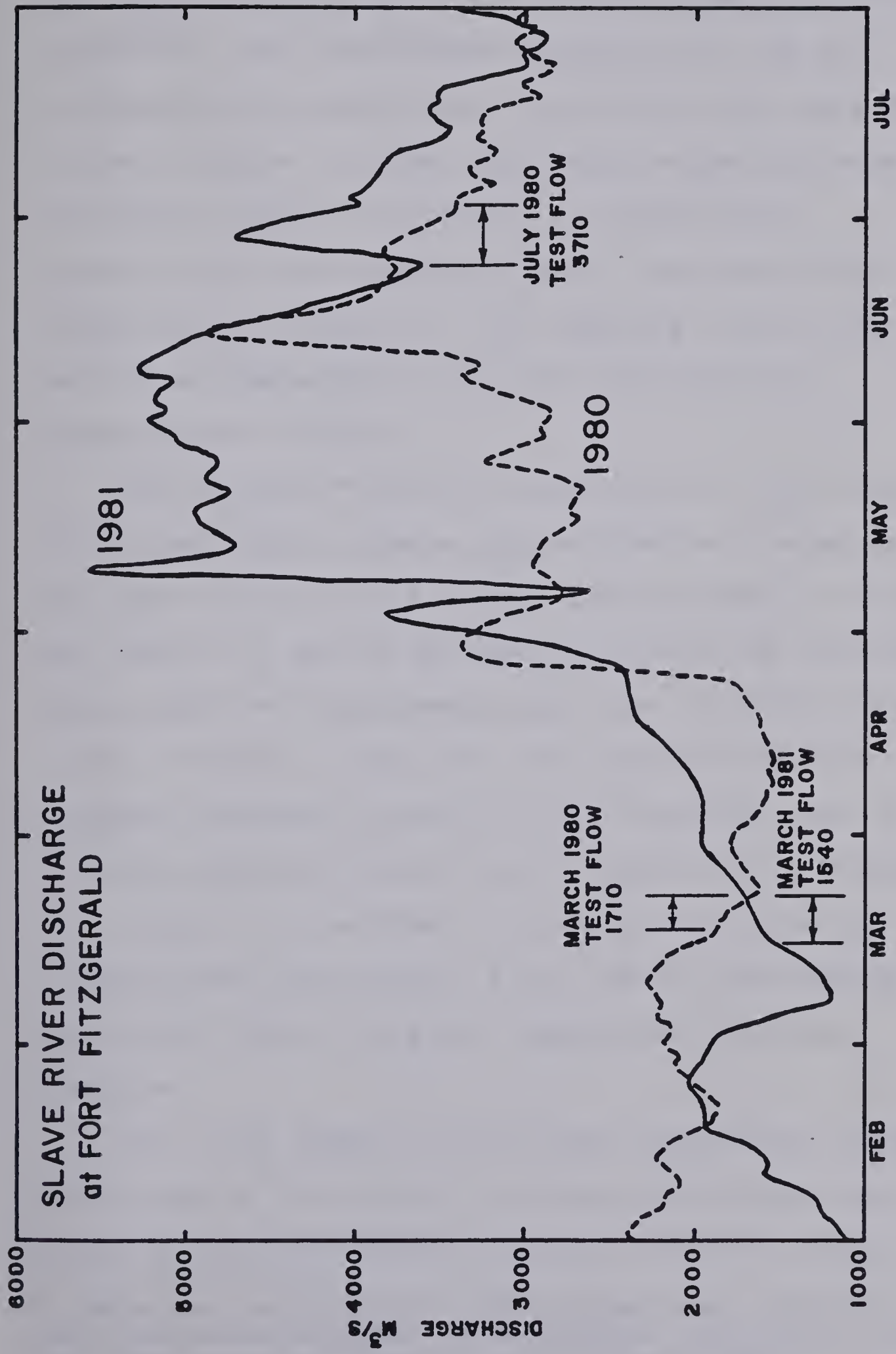


Figure 4.6 Slave River Discharge at Fort Fitzgerald  
-data from Water Survey of Canada





study.' The dye is supplied as a 20% by weight solution and was further diluted prior to injection. Data on the dye injection, river background concentration, and the estimated fully mixed river concentration for each test is listed in Table 4.1. The long injection periods were required to ensure an interval of steady-state concentration for sampling at each cross section as illustrated in Figure 4.7. The sampling time at each section was selected to be within its constant concentration 'window'.

The constant injection rate during the 1980 tests was controlled using a simple constant head weir apparatus fed by siphon action from a storage drum as shown in Figure 4.8 and Plate 4.8. During the March 1981 test the variable speed positive displacement pump shown in Plate 4.9 was used to control the dye flow. The pump allowed more accurate and easier control of the injection rate. In each case the apparatus was set up in a tent over a manhole on the outfall line as shown in Plate 4.10 and the dye injected into the effluent flow. The tent was heated during the winter tests to prevent freezing of the tracer solution.

The first sampling section was located far enough downstream of the outfall to ensure the effluent and tracer would be uniformly mixed vertically. Only one tracer sample

-----  
' Feuerstein and Selleck (1963) present an excellent review of fluorescent tracers and fluorescent tracing procedures are comprehensively described by Wilson (1968).



Table 4.1 Tracer Injection Data

Test	Injection Conc. %	Injection Flow mL/s	Period hr	Background River Conc. ppb	Fully Mixed River Conc. ppb	Avg. River Discharge cms
March 1980	4.05	2.97	23.24	0.03	0.07	1730
July 1980	4.77	6.83	17.67	0.10	0.09	3710
March 1981	9.42	1.93	31.55	0.03	0.12	1560

\* in excess of background



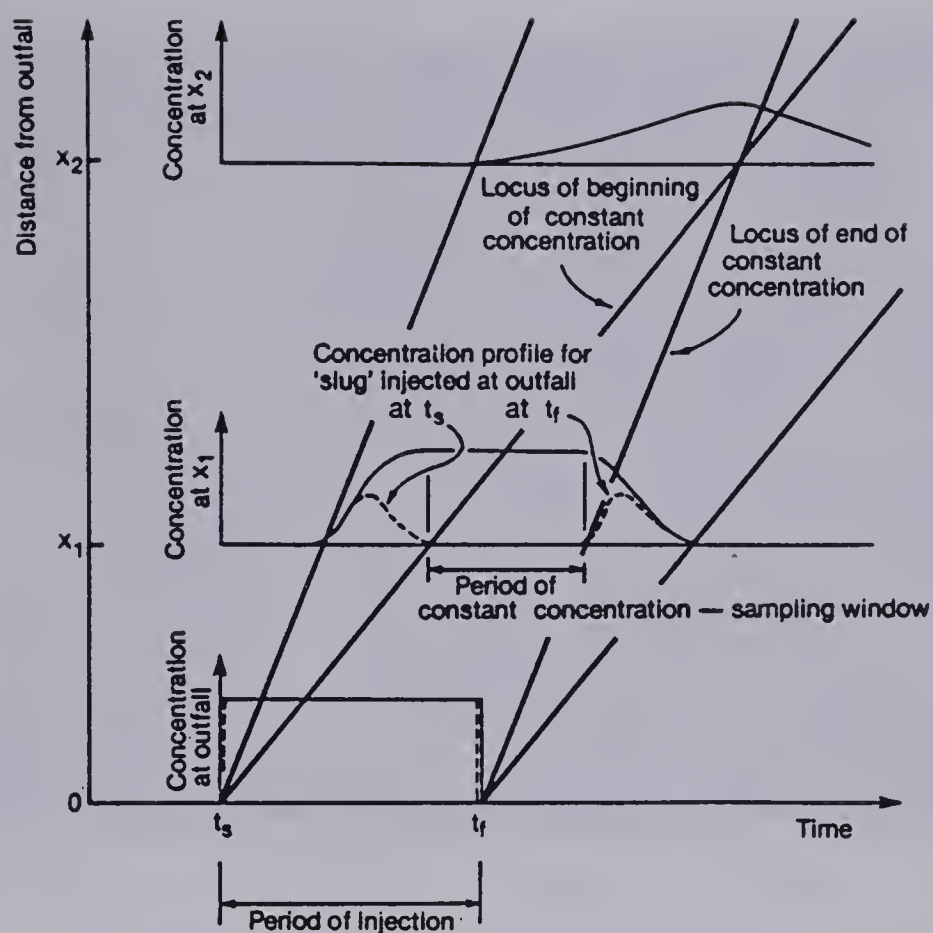


Figure 4.7 Illustration of Variation in Tracer Concentration with Time and Distance following a Finite Duration Constant Rate Injection  
—from Smith and Gerard (1981)

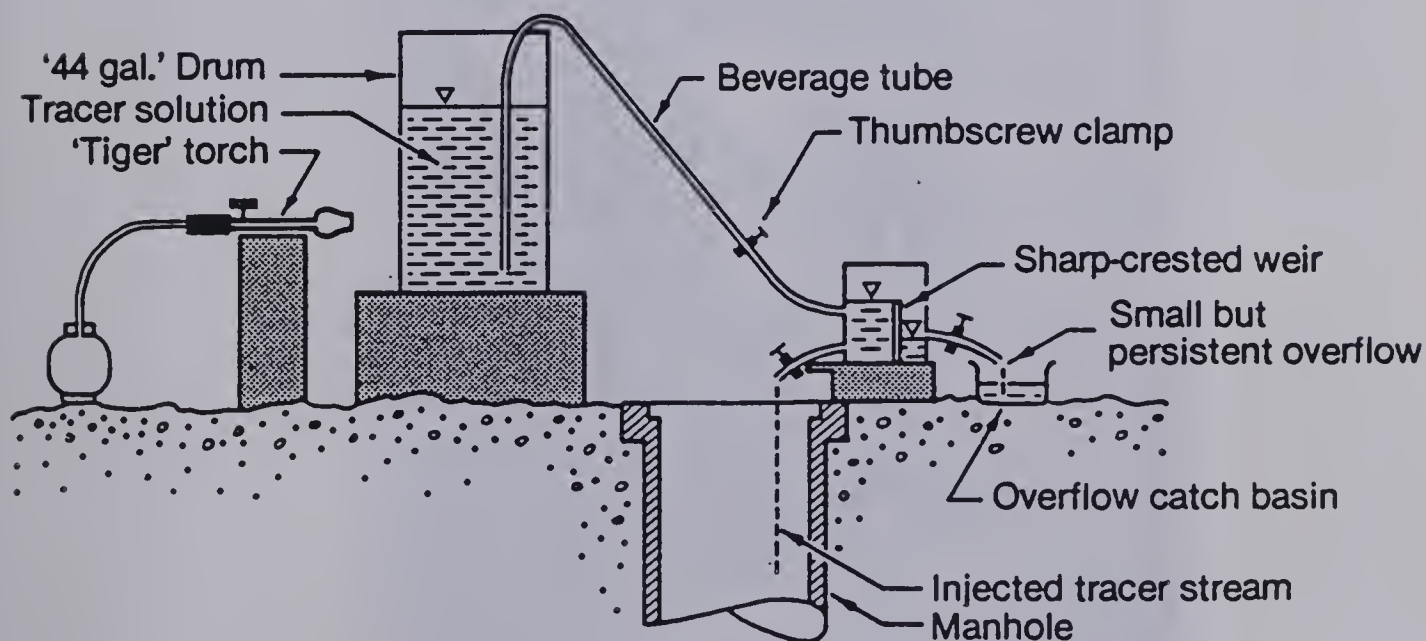


Figure 4.8 Weir Apparatus for Tracer Injection  
—from Smith and Gerard (1981)







Plate 4.8 Constant Head Weir



Plate 4.9 Pump Apparatus for Tracer Injection





Plate 4.10 Winter Injection Tent



from each sampling location was required due to this uniform concentration with depth. In the winter tracer samples were collected at each hole from under the ice sheet (see Plate 4.11) using the tracer sampling rod and 125 ml plastic bottle shown in Figure 4.9. The bottles were simply hand dipped below the water surface during the summer test. Insulated containers, which prevented freezing during the winter and provided isolation from sunlight, were used to transport the samples to the University of Alberta for analysis.

### **Sample Analysis and Results**

The tracer concentration in each sample was determined in the laboratory using the Turner Designs field-model fluorometer shown in Plate 4.12. The samples were stored to allow sediment to settle out and temperatures to equalize before analysis. This eliminated light scatter and temperature effects. Reanalysis of the samples was conducted with the sediment fully mixed to assess any differences in measured concentration.

Ice cover conditions correspond to periods of extremely low sediment load of the river due to reduced flows and therefore, the settled and fully mixed sediment measurements of tracer concentration for these periods were not significantly different. However, the peak flows of June and July correspond to periods of high sediment load and not surprisingly significant differences in tracer







Plate 4.11 Winter Sampling



Plate 4.12 Fluorometer





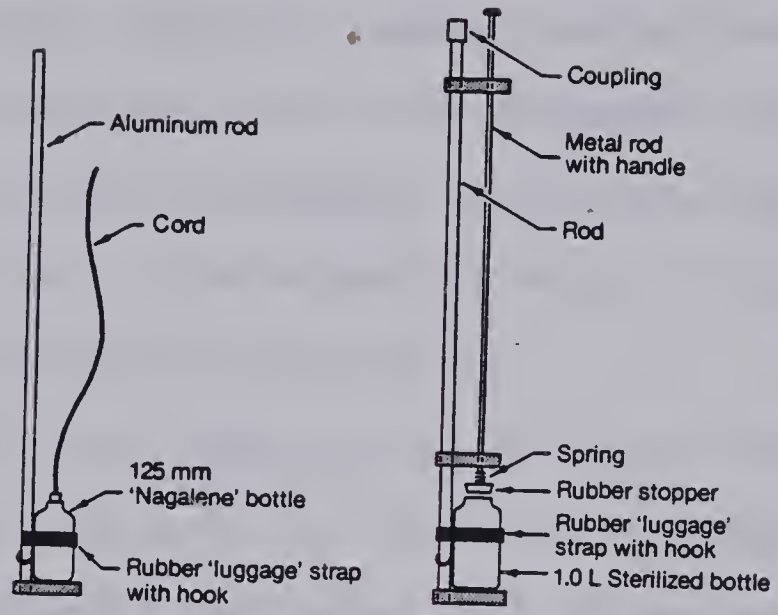


Figure 4.9 Sampling Rods  
-from Smith and Gerard (1981)



concentrations in the settled and fully mixed measurements were evident for the summer test.

Subsequent mass balance analysis of the tracer flux at each measured section indicated incomplete recovery of the input tracer mass. Possible removal mechanisms are adsorption of the tracer onto the suspended sediments, the stream boundaries or the sample containers and destruction of the tracer due to photochemical decay or chemical oxidation resulting from agitation.

In an effort to identify the source of this mass loss adsorption tests were run on Rhodamine WT dosed samples of distilled water and river water of high sediment content. The samples were stored in glass and plastic bottles isolated from light contact. The results of the tests indicated that although a small amount of tracer was lost to the sediment (less than 5 percent) the most significant losses were due to adsorption to surfaces of the plastic sampling bottles. A summary of the adsorption analysis and the resulting plastic adsorption correction are given in Appendix IV.

The estimated tracer recovery for the winter tests, after correction for the adsorption onto the plastic bottles, was generally in the range of 90 to 100 percent. Recoveries in this range are excellent considering the accuracy of the flow measurements used in the mass balance calculations would generally be in the range of  $\pm 10$  percent. Error associated with calibration and reading of



the fluorometer and adsorption losses to the extremely low sediment content in winter are minimal compared to the error associated with estimating the distribution and magnitude of river flow.

Unfortunately the corrected recovery during the summer test was much lower, generally in the range of 75 to 85 percent. Again inaccuracy in flow estimation may account for a major portion of this discrepancy, however, some additional removal mechanisms must be active during the summer which are not present during winter.

The most probable mechanism is photochemical decay which is eliminated by ice cover during the winter tests. Outdoor jar experiments conducted by Feuerstein and Selleck (1963) indicated concentrations may decay by as much as 1 to 2 percent per hour. These rates probably represent upper limits in natural streams, however, losses in the order of 10 to 20 percent would not be unreasonable within the reach sampled. Minor absorption losses due to high sediment content in summer and chemical oxidation would also contribute to the increased tracer loss. Considering the combined effects of photochemical decay, oxidation and adsorption onto sediment tracer recovery of 10 to 15 percent less than the winter tests is not unreasonable.

The estimated dye recoveries at each section for the three tests are shown in Table 4.2.





Table 4.2 Tracer Recoveries

X-Section	%Recovery		
	March 1980	July 1980	March 1981
2.0 km	1.00	.70	.97
5.5 km	.99	.74	.98
12.0 km	1.03	.81	.98
13.0 km	-	-	1.03
14.2 km	1.00	.81	.95
15.8 km	.93	.81	.95
22.9 km LC	-	.84	.87
27.8 km	.65	.70	.90
39.9 km	-	-	1.02



The measured tracer concentrations (corrected for adsorption) are plotted in Figures 4.10, 4.11 and 4.12 in dimensionless form,  $c'$  being given by Equation 2.24. The transverse coordinate of the plots is the dimensionless cumulative flow discussed earlier and shown in the section plots. The plots of Figures 4.10, 4.11 and 4.12 vividly illustrate the two-dimensional nature of the mixing which occurs downstream of a bank outfall discharging to a wide river. At approximately 40 km downstream of the outfall during the March 1981 test, the edge of the plume is only approaching a distance across the channel equivalent to half the total river discharge. Evidently a very long distance is required before complete mixing of the effluent occurs for these conditions.

#### D. Bacteriological Methods

##### Sampling

River samples for microbiological analysis were collected using the bacteriological sampling rod shown in Figure 4.9 and Plate 4.13. The spring loaded rubber stopper of the sampler allowed the sample bottle to be lowered below the ice in winter or the water surface in summer, filled, closed and removed. The sampling bottles were sterilized and sealed prior to shipment to Fort Smith and, other than contact with the stopper, the bottle mouth and



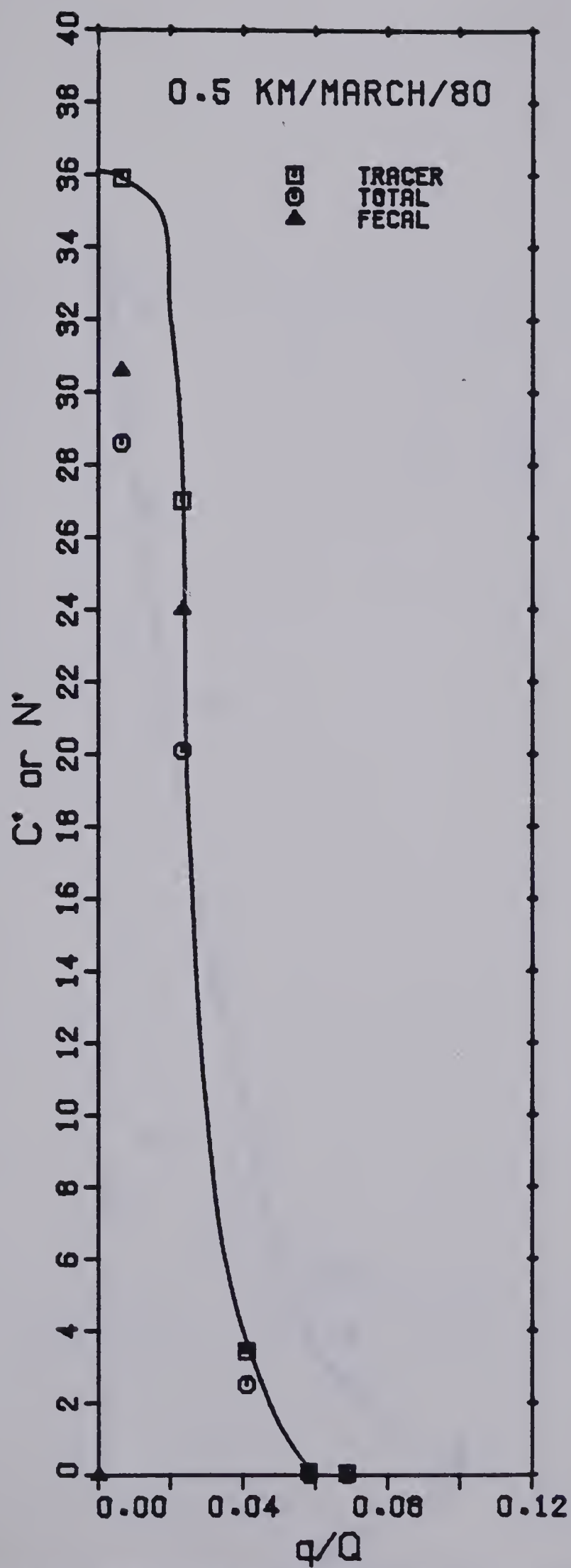


Figure 4.10(a) Dimensionless Tracer and Microorganism Concentrations  
March 1980



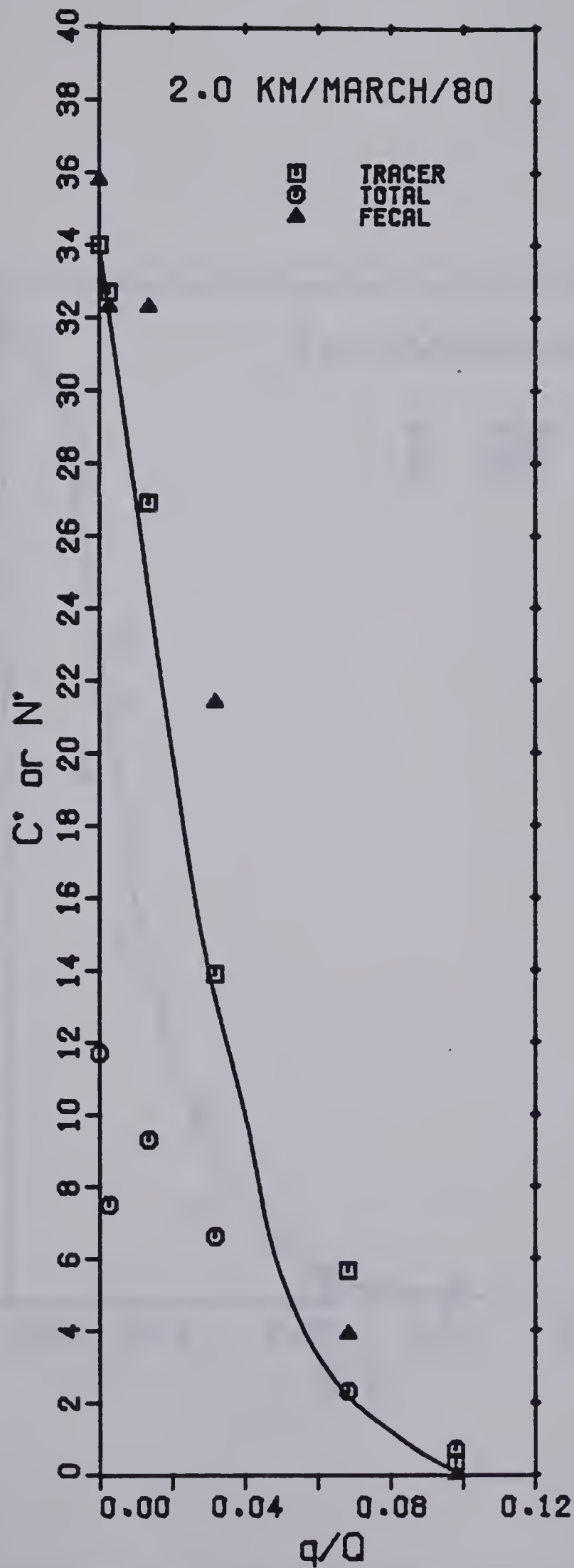


Figure 4.10(b) Dimensionless Tracer and Microorganism Concentrations  
March 1980





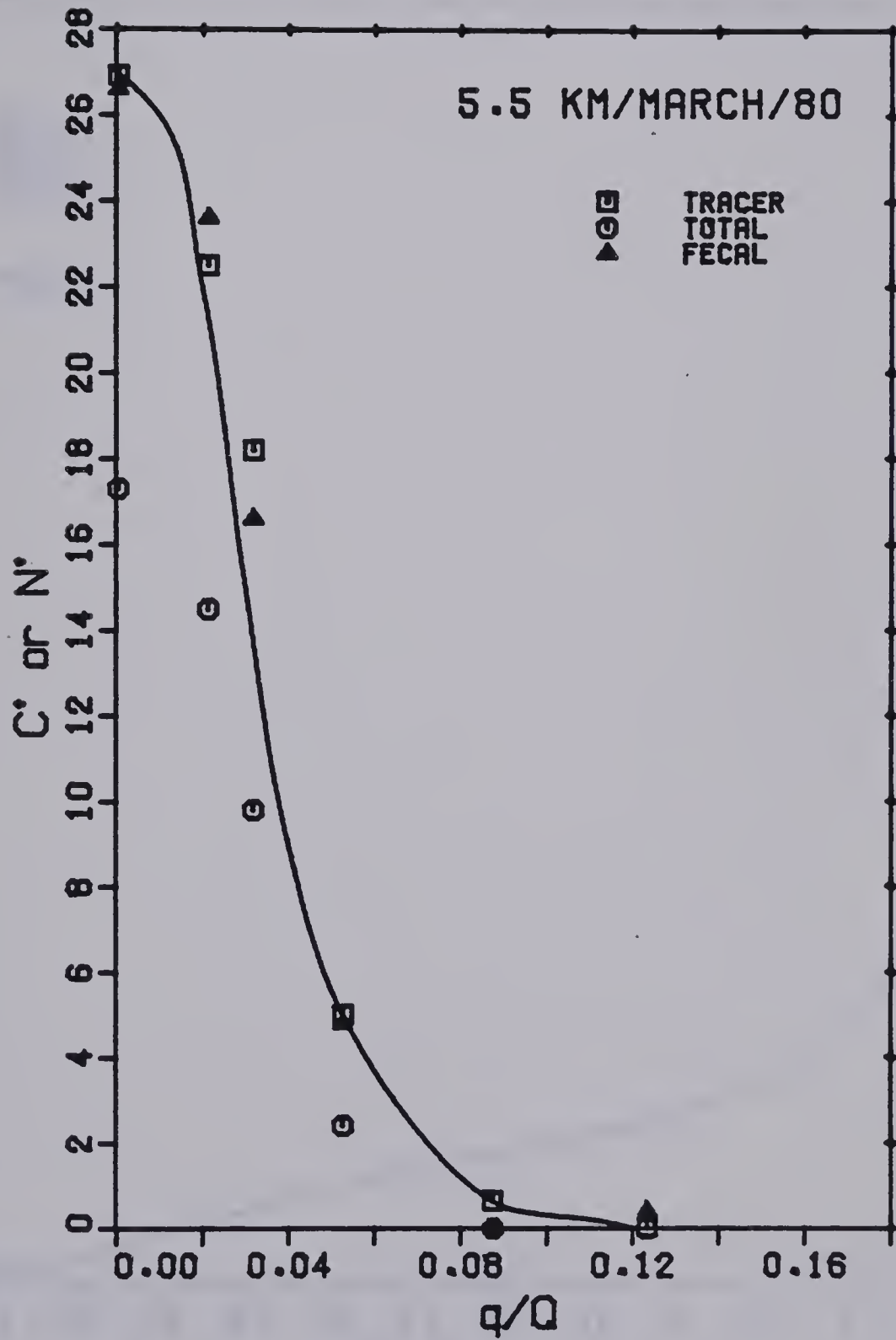


Figure 4.10(c) Dimensionless Tracer and Microorganism Concentrations  
March 1980



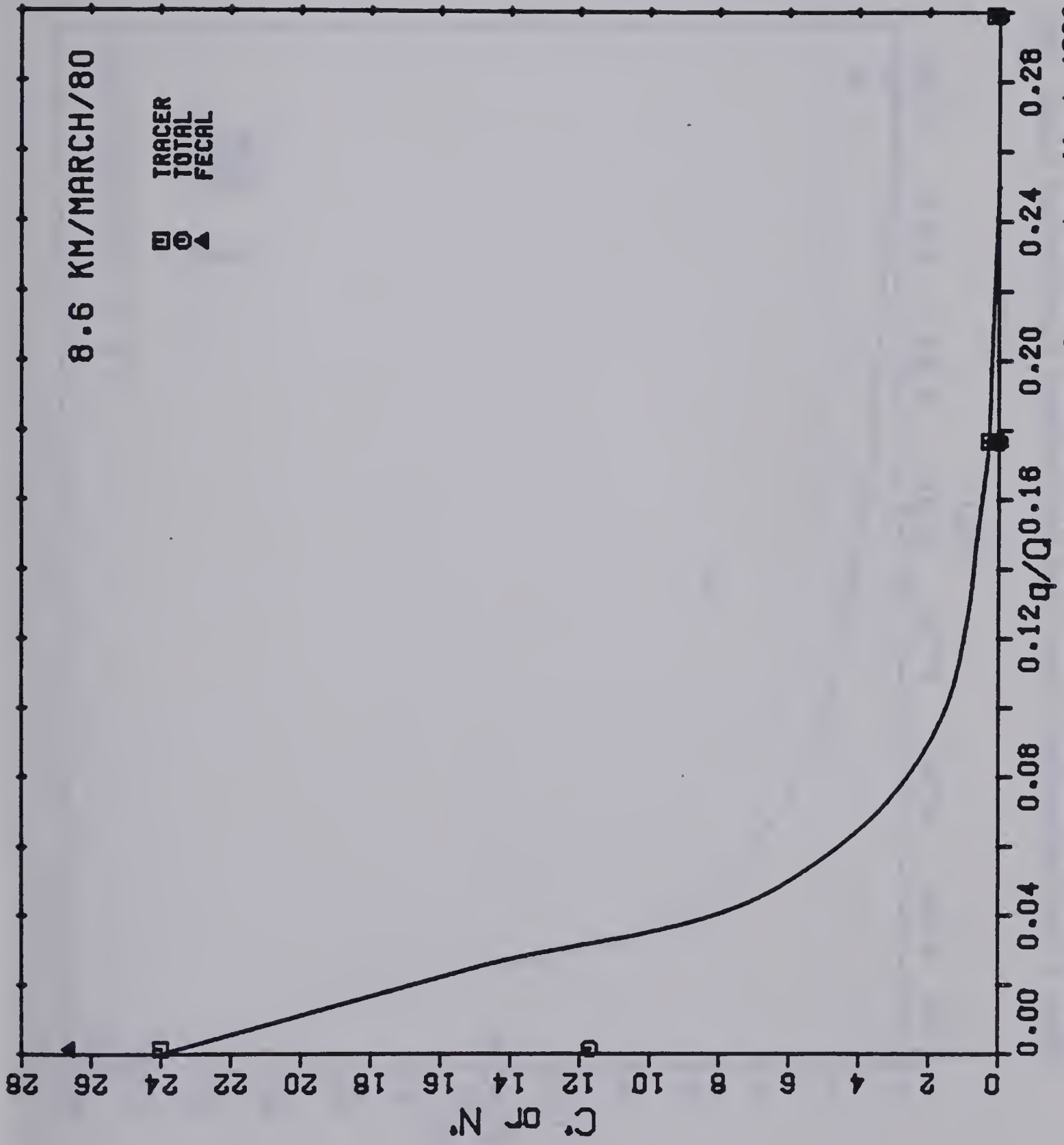


Figure 4.10(d) Dimensionless Tracer and Microorganism Concentrations March 1980



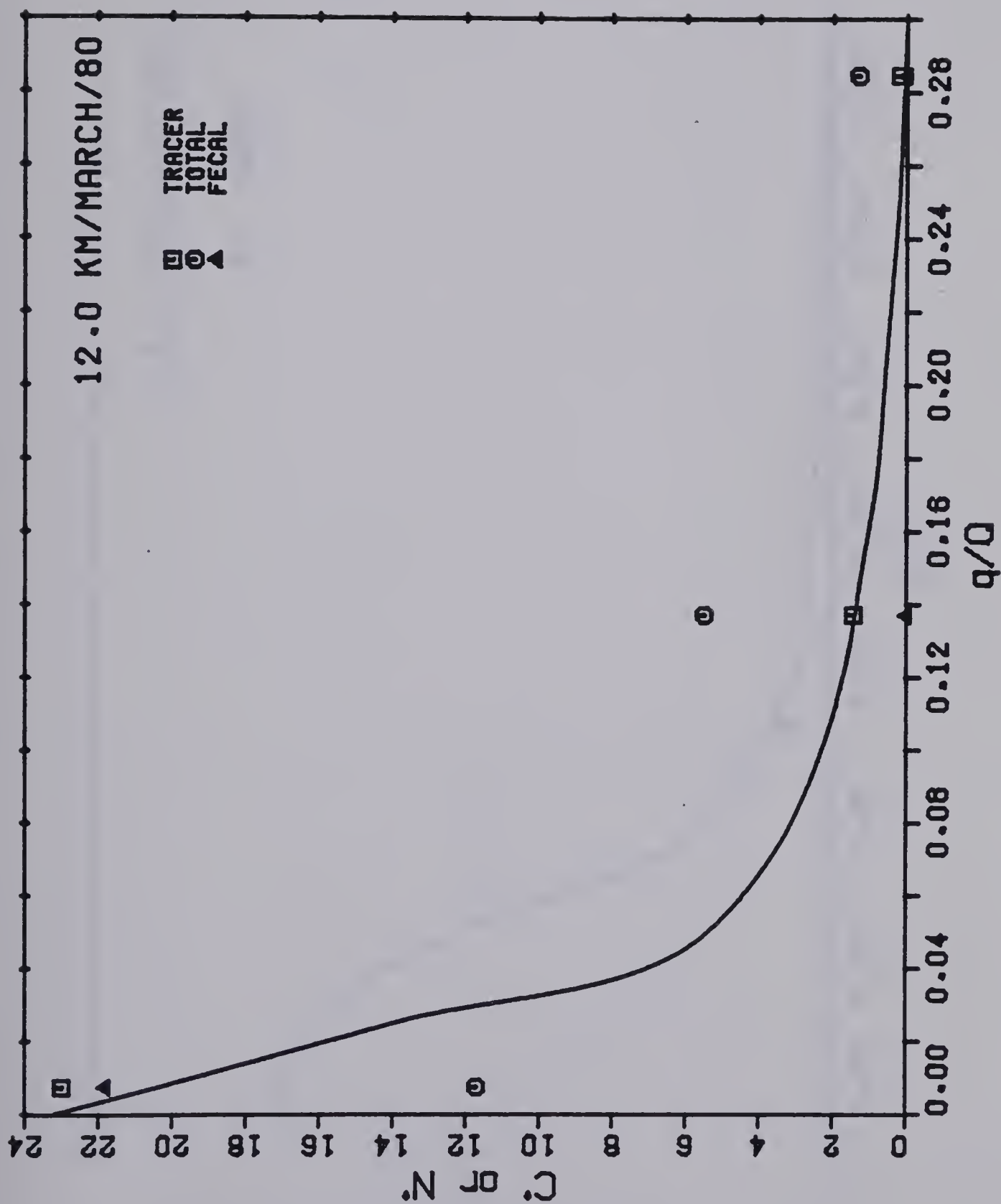


Figure 4.10(e) Dimensionless Tracer and Microorganism Concentrations March 1980





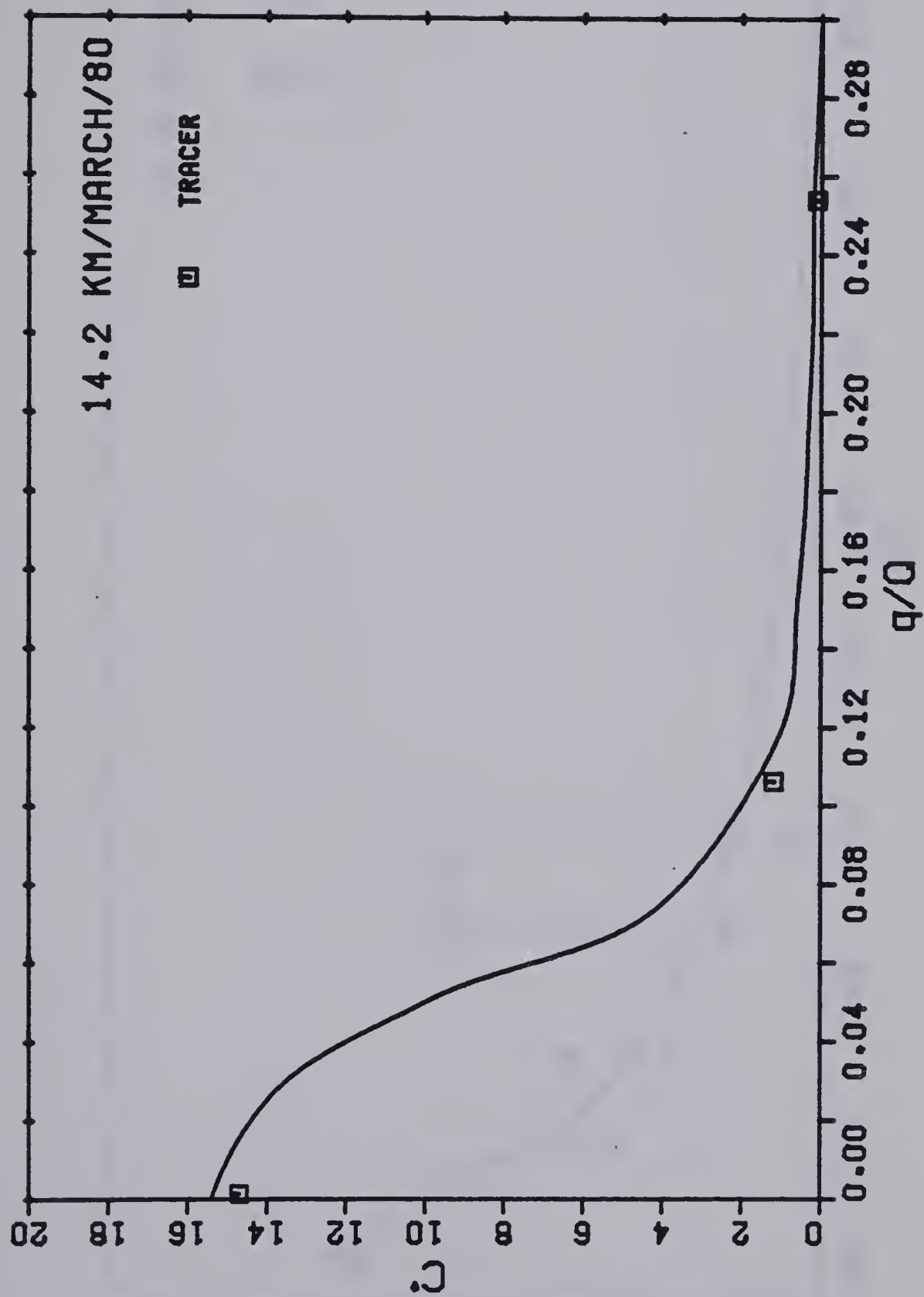


Figure 4.10(f) Dimensionless Tracer and Microorganism Concentrations March 1980



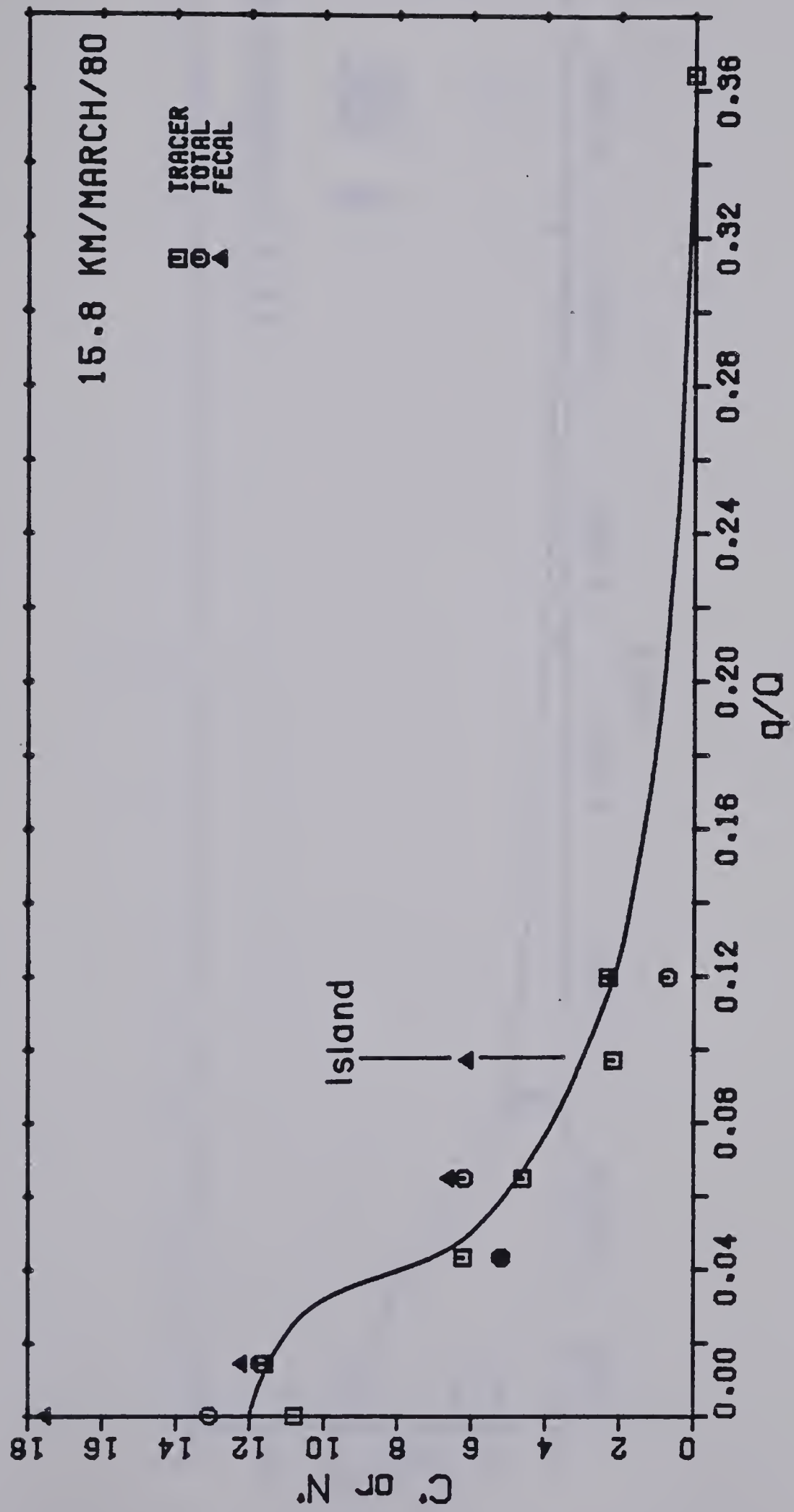


Figure 4.10(g) Dimensionless Tracer and Microorganism Concentrations March 1980



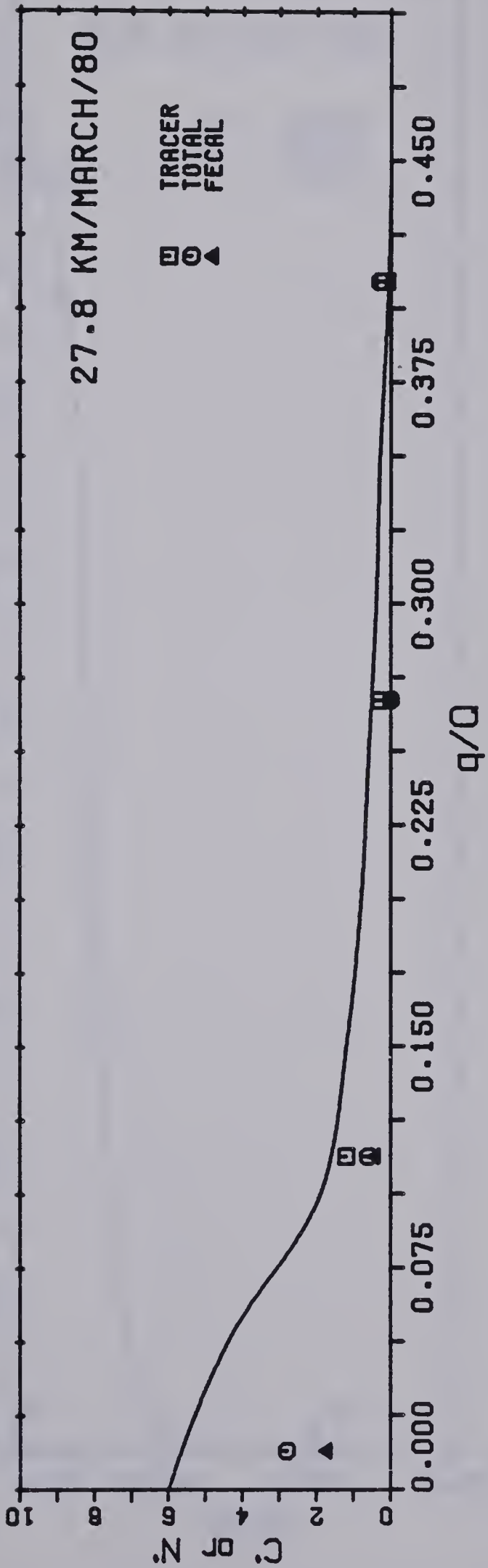


Figure 4.10(h) Dimensionless Tracer and Microorganism Concentrations March 1980



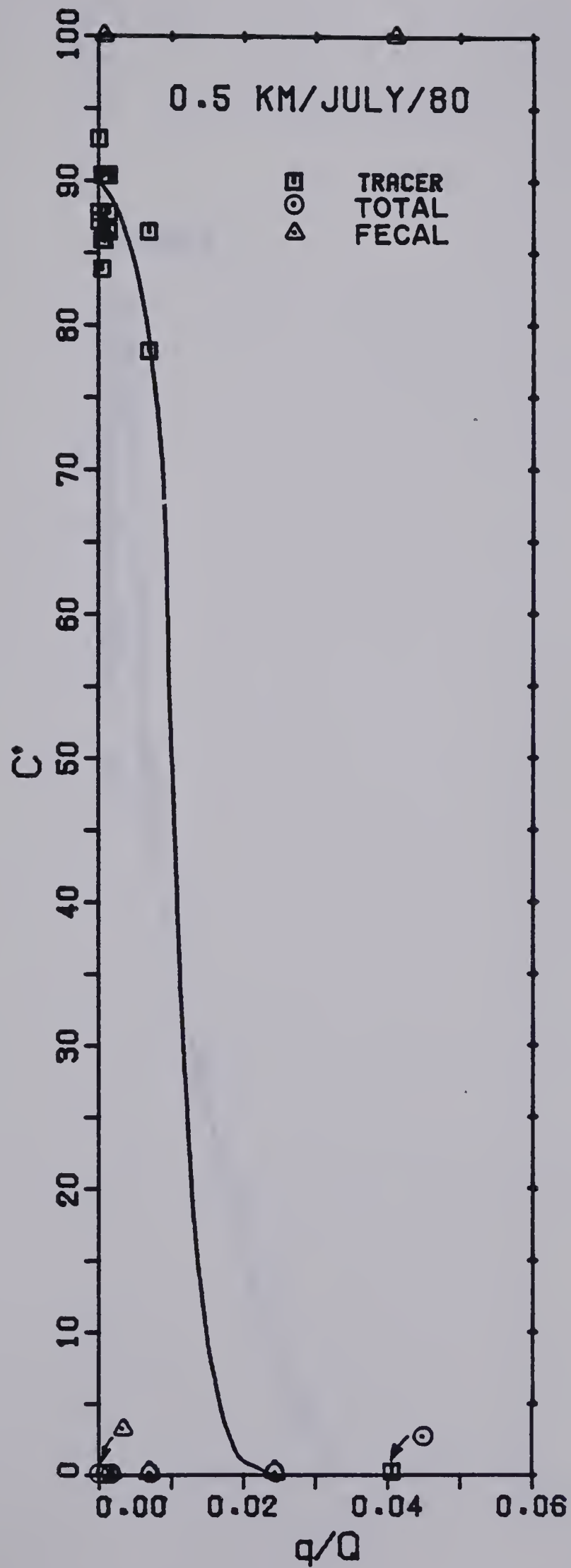


Figure 4.11(a) Dimensionless Tracer and Microorganism Concentrations  
 July 1980





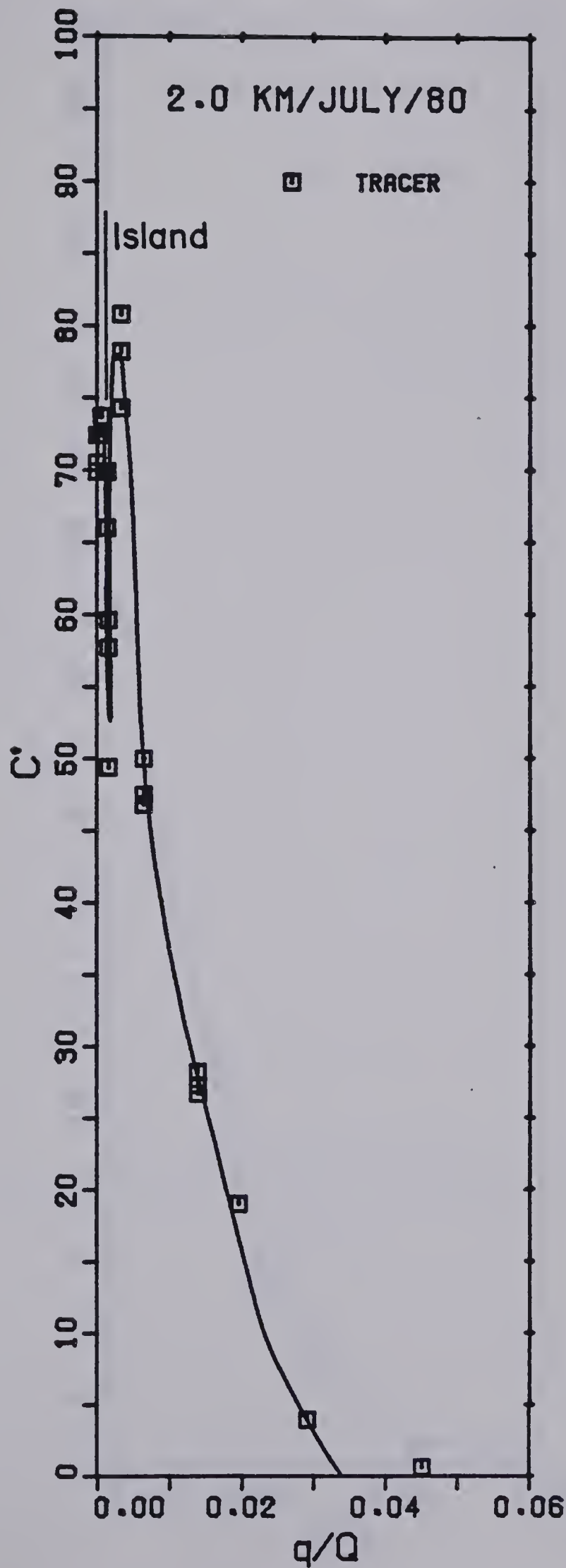


Figure 4.11(b) Dimensionless Tracer and Microorganism Concentrations  
July 1980



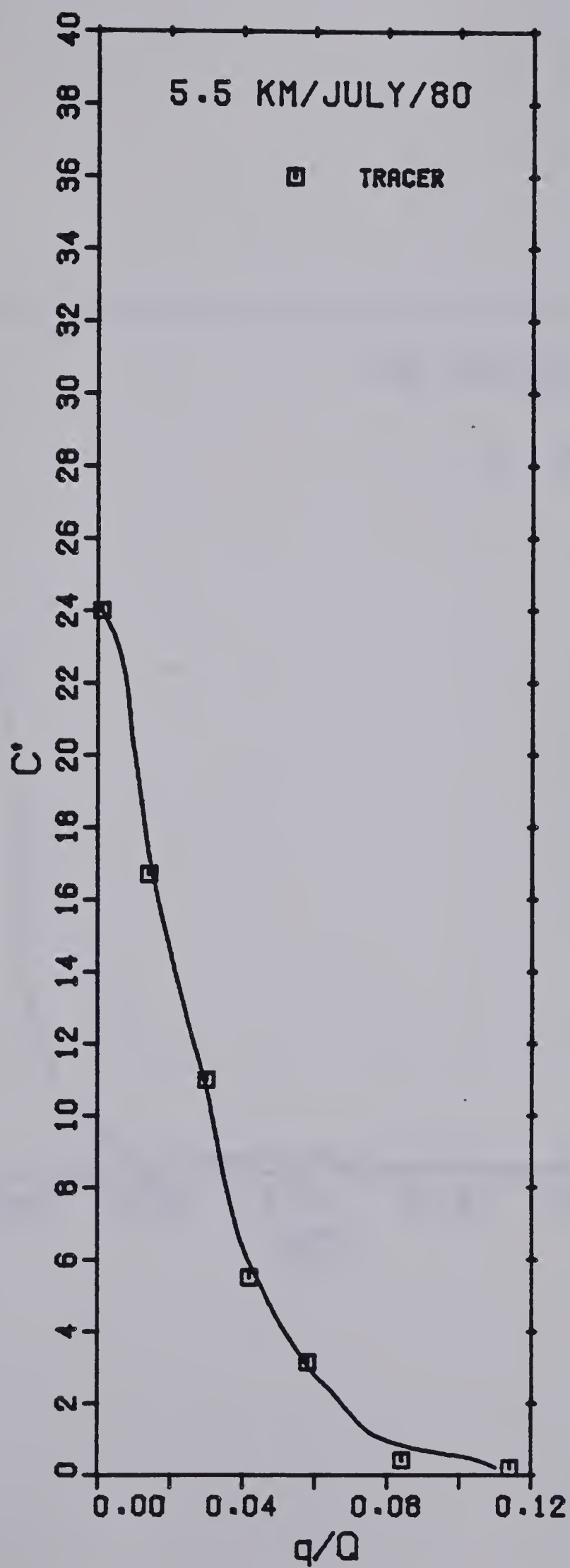


Figure 4.11(c) Dimensionless Tracer and Microorganism Concentrations  
July 1980



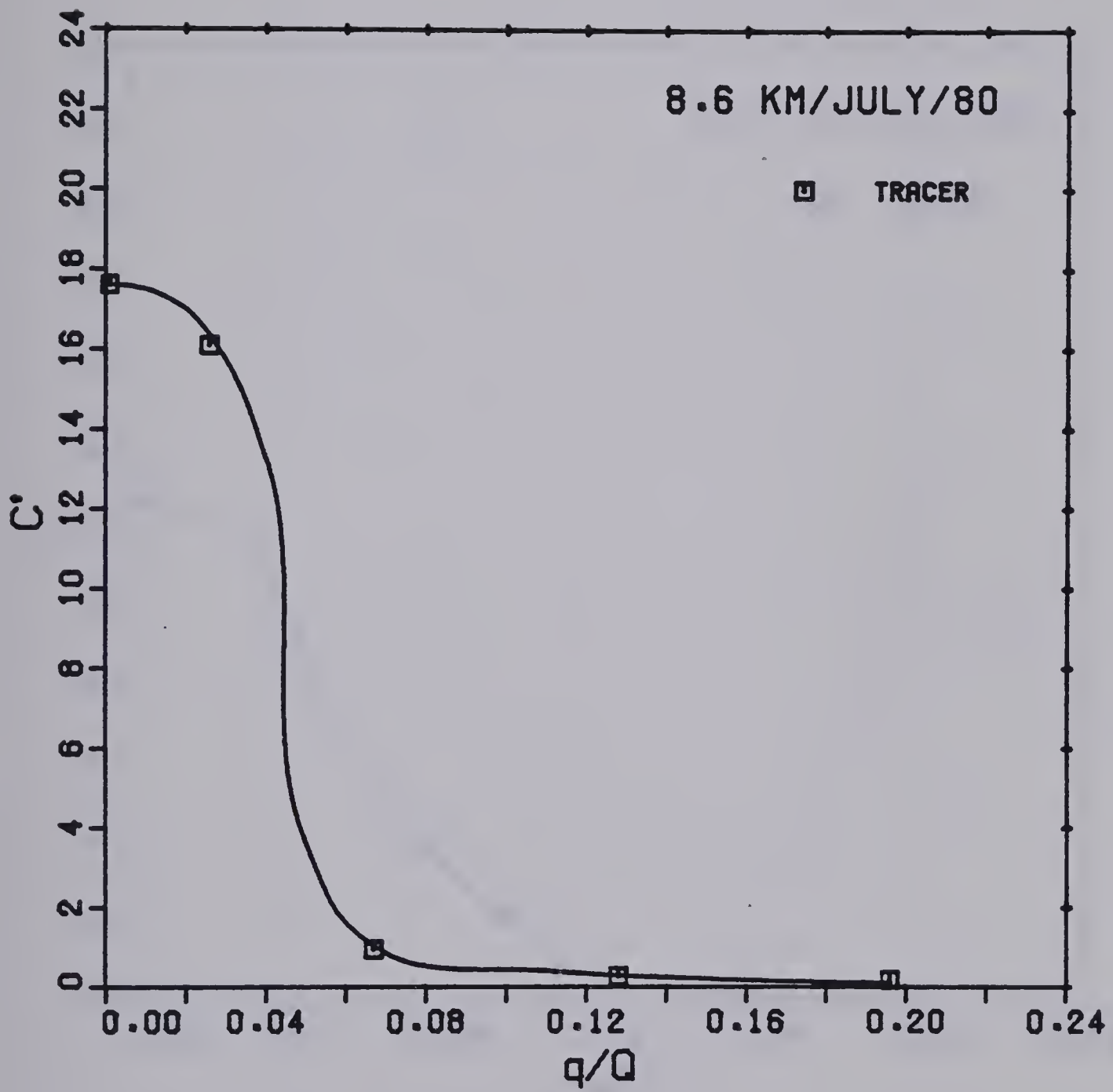


Figure 4.11(d) Dimensionless Tracer and Microorganism Concentrations  
July 1980





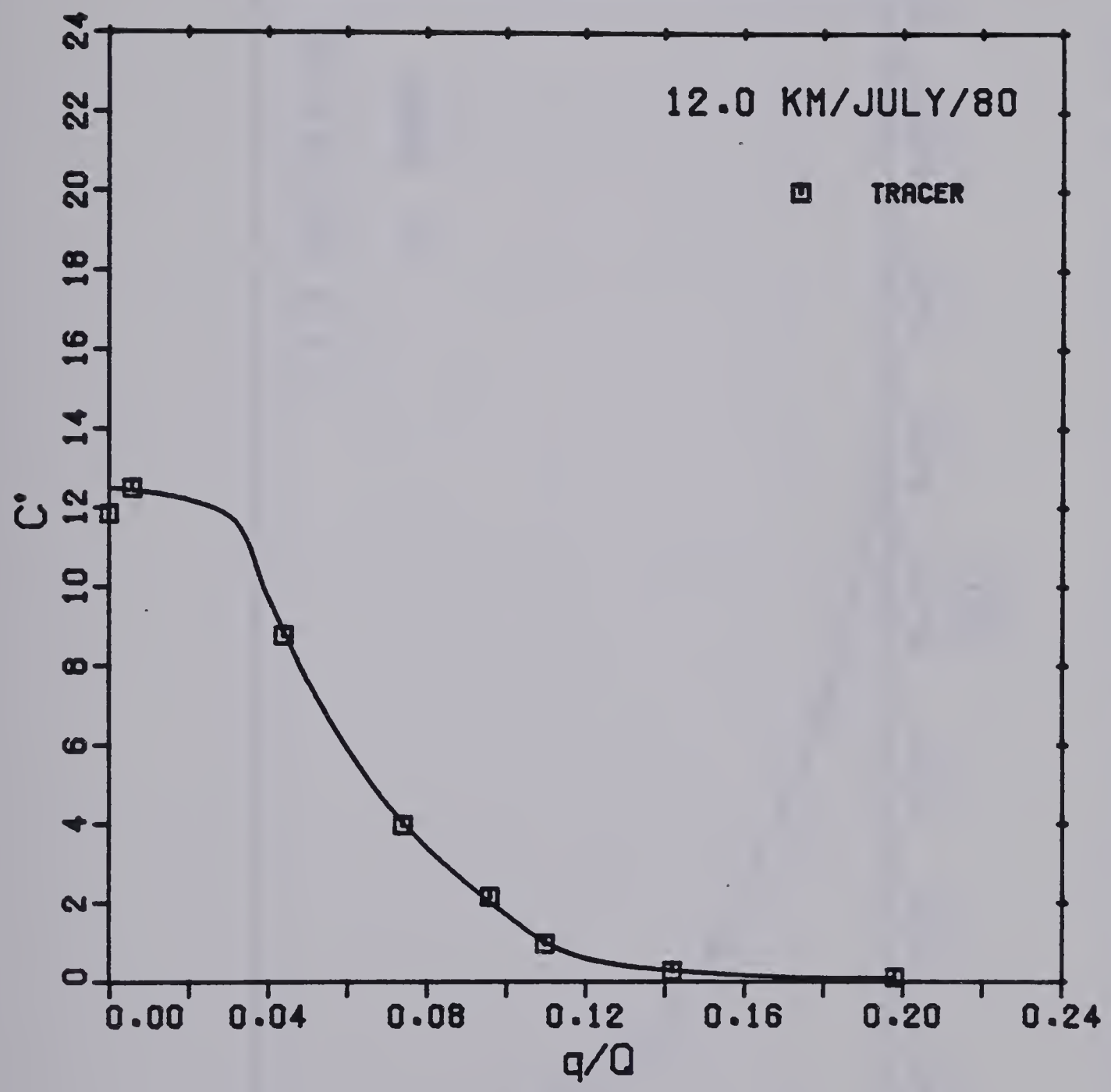


Figure 4.11(e) Dimensionless Tracer and Microorganism Concentrations  
July 1980



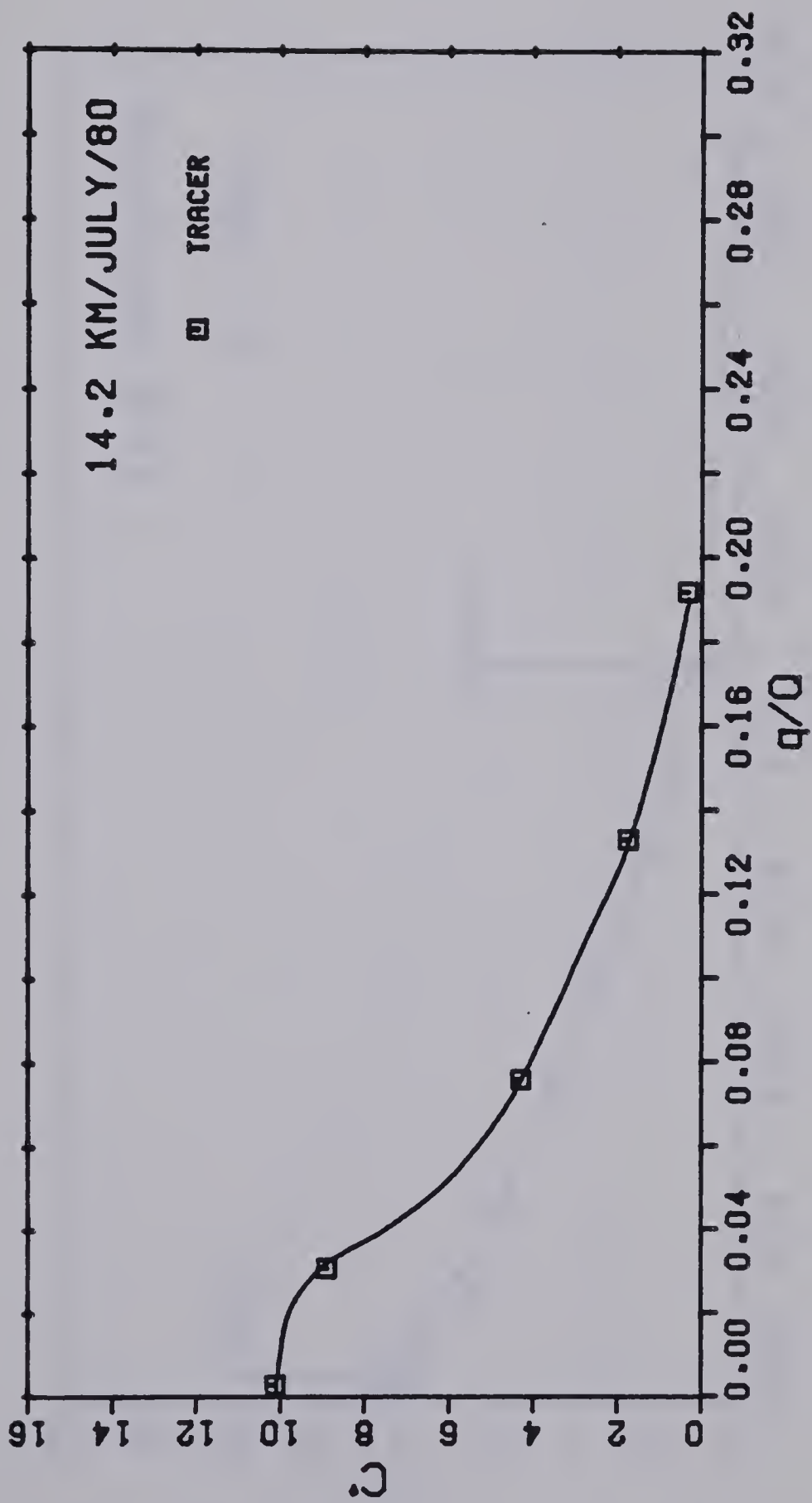


Figure 4.11(f) Dimensionless Tracer and Microorganism Concentrations July 1980



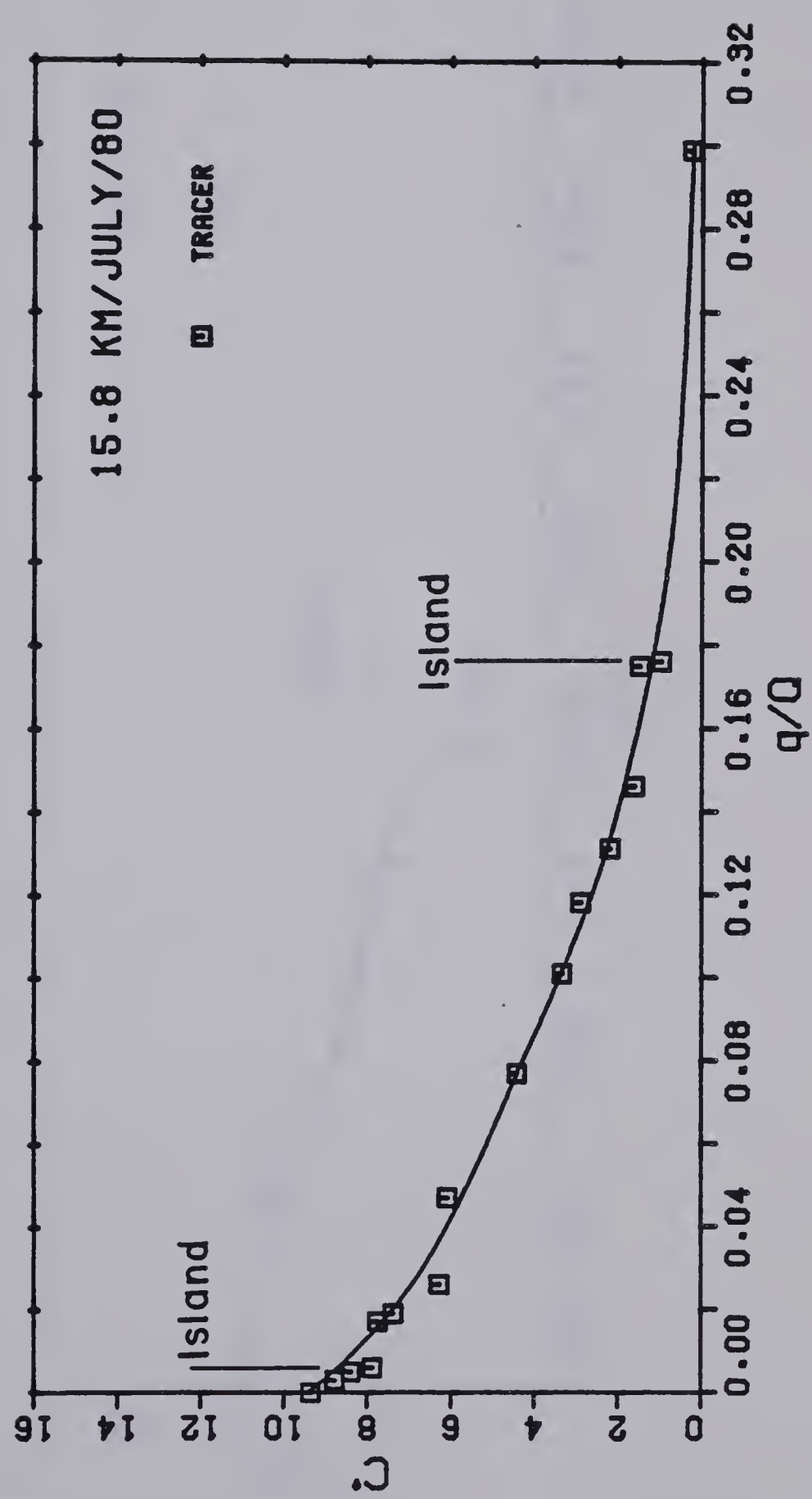


Figure 4.11(g) Dimensionless Tracer and Microorganism Concentrations July 1980



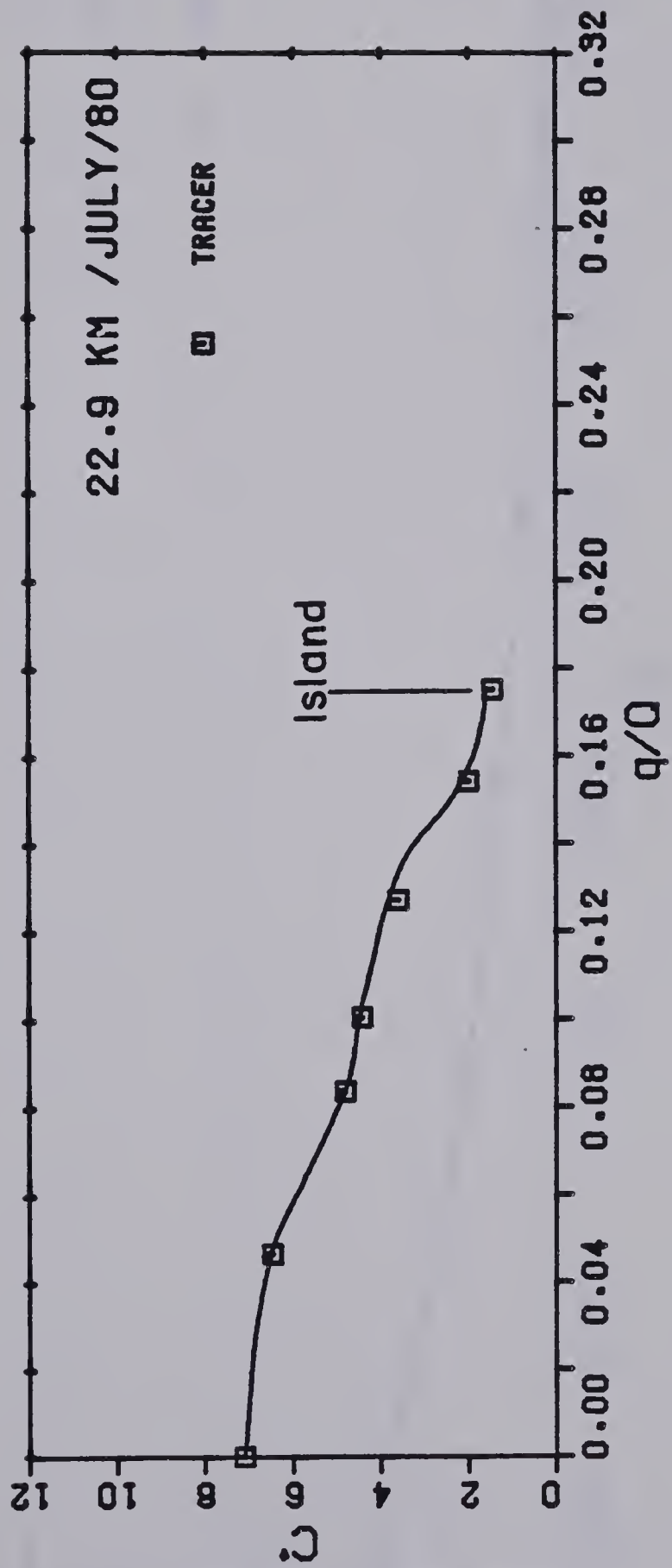


Figure 4.11(h) Dimensionless Tracer and Microorganism Concentrations July 1980





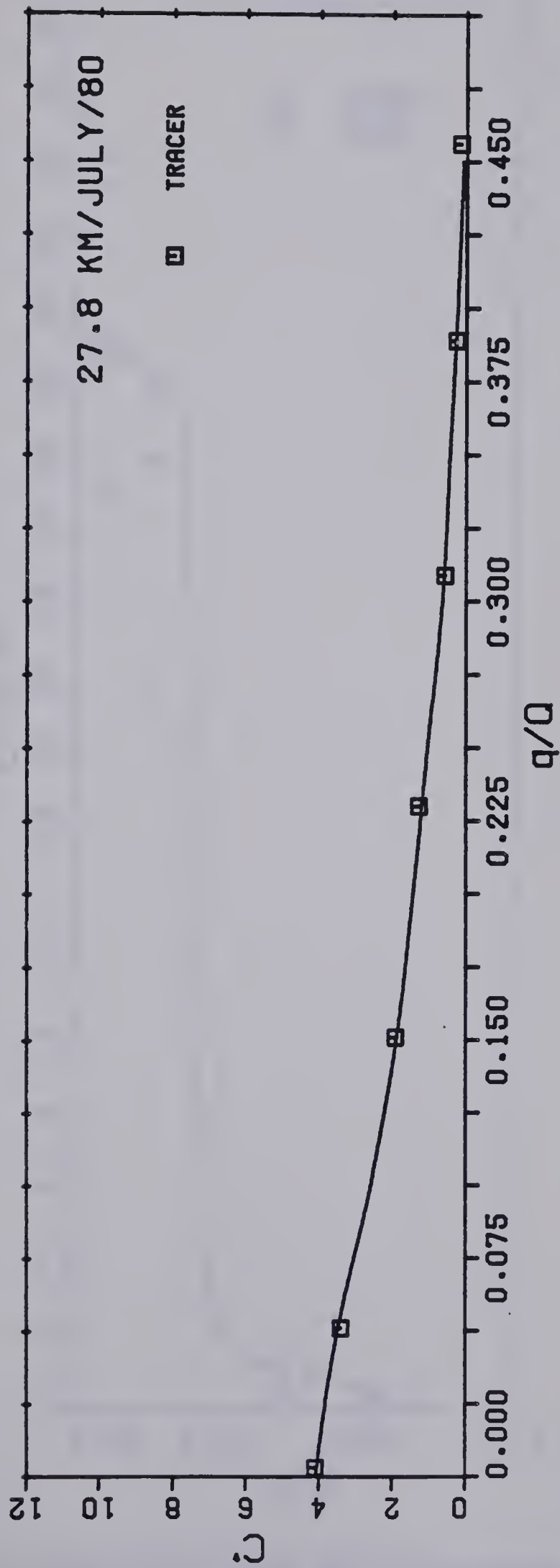


Figure 4.11(i) Dimensionless Tracer and Microorganism Concentrations July 1980



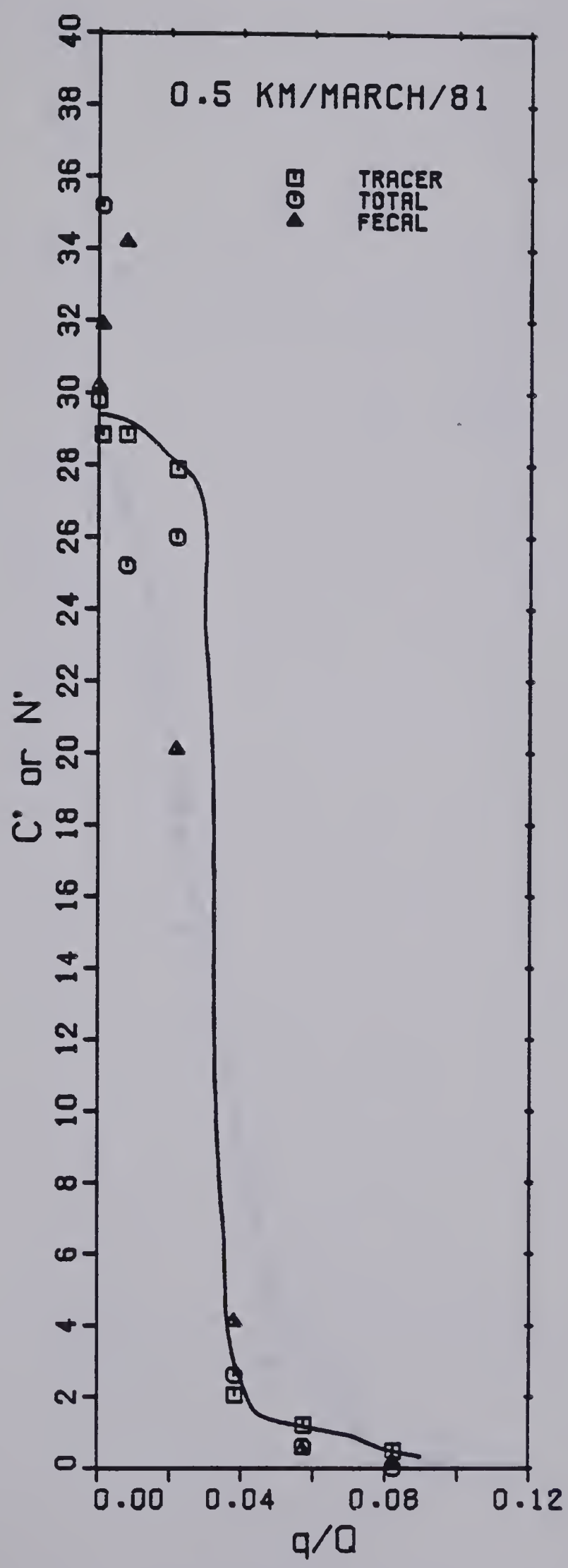


Figure 4.12(a) Dimensionless Tracer and Microorganism Concentrations  
March 1981



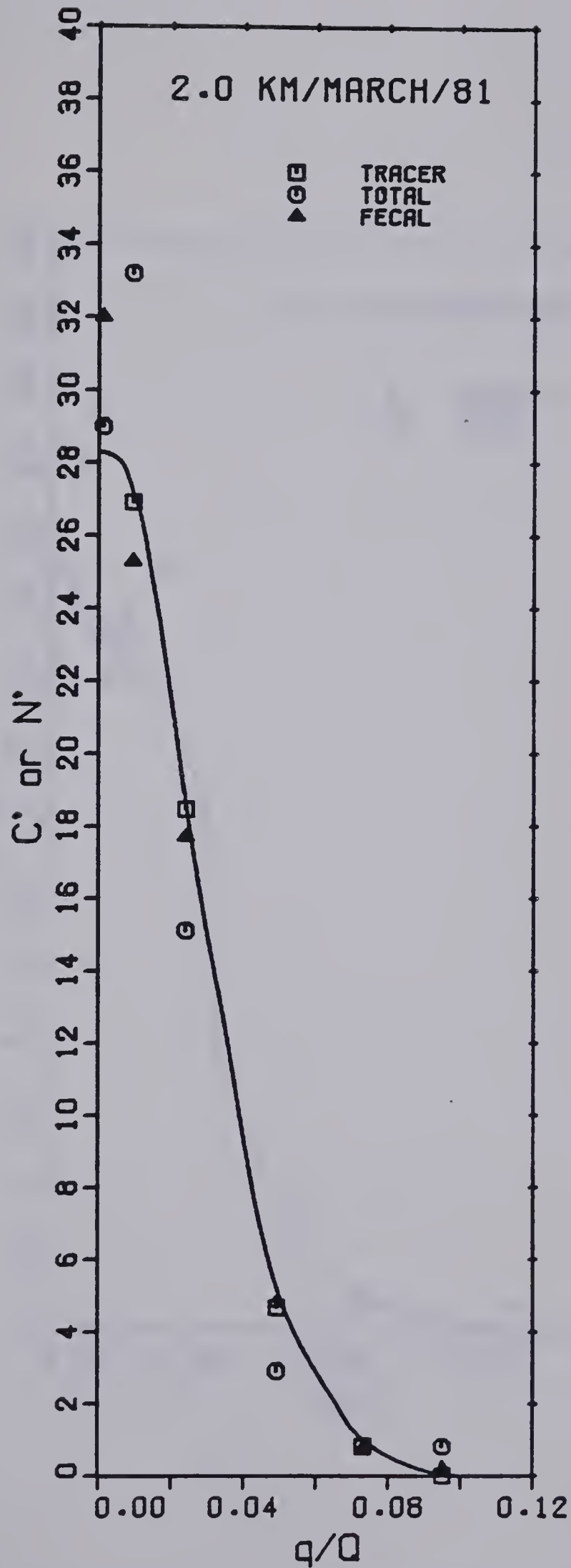


Figure 4.12(b) Dimensionless Tracer and Microorganism Concentrations  
March 1981





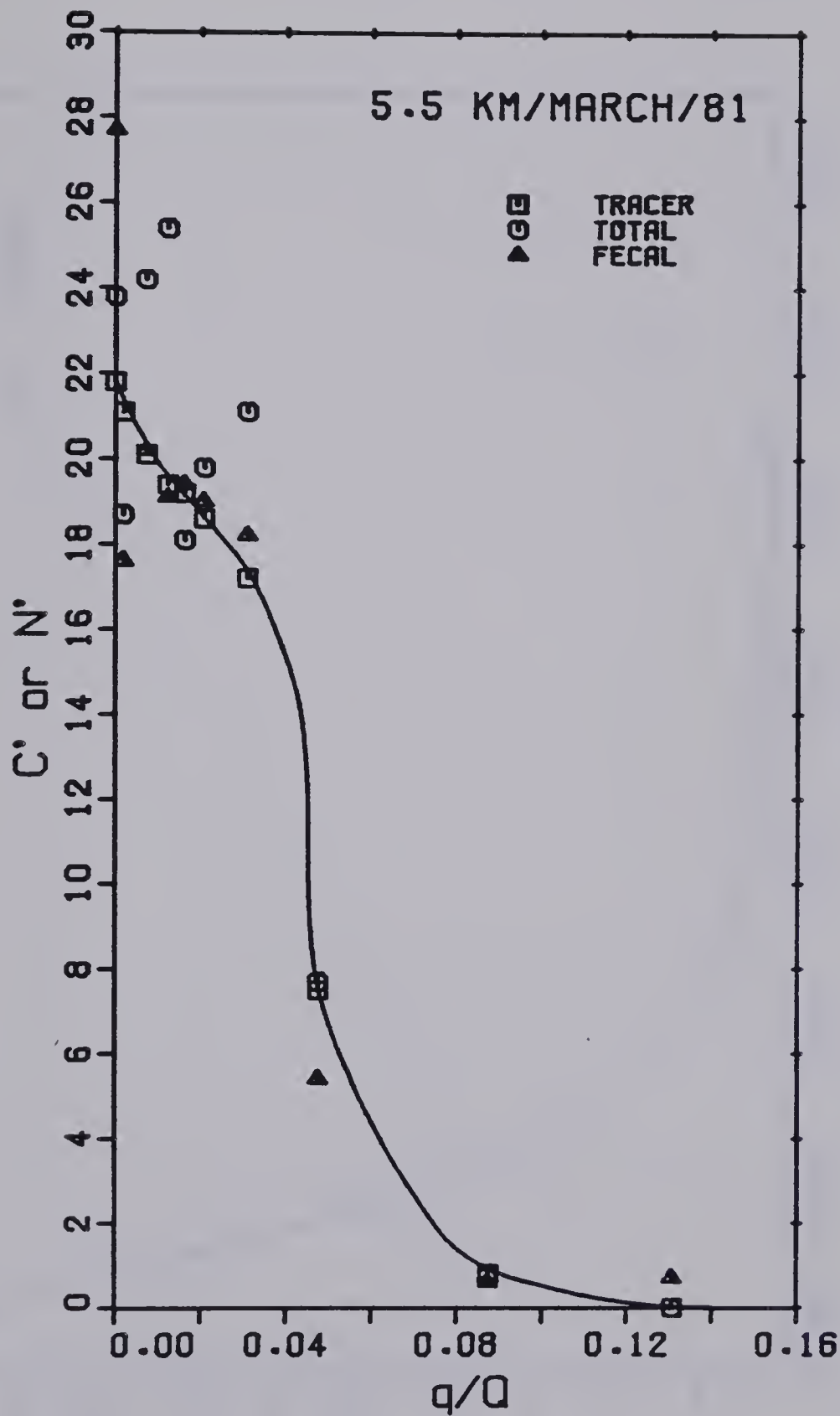


Figure 4.12(c) Dimensionless Tracer and Microorganism Concentrations  
March 1981



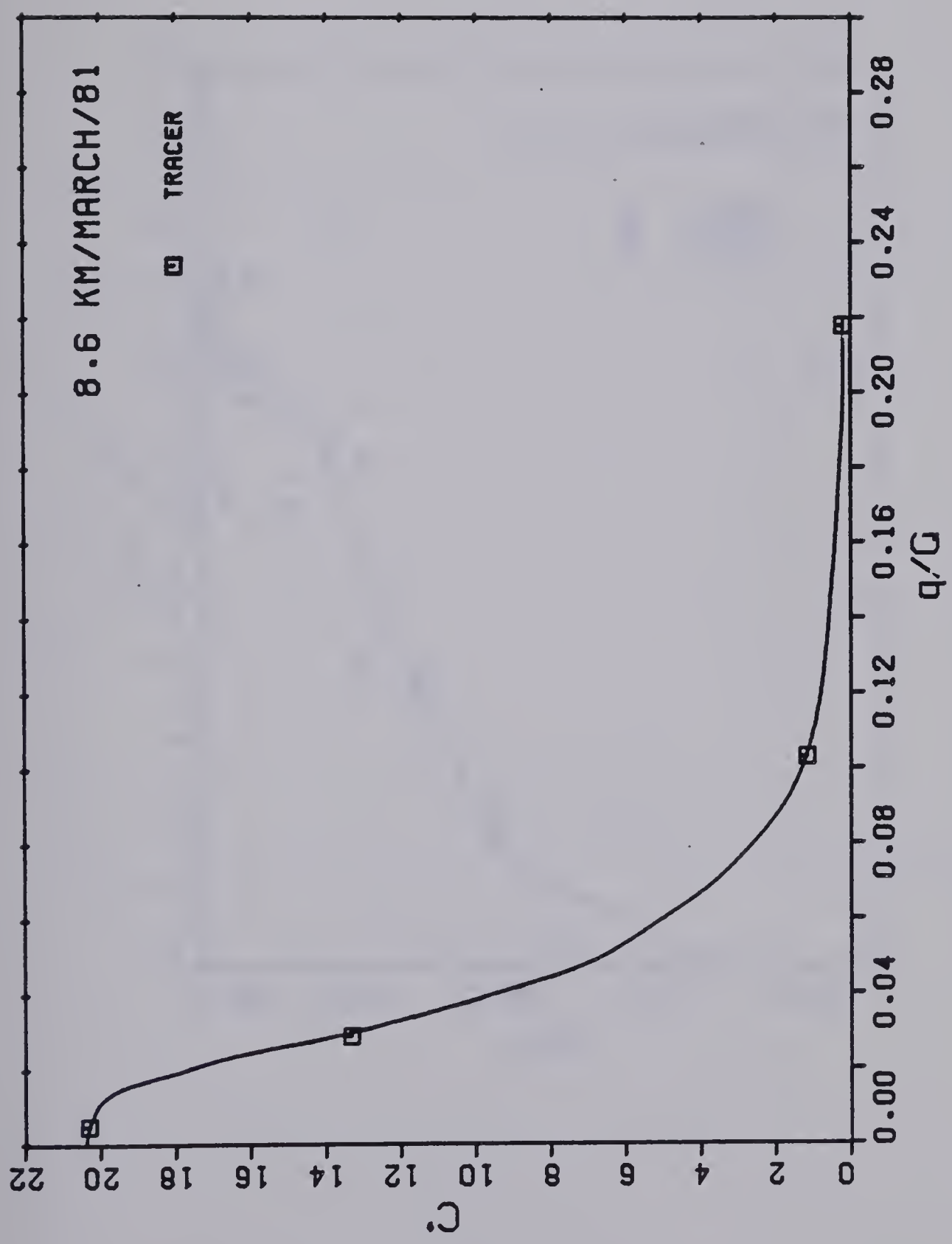


Figure 4.12(d) Dimensionless Tracer and Microorganism Concentrations March 1981



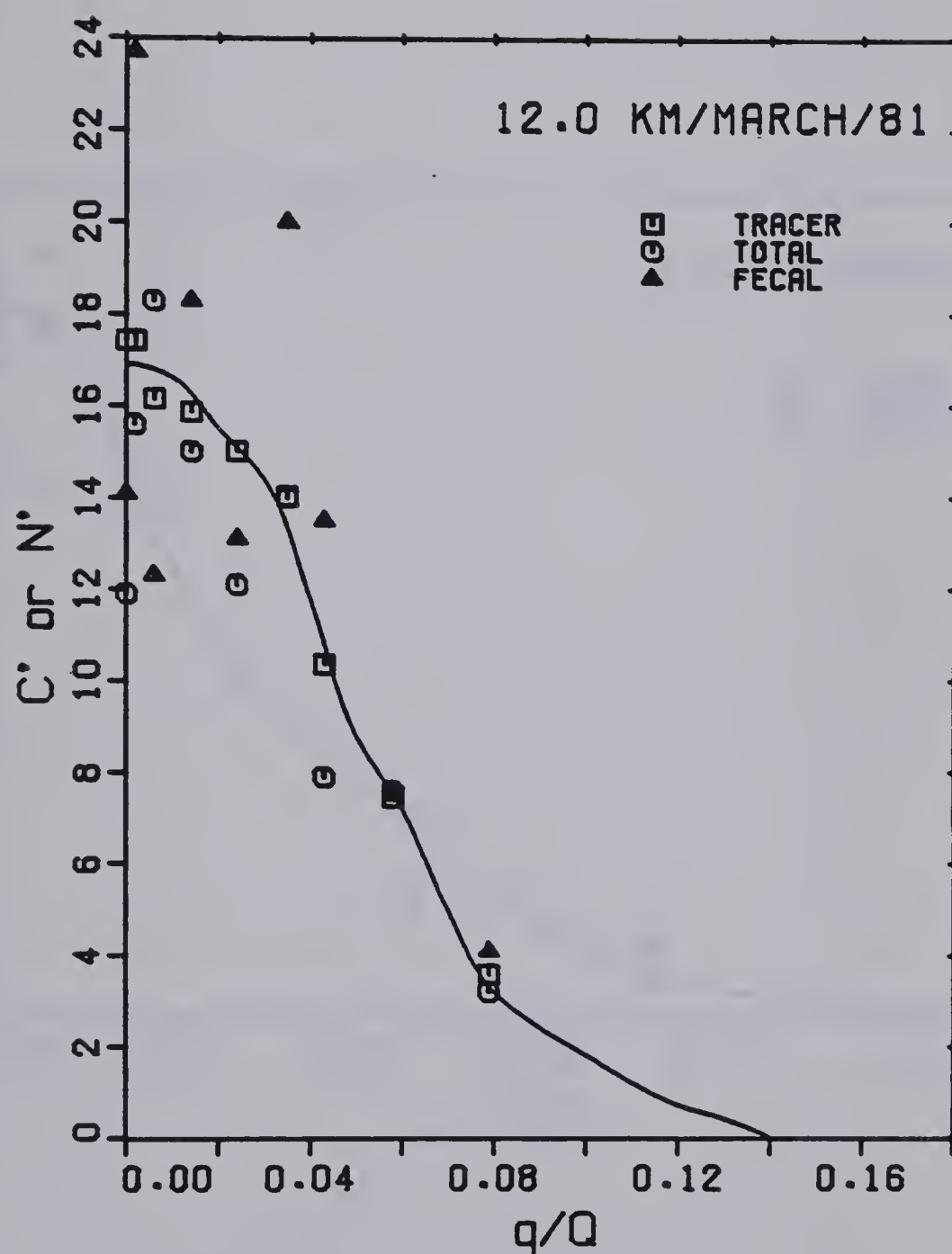


Figure 4.12(e) Dimensionless Tracer and Microorganism Concentrations  
March 1981



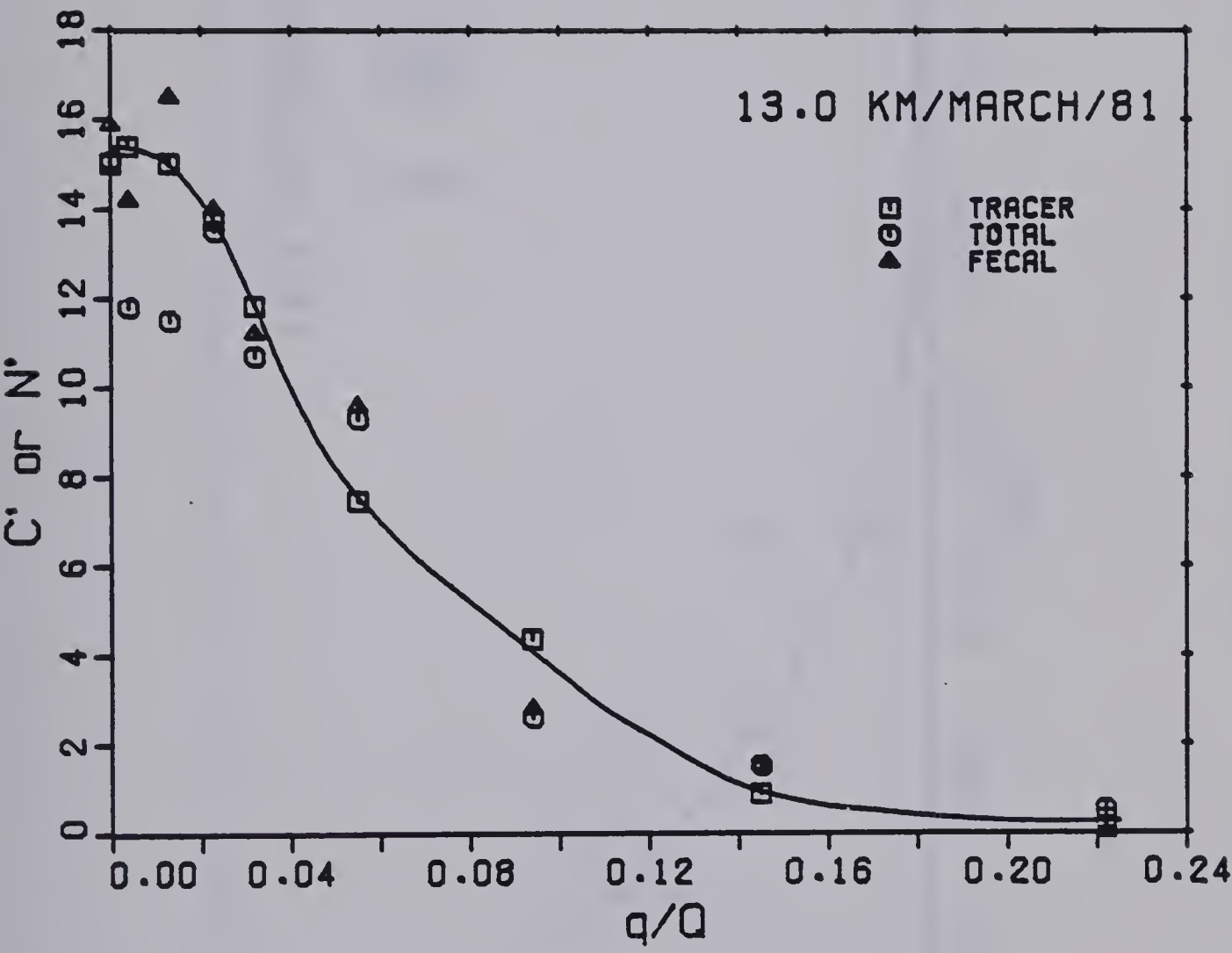


Figure 4.12(f) Dimensionless Tracer and Microorganism Concentrations  
March 1981





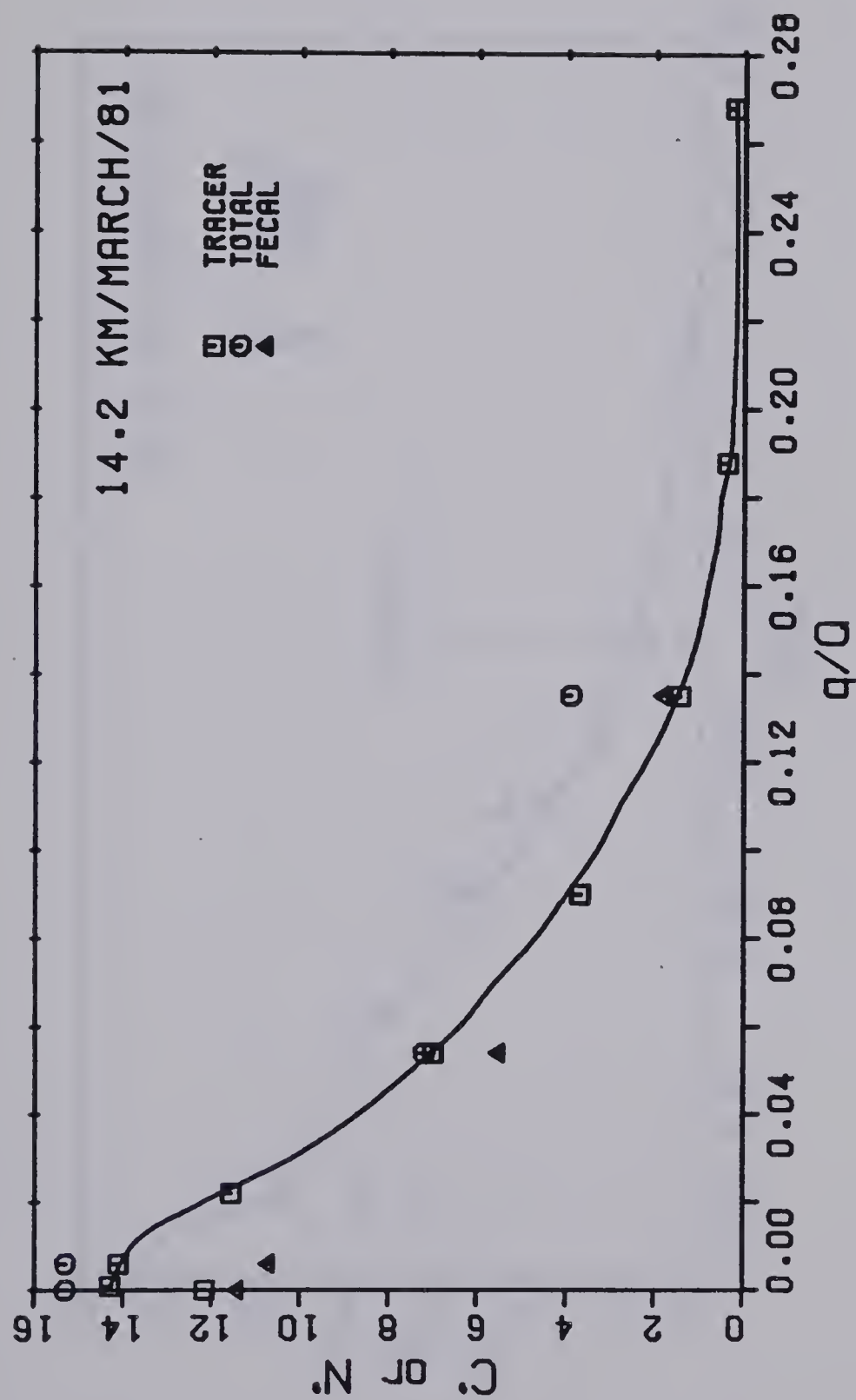


Figure 4.12(g) Dimensionless Tracer and Microorganism Concentrations March 1981



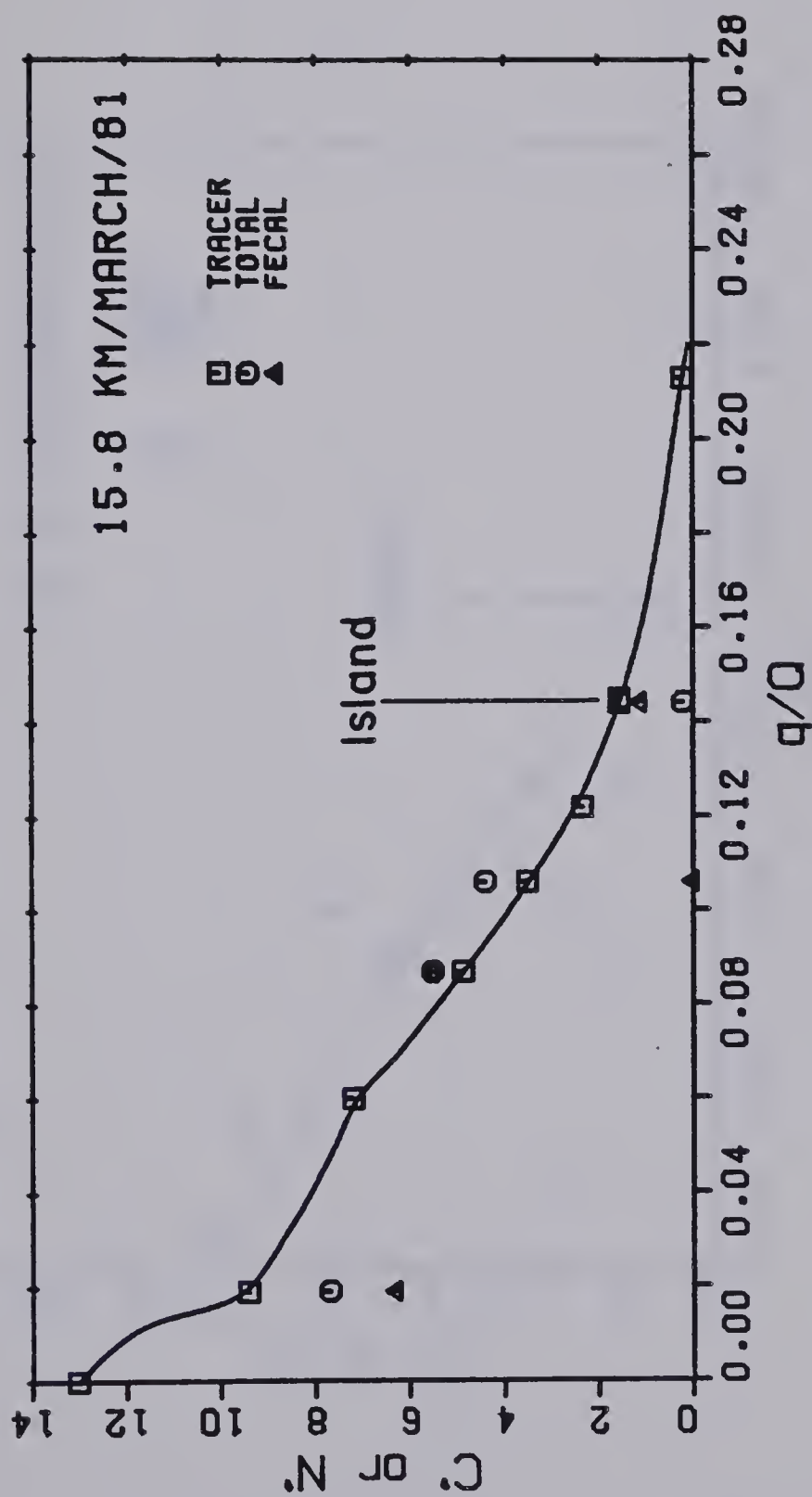


Figure 4.12(h) Dimensionless Tracer and Microorganism Concentrations March 1981



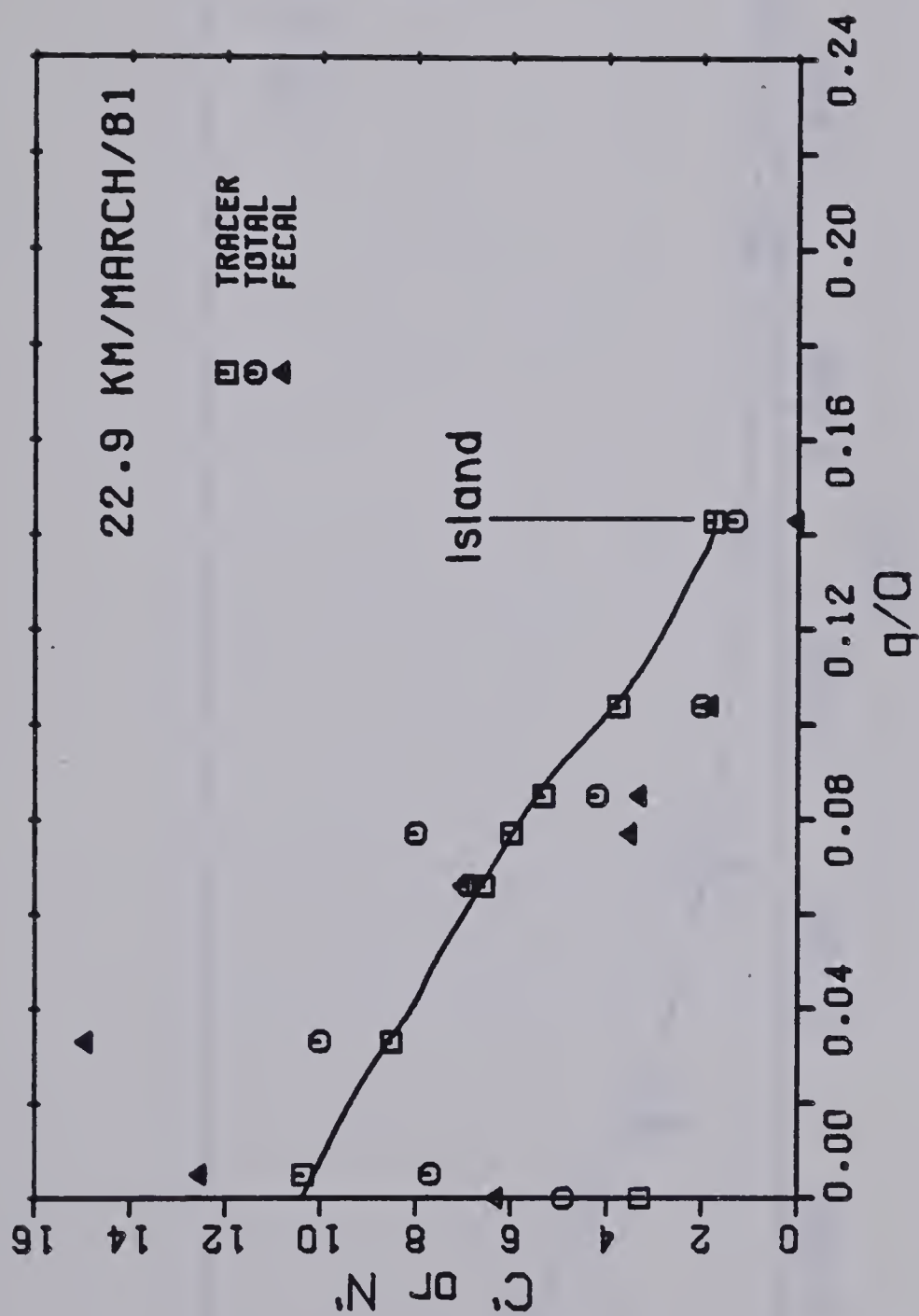


Figure 4.12(i) Dimensionless Tracer and Microorganism Concentrations March 1981





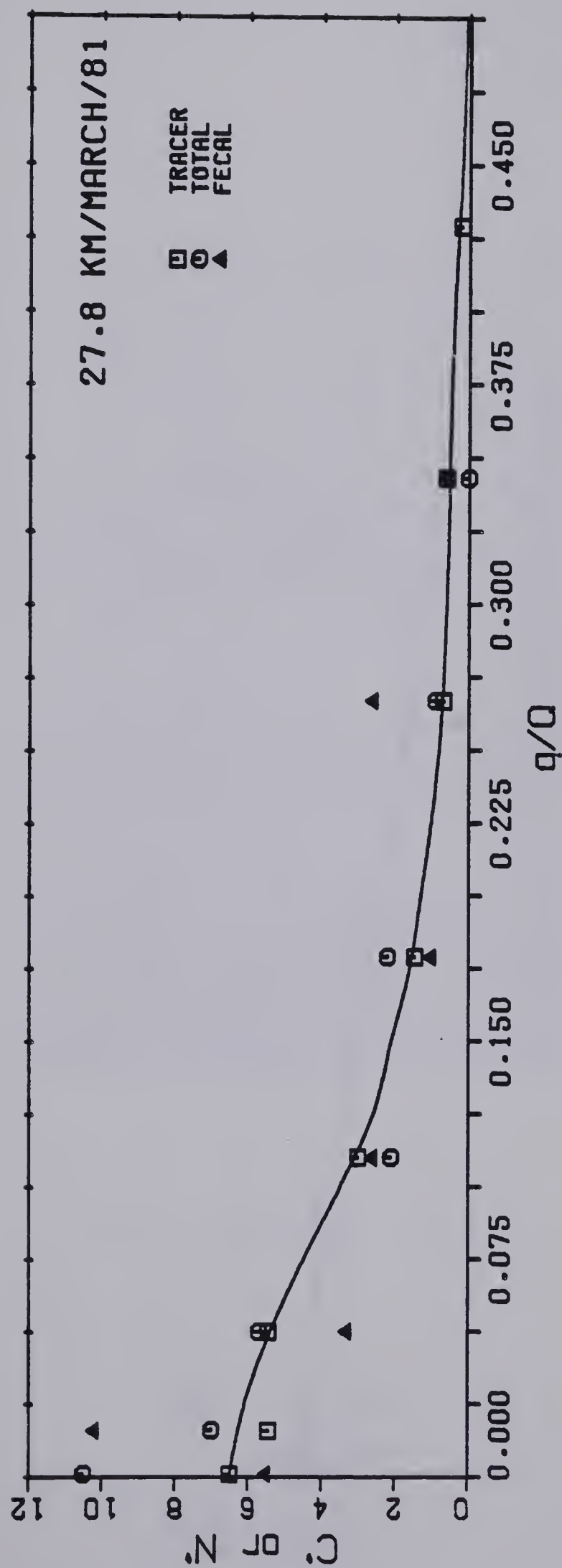


Figure 4.12(j) Dimensionless Tracer and Microorganism Concentrations March 1981



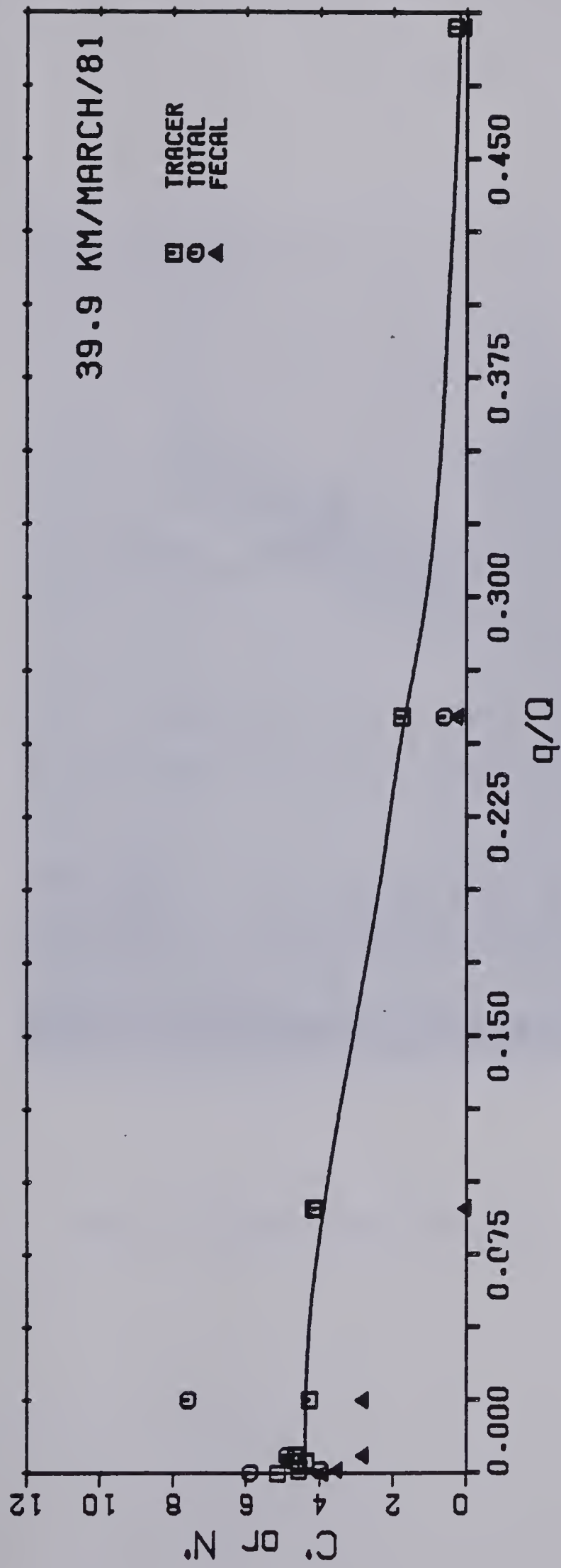


Figure 4.12(k) Dimensionless Tracer and Microorganism Concentrations March 1981





Plate 4.13 Bacteriological Sampling



lid underside were not touched during the sampling procedure. No investigations into possible contamination due to contact with the stopper were conducted. Raw effluent samples from the manhole located on the outfall line were also collected for analysis. Following sampling the bottles were immediately placed in an insulated container for storage and shipment to the laboratory for analysis.

A critical component of the bacteriological sampling was transporting the samples from the river to the laboratory. The relatively isolated location of Fort Smith and the absence of adequate laboratory facilities during the winter tests required transport of the samples by air 700 km south to Edmonton for analysis. Table 4.3 lists the activities and estimated delays between sampling and analysis at the Environmental Protection Service Laboratory in Edmonton. The elapsed times listed in the table represent maximums and in general analysis was begun within the recommended 8 hour period following sampling. Mobile laboratory facilities of the Environmental Protection Service were available for the summer test and these samples were analysed in Fort Smith within 3 to 4 hours after collection.

### Laboratory Analysis and Results

Total coliform, fecal coliform, fecal streptococci, and 20° and 30° C standard plate counts were enumerated by





Table 4.3 Bacteriological Sample Time Information for Winter Tests

Activity	Time Period	Elapsed Time , hr
Collection	8:00 to 11:30	1-3.5
Transport to Airport	11:30 to 12:30	1.0
Air Travel to Edmonton	12:30 to 15:00	2.5
Delivery to Laboratory	15:00 to 16:00	1.0
Laboratory Work	16:00 to 20:00	1-4.0



membrane filtration procedures according to **Standard Methods** 909A, 909C, 910B and 907 at specified temperatures for each sample.<sup>1</sup> Total and fecal coliform concentrations were selected for decay analysis because they are better indicators of enteric wastes than the total plate counts. Although fecal streptococci are an excellent indicator of recent fecal contamination their low raw effluent concentration caused rapid dilution to background levels within the river rendering them unsuitable for decay analysis. Geometric averages of the measured concentrations of fecal and total coliforms at each sampling locations are given in Appendix V along with estimated values of the river background concentrations.

The raw effluent concentrations of total and fecal coliforms measured during the summer test were extremely low indicating high efficiency of treatment in the lagoon system. Unfortunately even the limited dilution between the outfall and 0.5 km was sufficient to reduce the indicator concentrations to levels which are masked by the variation in background values. Although decay undoubtedly occurs during summer conditions it is impossible to evaluate with the present data due to the high effluent quality and dilution effects.

-----  
<sup>1</sup> Davenport, Sparrow, and Gordon (1976) maintain the membrane filter technique has a high degree of precision for enumerating indicator bacteria in river water samples and with good laboratory technique the errors contributing to the distribution of enumeration data may be minimized.



To evaluate microorganism decay it is necessary to first know the rate at which microorganisms are discharged to the river (the total microorganism flux). The total flux may be determined by measurement of the raw effluent flow and microorganism concentration.

The raw effluent concentrations measured are listed in Appendix V and the geometric mean of the measurements are given in Table 4.4. The lagoon effluent concentration was assumed constant and equal to the geometric mean since fluctuations in input concentration to the lagoon system would not be detectable after 90 days of retention. Originally effluent flow was to be measured at a sharp crested weir installed along the outfall line. However mass balance analysis of tracer samples taken during the March 1980 test from the outfall line downstream of the injection point indicated the weir calibration was in error, probably due to the approach velocity. Observation of the head on the weir was still useful in that it indicated the effluent flow was nearly constant for all three sampling periods. The size of the lagoon system evidently was sufficiently large enough to dampen out fluctuations of the input flow.

Effluent flow for the March 1980 test was calculated using mass balance of the effluent tracer concentration compared to the injected tracer concentration and flow. Unfortunately during the March 1981 test the downstream manhole was not accessible and tracer samples could not be taken. The fully mixed microbial concentrations for this





Table 4.4 Effluent Parameters

Test	Effluent Flow L/s	River Flow cms	Concentration*			
			Effluent		Fully Mixed**	
			TC	FC	TC	FC
March 1980	11.0	1730	$1.2 \times 10^6$	$3.6 \times 10^5$	7.1	2.3
July 1980	7.4***	3710	5700	3100	.01	.01
March 1981	11.3***	1560	$8.7 \times 10^5$	$3.6 \times 10^5$	6.1	2.7

\* geom avg /100mL  
 \*\* in excess of background  
 \*\*\* estimated flow



test were calculated on the basis of a normalized average flux of bacteria in comparison to the tracer flux at the 0.5 km section. This approach assumes that decay within this distance was negligible for winter conditions.<sup>1</sup> The effluent flow during the summer could only be estimated using the weir measurements and an assumed error due to the approach velocity. The estimated fully mixed microbial concentrations in excess of background are given in Table 4.4 with the effluent flows. The indicator concentrations measured at each section are shown in Figures 4.10, 4.11, and 4.12 in dimensionless form.<sup>2</sup> Calculation of the dimensionless concentrations is identical to the method used for the tracer (Equation 2.24).

The concentration plots for the ice cover tests indicated the microorganism distributions, although subject to some scatter, closely match the tracer distributions, which represent a condition of no decay. As mentioned previously the summer concentrations rapidly drop to background level and are not detectable beyond the section at 0.5 km. Scatter of biological data is common and should be expected since the geometric means were calculated from a limited number of samples. The problem of discerning any decay during the winter tests will be addressed in the next chapter.

-----  
<sup>1</sup> This assumption is supported well by close agreement of the dimensionless concentration distributions of tracer and indicator at 0.5 km for the March 1980 test.

<sup>2</sup> Only indicator concentrations at 0.5 km are plotted in Figure 4.11 to illustrate the rapid decline in numbers.



## V. MATHEMATICAL ANALYSIS OF FIELD RESULTS

### A. Tracer Analysis

The basic theory describing transverse mixing in natural channels was outlined in Chapter II. The primary objective of the tracer field studies was to provide a datum of effluent dilution against which to judge decay downstream of the outfall. However, they could also be used to find values of the transverse mixing coefficient for various flow conditions. The coefficient values may then be used in Equation 2.20 to predict river concentrations of conservative pollutants for known input concentration and boundary conditions.

The transverse mixing coefficient is closely related to the rate of lateral spread of the effluent plume across the channel. The amount of spread can be quantitatively represented by the variance of the concentration distribution across the stream at each measured section. Beltaos (1979) has shown that the variance is a linear function of an integral value  $I$  (see Equation 2.26) provided the term  $uh^2E_z$  may be assumed constant and equal to a reach-averaged value (see Equation 2.21). A reach-averaged value of  $E_z$ , the transverse mixing coefficient, may be calculated from the slope of a plot of variance versus  $I$  using Equation 2.27 and reach-averaged values of velocity  $V$ , depth  $H$  and shape factor  $\psi$ .





The analysis of side discharges into wide streams may be simplified by using the method of images and considering the measured plume concentration distributions (as shown in Figures 4.10, 4.11 and 4.12) as half of those resulting from a midflow injection of rate  $2Q_0$  into an imaginary stream of total discharge  $2Q$ . The integral  $I$  then simply reduces to the distance  $x$  from the outfall within the region where the bank concentrations of the imaginary plume are zero (ie. the crossing distance).

The variance of each  $c'$ - $\eta'$  distribution is given by

$$\sigma^2 = \int_0^1 (\eta' - \mu)^2 c' d\eta' \quad (5.1)$$

where  $\eta' = \eta/2$  to allow for the doubled discharge in the hypothetical stream and  $\mu$  is the first moment, which equals 0.5 because the imaginary distributions are symmetrical about the midflow point. The variance calculated for each section is in terms of the dimensionless transverse coordinate  $\eta'$  and therefore is dimensionless itself. Plots of the variance of the imaginary plume concentration distributions versus  $x$  for the three tracer studies are shown in Figure 5.1.

The points plotted for each test in Figure 5.1 tend to define a curve bounded by two straight lines rather than a single straight line which the analytical solution of Yotsukura and Cobb (1972) would predict. These results are not unexpected because the change in variance with  $x$  is





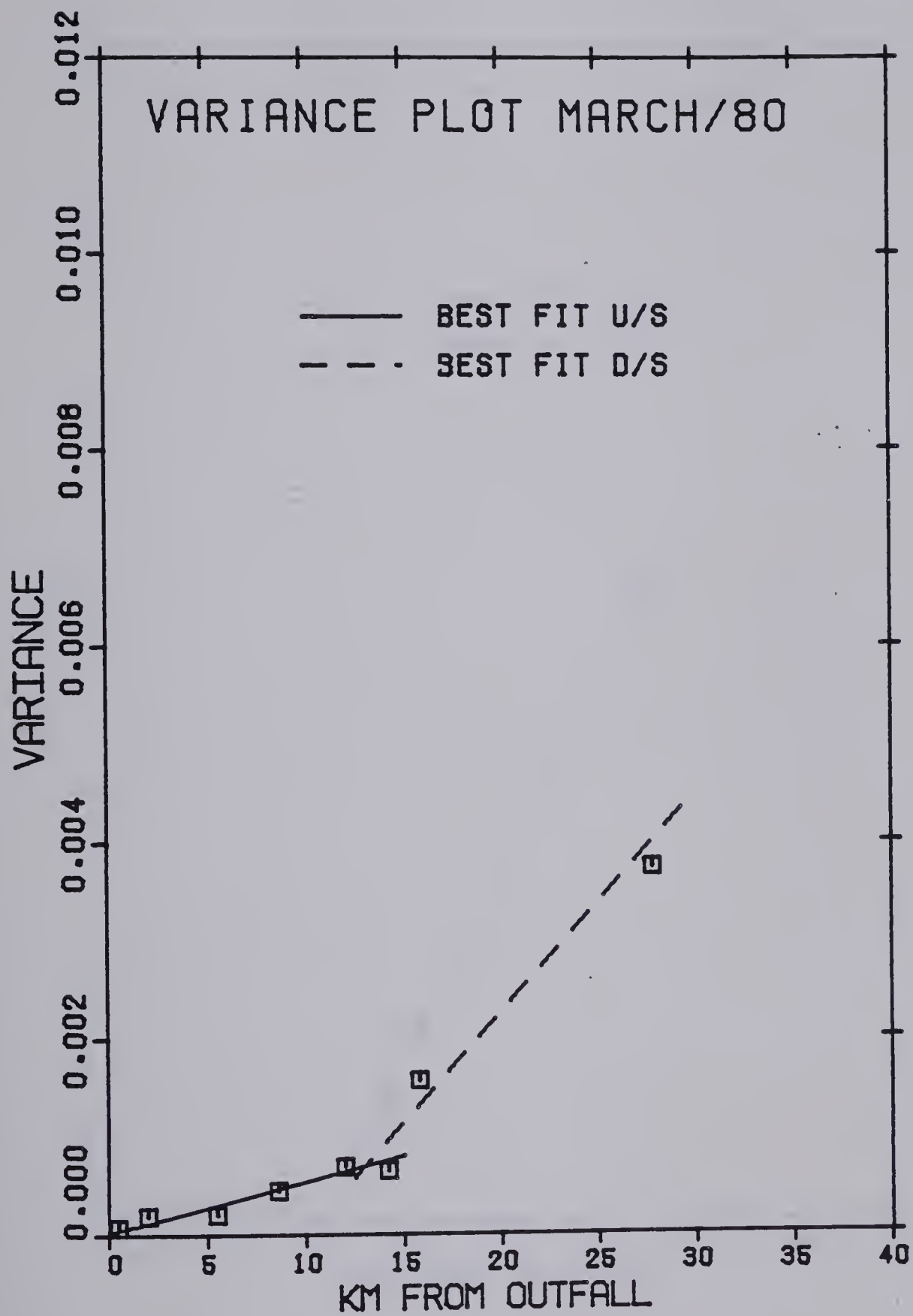


Figure 5.1(a) Change in Variance of Best Fit Tracer Distributions with Distance from the Outfall



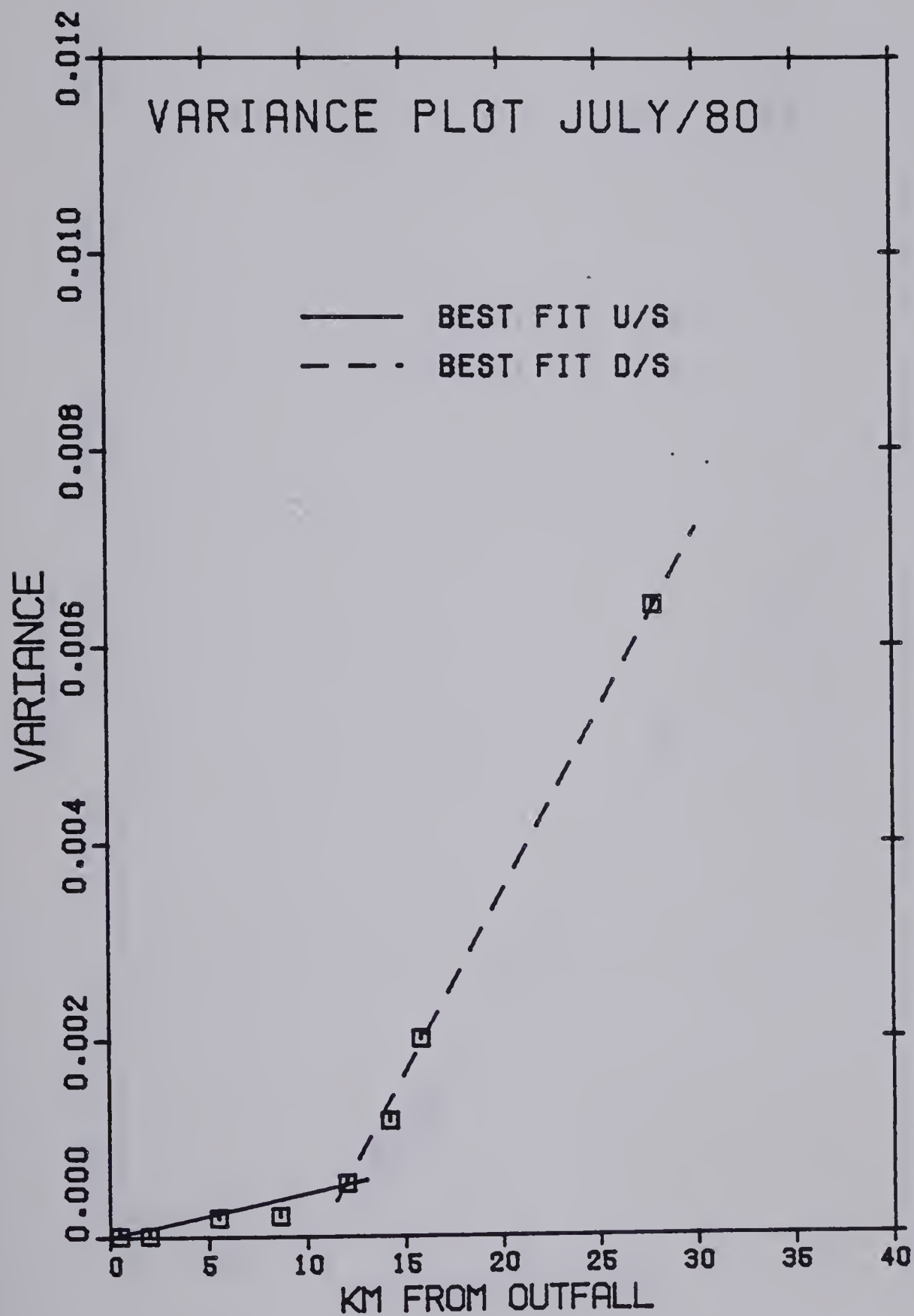


Figure 5.1(b) Change in Variance of Best Fit Tracer Distributions with Distance from the Outfall



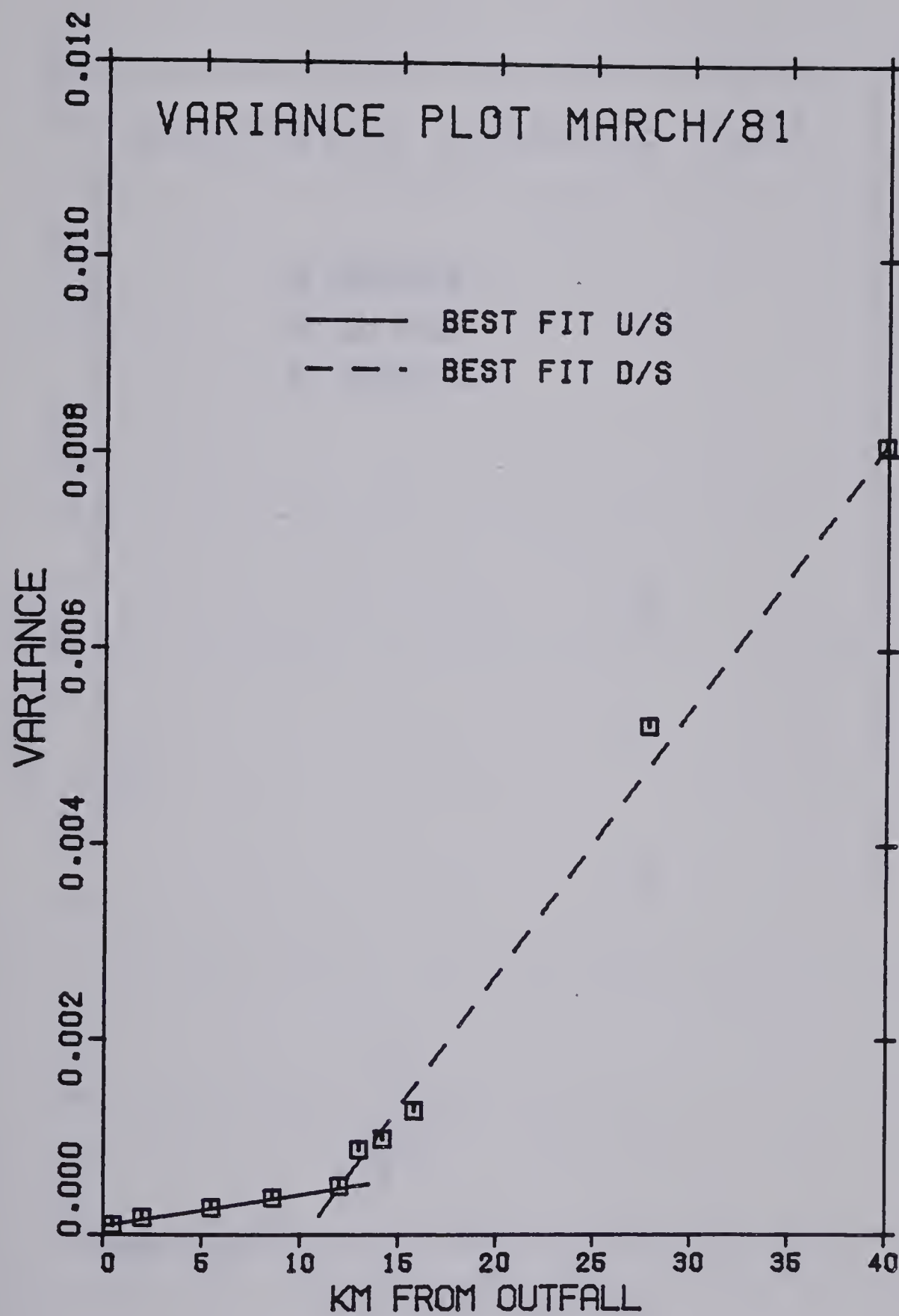


Figure 5.1(c) Change in Variance of Best Fit Tracer Distributions with Distance from the Outfall





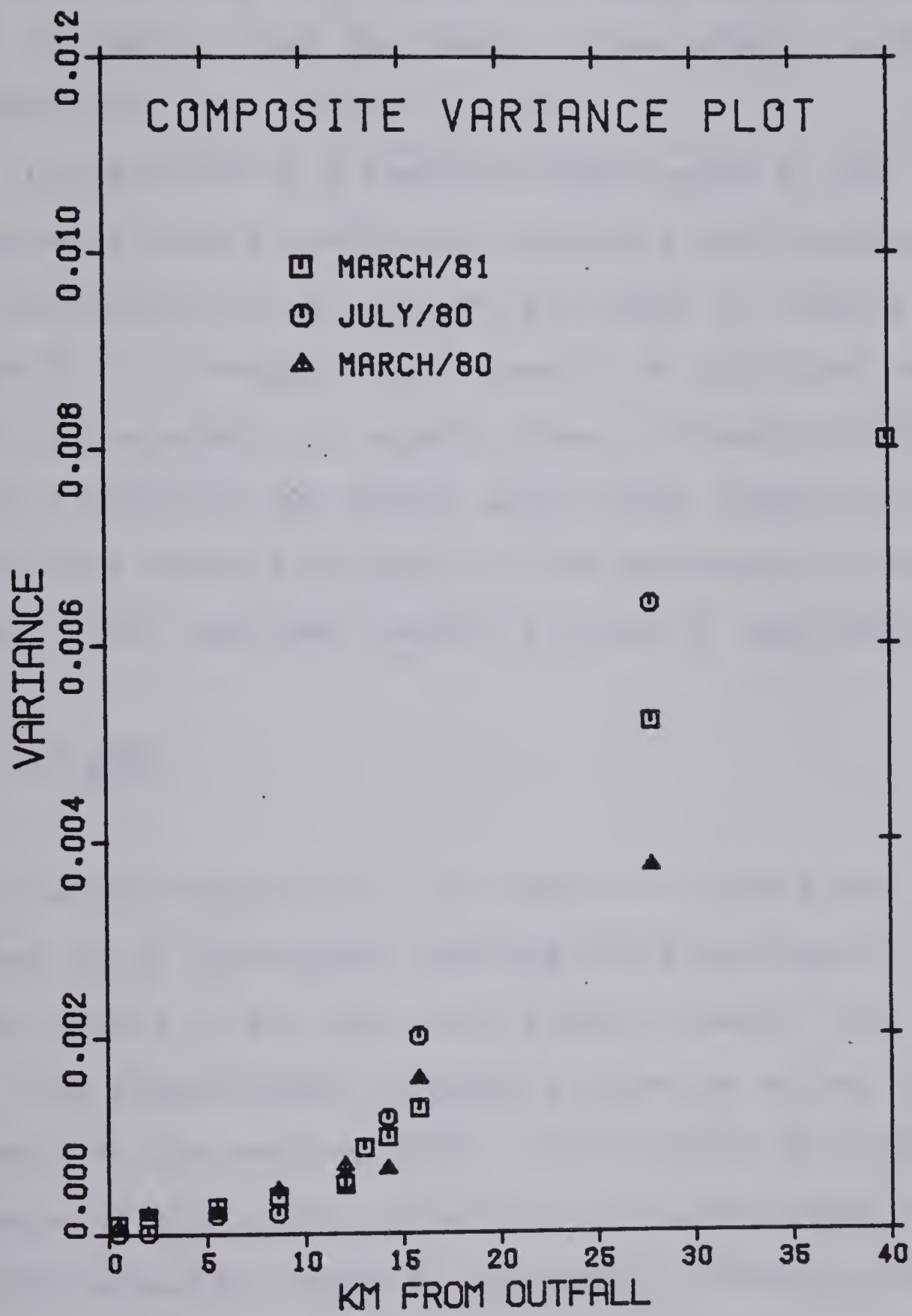


Figure 5.1(d) Change in Variance of Best Fit Tracer Distributions with Distance from the Outfall



proportional to the term  $uh^2E_z$  (see Equations 2.21 and 2.25). Near the banks, where local values of  $u$  and  $h$  are small, the change in variance and hence the slope of the plot is smaller than for those regions where  $u$  and  $h$  approach the mean channel values.

Calculation of a reach-averaged value of the transverse mixing coefficient upstream and downstream of the breakpoints in the curves are shown in tabular form in Table 5.1. To compare these results to published values of  $E_z$ , it is necessary to express them in dimensionless form using a velocity and length scale which characterizes the turbulence causing the mixing. The appropriate velocity scale is  $V_*$ , the shear velocity given by the Equation 2.8

$$V_* = \sqrt{gRS} \quad (2.8)$$

The average slope within the reach is 0.00005 m/m. Average values of  $V_*$  calculated upstream and downstream of the break-points in the plots are given in Table 5.2.

The length scale is usually taken as either  $R$  or  $H$ . However  $W$ , the average width, which should be a better measure of the lateral dimensions of large scale turbulence and disturbances caused by geomorphic irregularities is another alternative as discussed earlier.

Values of the dimensionless coefficient calculated for the three alternative length scales upstream and downstream of the breakpoints in Figure 5.1 are given in Table 5.2.



Table 5.1 Calculation of Reach-Averaged  $E_z$

Test			slope (1/m)	$\psi$	V (m/s)	H (m)	$E_z$ (m <sup>2</sup> /s)
March 1980	U/S		$52 \times 10^{-9}$	2.21	.51	4.82	.0119
	D/S		$224 \times 10^{-9}$	1.54	.55	4.66	.0729
July 1980	U/S		$44 \times 10^{-9}$	2.87	.80	5.36	.0183
	D/S		$369 \times 10^{-9}$	1.67	.87	5.38	.2430
March 1981	U/S		$32 \times 10^{-9}$	2.61	.38	5.09	.0059
	D/S		$273 \times 10^{-9}$	1.54	.43	4.90	.0811



Table 5.2 Calculation of Dimensionless  $E_z$

Test		$V_*$ (m/s)	H (m)	R (m)	W (m)	$E_z$ (m <sup>2</sup> /s)	$E_z/V_*H$	$E_z/V_*R$	$E_z/V_*W$
March 1980	U/S	.0344	4.82	2.41	787	.0119	.072	.144	.439x10 <sup>-3</sup>
	D/S	.0344	4.66	2.33	777	.0729	.463	.926	2.78x10 <sup>-3</sup>
July 1980	U/S	.0531	5.36	5.36	879	.0183	.067	.067	.397x10 <sup>-3</sup>
	D/S	.0514	5.38	5.38	864	.2340	.879	.879	5.47x10 <sup>-3</sup>
March 1980	U/S	.0353	5.09	2.55	836	.0059	.033	.065	.196x10 <sup>-3</sup>
	D/S	.0347	4.90	2.45	785	.0811	.477	.954	2.98x10 <sup>-3</sup>





The range of values of the dimensionless parameter found by other investigators for streams similar to the Slave River are given in Table 5.3. Comparison of these ranges with the calculated values indicates the upstream portion of the reach has a mixing coefficient almost an order of magnitude lower than expected for all three test results.

This disparity, and the non-linear relationship of variance with  $x$ , suggests that the assumption that the term  $uh^2E_z$  in Equation 2.20 can be replaced by a constant reach-averaged value  $D_z$  is not reasonable for side injection into a wide natural river, and supports the similar finding by Lau and Krishnappan (1981). Analytical solutions are not available for Equation 2.20 with a variable  $uh^2E_z$  term. Reasonable estimates of  $E_z$  can therefore only be obtained by solving numerically for trial values of  $E_z$  and comparing the predicted concentration distributions to those measured in the field. Numerical solution to find the best estimate of  $E_z$  and computer modelling of the mixing process will be addressed in Chapter VI.

## **B. Microorganism Decay Analysis**

Decay analysis was only conducted for ice covered conditions because of the rapid decrease of indicator bacteria to background levels which occurred during the summer test.



Table 5.3 Dimensionless  $E_z$  from Other Investigations

Stream Description	W (m)	W/H	Irregularity Rank	$E_z/V\Delta W$	$E_z/V\Delta H$	$E_z/V\Delta R$
Missouri R.: severe bends	234	59.1	1	.0560	3.31	3.31
Beaver R.: regular meanders point bars, large dunes : ice covered	42.7 38.7	44.6 63.5	2 3	.0230 .0200	1.03 1.27	1.03 2.54
Lesser Slave R.: severe bends :ice covered	43.0 36.3	17.0 17.5	4 5	.0190 .0100	.323 .175	.646 .350
Missouri R.: two mild bends	183	68.7	6	.0087	.598	.598
South R.: few mild bends	18.2	46.2	7	.0065	.300	.300
Columbia R.	305	100	8	.0074	.740	.740
Athabasca R. below Ft. McMurray: straight with islands, mid channel bars :ice covered	373 252	170 131	9 10	.0044 .0044	.748 .576	.748 1.15
Athabasca R. below Athabasca: irregular with occasional islands, bars :ice covered	320 276	156 288	11 12	.0026 .0010	.406 .288	.406 .576
Danube R.: one moderate and one very mild bend	500	100	13	.0012	.120	.120



Manpower and time constraints during the March 1980 test prevented more than one sampling of the majority of holes. During the March 1981 test the majority were sampled at least twice. Nevertheless considerable scatter must still be expected due to the nature of bacteriological enumeration data. The March 1981 test results are considered more representative and superior to the March 1980 test for decay analysis and therefore will serve as the sole basis for the following calculations. A preliminary assessment of decay based upon the limited March 1980 data was presented by Smith and Gerard (1981).

The plots of dimensionless concentrations of total and fecal coliforms shown in Figure 5.2 were chosen for decay analysis. The sections at 14.2 km and 15.8 km were rejected because they were only sampled once, and the 39.9 km section because the concentration levels within the effluent plume had dropped to near background levels. The estimated mean travel times to each section are given on the individual plots of Figure 5.2.

The results of the March 1980 study reported by Smith and Gerard (1981) indicated there was no discernable die-off of microorganisms within approximately an 18 hour period following discharge to the river. The plots of Figure 5.2 appear to support the 1980 results. A standard 't' test of the ratio of microorganism concentration to measured tracer concentration compared to unity was run at 13.0 km and 27.8 km to ascertain if there was any





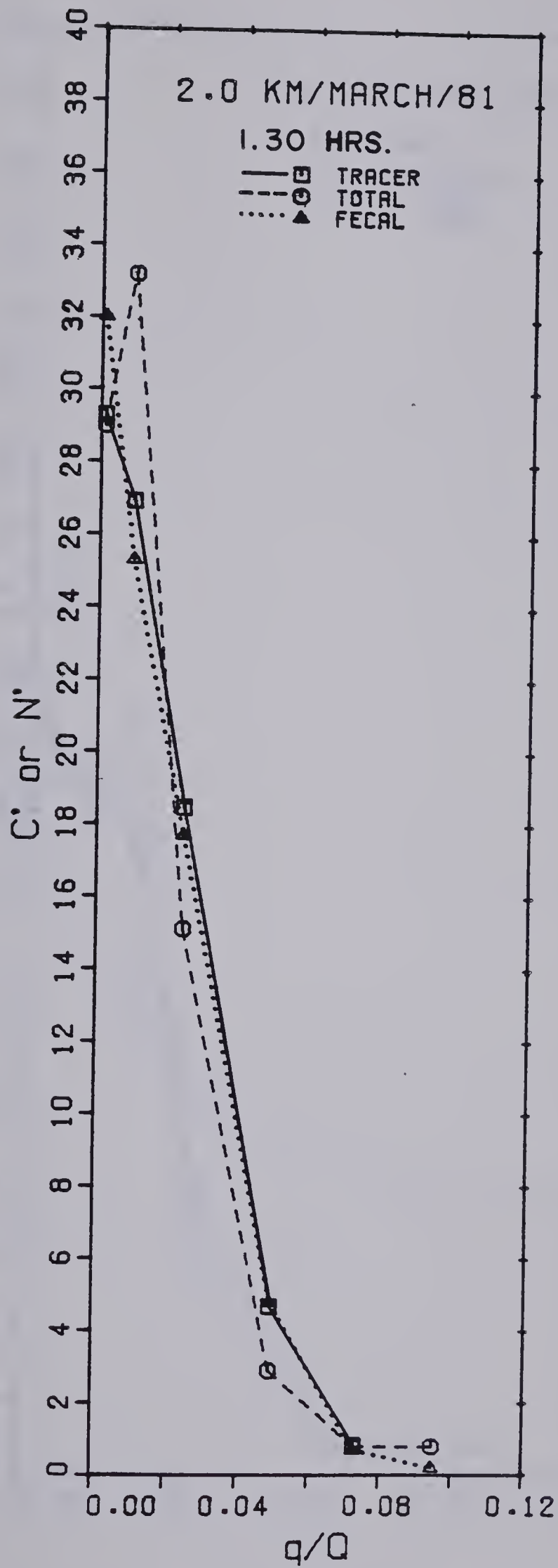


Figure 5.2(a) Selected Distributions for Microorganism Decay Analysis



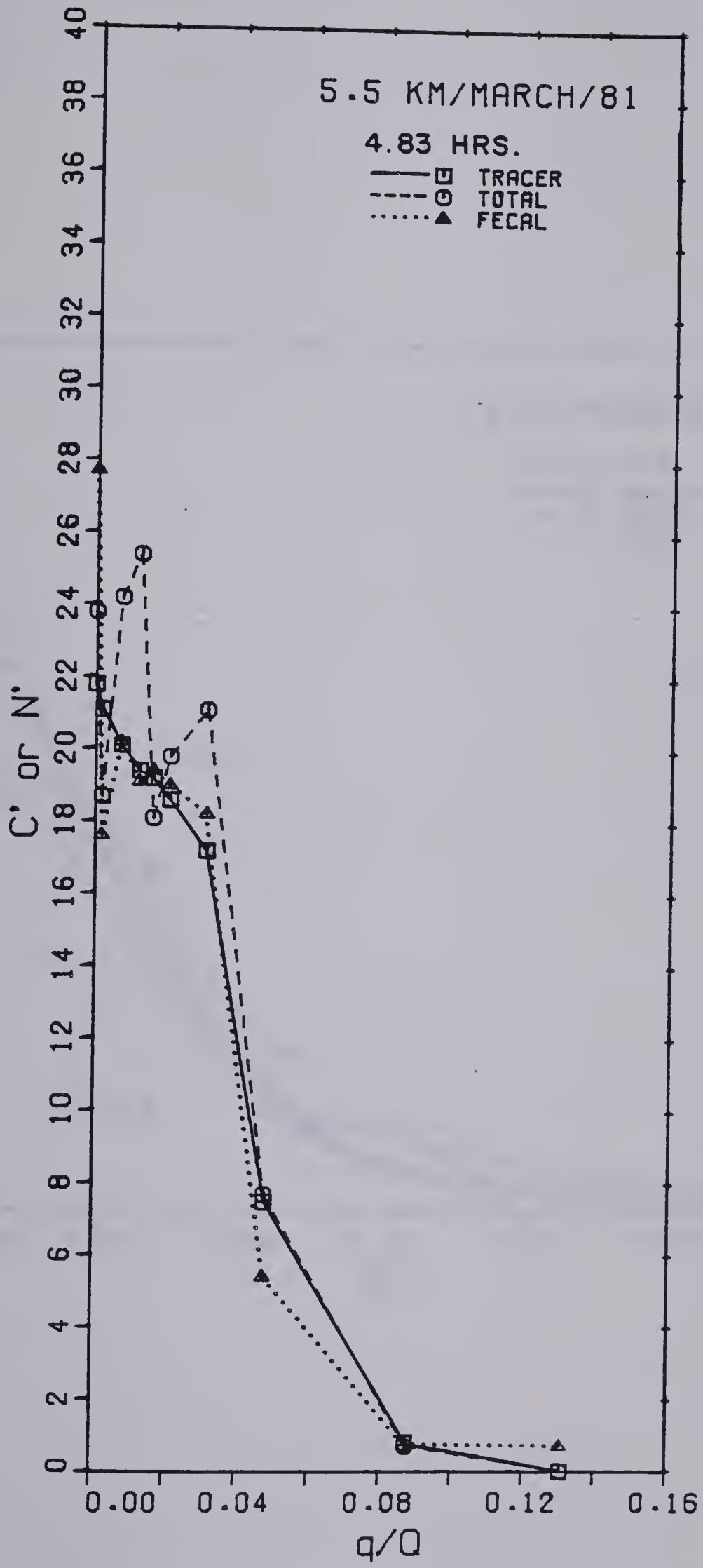


Figure 5.2(b) Selected Distributions for Microorganism Decay Analysis



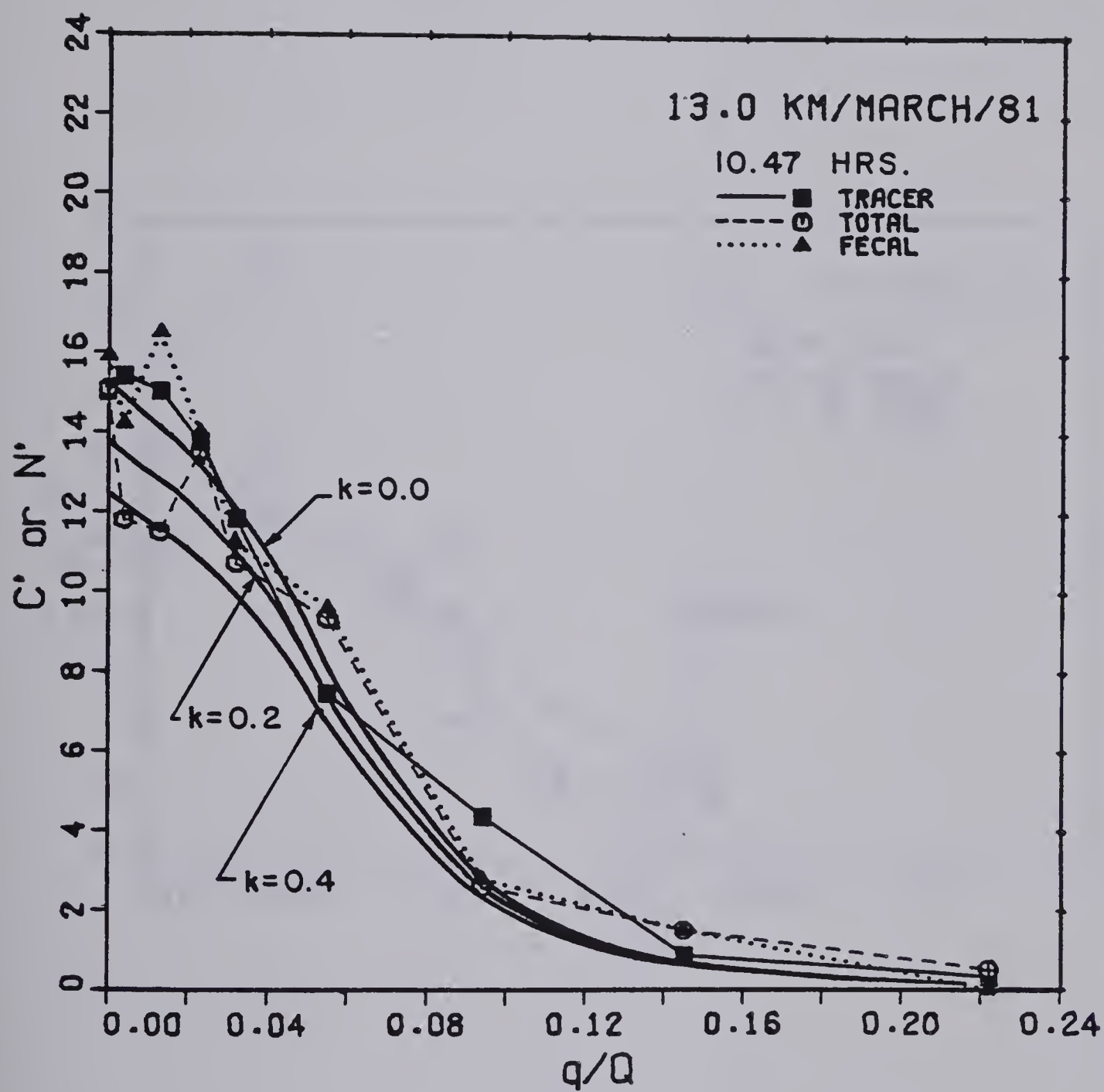


Figure 5.2(c) Selected Distributions for Microorganism Decay Analysis



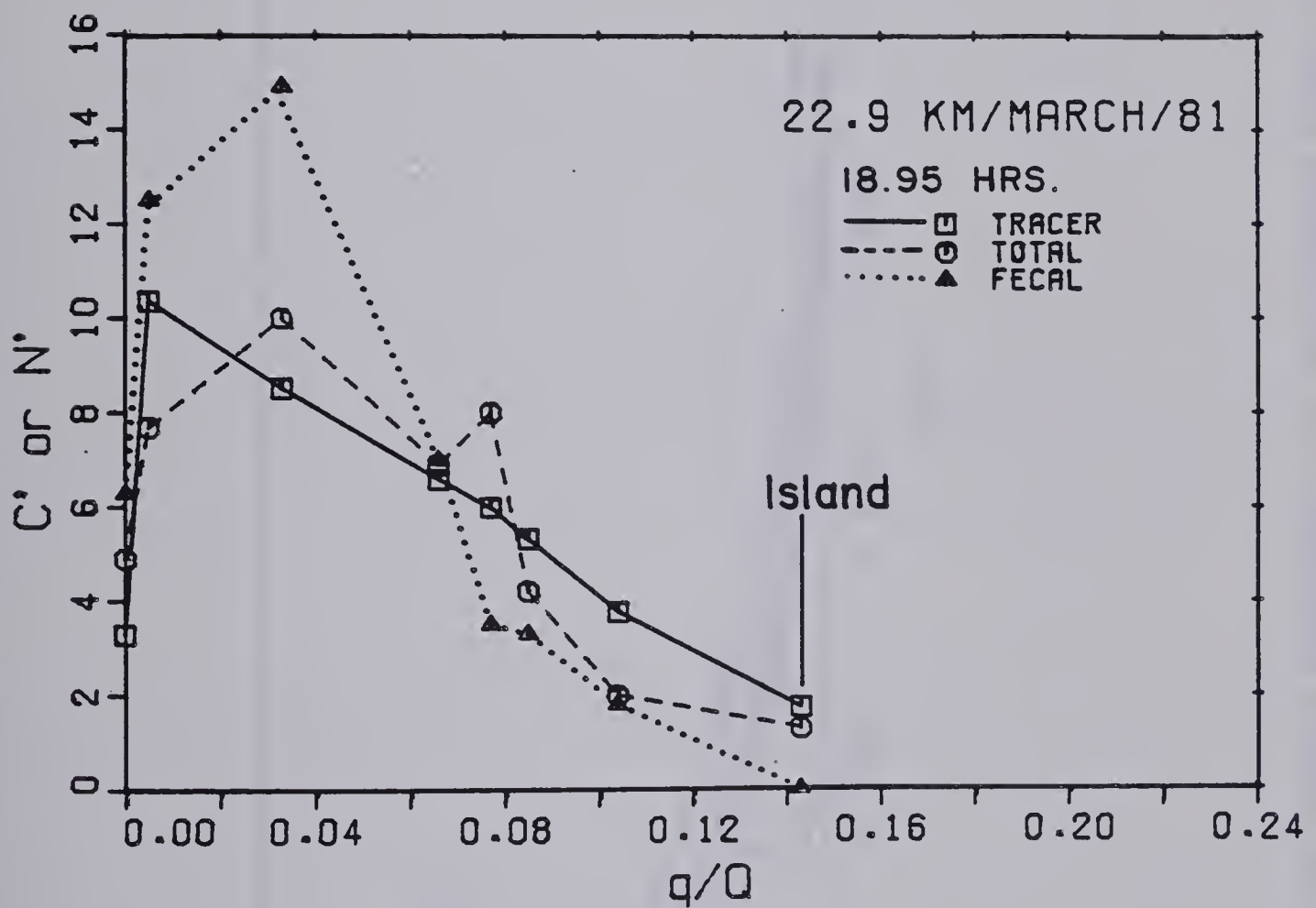


Figure 5.2(d) Selected Distributions for Microorganism Decay Analysis





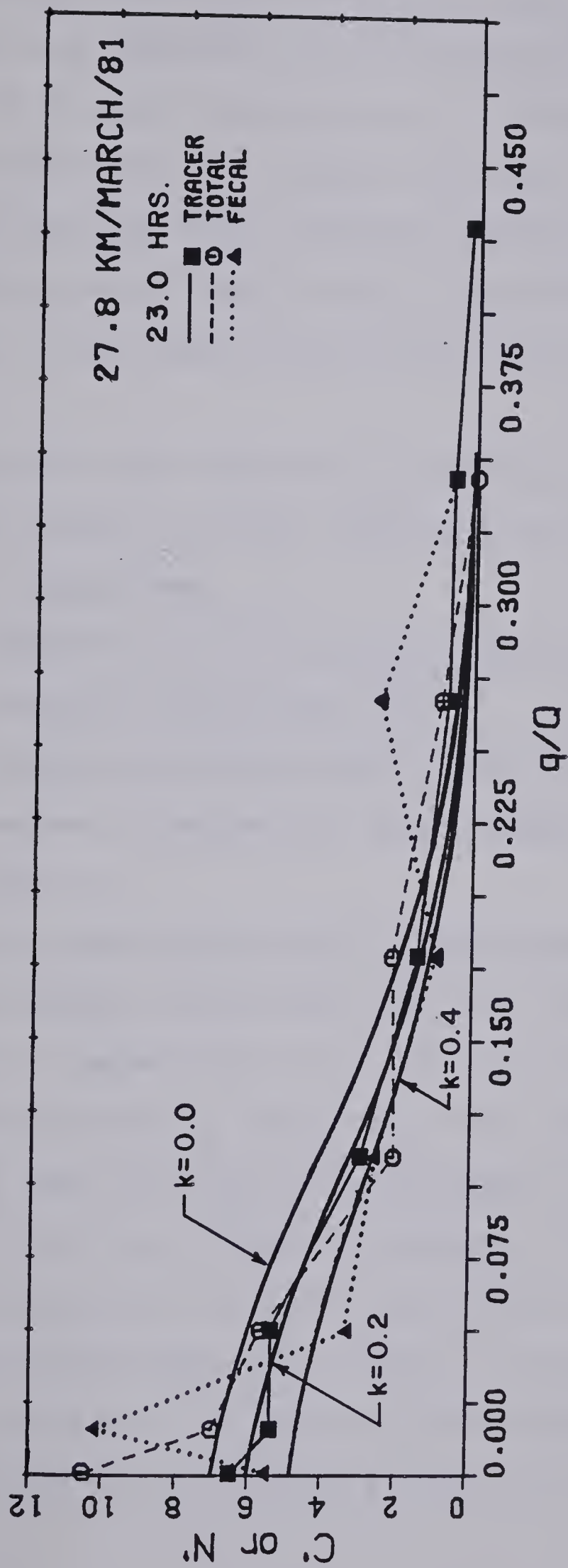


Figure 5.2(e) Selected Distributions for Microorganism Decay Analysis



statistically significant difference. The test was conducted with measured concentrations greater than 10 percent of the peak concentration to eliminate some of the background effects. The results are shown in Table 5.4. Both the total and fecal coliform concentration distributions were found to be not significantly different from that of the tracer over the 23 hours of flow time sampled.

A die-off not significantly different from zero in this reach under ice cover conditions can be supported by two other approaches:

- a. comparison of the boundary region concentrations along the river reach, and
- b. evaluation of the number of microorganisms in excess of background values present at each section.

The average concentration of microorganisms along the left bank boundary should show the most significant decreases in comparison to the tracer if the decay proceeded according to Chick's Law (see Equation 2.35). The average of the first two or three sampling holes adjacent to the left bank was chosen to represent the boundary region concentration to reduce the effects of scatter of the microorganism data. The results of the analysis are shown in Table 5.5. The ratios of microorganism to tracer concentrations are consistently close to 1.0.



Table 5.4 t Test at 13.0 km and 27.8 km

Section (km)	Parameter	N.P. *	D.F. **	t	95% confidence interval***
13.0	TC	21	40	-.700	-2.02 to 2.02
13.0	FC	21	40	-.156	-2.02 to 2.02
27.8	TC	6	10	.820	-2.22 to 2.22
27.8	FC	6	10	-.782	-2.22 to 2.22

\* number of paired data points  
\*\* degrees of freedom  
\*\*\* the range of t for which there is a 95 percent chance the difference between the microbial and tracer distribution may occur due to random chance rather than actual decay. The t values are within the intervals therefore the differences in the distributions are not significant at the 5 percent significance level

Table 5.5 Near Left Bank Concentrations

Section (km)	Tracer T	Dimensionless Concentrations		Ratio	
		TC	FC	TC/T	FC/T
2.0	28.1	31.2	28.6	1.11	1.02
5.5	21.1	22.3	21.8	1.06	1.04
13.0	15.1	12.8	15.5	0.85	1.03
22.9	9.5	8.9	13.7	.94	1.44
27.8	5.8	7.7	6.3	1.32	1.09





The total flux of microorganisms entering the river at the outfall must be accounted for at each downstream section if no significant die-off occurs. The plots of Figure 5.2 are in dimensionless form corrected for background values and therefore the area under each curve should be 1.0 if no die-off occurs. The areas<sup>1</sup> are given in Table 5.6. The recovery at section 22.9 km should be considered in relation to the tracer recovery since only the left channel of the river was sampled. The results are consistent with the premise of no significant die-off.

Generally, under warmer conditions bacterial concentrations are a non-conservative parameter with a discernable decay rate. Prediction of the concentration distribution of non-conservative parameters, and estimation of the decay coefficient,  $k$ , may be accomplished by incorporating a decay term into Equation 2.20 and solving numerically. This method will be presented in Chapter VII.

-----  
<sup>1</sup> The areas were calculated using simple trapezoidal approximations rather than attempting to fit a curve to the data.



Table 5.6 Microorganism Recovery

Section (km)	Tracer T	Dimensionless TC	Area FC	Ratio TC/T	FC/T
2.0	0.96	0.95	0.94	0.99	0.98
5.5	0.98	1.08	1.00	1.10	1.01
13.0	1.11	1.06	1.11	0.96	1.00
22.9	0.87	0.82	0.98	0.95	1.13
27.8	0.89	0.93	0.97	1.05	1.09



## VI. COMPUTER MODELLING

### A. Tracer Modelling

#### July 1980 and March 1981 Tests

Analytical analysis of the field tracer tests given in the previous chapter proved unsatisfactory. A numerical solution was required.

An implicit finite difference scheme first proposed by Stone and Brian (1963) for numerical solution of diffusion problems in the form of Equation 2.20 was used in the modelling procedure. As mentioned in Chapter II this method was recently used by Lau and Krishnappan (1981) to analyse transverse mixing in a much smaller natural stream. Details of the finite difference scheme and the computational method are given in Appendix VI.

The numerical modelling scheme has the additional advantage of allowing a consideration of the change in boundary conditions and the difference in minor channel lengths around islands. The solution distribution may be split at the upstream end of an island, new boundary conditions established, and calculations continued along the individual channels. At the downstream end of the island the full channel boundary conditions may be reestablished and the solution continued with a discontinuous concentration profile formulated from the individual channel distributions.



Modelling was first conducted for the March 1981 and July 1980 tests representing ice cover and summer conditions. The river reach was divided into longitudinal river portions in which the channel geometry and flow characteristics could be represented by one of the surveyed cross sections. The variations in  $uh^2$  (the term accounting for the local depth and velocity in the transverse direction) were derived from the section geometry plots and cumulative flow distributions shown in Figure 4.4. The normalized concentration distribution measured at 0.5 km was used as the input distribution. Values of  $E_z$  were determined for each longitudinal river portion to give a best fit to the normalized measured tracer distribution contained within that particular river portion. The results of the modelling for each test are shown in Figure 6.1 and 6.2 and Tables 6.1 and 6.2.

#### Dimensionless Transverse Mixing Coefficient

Extrapolation of these results to other locations requires the determination of parameters on which to scale  $E_z$ . As mentioned in Chapter V, reach-averaged value of shear velocity and either reach-averaged depth, hydraulic radius or width have generally been used. However, as pointed out by Smith and Gerard (1981) this seems unreasonable for a situation where the plume occupies such a small portion of the total stream width. Local parameters would seem more appropriate. Suggested scaling factors are:





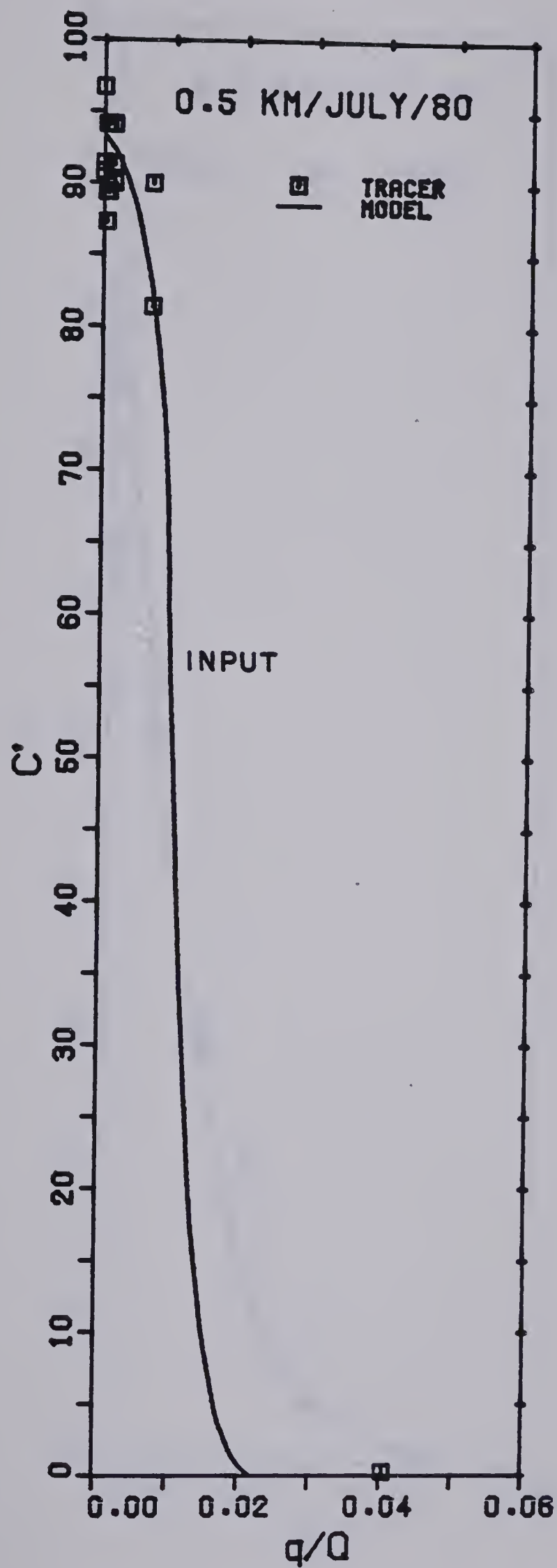


Figure 6.1(a) Computer Modelling of Normalized Tracer Distributions July 1980



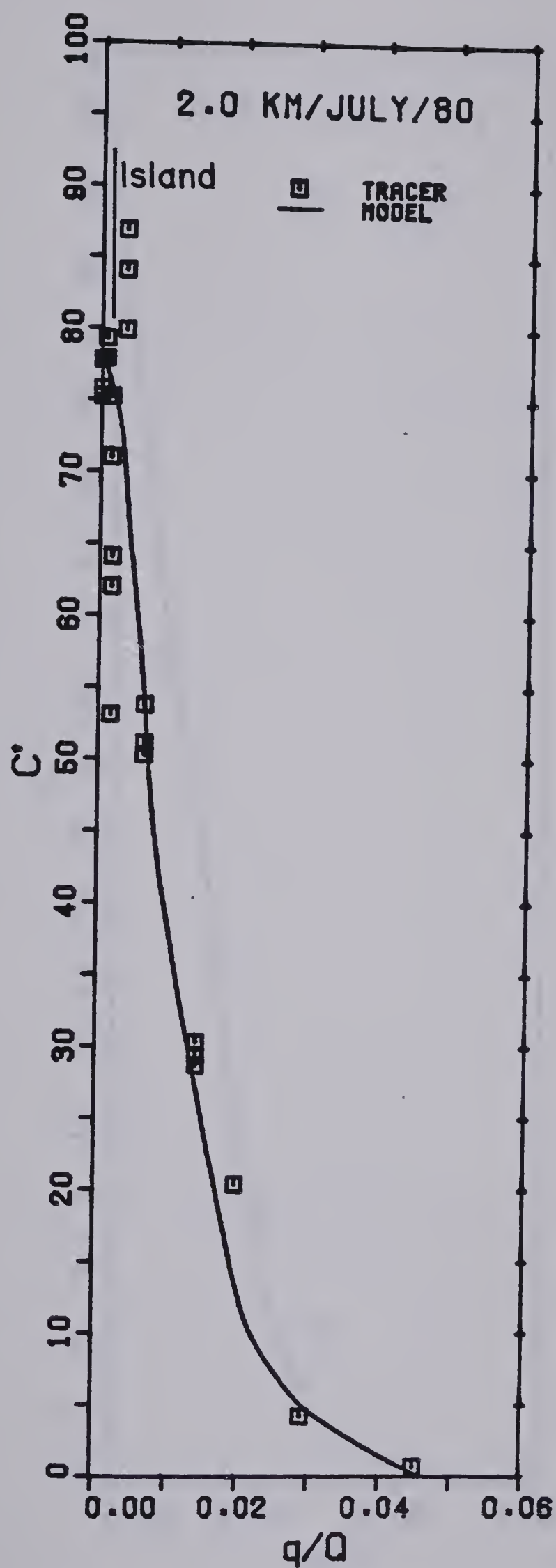


Figure 6.1(b) Computer Modelling of Normalized Tracer Distributions July 1980



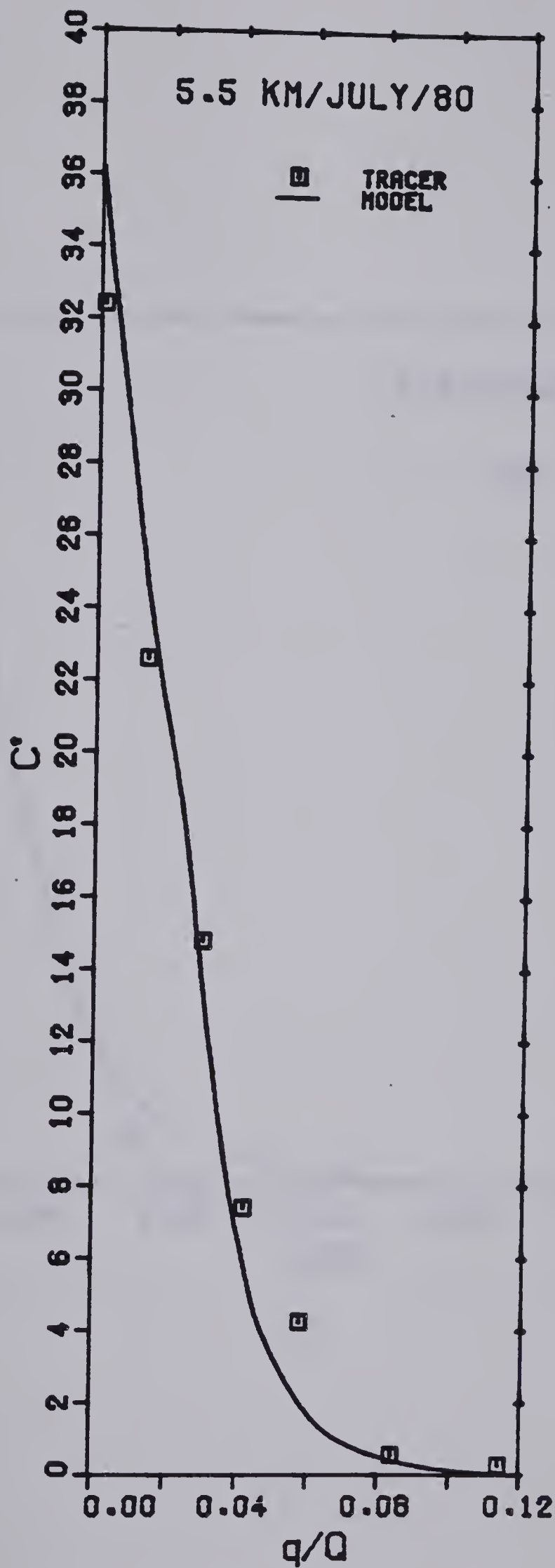


Figure 6.1(c) Computer Modelling of Normalized Tracer Distributions July 1980





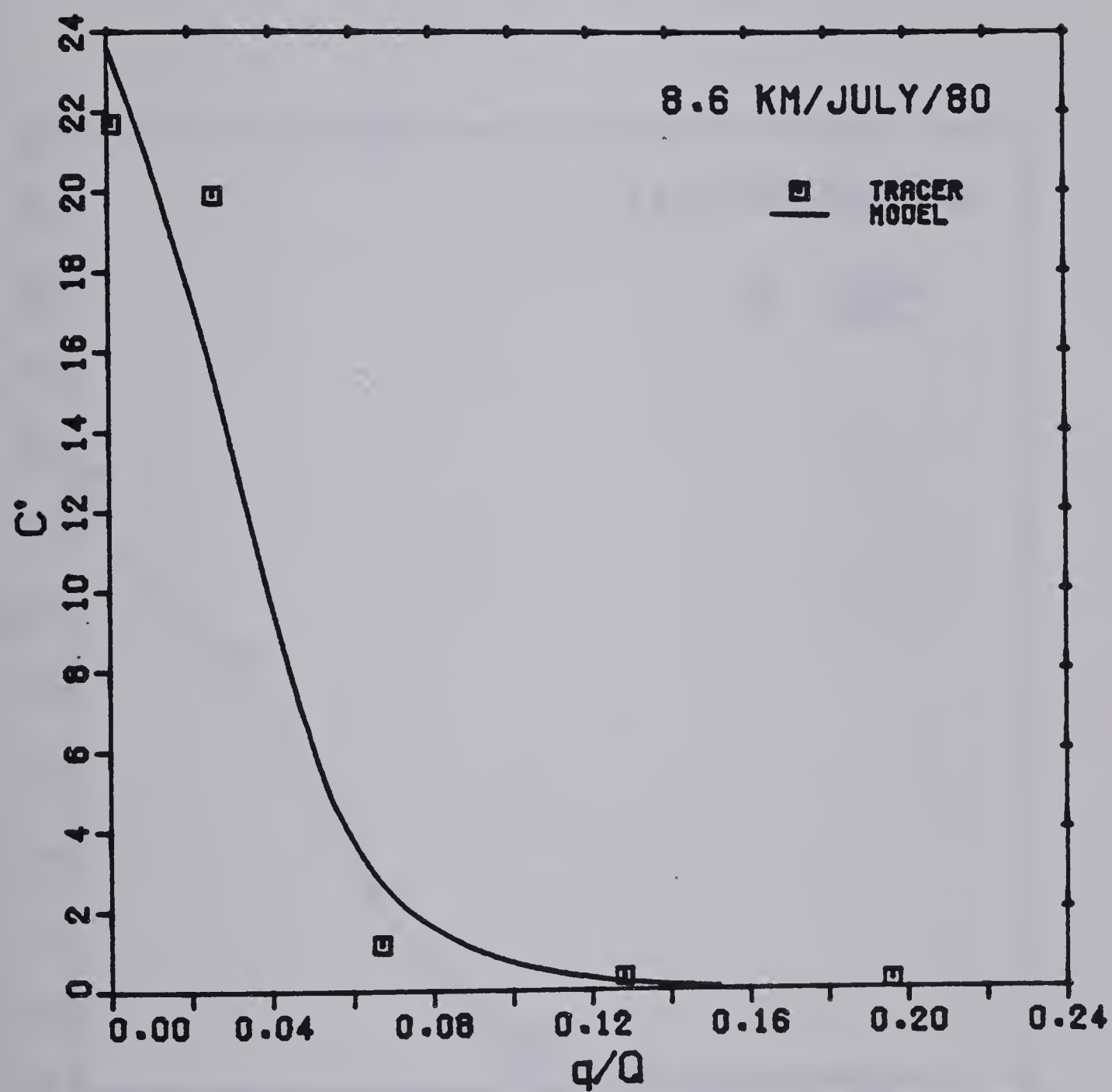


Figure 6.1(d) Computer Modelling of Normalized Tracer Distributions July 1980



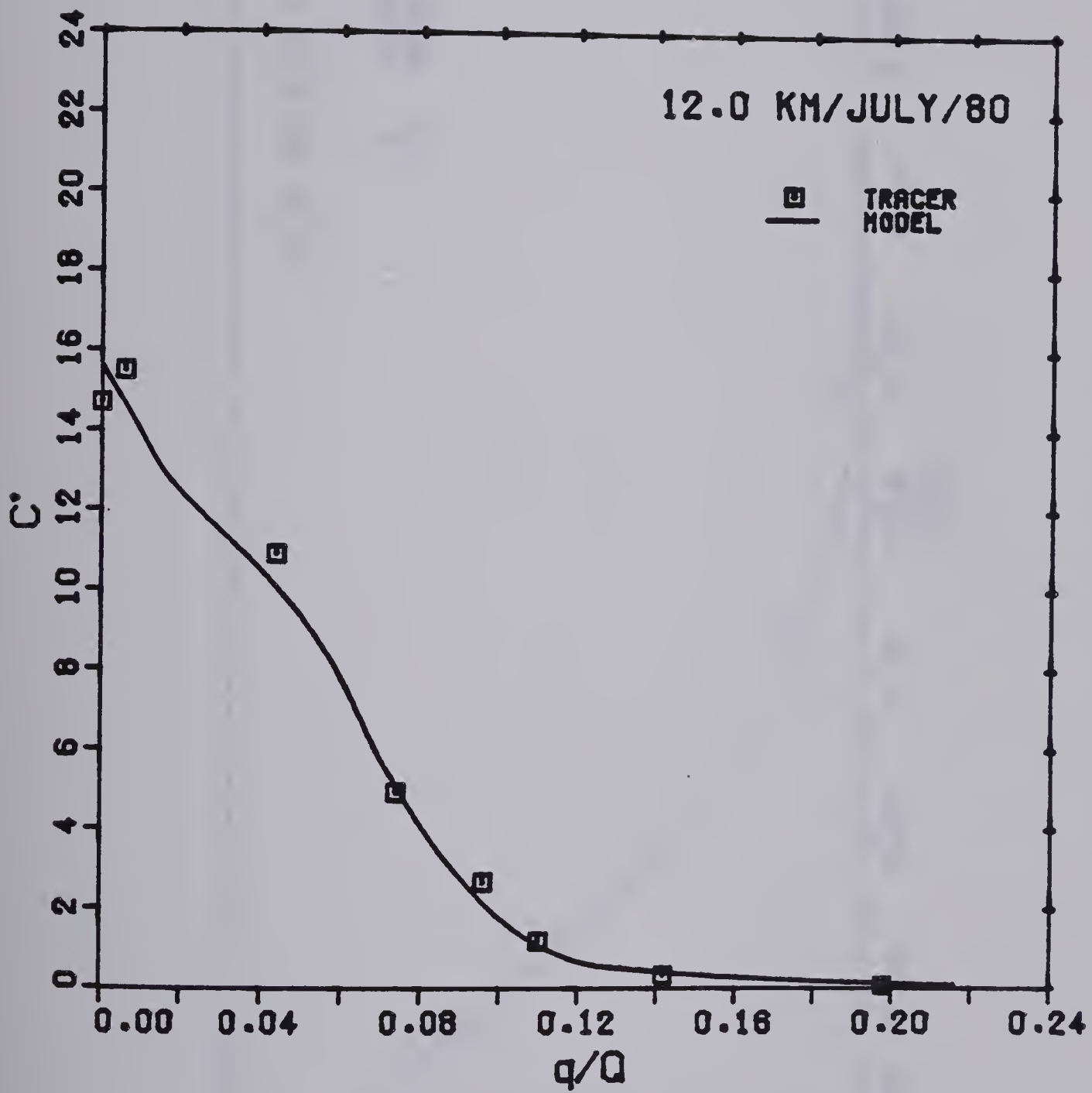


Figure 6.1(e) Computer Modelling of Normalized Tracer Distributions July 1980



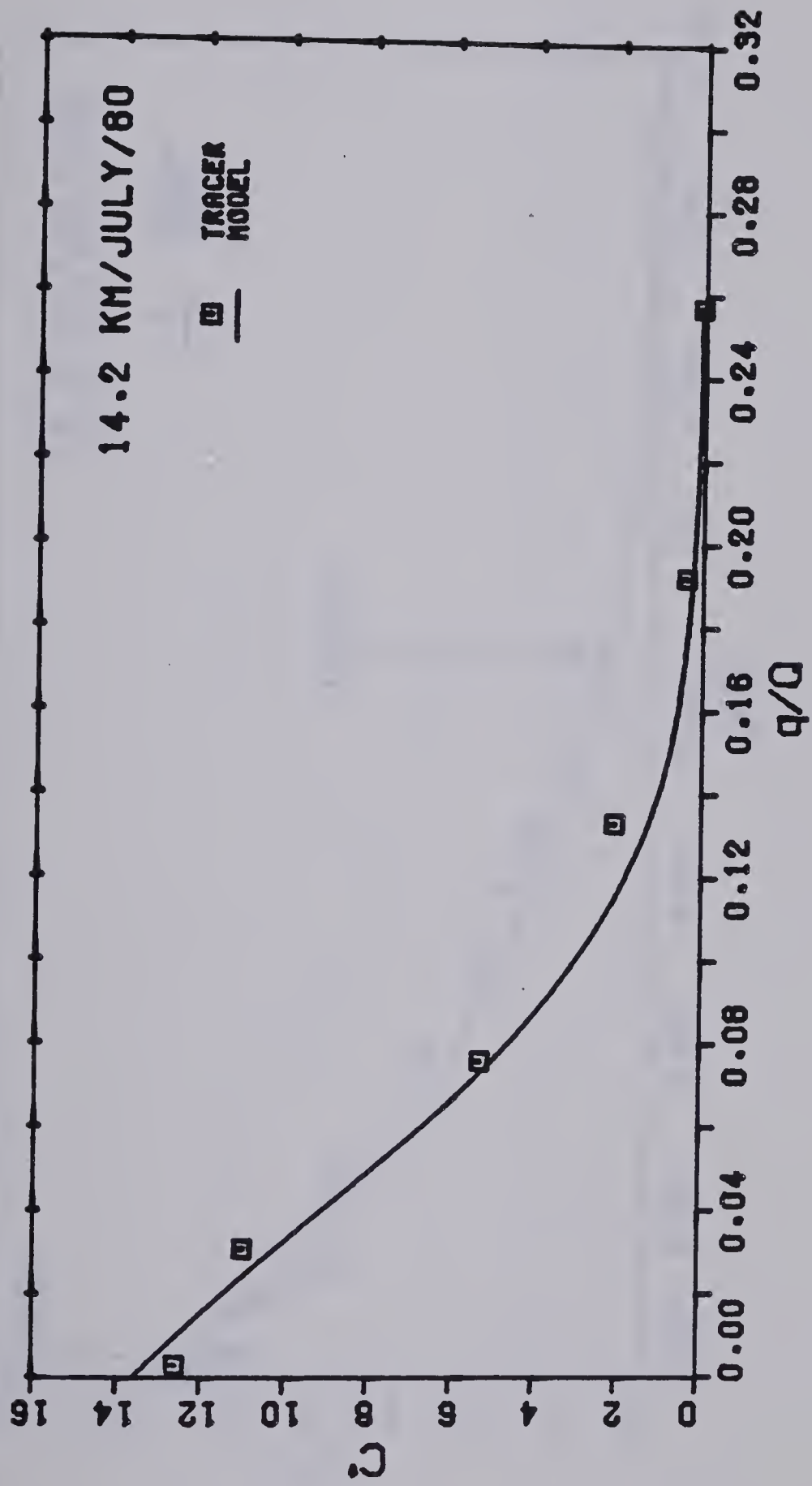


Figure 6.1(f) Computer Modelling of Normalized Tracer Distributions July 1980



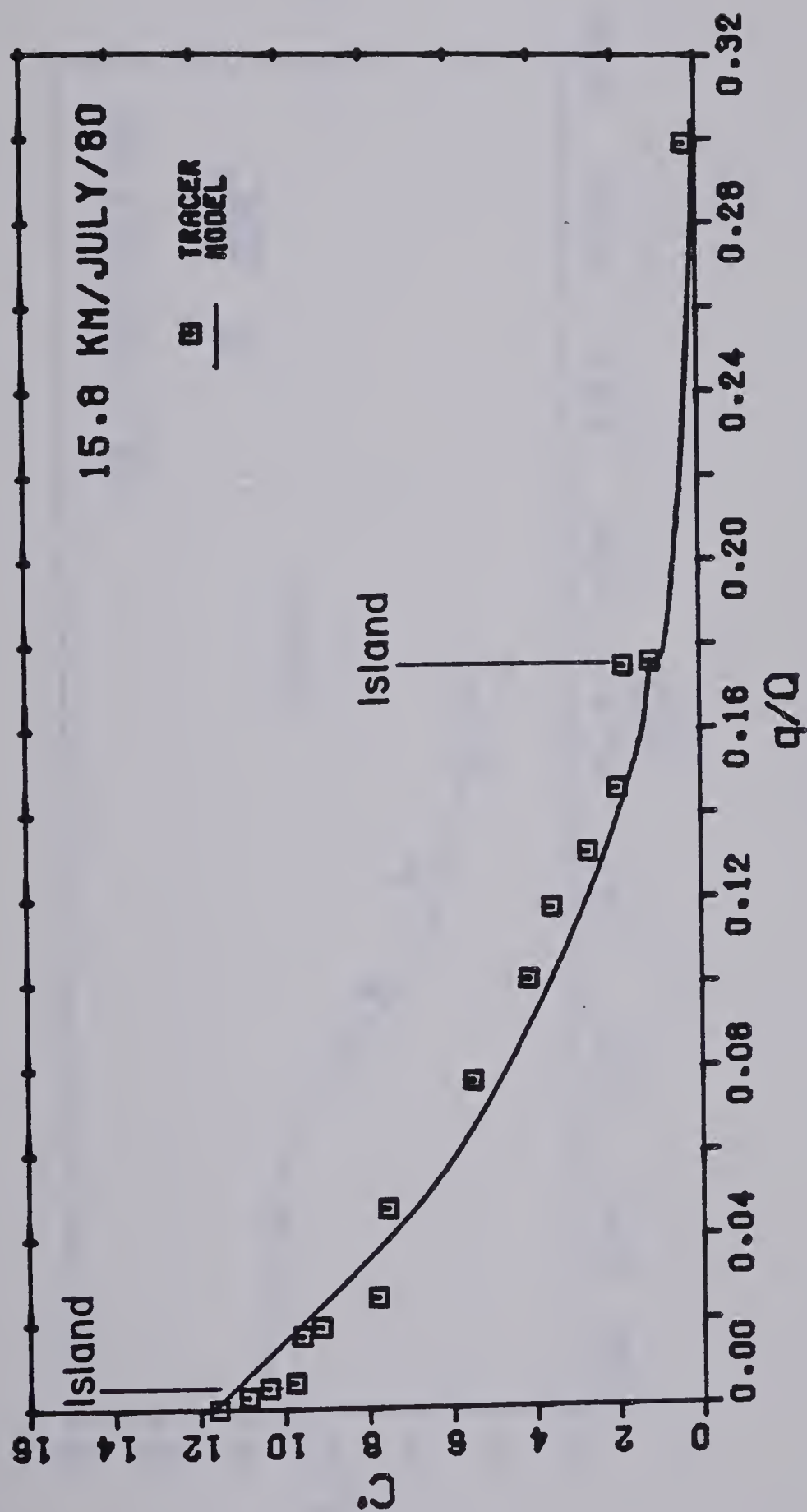


Figure 6.1(g) Computer Modelling of Normalized Tracer Distributions July 1980





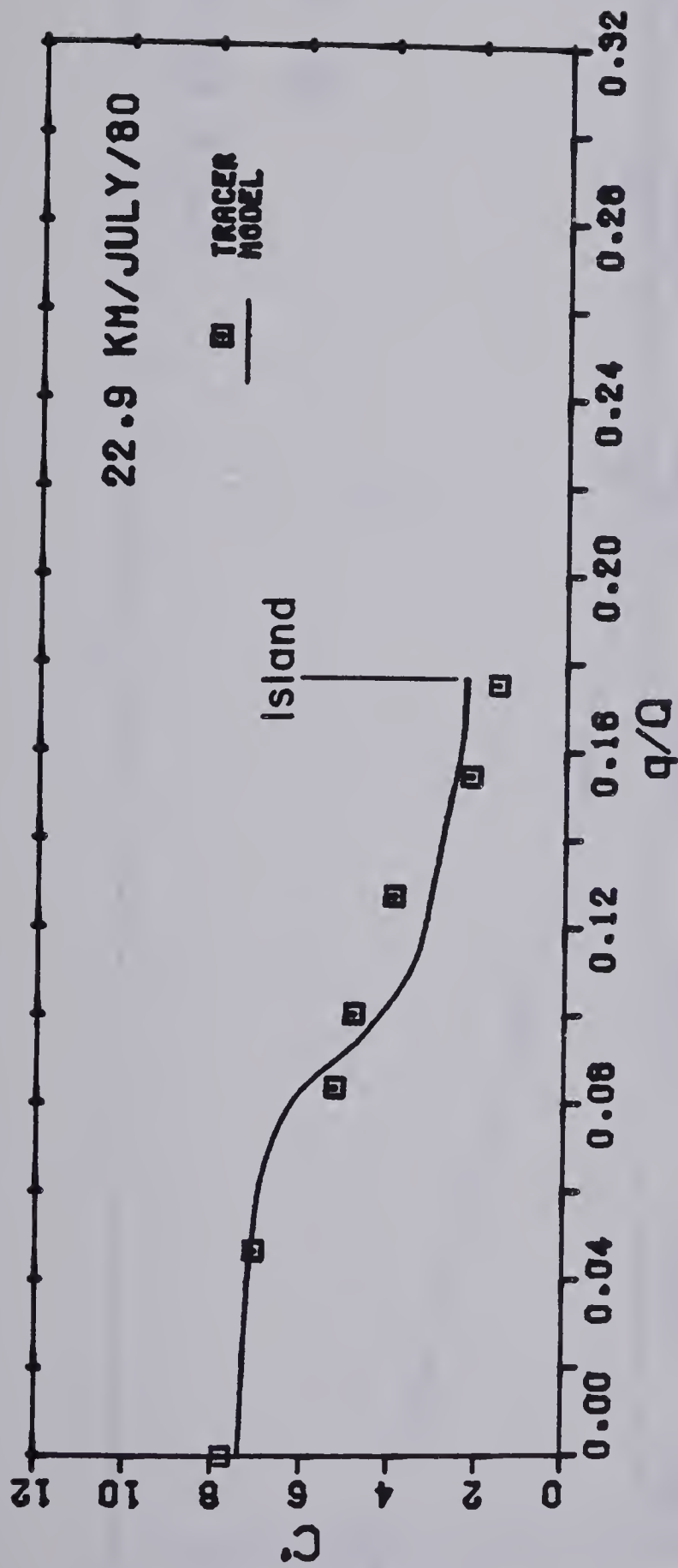


Figure 6.1(h) Computer Modelling of Normalized Tracer Distributions July 1980



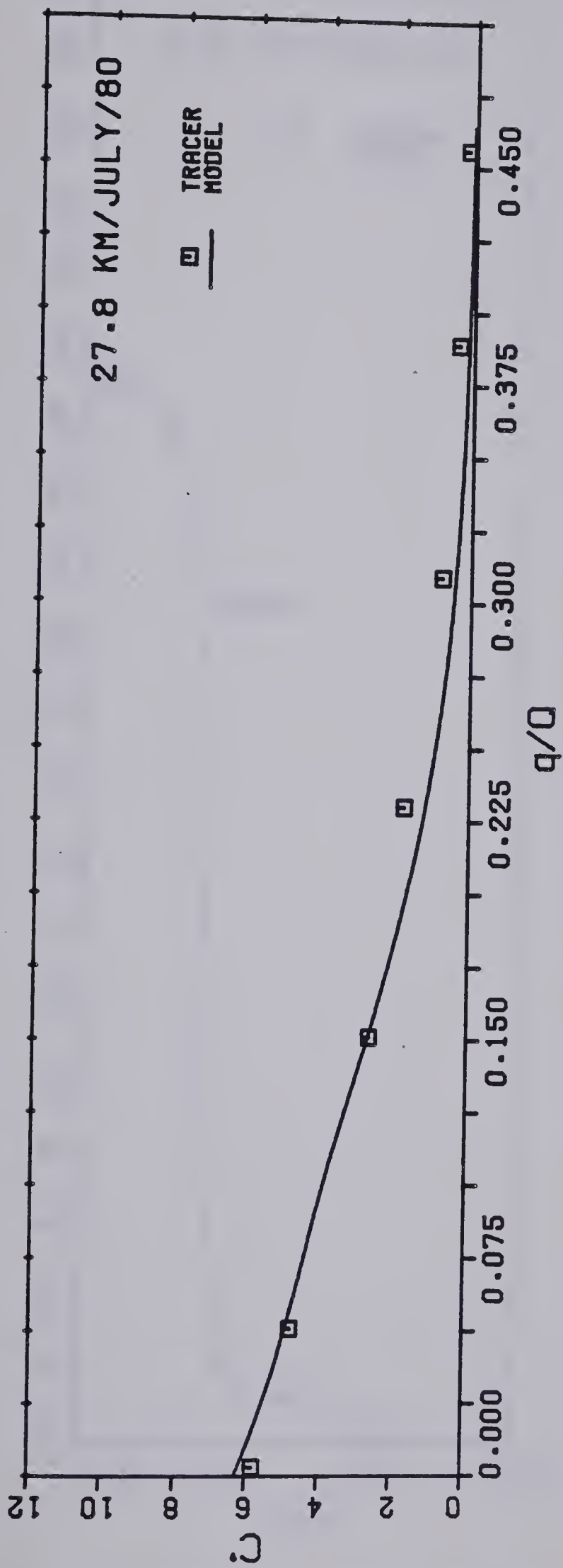


Figure 6.1(i) Computer Modelling of Normalized Tracer Distributions July 1980



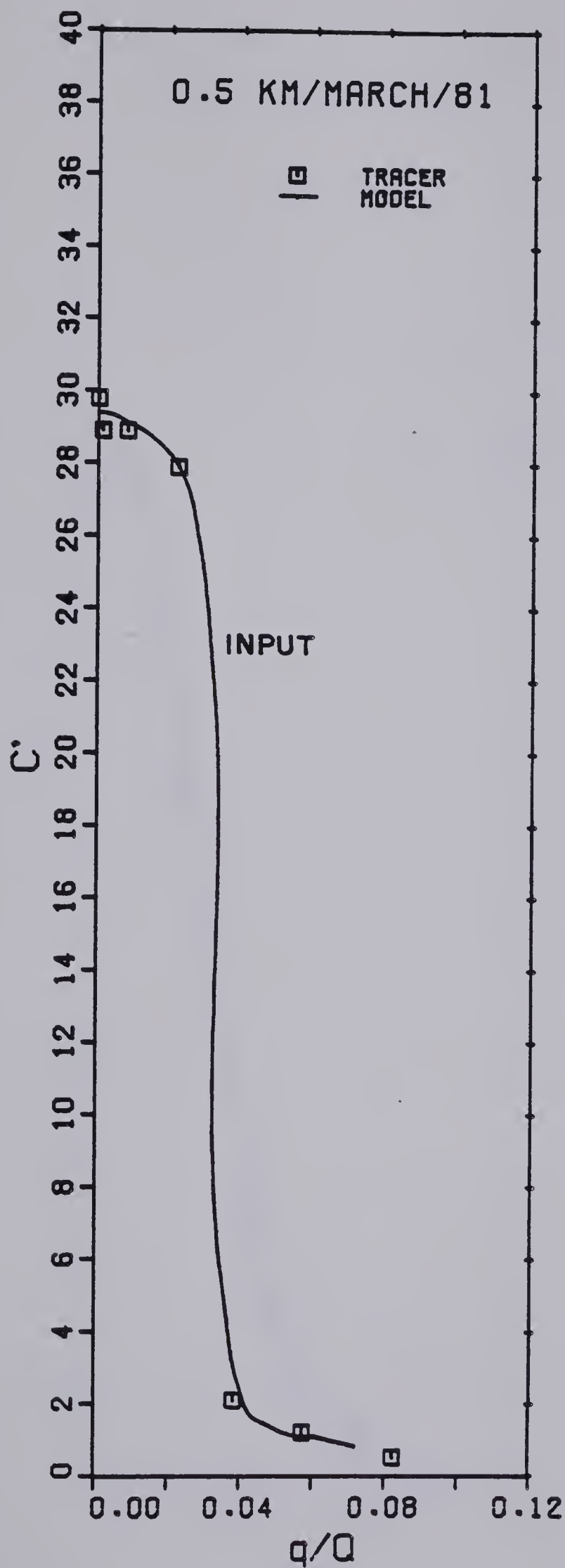


Figure 6.2(a) Computer Modelling of Normalized Tracer Distributions March 1981





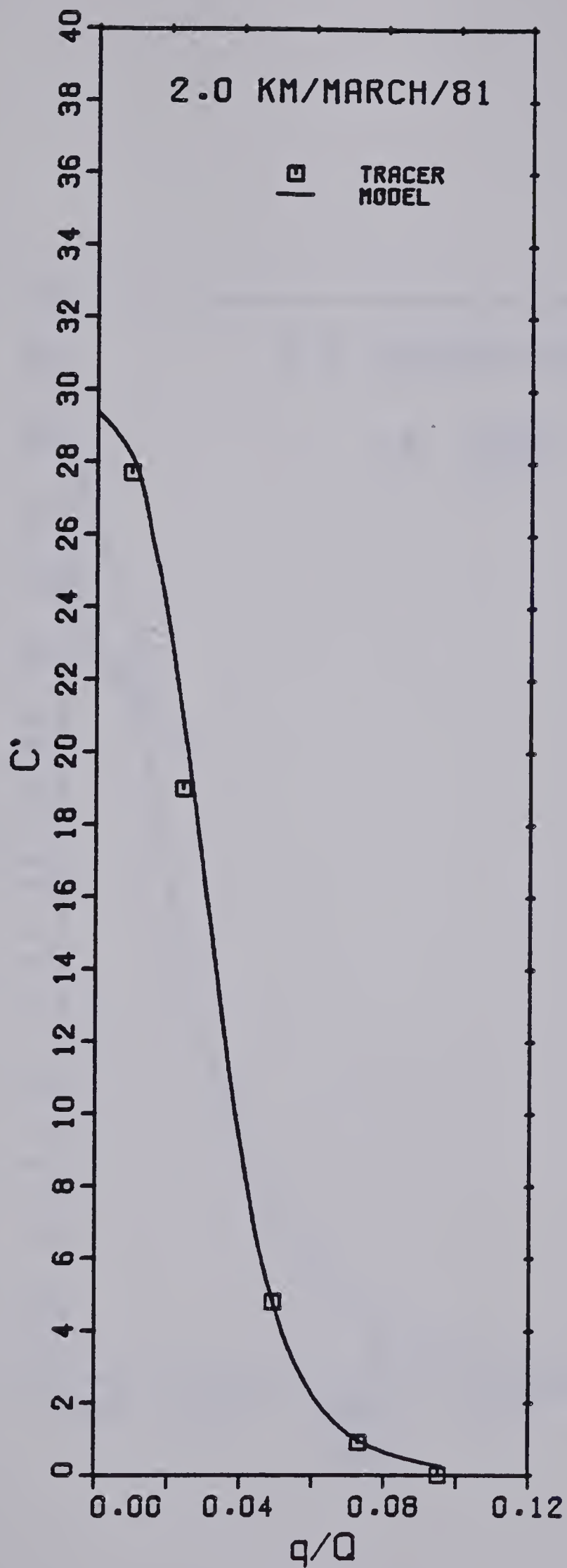


Figure 6.2(b) Computer Modelling of Normalized Tracer Distributions March 1981



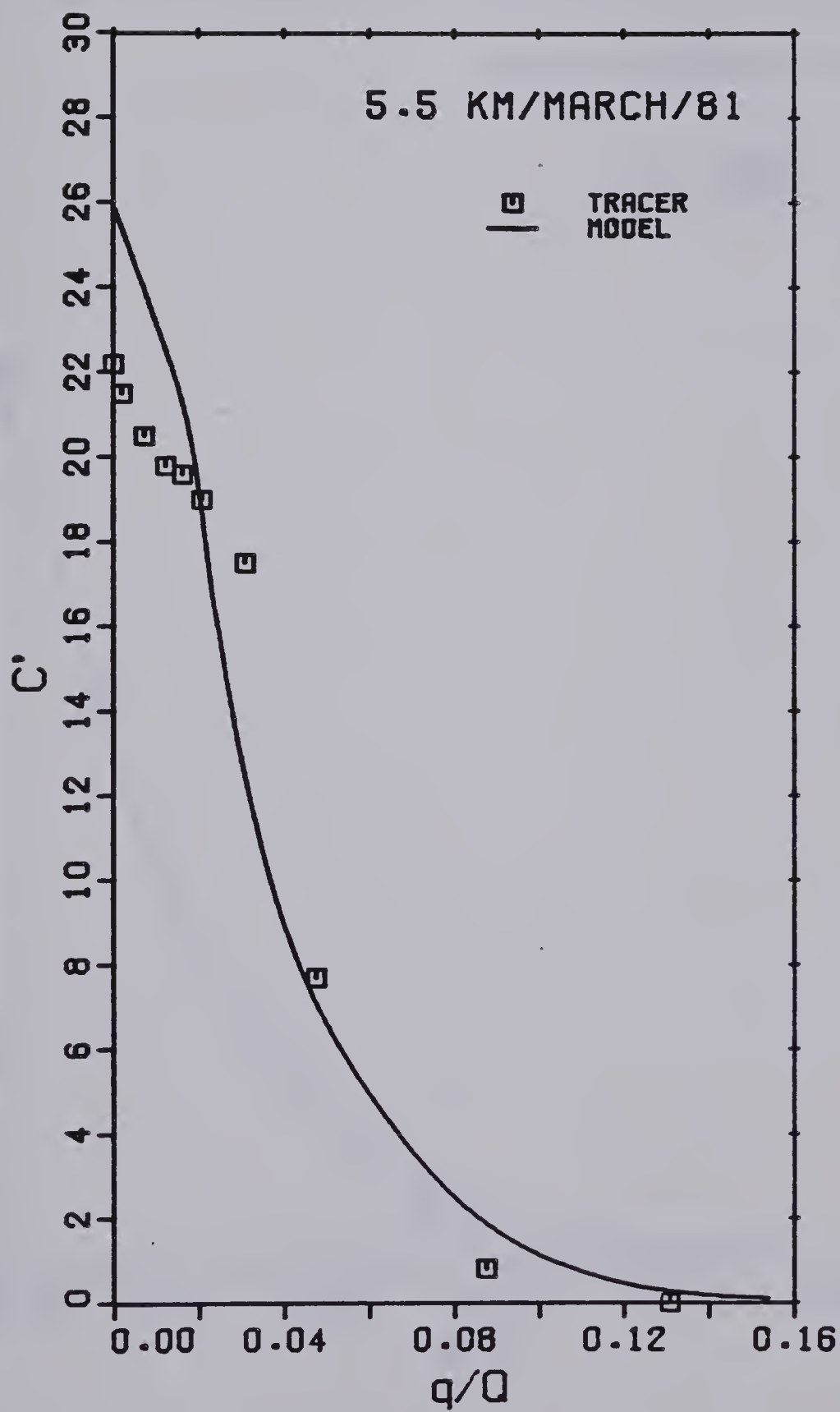


Figure 6.2(c) Computer Modelling of Normalized Tracer Distributions March 1981



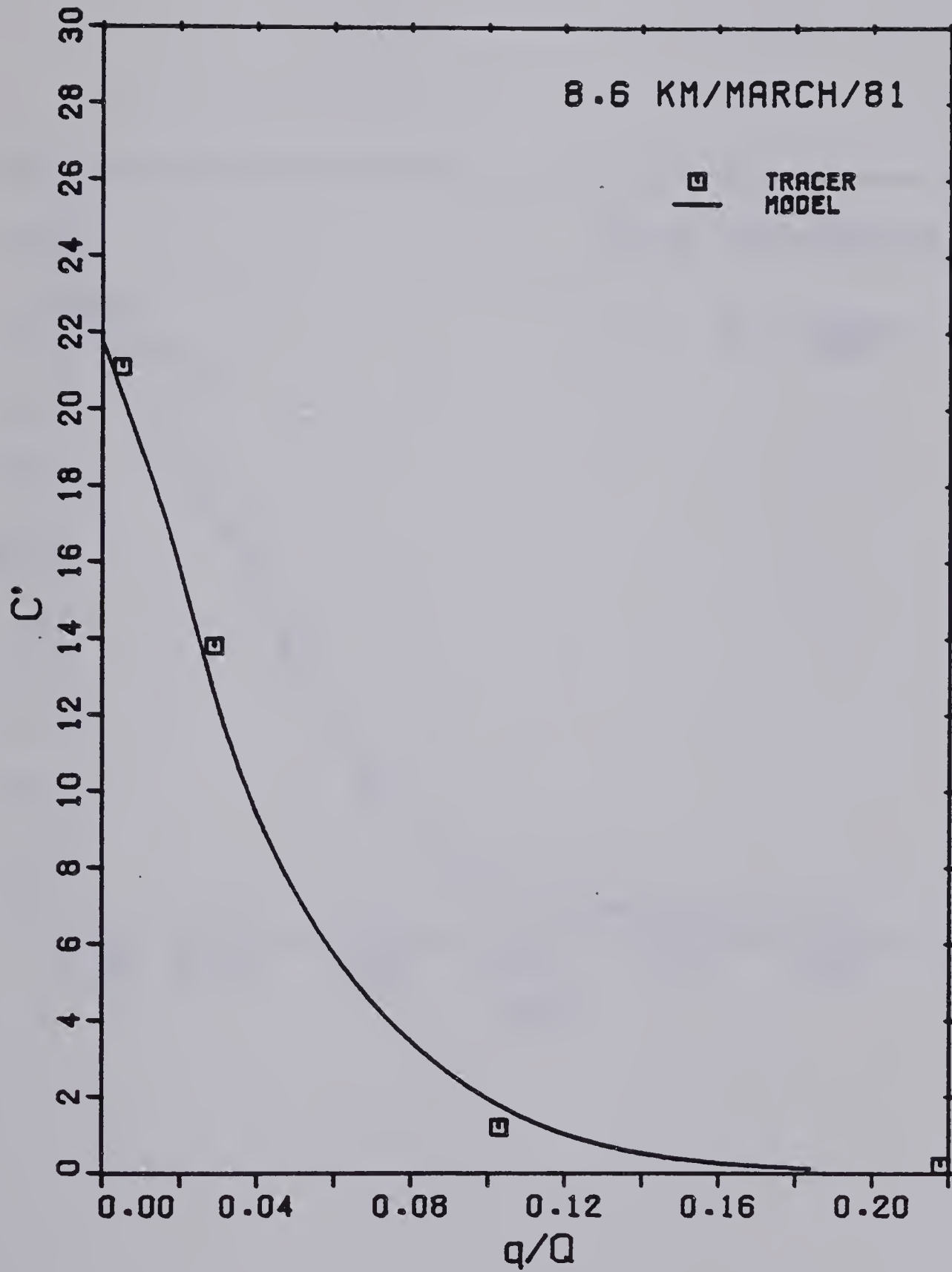


Figure 6.2(d) Computer Modelling of Normalized Tracer Distributions March 1981



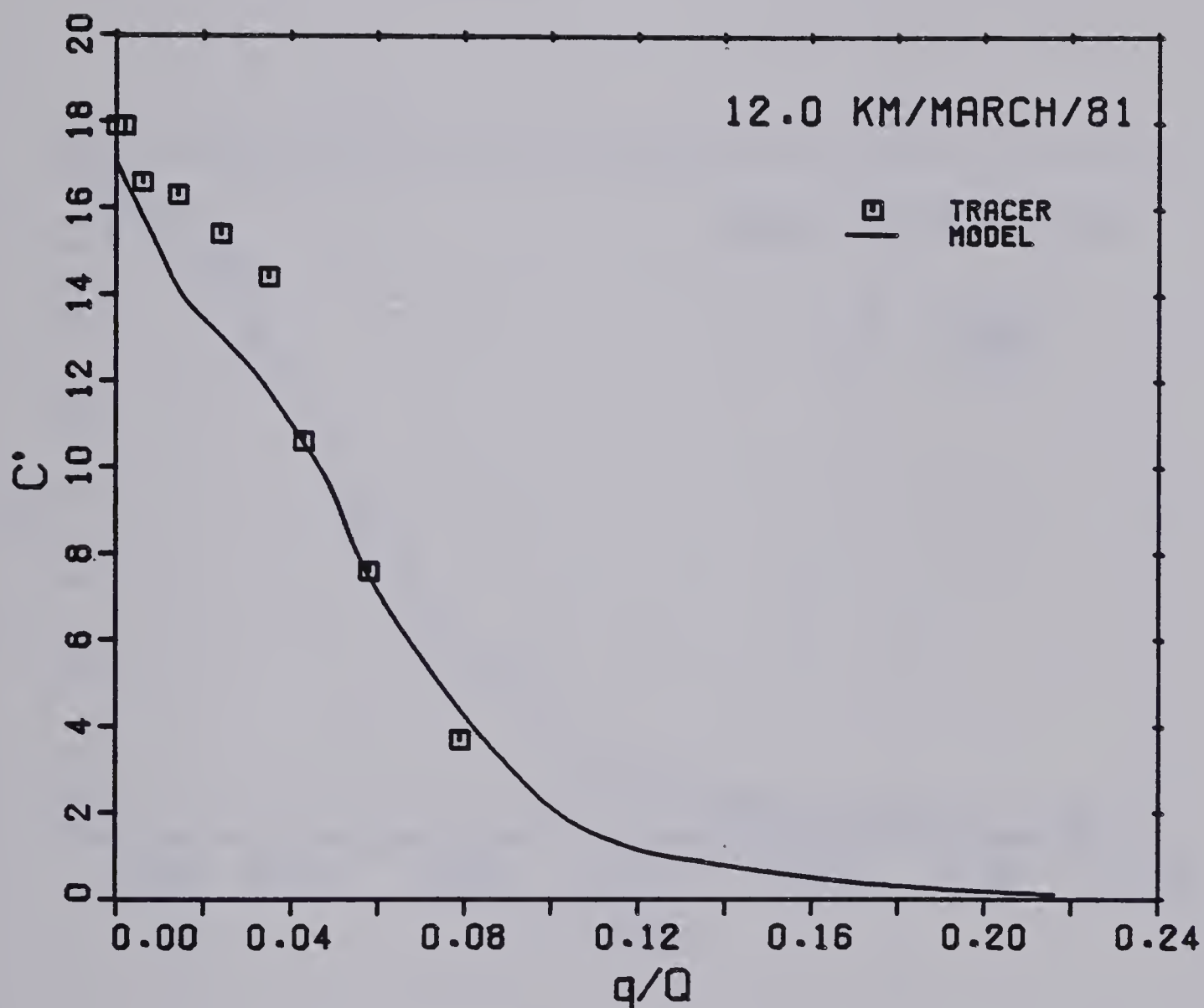


Figure 6.2(e) Computer Modelling of Normalized Tracer Distributions March 1981





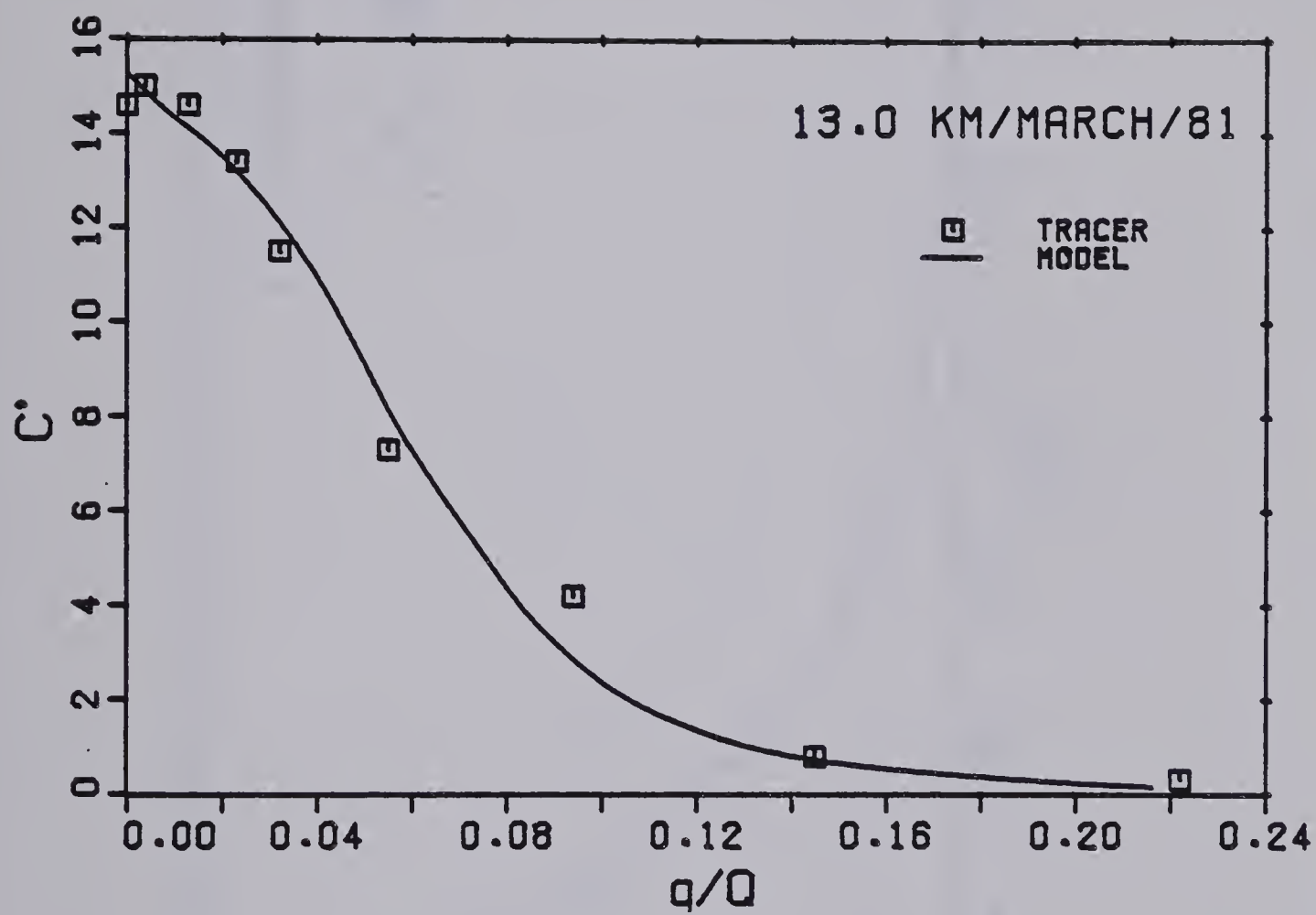


Figure 6.2(f) Computer Modelling of Normalized Tracer Distributions March 1981..



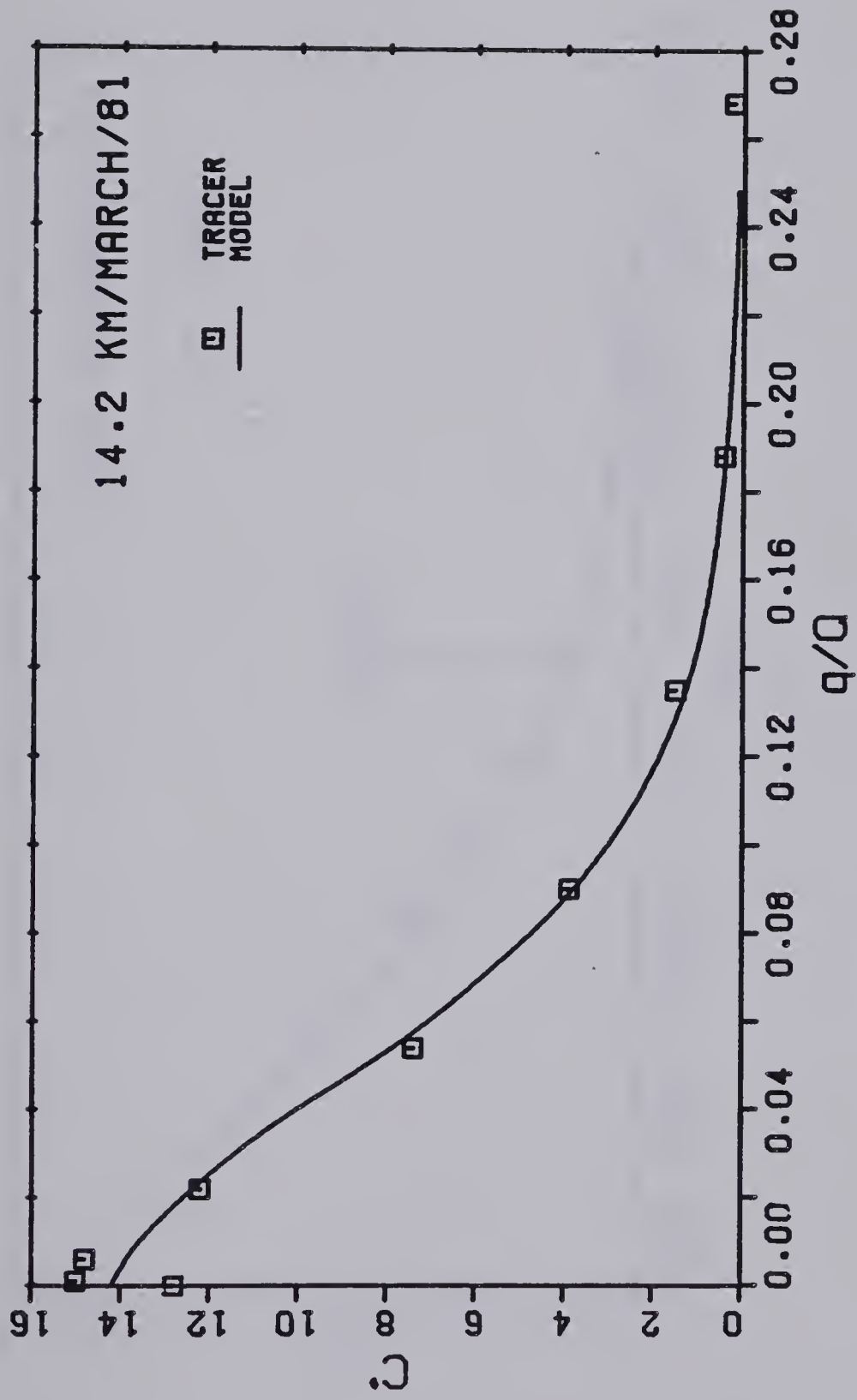


Figure 6.2(g) Computer Modelling of Normalized Tracer Distributions March 1981



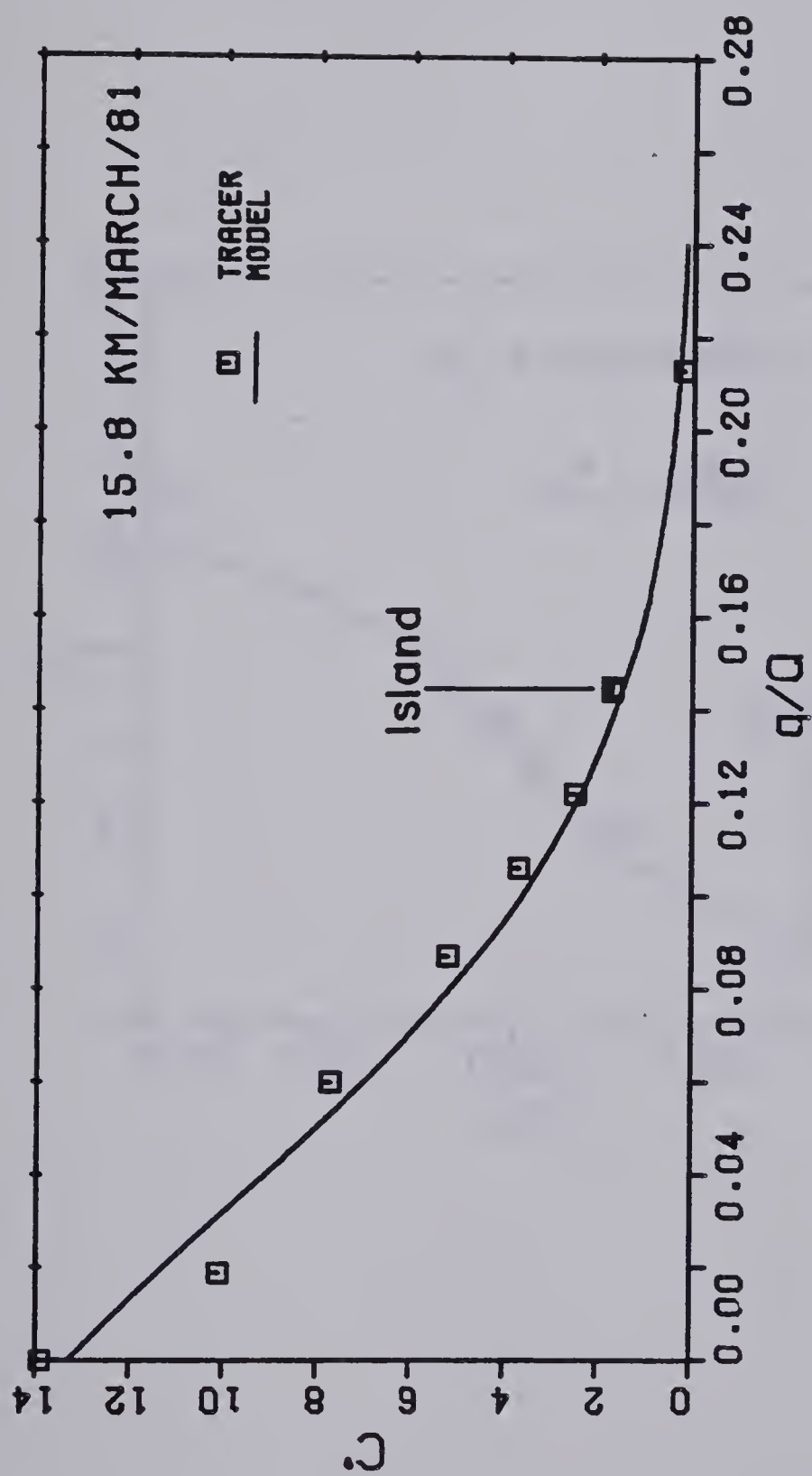


Figure 6.2(h) Computer Modelling of Normalized Tracer Distributions March 1981





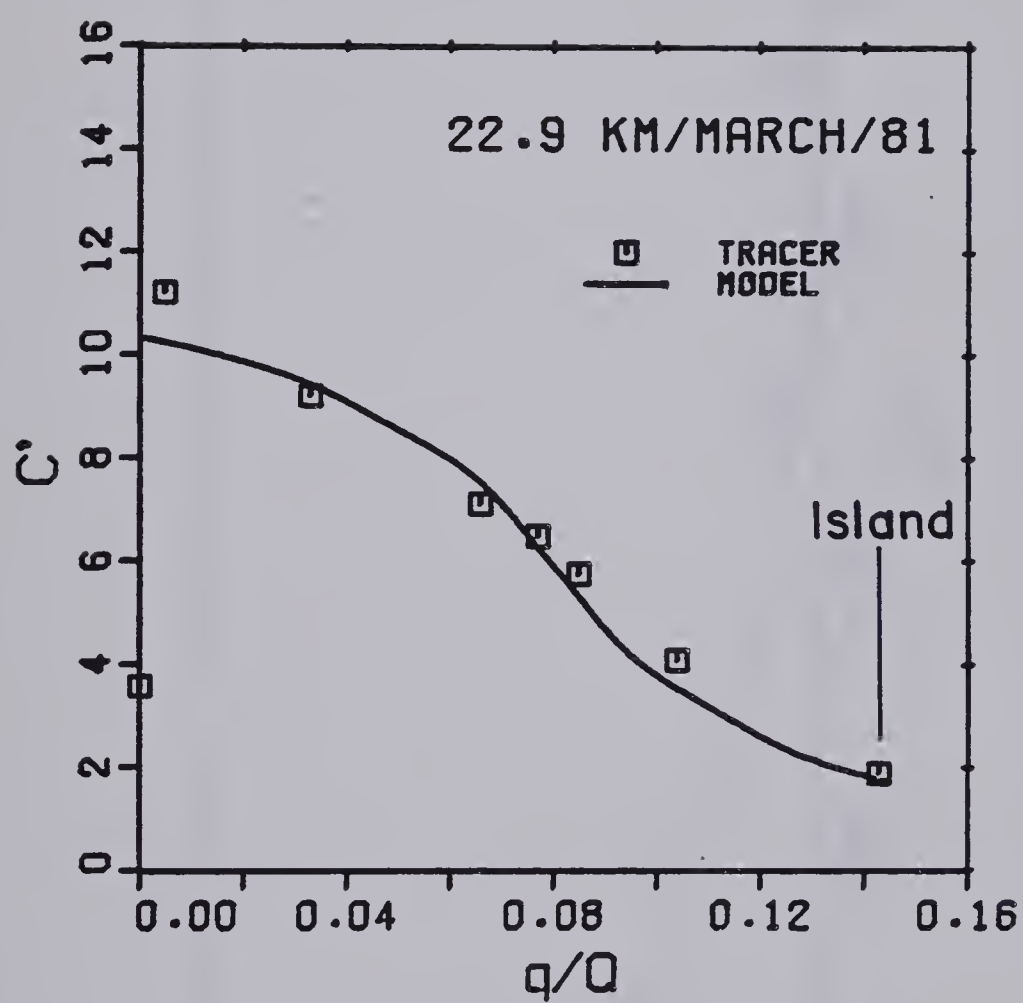


Figure 6.2(ii) Computer Modelling of Normalized Tracer Distributions March 1981



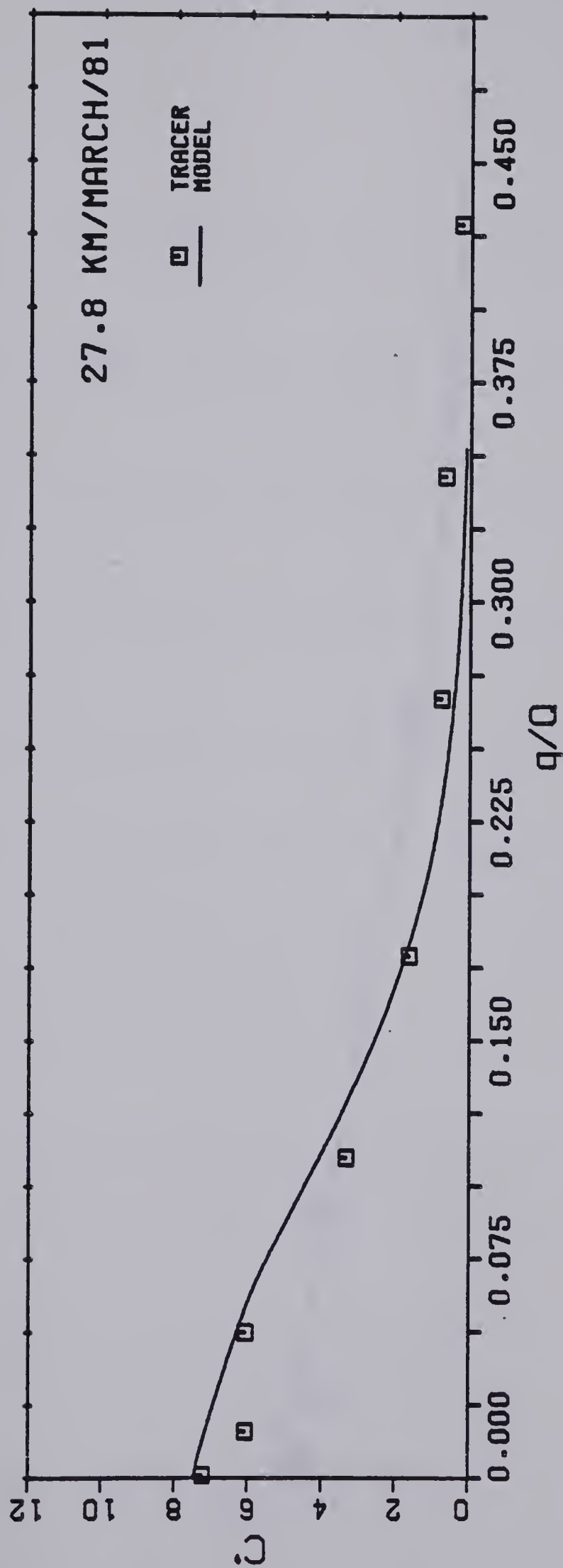


Figure 6.2(j) Computer Modelling of Normalized Tracer Distributions March 1981



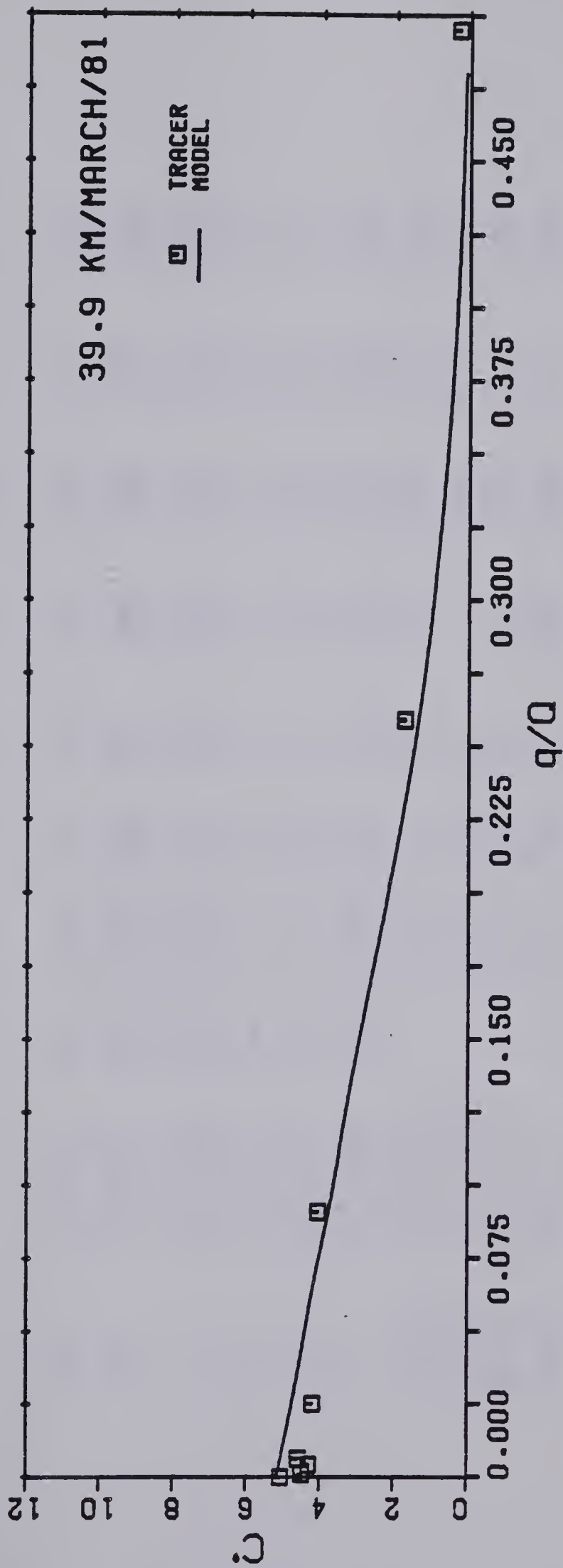


Figure 6.2(k) Computer Modelling of Normalized Tracer Distributions March 1981



Table 6.1 Numerical Solution and Plume Characteristics July 1980

X-Section (km)	Interval	$\Delta\eta$	Plume Characteristics				$E_z/\bar{h}u^*$	$E_z/\bar{b}u^*$
			$u^*$ m/s	$\bar{h}$ m	$\bar{b}$ m	$E_z$ m <sup>2</sup> /s		
0.5	0.5-0.9	.017	.0415	4.15	18@	.0406	0.01	.050
2.0	0.9-2.0	.029	.0220	0.99	225	.2471	11.34	.050
	2.0-2.3	.029	.0220	0.99	187	.2069	9.45	.050
5.5	2.3-4.85	.064	.0370	2.79	126@	.2531	2.45	.054
	4.85-7.80	.064	.0370	2.79	65	.1328	1.29	.055
8.6	7.8-10.4	.054	.0441	3.96	53	.1160	0.66	.050
12.0	10.4-12.6	.120	.0421	3.61	82	.1903	1.25	.055
14.2	12.6-14.2	.180	.0510	5.31	61	.1719	0.64	.055
	14.2-15.6	.180	.0510	5.31	161@	.4488	1.66	.055
15.8LC	15.6-20.0LC	-	.0326	2.17	260	.4655	6.58	.055
15.8RC	15.6-22.4RC	-	.0326	6.13	54	.1609	0.53	.060
22.9LC	20.0LC-25.0LC	-	.0347	2.46	342	.6534	7.65	.055
25.8@@	23.7-26.2	-	.0376	2.88	340*	.6956	6.42	.054
27.8	26.2-27.8	.400	.0547	6.11	220*	.6652	1.99	.055
Reach Average							4.30	.053

@ estimated value

@@ 25.8 km section is a composite of the geometry at 22.9 km and 15.8RC km, note 25.0LC, 22.4RC, and 23.7 km are the same location, 23.7 km is the average distance while the others represent the distances along the right and left channels past Sawmill Island.





Table 6.2 Numerical Solution and Plume Characteristics March 1981

X-Section (km)	Interval	$\Delta \eta$	Plume Characteristics				$E_z$ m <sup>2</sup> /s	$E_z/\bar{h}U^*$	$E_z/\bar{r}U^*$	$E_z/\bar{b}U^*$
			$U^*$ m/s	$\bar{h}$ m	$\bar{b}$ m	$b$ m				
0.5	0.5-0.9	.048	.0303	3.74	25 <sup>Ⓢ</sup>	34 <sup>Ⓢ</sup>	.0152	0.13	.27	.020
2.0	0.9-2.3	.072	.0206	1.73	132	190	.0659	1.85	3.70	.024
5.5	2.3-7.80	.088	.0263	2.82	128	180	.0763	1.03	2.06	.023
8.6	7.8-10.4	.112	.0295	3.54	37	68	.0266	0.25	0.51	.024
12.0	10.4-12.6	.120	.0287	3.37	68	186	.0373	0.39	0.77	.019
13.0	12.6-13.6	.152	.0351	5.02	57	105	.0386	0.22	0.44	.019
14.2	13.6-15.6	.168	.0361	5.31	57	113	.0469	0.25	0.49	.023
15.8LC	15.6-20.0LC	-	.0214	1.86	127 <sup>ⓈⓈ</sup>	250 <sup>ⓈⓈ</sup>	.0428	1.08	2.15	.016
15.8RC	15.6-22.4RC	-	.0360	5.28	25	-	.0180	0.10	0.19	.020
22.9LC	20.0LC-25.0LC	-	.0223	2.02	204	350	.0781	1.73	3.46	.017
25.8 <sup>ⓈⓈⓈ</sup>	23.7-26.2	-	.0257	2.69	250 <sup>Ⓢ</sup>	450 <sup>Ⓢ</sup>	.1285	1.86	3.72	.020
27.8	26.2-27.8	.432	.0379	5.86	160 <sup>Ⓢ</sup>	350 <sup>Ⓢ</sup>	.1023	0.46	0.92	.031
	27.8-38.8	.432	.0379	5.86	68	200	.0606	0.27	0.55	.022
39.9	38.8-39.9	.480	.0372	5.64	134 <sup>Ⓢ</sup>	258	.0893	0.41	0.83	.019
			Reach Average to 27.8 km					1.02	2.04	.021

<sup>Ⓢ</sup> estimated value  
<sup>ⓈⓈ</sup> allowing 40m for mid-channel bar  
<sup>ⓈⓈⓈ</sup> 25.8 km section is a composite of the geometry at 22.9 km and 15.8RC km, note 25.0LC, 22.4RC, and 23.7 km are the same location, 23.7 km is the average distance while the others represent the distances along the right and left channels past Sawmill Island.



- a. the average plume-region shear velocity, this being a measure of the intensity of the turbulence, and
- b. a length scale, representative of the large scale components of the turbulence and other flow conditions responsible for lateral mixing within the plume. Suggested length scales are:
  - 1)  $\bar{b}$ , the distance between  $c'_{\max}$  and  $0.5 c'_{\max}$ , (termed the half-plume width) a characteristic of the plume width, and a measure of the size of the larger scale eddies within the plume-region, or
  - 2)  $\bar{r}$ , the average plume-region hydraulic radius, or
  - 3)  $\bar{h}$ , the average plume-region depth or depth below the ice cover

It should be noted that the use of such plume-dependent scaling parameters in a design situation would require an iterative type solution. However, because the solution converges rapidly, this is not considered particularly detrimental.

The correct scaling factors should give a dimensionless mixing coefficient more or less constant along the length of the plume. The diffusion coefficient within each river portion was assumed to scale on the average plume region' shear velocity  $U^*$  and a length scale

-----  
'The plume region being defined as the transverse distance between the left bank (the injection bank) and the point at which the tracer concentration has been reduced to 5 percent of the peak concentration.



such that

$$E_z = \beta l U^* \quad (6.1)$$

where  $\beta$  is a constant of proportionality and  $U^*$  is given by Equation 2.8 with  $R$  equal to the plume region hydraulic radius  $\bar{r}$ . The estimated reach-averaged value of  $S$  (0.00005 m/m) was used in the calculation of  $U^*$  for each river portion. Ideally local values of shear velocity could be calculated for each portion if an accurate slope profile of the river reach was available. Incremental values of the dimensionless coefficients for each test are given in Tables 6.1 and 6.2 and plotted against distance in Figure 6.3. Reach-averaged values of the dimensionless coefficients for each test are also listed in the tables.

Scatter of the dimensionless mixing coefficient over approximately one order of magnitude remains after using either  $\bar{r}$  or  $\bar{h}$  as the length scale. However, using  $\bar{b}$  gives quite constant results for the individual summer and winter tests.

Regardless of the length scale chosen a disparity in the reach-averaged summer and winter results is evident. Comparing the magnitude of the disparity using either of the vertical length scales,  $\bar{r}$  or  $\bar{h}$ , indicates the hydraulic radius is a better measure of the length scale of turbulence under ice cover than is the depth. The disparity between reach-averaged dimensionless coefficients for







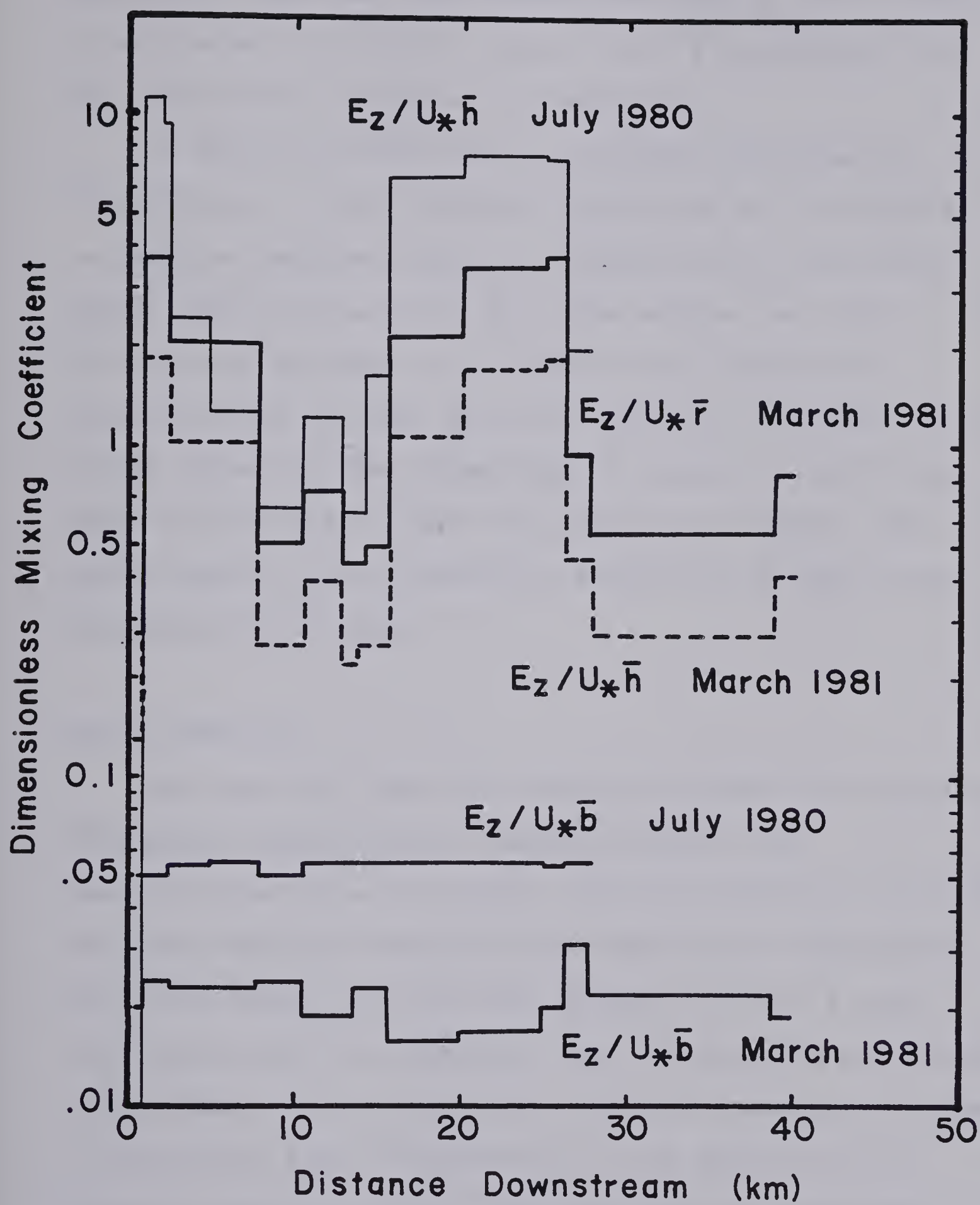


Figure 6.3 Dimensionless Mixing Coefficient versus Distance



summer and winter, using either  $\bar{r}$  or  $\bar{b}$ , is roughly of equivalent magnitude. Non-dimensionalizing  $E_z$  with  $U^*$  and  $\bar{b}$  gives the most consistent results and is considered the most appropriate method of extrapolation.

In design calculations an estimated concentration distribution, a short distance downstream of the outfall, is required because numerical simulations of the mixing cannot begin from a point or a line source. An input distribution can best be estimated using analytical solutions such as those given by Yotsukura and Cobb (1972). Errors caused by the assumptions of constant velocity and depth within this initial river portion are small, and become smaller as the numerical simulation of the mixing progresses downstream.

### March 1980 Test

The numerical model was tested by predicting the March 1980 plume characteristics using the March 1981 reach-averaged value of  $E_z/\bar{b}U^*$ , the March 1980 section data and the normalized concentration distribution measured at 0.5 km as input. Initial trial values of  $U^*$  and  $\bar{b}$  were calculated using the geometric data and assuming the spread of the plume in the transverse direction (measured in terms of cumulative flow) proportional to the square root of distance from the outfall. The model was run using the trial  $\bar{b}$ ,  $U^*$  and reach-averaged  $E_z/\bar{b}U^*$  to calculate input coefficients for each river portion. The output



distributions were then used to update the trial values for the second iteration and the process repeated until  $\bar{b}$  and  $U^*$  converged. The model was not run beyond 15.8 km because the measured tracer distribution at 27.8 km was poor for comparison purposes and actual stream geometry data between 15.8 and 27.8 km was not available for the March 1980 test.

The trial calculations are shown in Table 6.3 and the output from the final iteration plotted with the normalized measured concentrations in Figure 6.4. The plots indicate the tracer distributions are satisfactorily represented. Despite this success, the validity of using the plume  $U^*$  and  $\bar{b}$  as general scales for non-dimensionalizing  $E_z$  should be tested with other field data to ensure they are applicable to other locations.

## B. Microorganism Modelling

The non-conservative bacterial concentrations may be predicted by modifying the numerical model used for the conservative tracer. The modification requires the addition of a decay term to Equation 2.20. Chick's Law (Equation 2.35) can be written in differential form as

$$\frac{dN}{dt} = -kN \quad (6.2)$$

Following Beltaos (1981) Equation 6.2 may be substituted into the unsteady version of Equation 2.20 to give:





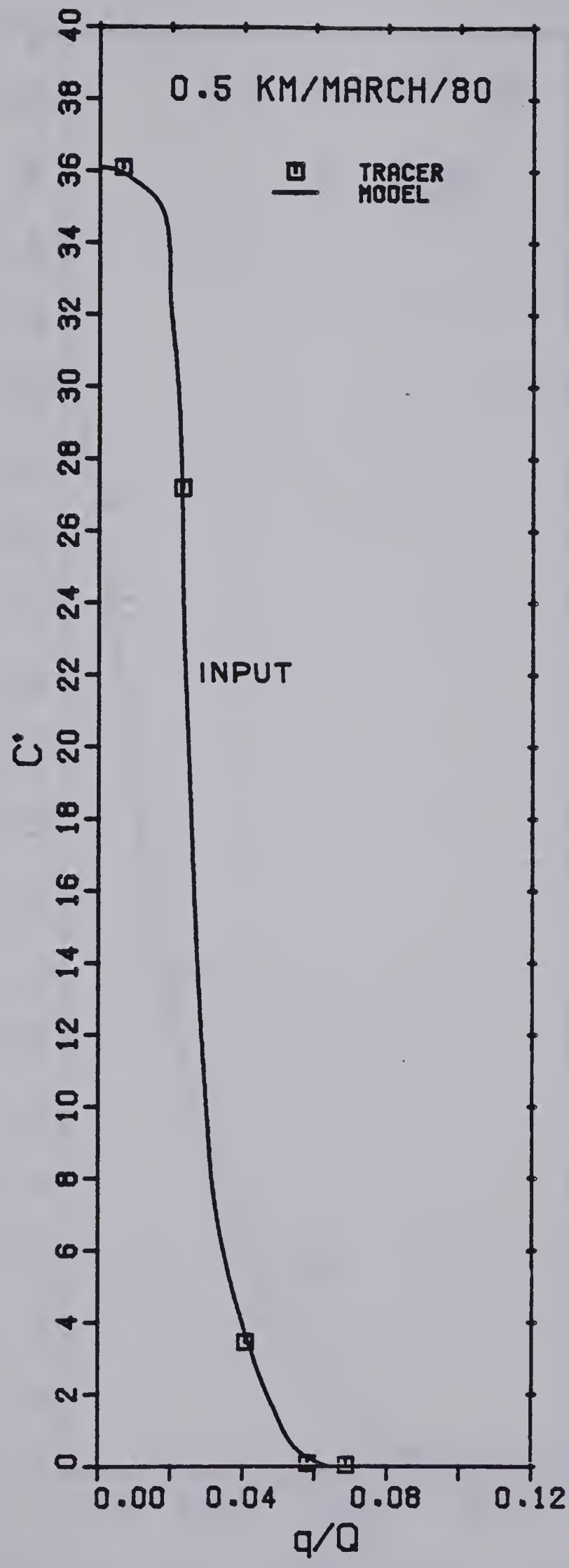


Figure 6.4(a) March 1980 Computer Modelling





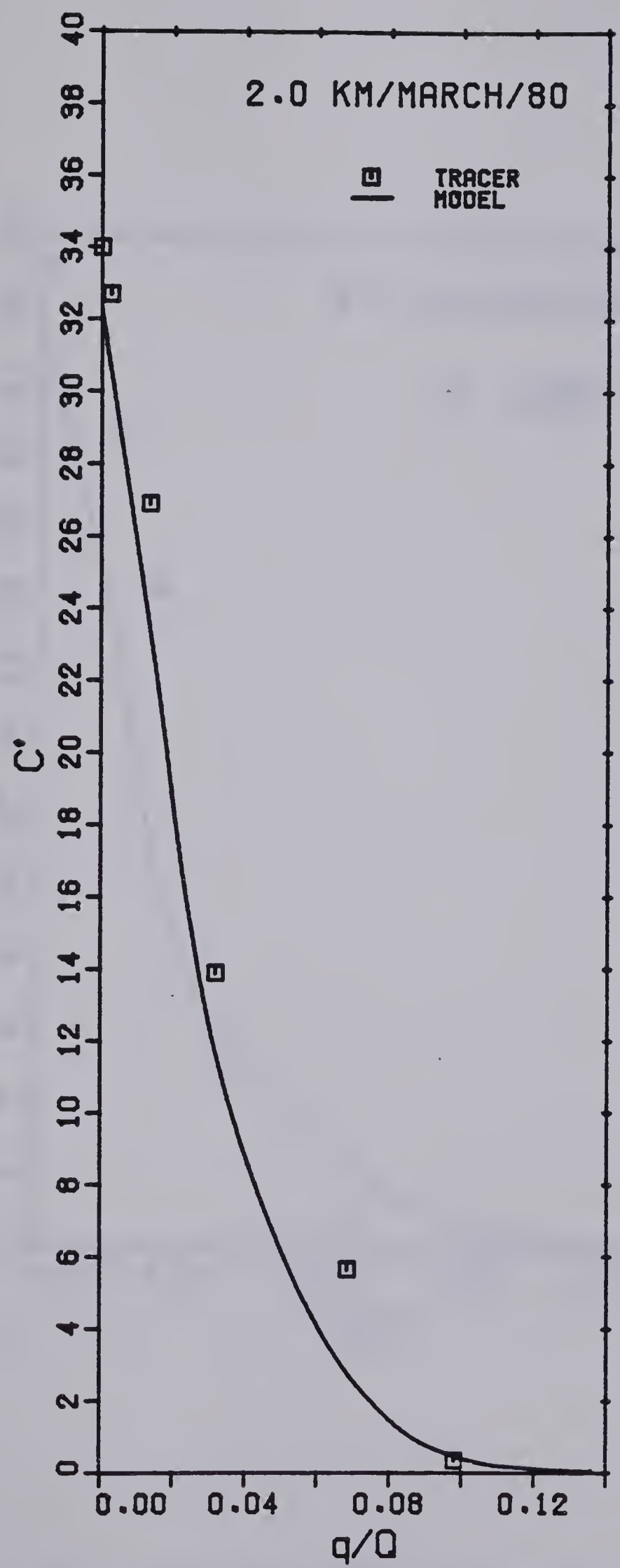


Figure 6.4(b) March 1980 Computer Modelling



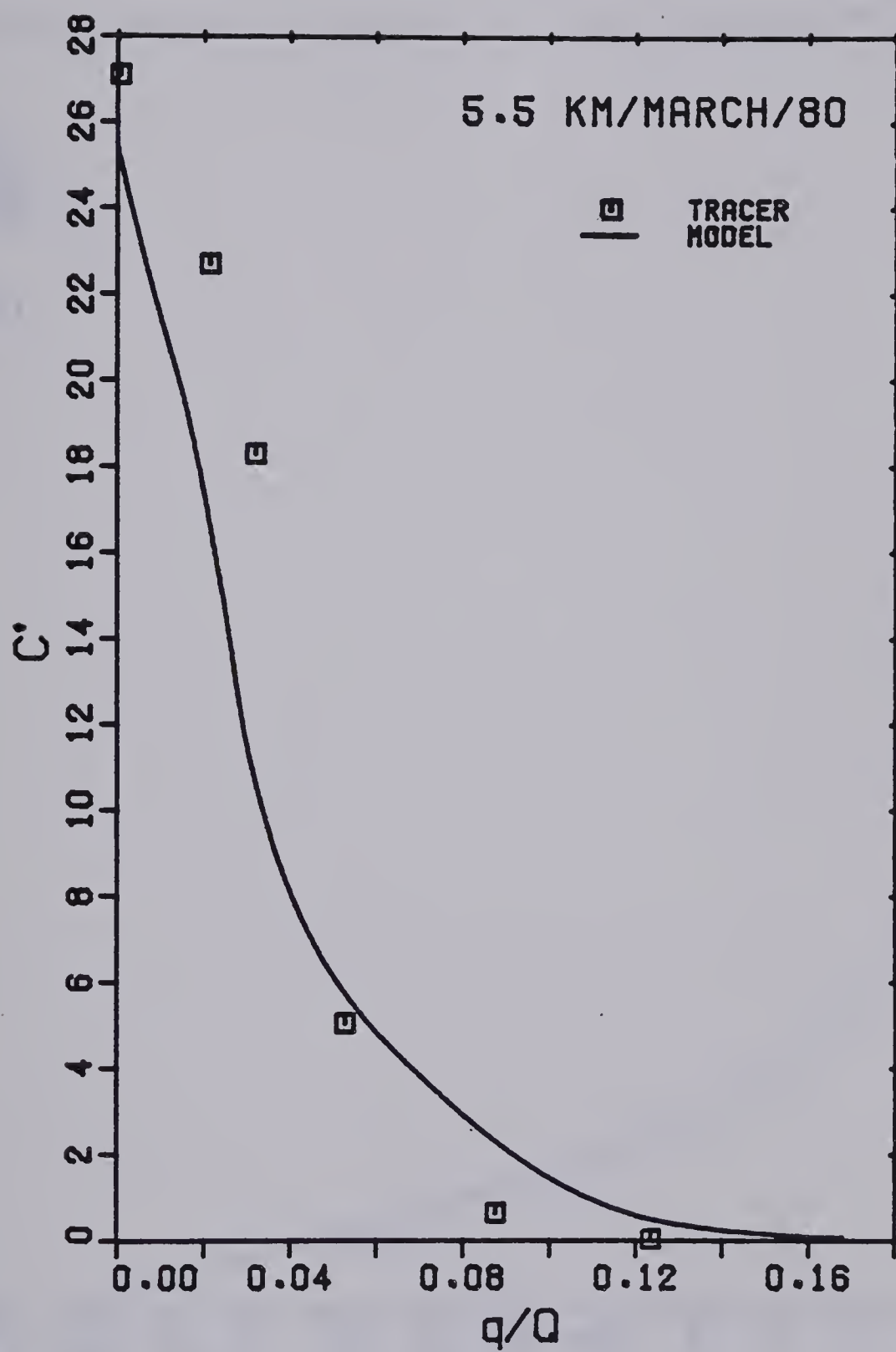


Figure 6.4(c) March 1980 Computer Modelling



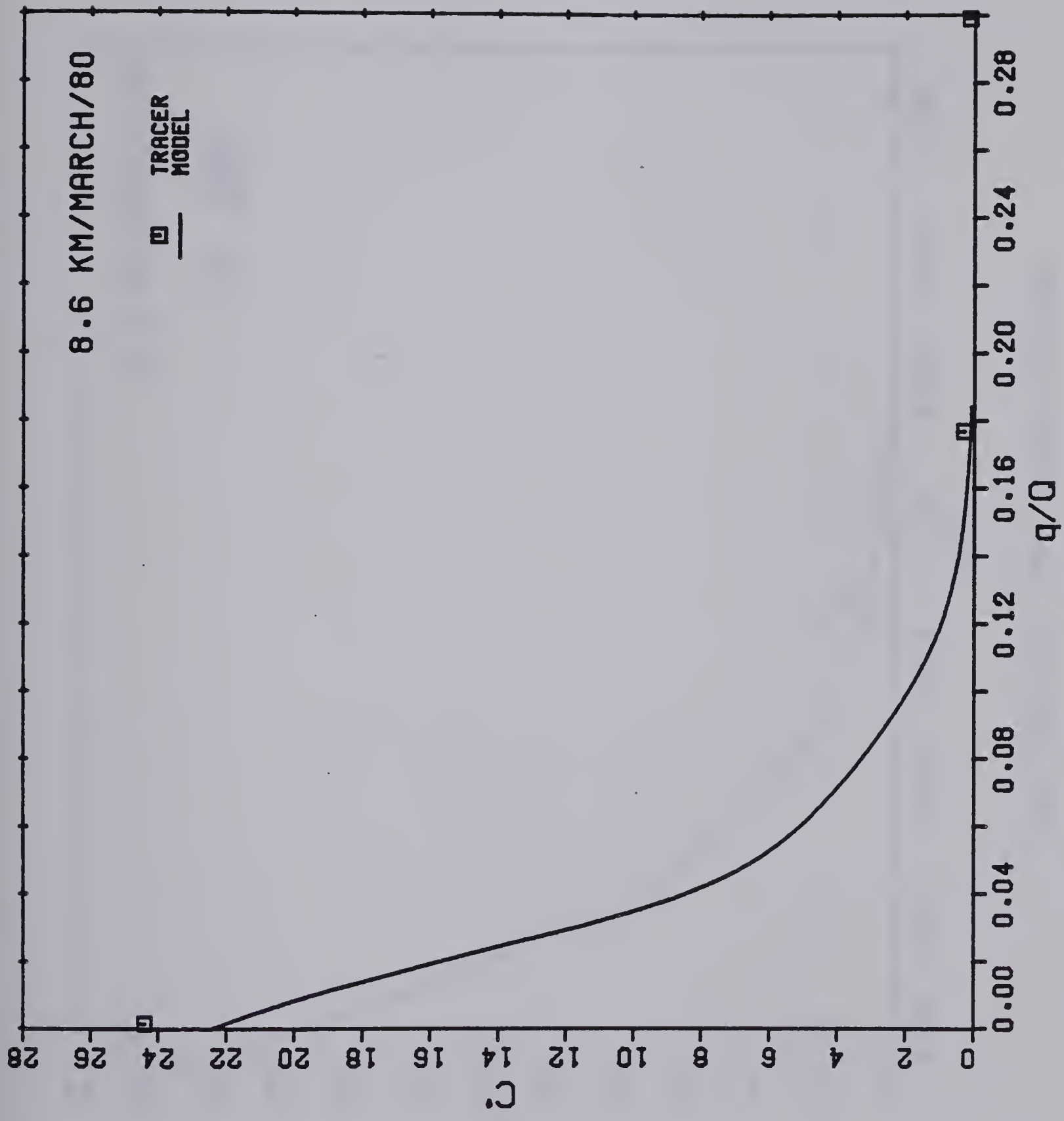


Figure 6.4(d) March 1980 Computer Modelling



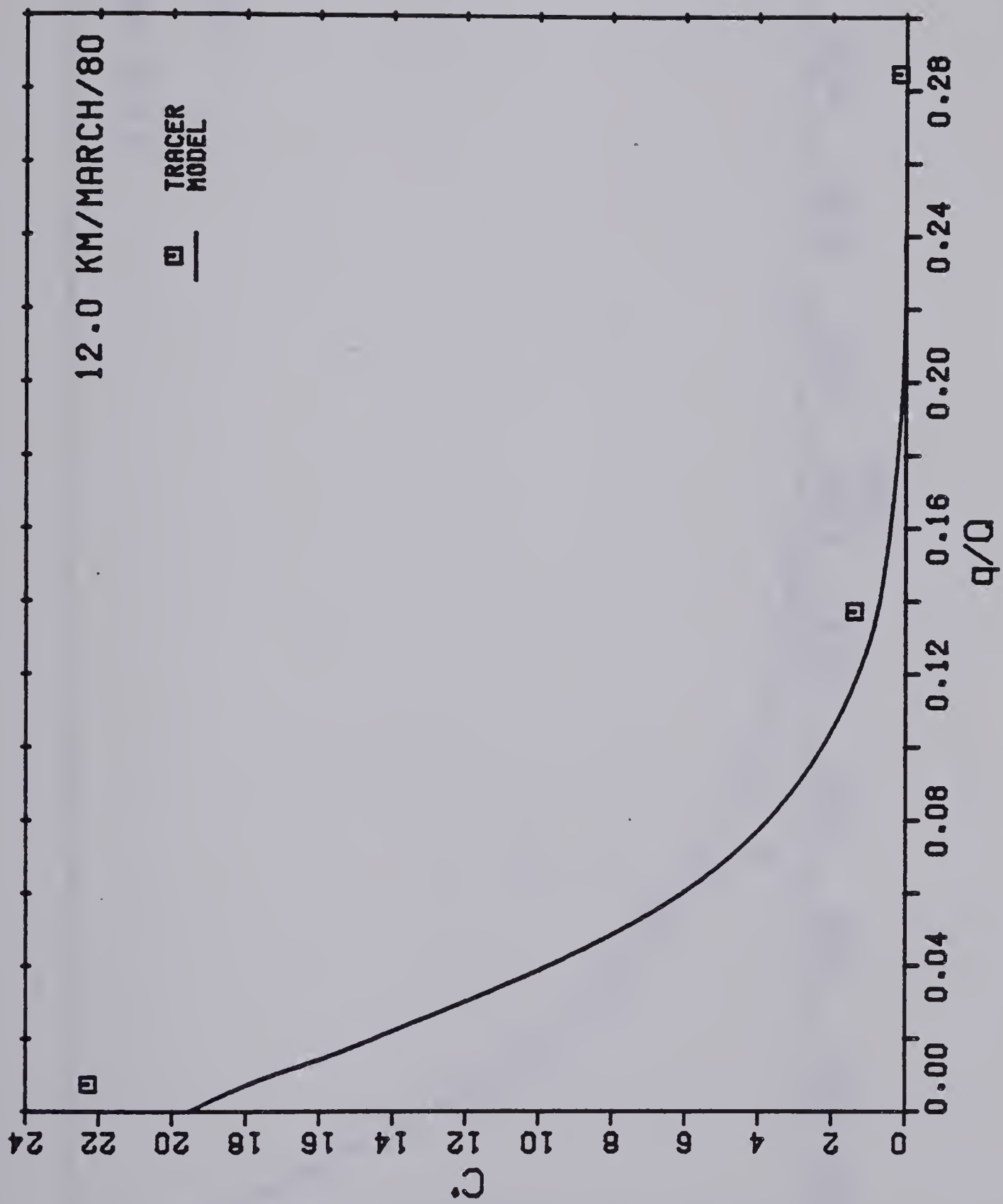


Figure 6.4(e) March 1980 Computer Modelling





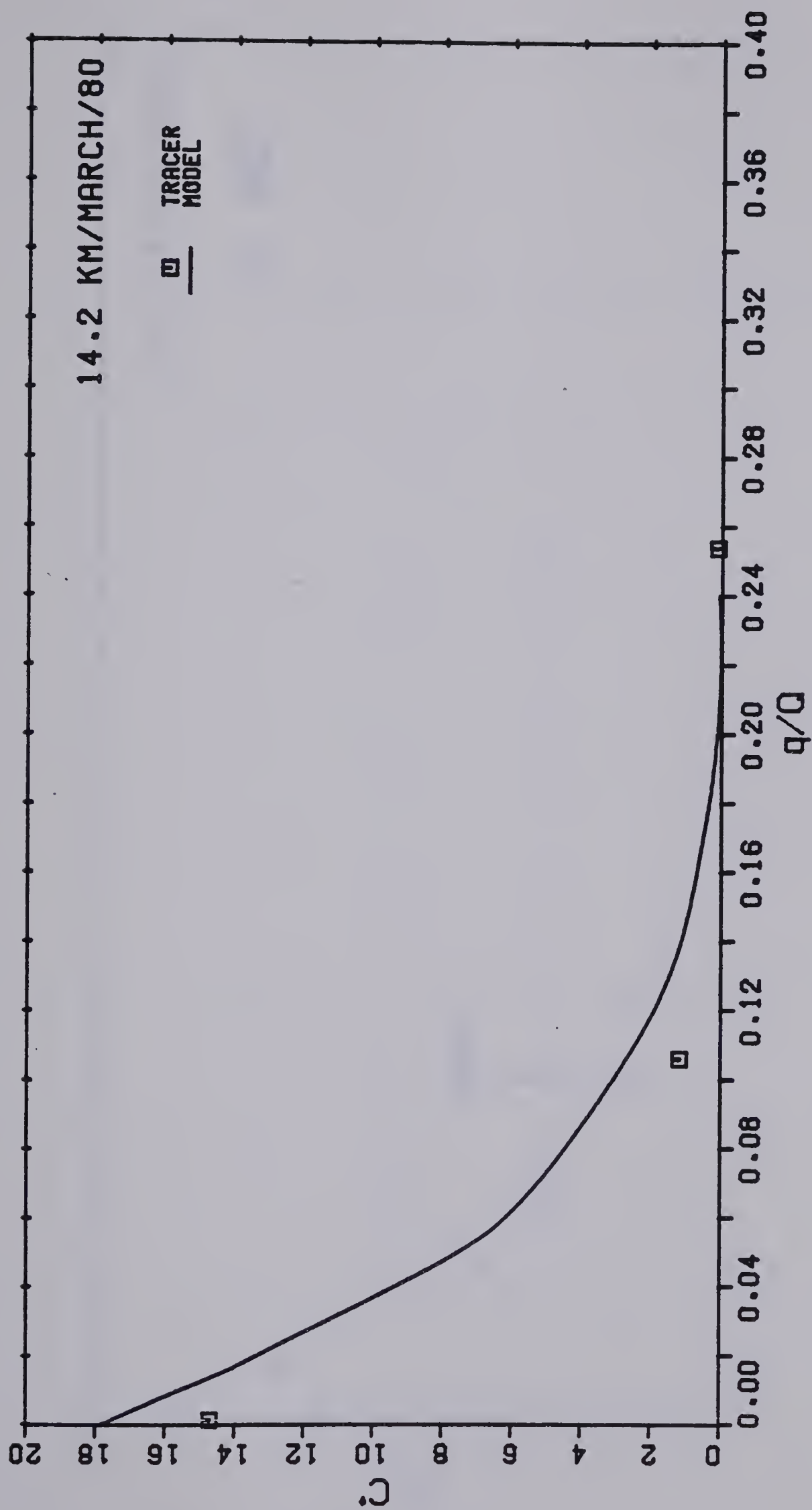


Figure 6.4(f) March 1980 Computer Modelling



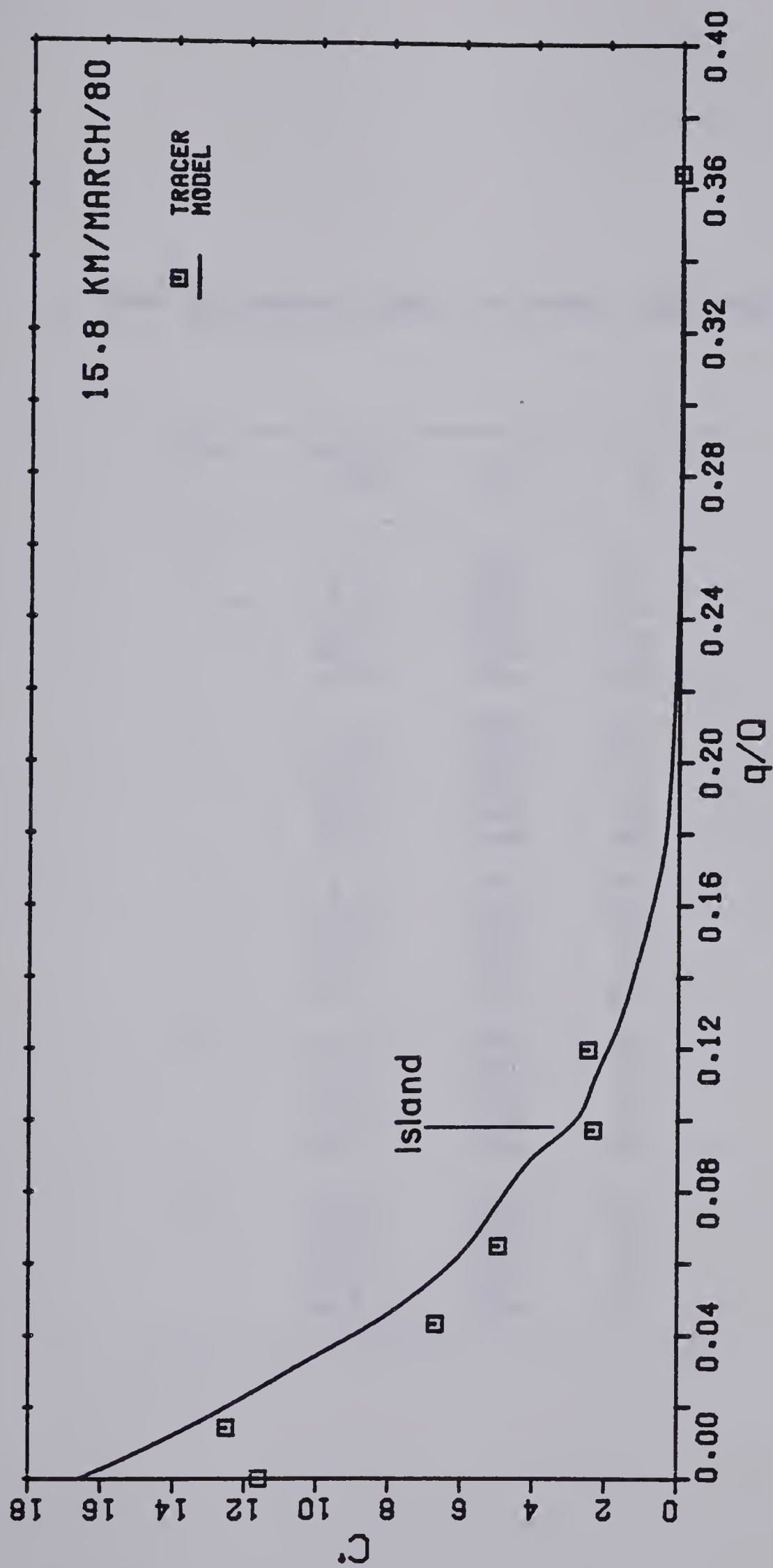


Figure 6.4(g) March 1980 Computer Modelling



Table 6.3 Iterative Solution for March 1980 Mixing

Trial	Section (km)	U* m/s	b m
1	2.0	.0229	198
	5.5	.0244	97
	8.6	.0237	36
	12.0	.0272	50
	14.2	.0310	48
	15.8	.0188	208
2	2.0	.0249	227
	5.5	.0254	110
	8.6	.0241	32
	12.0	.0273	51
	14.2	.0323	52
	15.8	.0188	200
3	2.0	.0252	227
	5.5	.0257	115
	8.6	.0267	33
	12.0	.0282	54
	14.2	.0327	54
	15.8	.0188	207
4	2.0	.0252	227
	5.5	.0257	115
	8.6	.0268	33
	12.0	.0284	54
	14.2	.0328	55
	15.8	.0188	210
5	2.0	.0252	227
	5.5	.0257	115
	8.6	.0268	33
	12.0	.0284	54
	14.2	.0329	55
	15.8	.0188	211



$$hu \frac{\partial N}{\partial x} = \frac{\partial}{\partial z} (h \epsilon_z \frac{\partial N}{\partial z}) - h k N \quad (6.3)$$

Using the 'q' transformation, non-dimensionalizing N and q and replacing  $\epsilon_z$  with  $E_z$  gives

$$\frac{\partial N'}{\partial x} = \frac{1}{Q^2} \frac{\partial}{\partial \eta} (u h^2 E_z \frac{\partial N'}{\partial \eta}) - \frac{k N'}{u} \quad (6.4)$$

Equation 6.4 can be solved numerically using the method outlined for the tracer (see Appendix VI and VII). The computer model was run for the March 1981 geometry and flow conditions using the optimum value of  $E_z$  for each river portion found for the tracer. The results for several trial k values are plotted in Figure 5.2 with the measured microorganism concentrations at 13.0 km and 27.8 km.

Comparison of the predicted distributions with the measured concentrations indicate the decay coefficient k could conceivably be between 0.0 and 0.4/day for the first 23 hours following discharge. The similarity of the generated curves illustrates a possible explanation for an indiscernable die-off rate within this period. The scatter of the data is of the same magnitude as any actual decay indicated by the solution curves. Measurement of the die-off rate over two to three days of travel is required to get a good indication of trends. Unfortunately in the present study the relatively low strength of the effluent and extremely high dilution capacity of the river cause the microorganism counts to fall to levels approaching





background within approximately one day of travel time.

A rough estimate of the optimum decay coefficient may be made by comparing the ratio of the geometric average of the measured dimensionless microbial concentrations to the solution concentrations generated for 13.0 and 27.8 km (see Figure 5.2(c) and (e)). The average ratios for all the sampling points with greater than 10 percent of the peak concentration are shown in Table 6.4. The results of the analysis once again illustrates the difficulty in discerning a decay rate. Any value in the range of 0.0 to 0.2/day would be appropriate, however a decay coefficient of approximately 0.1/day for both total and fecal coliforms appears to be the best estimate that can be made at present.



Table 6.4 Ratio of Measured Microbial Concentrations to Time-Dependent Decay Curves

Indicator	Decay Coefficient (1/d)		
	0.0	0.2	0.4
Total Coliforms	0.97	1.12	1.20
Fecal Coliforms	0.93	1.07	1.44



## VII. DISCUSSION

### A. Transverse Mixing

The tracer tests of this study have shown extremely slow lateral (transverse) mixing of effluent when discharged within the near bank region of a large natural stream. Here an assumption of complete lateral mixing a short distance downstream of an outfall would be completely invalid and decay analysis conducted on this basis would be in error. Rudimentary treatments of mixing such as that used by Frost and Streeter (1924) can also lead to confusing results. In their method the channel was divided into thirds on the basis of area and each fractional region represented by a single sampling point. A region was not considered in the calculation of the section average microbial concentration until microorganisms were detected in significant numbers at its sampling point. However, slow lateral plume spread could cause the concentrations at the first sampling point at each section to first increase, then decline as one moved downstream (see Figure 7.1). This process may explain some of the cases of aftergrowth reported in the literature.

Without steady-state tracer tests a true evaluation of microorganism decay can not be conducted until complete lateral mixing of the effluent has occurred. Unfortunately uniform lateral concentration may only be established far downstream of the river reach in which water quality is to



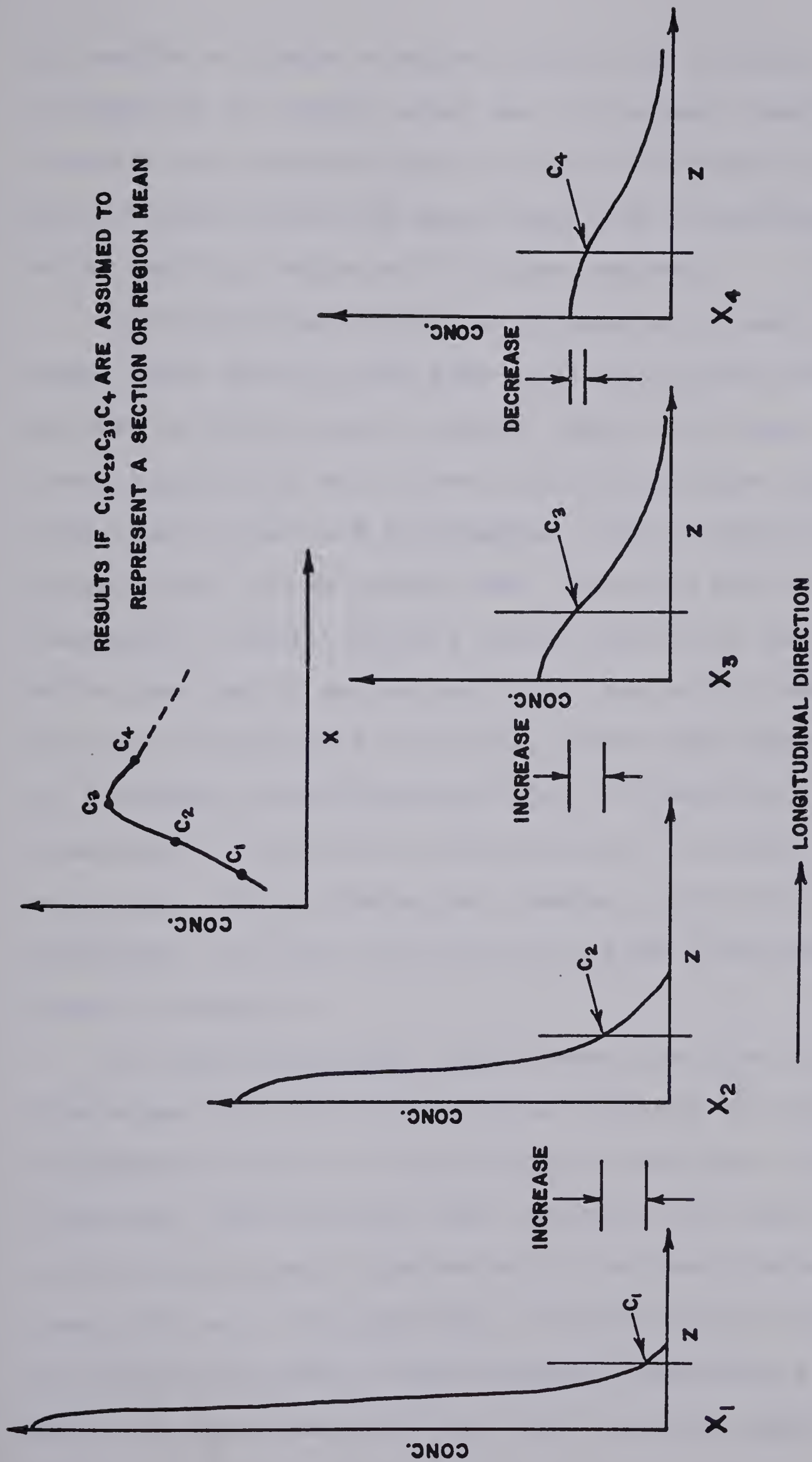


Figure 7.1 Apparent Increase in Bacterial Population due to Improper Consideration of Mixing





be studied or there is major concern due to casual consumption or contact water use. In general reaches of interest are located close to points of effluent discharge and effluent mixing and decay must both be considered in water quality studies within these regions.

Difficulty may arise when attempting to analytically model water quality data even with river mixing adequately defined by field tracer studies. Results of other investigators for mid-stream region injections (as summarized by Lau and Krishnappan (1981)) indicate  $E_z$  is proportional to the product  $WV^*$ . Generally  $WV^*$  is reasonably constant along a reach, and within the mid-stream region variations in  $uh^2$  are minor. Hence the success of analytical techniques, based upon the assumption of a constant reach-averaged  $uh^2E_z$ , in predicting transverse concentration distributions downstream of mid-stream region discharges. However, analytical techniques can prove unreliable for side discharges as shown in Chapter V.

Lau and Krishnappan (1981) have shown that for side discharges the variation in plume region  $E_z$  in the streamwise direction (from section to section) could not be neglected. Additionally, near the banks, the term  $uh^2$  varies significantly transversely. For bank discharges the term  $uh^2E_z$  will only approach a constant after the majority of tracer has moved to mid-stream and therefore a numerical solution, which accounts for local velocity, depth, and



plume-region  $E_z$ , is required.

Numerical simulation of the mixing along the Slave River study reach indicated  $E_z$  is proportional to the product  $\bar{b}U^*$  within the bank region. Other investigations for mid-stream region discharges suggest  $E_z$  is proportional to  $WV^*$ . Apparently the length scale  $\ell$ , which characterizes the size of the lateral eddies influencing the transverse mixing, varies with distance from the stream bank. Near the banks  $\ell$  appears proportional to the half-plume width while within the mid-stream region  $\ell$  is independent of plume size but proportional to stream width. For bank discharges a transition between appropriate length scales, defined by  $\bar{b}$  or  $W$ , must therefore occur as the plume spreads across the channel. The transition is illustrated in Figure 7.2 in which the dimensionless mixing coefficient is plotted against  $\bar{b}/W$ . For  $\bar{b}/W$  less than about 0.35,  $E_z/WU^*$  consistently decreases with decreasing  $\bar{b}/W$ , while  $E_z/\bar{b}U^*$  is reasonably constant. For  $\bar{b}/W$  greater than about 0.35,  $E_z/WU^*$  approaches a constant value while  $E_z/\bar{b}U^*$  begins to decline. Apparently  $\bar{b}/W$  of approximately 0.35 represents the transition between  $\ell \propto \bar{b}$  and  $\ell \propto W$  for ice covered conditions.

The transition region is not evident for the summer data shown in Figure 7.3. Local increases in mixing due to the presence of numerous side and mid-channel bars between 15.8 and 25.0 km may interfere with the trend observed in Figure 7.2. A second possibility is the transition may



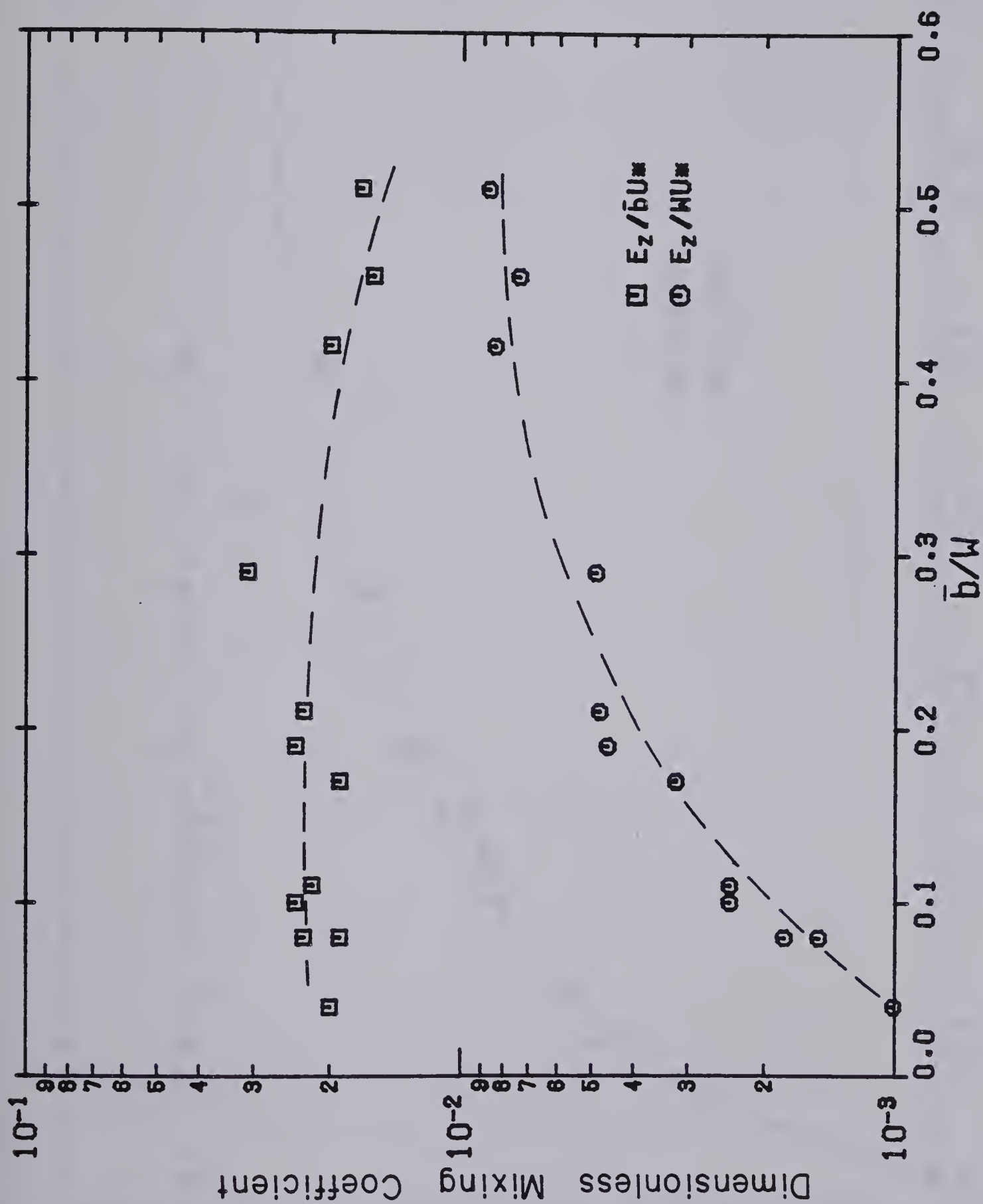


Figure 7.2 Dimensionless Mixing Coefficient versus Lateral Distance from the Left Bank, March 1981





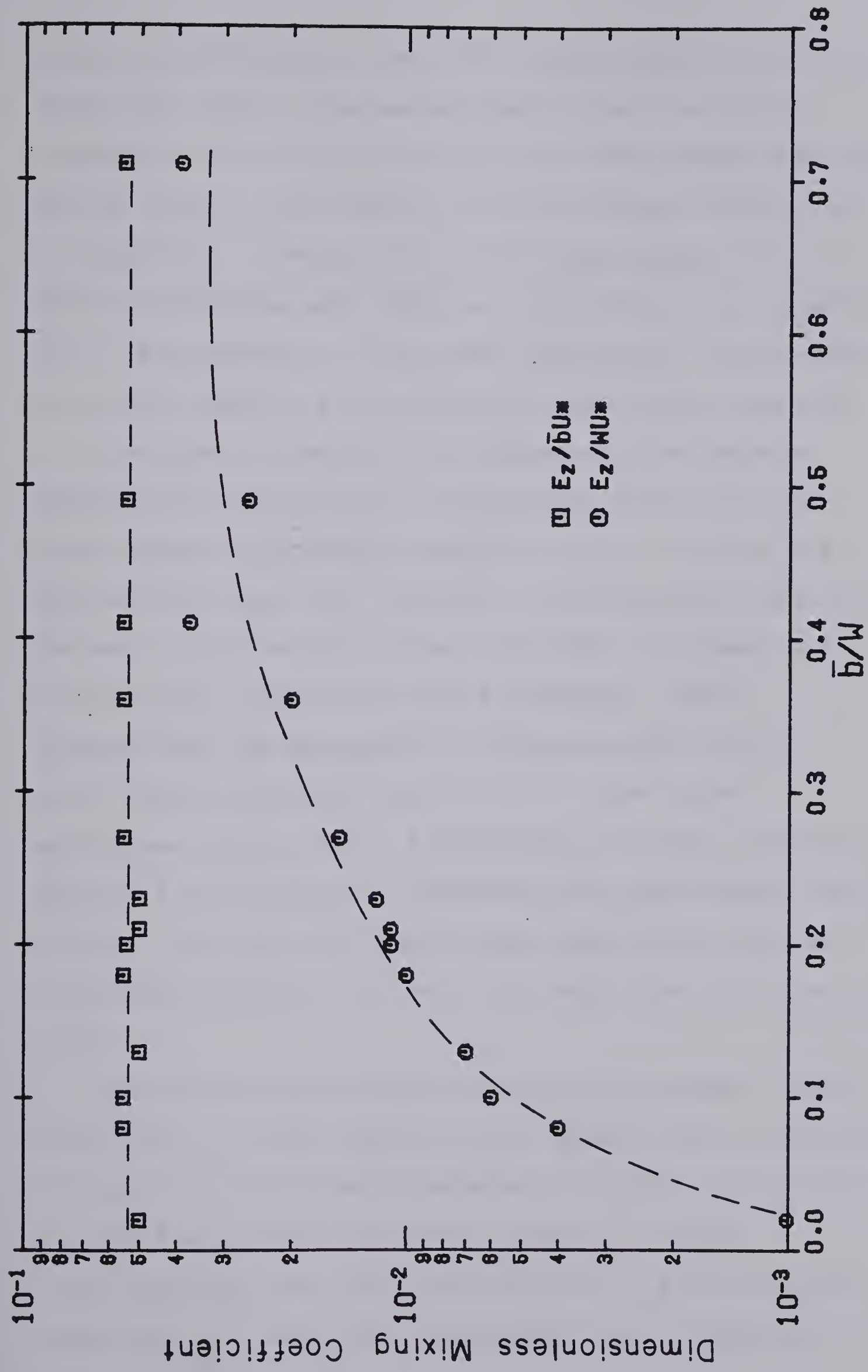


Figure 7.3 Dimensionless Mixing Coefficient versus Lateral Distance from the Left Bank, July 1980





occur for  $\bar{b}/W$  greater than 0.35. During the winter the ice cover may restrict the maximum eddy size to a certain proportion of  $W$ , while for open water the maximum eddy size may be larger. Unfortunately with the present data it is not possible to deduce the actual relationship of  $\ell$  to distance from the bank. Such a relationship would greatly aid in the selection of the most appropriate length scale to use for various flow conditions and outfall location.

As noted in Chapter VI,  $\bar{b}$  appears to be the most appropriate length scale of turbulence along the study reach because reasonably constant values of  $E_z/\bar{b}U^*$  are obtained for each test. However, an unexplained disparity between reach-averaged values of  $E_z/\bar{b}U^*$  for summer and winter tests remains. Lau and Krishnappan (1981) demonstrated the dependence of dimensionless mixing coefficient upon aspect ratio  $W/H$  for open water, mid-stream region tests. A difference in aspect ratio may account for the disparity between winter and summer data. However, the ratio  $W/R$  may be more appropriate because  $R$  implicitly accounts for restricted eddy size due to an ice cover.

For bank region mixing the appropriate aspect ratio would be  $b/\bar{r}$  or  $b/\bar{h}$  where  $b$  is the plume width as defined in Chapter VI. The reach-averages of  $E_z/\bar{b}U^*$ ,  $b/\bar{r}$  and  $b/\bar{h}$  for the Slave River are given in Table 7.1. The reach-averages were only calculated to 27.8 km to allow comparison of summer and winter data over an identical



Table 7.1 Dimensionless Mixing Coefficient versus Plume-Region Aspect Ratio

Test	$E_z/bU^*$	$b/\bar{r}$	$b/\bar{h}$
July, 1980	.053	115	115
March, 1981	.021	195	98



river reach. The data indicates a two to three fold increase in dimensionless mixing coefficient for approximately a 50 percent reduction in  $b/\bar{r}$ . This is the most comparable to the trend indicated in Figure 2.5 for strictly open water data. The disparity between summer and winter data therefore appears to be the result of plume region aspect ratio defined by  $b/\bar{r}$ .

Beltaos reported the results of two ice covered mid-stream region tests with reach sinuosities of approximately 1.0. Assuming  $W/R$  is the most appropriate aspect ratio, as indicated by the Slave River tests, values of  $E_z/WV^*$  for these winter tests are plotted in Figure 7.4 with the data previously given in Figure 2.5. The results of these ice cover tests agree with the trend indicated for open water.

The Slave River data can not be directly compared to the test results summarized by Lau and Krishnappan (1981) because the mixing coefficients are non-dimensionalized with different length scales. Direct comparison would require knowledge of the correct scale  $\ell$  for each test. Unfortunately the present data is insufficient to predict the proportionality of  $\bar{b}$  to  $\ell$  or  $W$  to  $\ell$  within their respective regions of applicability. However, the magnitude of the difference in dimensionless coefficient can be roughly estimated from Figure 7.2 and 7.3. Assuming  $\bar{b}/W$  of 0.35 represents the transition region in which either scale is appropriate then 0.35 times  $E_z/\bar{b}U^*$  should be roughly



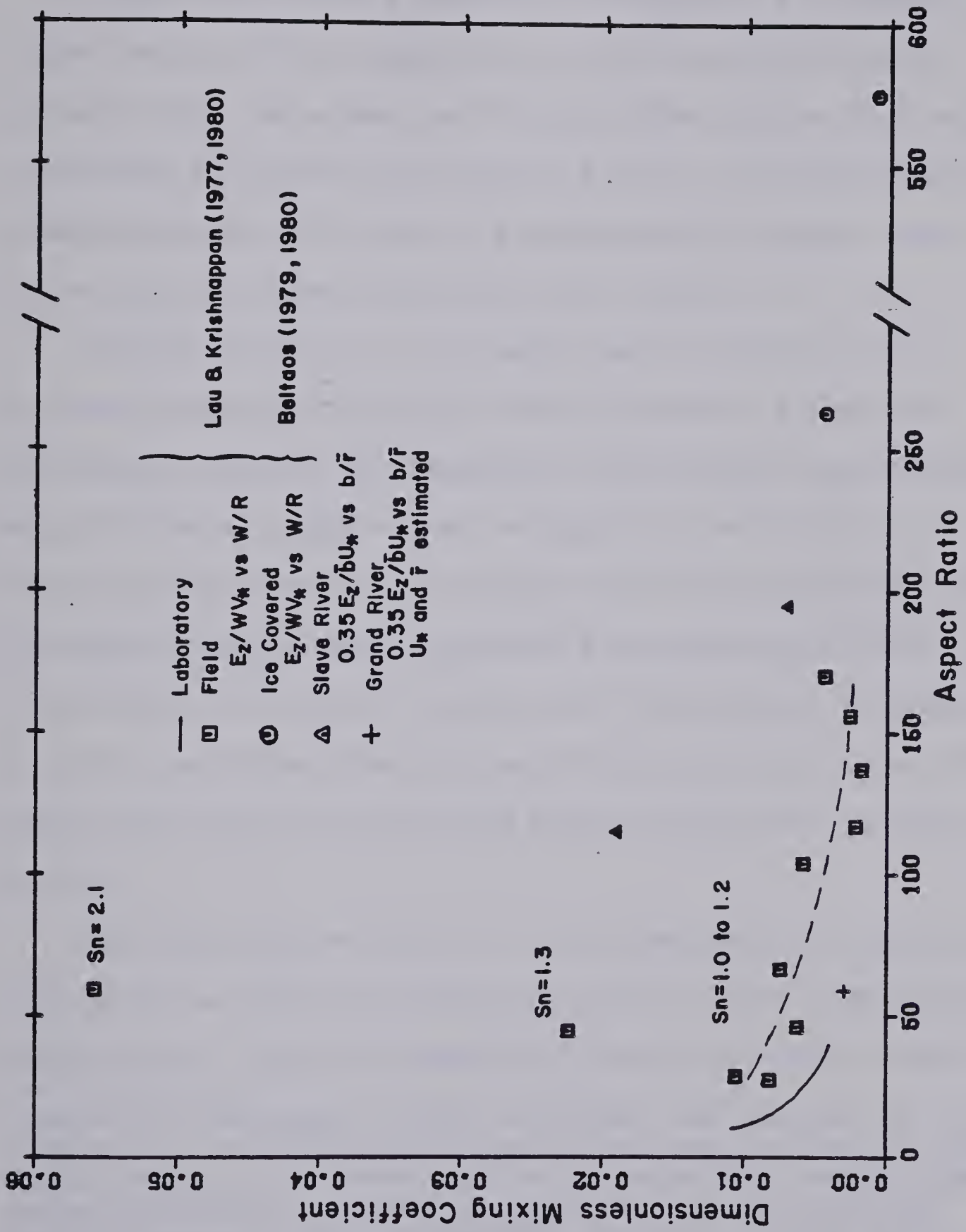


Figure 7.4 Dimensionless Mixing Coefficient versus Aspect Ratio







equivalent to  $E_z/WV^*$ . Multiplying the Slave River reach averages by 0.35 gives 0.007 for winter and 0.019 for summer.

These results are plotted in Figure 7.4, assuming the plume region  $b/\bar{r}$  is equivalent to  $W/R$  for mid-channel plumes. Both the summer and winter data points plot above the curve for points with  $Sn$  of 1.0 to 1.2. The summer dimensionless coefficient is considerably higher than the curve, plotting near the point for  $Sn$  of 1.3.'

The sinuosity of the study reach is difficult to estimate because the down valley distance is hard to accurately define. The sinuosity calculated from distances scaled from air photos and navigation charts is 1.3 assuming the down valley distance may be represented by a straight line between the outfall and the Salt River confluence. This value agrees with the average sinuosity of 1.3 for the Slave River between Fort Smith and Great Slave Lake calculated from distances scaled from the navigation charts.

If the value of  $Sn$  of 1.3 is accepted the Slave River data and the previous data point for  $Sn$  of 1.3 define a second curve relating dimensionless mixing coefficient to

-----  
'Lau and Krishnappan (1981) analysed the results of a side injection into the Grand River using section rather than plume-region parameters. Accurate reanalysis using plume region parameters is not possible due to the limited section geometry data presented. However, assuming  $U^*$  equivalent to  $V^*$  gives an estimated plume-region  $E_z/\bar{b}U^*$  of 0.003 for average  $b/\bar{r}$  of 59. Comparing this point to the data in Figure 7.4 indicates reasonably close agreement considering the value of  $U^*$  would tend to be lower than estimated.



aspect ratio. The functional relationship for dimensionless mixing coefficient, given by Equation 2.32, appears to be represented by a family of curves. Each curve represents a value of  $S_n$  and has decreasing values of dimensionless coefficient for increasing aspect ratio. This is not unexpected because the magnitude of secondary currents at bends diminish with the depth due to increasing resistance to lateral fluid motion.

Although the Slave River data appears to support the functional relationship proposed by Lau and Krishnappan (1981) more data for natural streams of higher sinuosity is required before any general conclusions can be made. The summer dimensionless mixing coefficient may be higher due to increased mixing caused by large side and mid-channel bars. These effects are less evident during the winter because flow over and around the bars is largely eliminated by the presence of the ice sheet.

## **B. Microorganism Decay**

With microorganism concentration reduction due to dilution accounted for, decreases attributable to true time-dependent decay may be evaluated. Ideally a large number of samples should be taken at each station because enumeration data is geometrically distributed. However, limited time, resources, and manpower prevented the desirable intensive sampling at each location and consequently some scatter of the data derived from



geometric averages resulted. A larger number of samples would allow a confidence interval to be associated with each point, but with the sample numbers available the data had to be considered more or less absolute.

The scatter of the data and the short flow time which could be accurately sampled both contribute to the difficulty in predicting a value of  $k$  for the reach under ice cover conditions. The best estimate of  $k$  from the ice covered results is in the range of 0.0 to 0.2/day for total and fecal coliforms. Within the reach sampled (likely the reach of most interest downstream of Fort Smith), to provide conservative estimates, the indicator bacteria should probably be considered a non-decaying pollutant under ice cover conditions (ie.  $k=0.0$ ).

As mentioned decay analysis of the summer data was not possible due to the low effluent strength and rapid decline of indicator bacteria concentrations to near background levels.

### C. Dimensionless Curves

Dimensionless treatment of the data has been used throughout the mixing and decay analysis. Non-dimensional plots have the advantage of applying to any input pollutant concentration of the same type and for the same source configuration. If the wastewater flow from Fort Smith doubled, the plume concentrations of a conservative parameter such as chlorides could easily be determined by





calculating the fully mixed concentration (see Equation 2.24) and then multiplying by the dimensionless concentration, shown in the plots for the conservative tracer, at any desired location. Similarly concentrations of any non-conservative pollutant of known  $k$  could be calculated using decay curve plots similar to those shown in Figure 5.2 for 13.0 km and 27.8 km. '

Although the tracer and microorganism curves only apply to the river flow conditions and source for which they were measured, calculations using the modelling procedure may accommodate variations in the flow, provided the mixing coefficient  $E_z$  is known. Ideally measured tracer curves should be available for a range of flows from worst conditions (generally ice covered) to typical spring or summer high water conditions to provide a relationship between  $E_z$  and stream discharge. The expected plume concentrations and characteristics may then be predicted for various flows using the modelling procedure. The

-----  
'As an example consider a serviced population increase to 5000 persons and an average wastewater production of 300L/person/day for Ft. Smith. The resulting wastewater flow would equal

$$5000 \text{ p} \times 300\text{L/p day} / 60 \times 60 \times 24 \text{ s/day} = 17.4 \text{ L/s}$$

Assuming a discharged effluent fecal coliform concentration of  $4 \times 10^5$ /100mL and a Slave River flow of 1560 cms under ice cover the fully mixed concentration would be

$$c_{\infty} = 4 \times 10^5 \times 17.4 / (1000 \times 1560) = 4.5 / 100\text{mL}$$

Referring to Figure 5.2 for 27.8 km and assuming a  $k$  value of 0.2/day indicates a dimensionless peak concentration of 6.0. Converting to an actual peak river concentration of fecal coliforms in excess of background gives

$$c_{\text{max.}} = 4.5 \times 6.0 = 27.0 / 100\text{mL}$$

If the decay coefficient was assumed zero (ie. the fecal coliforms behave as a conservative tracer ) the peak concentration at 27.8 km would be

$$c_{\text{max.}} = 4.5 \times 7.0 = 31.5 / 100\text{mL}$$





efficiency of different outfall configurations may also be evaluated by altering the shape of the input curve used in the numerical model.

#### D. Comparison of Results to Other Studies

It is difficult to make direct comparisons of the Fort Smith survey with other published data on bacterial self-purification for the following reasons:

- a. other tests are generally for much longer travel times,
- b. winter tests reported are from more temperate climates with much higher water temperatures, and generally with no ice cover,
- c. most have no assessment of mixing or, at best, only a rudimentary consideration, which undoubtedly causes errors in the initial sampling sections, and
- d. most tests have a decay curve similar to that first noted by Frost and Streeter (1924) in which two portions of the initial bacterial population die-off at different rates (The initial rapid decrease of the predominant fraction may however be significantly less than reported due to unaccounted-for mixing effects at the initial sampling stations).

An initial rapid decline of the indicator bacteria population, due to time dependent decay, is not evident within the Fort Smith effluent plume under ice cover



conditions (see Figures 4.10 and 4.12). Unlike the two phase curves of Frost and Streeter, the indicator population appears to consist of a single persistent fraction. Smith and Gerard (1981) suggested the retention time within the lagoon system may produce an acclimation effect. Acclimation or, alternatively, death of less persistent indicator bacteria within the lagoon system would eliminate the existence of a less persistent subpopulation within the river. Accepting this hypothesis, the decay rate downstream of Fort Smith should only be compared to that of the more persistent subpopulation of other studies in which no acclimation effect is evident. The die-off of the more persistent subpopulation in other studies can most accurately be estimated by assessing the reduction in numbers at the farther downstream sections. There, any effects of incomplete lateral mixing or of an initial less persist subpopulation are largely eliminated.

The best tests for comparison are those conducted on the Tanana River in Alaska under ice cover conditions (Gordon (1972), Davenport, Sparrow and Gordon (1976)). The effluent source for these tests is domestic wastewater from Fairbanks, Alaska discharged to the Chena River, a small tributary of the Tanana River. The initial sampling site on the Tanana was located a distance judged sufficiently far enough downstream of the Chena confluence to allow complete lateral mixing of the effluent. Results of the die-off analysis expressed as percentages of the initial mean



concentration at the first sampling section are given in Figure 7.5.

The rate of decline between the first and second sampling sections is slightly higher than farther downstream, the trend more pronounced for the initial test. This increased decline may be the result of incomplete lateral mixing or the existence of a less persistent fraction, which would not be unreasonable here, because the effluent was warm domestic sewage discharged directly into the near freezing river environment. A subpopulation sensitive to thermal shock would rapidly decay, the majority being eliminated before the second sampling section.

The more limited dilution capacity of the Tanana River in comparison to the Slave River allowed sampling of the effluent plume over seven days of flow time. Values of  $k$  for Equation 2.35 calculated from the slope of lines fitted to the data points beyond the second section are shown in Table 7.2. The estimated second fraction  $k$  values are well within the range of values estimated as feasible for the Slave River under ice cover conditions.

Other ice cover tests have been reported by Ballentine and Kitrell (1968) for the Red River and Mississippi River in the northern United States. Die-off curves for these tests are shown in Figure 7.6 and the estimated  $k$  values for the downstream sections included in Table 7.2. Here the  $k$  values are larger than found for the Fort Smith reach.





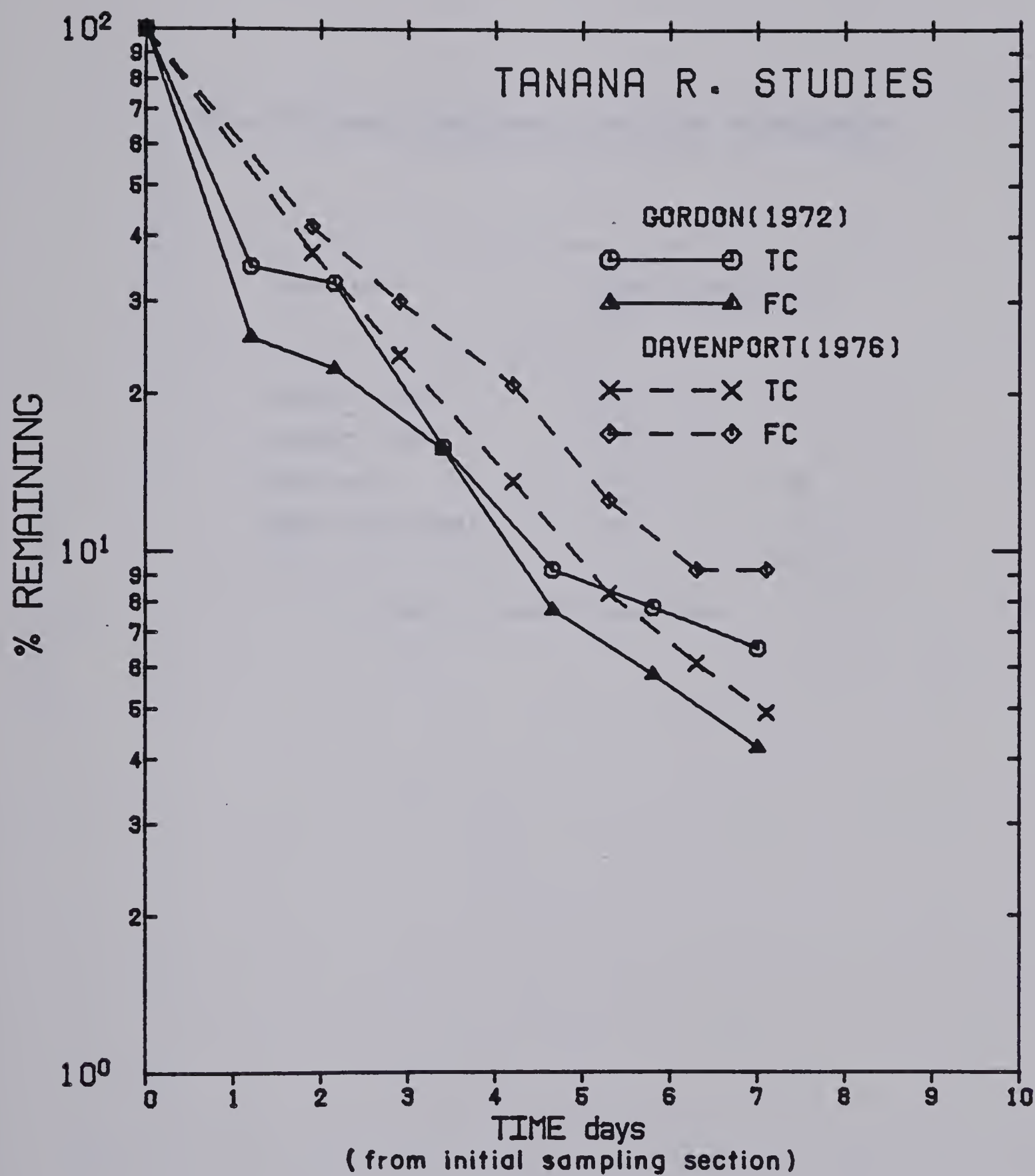


Figure 7.5 Tanana River Studies  
 -data from Gordon (1972) and Davenport, Sparrow and Gordon (1976)





Table 7.2 Decay Coefficients from Other Investigations

Location	Decay Coefficient *	
	TC	FC
Tanana R. 1970	.32	.27
Tanana R. 1975	.39	.31
Red River	.43	.35
Upper Mississippi R.	.54	.69

\* /day for natural logarithms



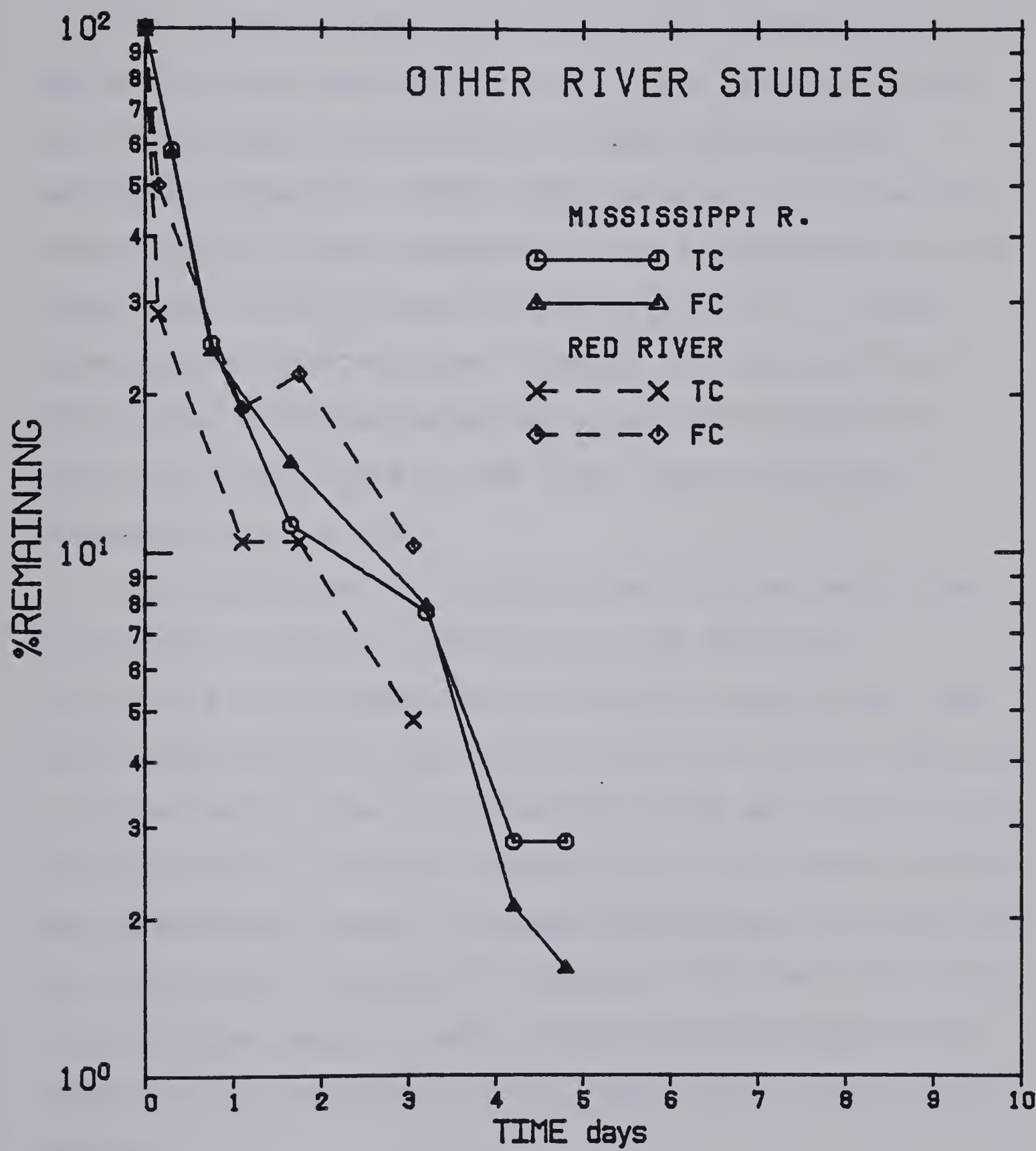


Figure 7.6 Other Ice Condition Decay Studies  
-data from Ballentine and Kittrell (1968)



However, the higher  $k$  values again may represent an inadequate assessment of dilution (mixing) or the initial presence of a significantly less persistent population fraction.

The results of the Slave River, the latter portion of the Tanana River and the Red River agree reasonably well with the  $k$  value predicted by the empirical formula developed by Mancini (1978). This formula, which predicts  $k$  on the basis of water temperature, salt concentration, and light input, gives a value of 0.48/day for 0° C, fresh water and no light exposure. Considering the scatter of points from which the relationship was derived and the absence of data points in the lower temperatures the agreement is quite good.

The Slave River and Tanana River studies verify the speculation of early investigators that bacterial persistence is extended under cold water conditions. The cold temperatures are generally thought to inhibit the rate of predation by other organisms and delay self-destruction of cells due to endogenous respiration. In northern rivers the persistence problem is compounded during the winter by ice cover which isolates the effluent from the lethal rays of sun. These factors clearly demonstrate the particular concern over contamination of northern waters by microbial wastes.

Effluent quality objectives for municipal wastewater discharges and receiving water quality objectives have both



been recently established by the Northwest Territories Waterboard.<sup>1</sup> In establishing regulations emphasis should be placed on a strategy of maintaining receiving water quality rather than setting stringent effluent quality or receiving water loading standards. In this regard a comprehensive evaluation of mixing, as demonstrated by the Slave River studies, is necessary to first simply identify plume regions to establish a proper receiving water quality monitoring program and secondly, to allow proper estimation of plume region and initial mixing zone concentrations as a guide to setting site specific regulations for effluent quality and loading rates.

-----  
<sup>1</sup> Guidelines for Municipal Type Wastewater Discharges in the Northwest Territories 1981, Northwest Territories Waterboard.





## VIII. CONCLUSIONS

Analytical solutions to the steady-state transverse mixing equation do not adequately describe the mixing of side discharges of effluent into a large natural channel. The transverse variations in stream geometry and velocity cannot be neglected near the stream boundaries and therefore a numerical solution with the capability of accounting for these variations is required to successfully model the process.

The results of this study indicate the transverse mixing coefficient is proportional to plume region characteristics rather than the reach averaged values generally used. The half-plume width used as a length scale, along with a plume region shear velocity as a velocity scale, appears to give consistent non-dimensional values of the transverse mixing coefficient along the study reach for both ice cover and open water conditions.

Although consistent results are obtained a disparity exists between reach-averaged dimensionless mixing coefficients for summer and winter data. The disparity is apparently the result of differences in plume region aspect ratio and the dimensionless mixing coefficient decreases with increasing aspect ratio as demonstrated by Lau and Krishnappan (1977, 1981). The Slave River data also appears to support Lau and Krishnappan's hypothesis that the dimensionless mixing coefficient for natural streams is dependent upon channel sinuosity. However, without more



data for natural streams with higher values of sinuosity, the functional relationship proposed by Lau and Krishnappan (1981) cannot be conclusively accepted.

The length of reach over which microorganisms decay could be studied under ice cover conditions was limited by low effluent concentration and the extreme dilution capacity of the Slave River. The ice cover data indicated die-off of total or fecal coliforms was barely discernable for approximately a one day period following effluent discharge to the river. Consequently the microorganism concentrations within this reach could be conservatively modelled by considering them as a tracer. The summer microorganism decay could not be quantified due to the high efficiency of treatment within the lagoon system and subsequent rapid dilution to background concentrations following discharge.

Microorganism mixing and decay may be modelled using the unsteady version of the mass balance equation describing transverse mixing and the numerical method employed for the conservative tracer. This method of modelling microorganism concentrations comprehensively considers both dilution effects and decay simultaneously. Utilizing this method represents an improvement over techniques employed in previous microbial self-purification studies.

Despite the success in modelling both conservative (tracer) and non-conservative (microorganisms) parameters



in this study caution must be employed when attempting to extrapolate results to other locations. The current uncertainty in estimating both transverse mixing and decay coefficients, and the requirement of stream geometry and velocity data for both analytical and numerical solutions of effluent mixing often limit their utility to preliminary studies. There is little doubt field mixing tests and bacteriological river sampling will continue to be desirable for the identification of plume regions for receiving water monitoring programs, assessment of effluent plume environmental impact and to aid in the establishment of site specific regulations regarding receiving and effluent water quality.





## BIBLIOGRAPHY

- American Public Health Association, American Water Works Association, and Water Pollution Control Federation, 1980. *Standard Methods for the Examination of Water and Wastewater*. 15th edition, Washington, D.C. pp. 786-824.
- Ballentine, R.K. and Kittrell, F.W. 1968. Observations of fecal coliforms in several recent stream pollution studies. *Proceedings of the Symposium on Fecal Coliform Bacteria in Water and Wastewater*, Bureau of Sanitary Engineering, California State Department of Public Health, Berkeley, California. 35 pp.
- Beltaos, S. 1975. Evaluation of transverse mixing coefficients from slug tests. *Journal of Hydraulic Research, International Association of Hydraulic Research* 13, 4, pp. 351-360.
- Beltaos, S. 1979. Transverse mixing in natural channels. *Canadian Journal of Civil Engineering, CSCE*, 6, 4, pp. 575,591.
- Beltaos, S. 1980. Transverse mixing tests in natural channels. *Journal of the Hydraulics Division, ASCE*, 106, HY10, pp. 1607-1625.
- Beltaos, S. 1981. Private communication.
- Butterfield, C.T. 1933. Observations on changes in numbers of bacteria in polluted water. *Sewage Works Journal*, 5, 4, pp. 600-622.
- Chick, H. 1908. Investigation of the laws of disinfection. *Journal of Hygiene*, 8, 1, pp. 92-158.
- Chick, H. 1910. The process of disinfection by chemical agencies and hot water. *Journal of Hygiene*, 10, 2, pp. 237-286.





- Dahling, D.R. and Saffermann, R.S. 1979. Survival of enteric viruses under natural conditions in a subarctic river. *Applied and Environmental Microbiology*, 38, 6, pp. 1103-1110.
- Davenport, C.V., Sparrow, E.B. and Gordon, R.C. 1976. Fecal indicator bacteria persistence under natural conditions in an ice-covered river. *Applied and Environmental Microbiology*, 32, 4, pp. 527-536.
- Davenport, C.V. and Gordon, R.C. 1978. Effect of holding temperature and time on total coliform density in sewage effluent samples. AERS Working Paper No. 31, Arctic Environmental Research Station, College, Alaska, 15 pp.
- Deaner, D.G. and Kerri, K.D. 1969. Regrowth of fecal coliforms. *Journal of the American Water Works Association*, 61, 9, pp. 465-468.
- Dutka, B.J. and Kwan, K.K. 1980. Bacterial die-off and stream transport studies. *Water Research*, 14, 7, pp. 909-915.
- Elder, J.W. 1959. The dispersion of marked fluid in turbulent shear flow. *Journal of Fluid Mechanics*, 5, 4, pp. 544-560.
- Engmann, J.E.O. and Kellerhals, R. 1974. Transverse mixing in an ice covered river. *Water Resources Research*, 10, 4, pp. 715-784.
- Fair, G.M. and Geyer J.C. 1954. *Water Supply and Wastewater Disposal*. John Wiley and Sons, New York, N.Y. pp. 831-835.
- Feurerstein, D.L. and Selleck, R.E. 1963. Fluorescent tracers for dispersion measurements. *Journal of the Sanitary Engineering Division, ASCE*, 89, SA4, pp. 1-21.
- Fischer, H.B. 1967. Transverse mixing in a sand bed channel. United States Geological Survey Professional Paper 575-D, pp. D267-D272.



- Fischer, H.B. 1967. The mechanics of dispersion in natural streams. *Journal of the Hydraulics Division, ASCE*, 93, HY6, pp. 187-216.
- Fischer, H.B., List, J.E., Koh, R., Imberger, J. and Brooks, N. 1979. *Mixing in Inland and Coastal Waters*. Academic Press, New York, N.Y., pp. 1-145.
- Gerald, C.F. 1980. *Applied Numerical Analysis*. 2nd edition, Addison Wesley, Reading, Mass. pp. 115-117.
- Glover, R.E. 1964. Dispersion of dissolved or suspended materials in flowing streams. United States Geological Survey Professional Paper 433-B, 32 pp.
- Gordon, R.C. 1972. Winter survival of fecal indicator bacteria in a subarctic Alaskan river. United States Environmental Protection Agency Report No. EPA-R2-72-013, Washington, D.C. 41 pp.
- Holley, E.R., Siemons, J. and Abraham, G. 1972. Some aspects of analyzing transverse diffusion in rivers. *Journal of Hydraulic Research*, 10, 1, pp. 27-57.
- Hoskins, J.K. 1925. Quantitative studies of bacterial pollution and natural purification in the Ohio and the Illinois Rivers. *Transactions of the ASCE*, 89, pp. 1365-1377.
- Hoskins, J.K. and Butterfield, C.T. 1933. Some observed effects of dilution on the bacterial changes in polluted water. *Sewage Works Journal*, 5, 5, pp. 763-773.
- Hrudey, S.E. and Raniga, S. 1980. Greywater characteristics, health concerns and treatment technology. *Design of Water and Wastewater Services for Cold Climate Communities*. 1981. Pergamon Press Ltd., London, pp. 137-154.



- Kittrell, F.W. and Kochtitzky, O.W. 1947. Natural purification characteristics of a shallow turbulent stream. *Sewage Works Journal*, 19, 6, pp. 1032-1048.
- Kittrell, F.W. and Furfari, S.A. 1963. Observations of coliform bacteria in streams. *Journal of the Water Pollution Control Federation*, 35, 11, pp. 1361-1385.
- Lau, Y.L. and Krishnappan, B.G. 1977. Transverse dispersion in rectangular channels. *Journal of the Hydraulics Division, ASCE*, 103, HY10, pp. 1173-1189.
- Lau, Y.L. and Krishnappan, B.G. 1981. Modelling transverse mixing in natural streams. *Journal of the Hydraulics Division, ASCE*, 107, HY2, pp. 209-226.
- Mahlock, J.L. 1974. Comparative analysis of modeling techniques for coliform organisms in streams. *Applied Microbiology*, 27, 2, pp. 340-345.
- Mancini, J.L. 1978. Numerical estimates of coliform mortality rates under various conditions. *Journal of the Water Pollution Control Federation*, 50, 11, pp. 2477-2484.
- Martin, J.D. 1982. Health Information on the Northwest Territories. *Proceedings of the Third Symposium on Utilities Delivery in Cold Regions, pre-prints* Edmonton, Alberta, 14 pp.
- McFeters, G.A. and Stuart, D.G. 1972. Survival of coliform bacteria in natural waters: field and laboratory studies with membrane-filter chambers. *Applied Microbiology*, 24, 5, pp. 805-811.
- McFeters, G.A., Bissonnette, G.A., Jezeski, J.J., Thompson, C.A. and Stuart, D.G. 1974. Comparative survival of indicator bacteria and enteric pathogens in well water. *Applied Microbiology*, 27, 5, pp. 823-829.
- Northwest Hydraulic Consultants Ltd. 1980. *Summary of Hydrological Assessments, Slave River Hydro Feasibility Study, Preliminary Report*. Edmonton, Alberta.





- Northwest Territories Waterboard. 1981. *Guidelines for Municipal Type Wastewater Discharges in the Northwest Territories, 1981*. Northwest Territories Waterboard, Yellowknife, N.W.T., 36 pp.
- Phelps, E.B. 1944. *Stream Sanitation*. John Wiley and Sons, New York, N.Y. pp. 201-221.
- Purdy, W.C. and Butterfield, C.T. 1918. The effect of plankton animals upon bacterial death rates. *American Journal of Public Health*, 8, 7, pp. 499-505.
- Sayre, W.W. and Chang, F.M. 1968. A laboratory investigation of open-channel dispersion processes for dissolved, suspended, and floating dispersants. United States Geological Survey Professional Paper 433-E, 71 pp.
- Shaw, M.K., Marr, A.G. and Ingraham, J.L. 1971. Determination of the minimal temperature for growth of *Escherichia coli*. *Journal of Bacteriology*, 105, 2, pp. 683-684.
- Shawinigan Stanley. 1982. *Final Report, Slave River Hydro Feasibility Study, Appendix B, Hydrology*. Edmonton, Alberta.
- Smith, D.W. and Gerard, R. 1981. Mixing and microorganism survival in the Slave River, N.W.T. *Proceedings of the Specialty Conference on the Northern Community: A Search for a Quality Environment*, Ed. T.E. Vinson, American Society of Civil Engineers, New York, N.Y. pp. 555-569.
- Stone, H.L. and Brain, P.L.T. 1963. Numerical solution of convective transport problems. *American Institute of Chemical Engineering Journal*, 9, 5, pp. 681-688.
- Streeter, H.W. 1934. A formulation of bacterial changes occurring in polluted water. *Sewage Works Journal*, 6, 2, pp. 208-233.
- Taylor, G.I. 1954. The dispersion of matter in turbulent flow through a pipe. *Proceedings, Royal Society of London, Series A*. Vol. 223, pp. 446-468.





- United States Public Health Service. 1924. A study of the pollution and natural purification of the Ohio River, Part II: Report on surveys and laboratory studies. Public Health Bulletin No. 143, Washington, D.C., 343 pp.
- Velz, C.J. 1970. *Applied Stream Sanitation*. Wiley-Interscience, New York, N.Y., pp. 234-248.
- Water Survey of Canada. (annual publications). Surface water data, Alberta, 1980 and 1981. Environment Canada, Inland Waters Directorate, Water Resources Branch, Ottawa.
- Weber, W.J. 1972. *Physicochemical Processes For Water Quality Control*. Wiley-Interscience, New York, N.Y. pp. 199-211.
- Wilson, J.F. 1968. Fluorometric procedures for dye tracing. Techniques of Water-Resources Investigations of the United States Geological Survey, Book 3, Chapter A12, 31 pp.
- Yotsukura, N., Fischer, H.B. and Sayre, W.W. 1970. Measurement of the mixing characteristics of the Missouri River between Sioux City, Iowa, and the Plattsmouth, Nebraska: United States Geological Survey Water-Supply Paper 1899-G, 29 p.
- Yotsukura, N. and Cobb, E.D. 1972. Transverse diffusion of solutes in natural streams. United States Geological Survey, Professional Paper 582-C, 19 pp.
- Yotsukura, N. and Sayre, W.W. 1976. Transverse Mixing in Natural Channels. *Water Resources Research*, 12, 4, pp. 695-704.



## APPENDIX I Derivation of the Pollutant Conservation Equation

The basis of all mathematical descriptions and studies of mixing is the pollutant conservation equation. The equation is derived by considering mass conservation of a pollutant within an element of the fluid body.

Concentration changes due to stream mixing alone may be described by assuming the total pollutant mass remains constant with time (ie. no time-dependent decay of concentration) and considering the pollutant to have a density equal to that of the fluid. Pollutants of this type are termed neutrally buoyant and conservative.

Considering only convective pollutant mass flow into and out of a small finite element in a Cartesian coordinate system (see Figure I-1) the following partial differential equation describing the pollutant concentration change within the element may be derived

$$\frac{\partial c}{\partial t} + \frac{\partial}{\partial x}(uc) + \frac{\partial}{\partial y}(vc) + \frac{\partial}{\partial z}(wc) = 0 \quad (I-1)$$

where the direction of the spatial and velocity components are given in Figure I-1.

In addition to mass transfer by bulk fluid flow mass flux occurs due to random molecular motion or diffusion within the fluid. Diffusive pollutant movement is similar to heat flow in a substance and follows the relationship known as 'Fick's Law'. The pollutant flux  $Q_n$  through a



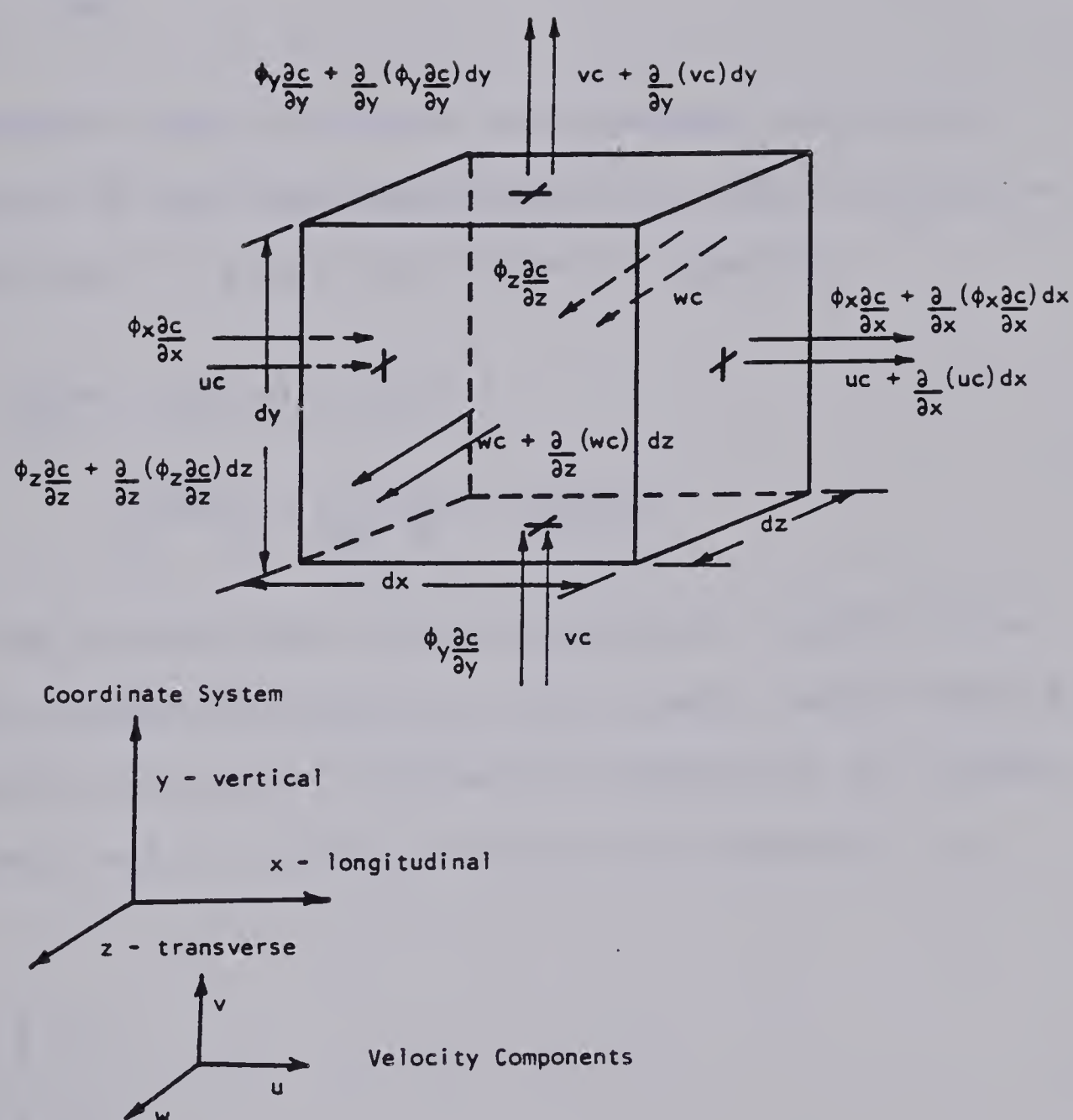


Figure I-1 Pollutant Flux In and Out of a Fluid Element in Cartesian Coordinates





plane perpendicular to the  $n$  direction is equal to the product of the concentration gradient  $\partial c / \partial n$  and a constant  $\phi_n$  called the molecular diffusion coefficient

$$Q_n = -\phi_n \frac{\partial c}{\partial n} \quad (I-2)$$

The negative sign indicates net movement is in the direction of the lower concentration. Adding diffusion flux to Equation I-1 gives the following equation

$$\begin{aligned} \frac{\partial c}{\partial t} + \frac{\partial}{\partial x}(uc) + \frac{\partial}{\partial y}(vc) + \frac{\partial}{\partial z}(wc) = \\ \frac{\partial}{\partial x}(\phi_x \frac{\partial c}{\partial x}) + \frac{\partial}{\partial y}(\phi_y \frac{\partial c}{\partial y}) + \frac{\partial}{\partial z}(\phi_z \frac{\partial c}{\partial z}) \end{aligned} \quad (I-3)$$

The velocity and concentrations at a point in a natural stream are generally not steady. Rather they are turbulent and can be considered composed of an average component and a randomly fluctuating component i.e.

$$\begin{aligned} u &= \bar{u} + u' \\ v &= \bar{v} + v' \\ w &= \bar{w} + w' \\ c &= \bar{c} + c' \end{aligned} \quad (I-4)$$

If a turbulent parameter for quasi-steady flow is time-averaged over a short period at a point the average component (ex.  $\bar{u}$ ) is constant and the resultant of the fluctuating component (ex.  $u'$ ) is zero. Substituting Equation I-4 into I-3 and taking the time average gives





$$\begin{aligned} \frac{\partial \bar{c}}{\partial t} + \frac{\partial}{\partial x} (\bar{u}\bar{c}) + \frac{\partial}{\partial y} (\bar{v}\bar{c}) + \frac{\partial}{\partial z} (\bar{w}\bar{c}) = \frac{\partial}{\partial x} (\phi_x \frac{\partial \bar{c}}{\partial x} - \overline{u'c'}) \\ + \frac{\partial}{\partial y} (\phi_y \frac{\partial \bar{c}}{\partial y} - \overline{v'c'}) + \frac{\partial}{\partial z} (\phi_z \frac{\partial \bar{c}}{\partial z} - \overline{w'c'}) \end{aligned} \quad (I-5)$$

where the overbars indicate time-averaged values.

The terms  $\overline{u'c'}$ ,  $\overline{v'c'}$ ,  $\overline{w'c'}$  represent time-averaged turbulent fluxes. These turbulent flux terms are generally expressed in the form of Fick's Law using a turbulent diffusion coefficient. For example the x direction component is:

$$\overline{u'c'} = -\epsilon_x \frac{\partial \bar{c}}{\partial x} \quad (I-6)$$

In general the turbulent diffusion in natural streams is much greater than molecular diffusion. Substitution of Equations I-6 into I-5 gives the pollutant conservation equation for turbulent flow

$$\begin{aligned} \frac{\partial \bar{c}}{\partial t} + \frac{\partial}{\partial x} (\bar{u}\bar{c}) + \frac{\partial}{\partial y} (\bar{v}\bar{c}) + \frac{\partial}{\partial z} (\bar{w}\bar{c}) = \\ \frac{\partial}{\partial x} (\epsilon_x \frac{\partial \bar{c}}{\partial x}) + \frac{\partial}{\partial y} (\epsilon_y \frac{\partial \bar{c}}{\partial y}) + \frac{\partial}{\partial z} (\epsilon_z \frac{\partial \bar{c}}{\partial z}) \end{aligned} \quad (I-7)$$

where it has been assumed the small molecular diffusion is included in  $\epsilon$ . The overbars in Equation I-7 are frequently omitted on the understanding all values are time-averaged.



## APPENDIX II Derivation of Mixing Equations for Wide Prismatic Channels

### Basic Equation

The general three-dimensional pollutant conservation equation was derived in Appendix I. Mixing within a wide prismatic channel may be represented by simplified forms of the general equation. The appropriate simplifications are dependent upon the flow characteristics and the distance downstream of the pollutant source.

Immediately following discharge a pollutant will mix in all directions. Most natural streams have a large aspect ratio (width to depth ratio) and the edges of the pollutant cloud will rapidly encounter the stream bed and the water surface. Therefore the pollutant quickly becomes well mixed in the vertical in comparison to the longitudinal and transverse directions. Generally the pollutant is well mixed in the vertical within about one hundred river depths downstream of the source. It is advantageous to work with a depth-averaged equation beyond this point. The time-averaged components of velocity and concentration in Equation I-7 may be considered to contain a depth-average component and a spatially fluctuating component whose depth-average is zero, ie.

$$\begin{aligned}\bar{c} &= \bar{\bar{c}} + c'' \\ \bar{u} &= \bar{\bar{u}} + u'' \\ \bar{v} &= \bar{\bar{v}} + v'' \\ \bar{w} &= \bar{\bar{w}} + w''\end{aligned}$$

(II-1)



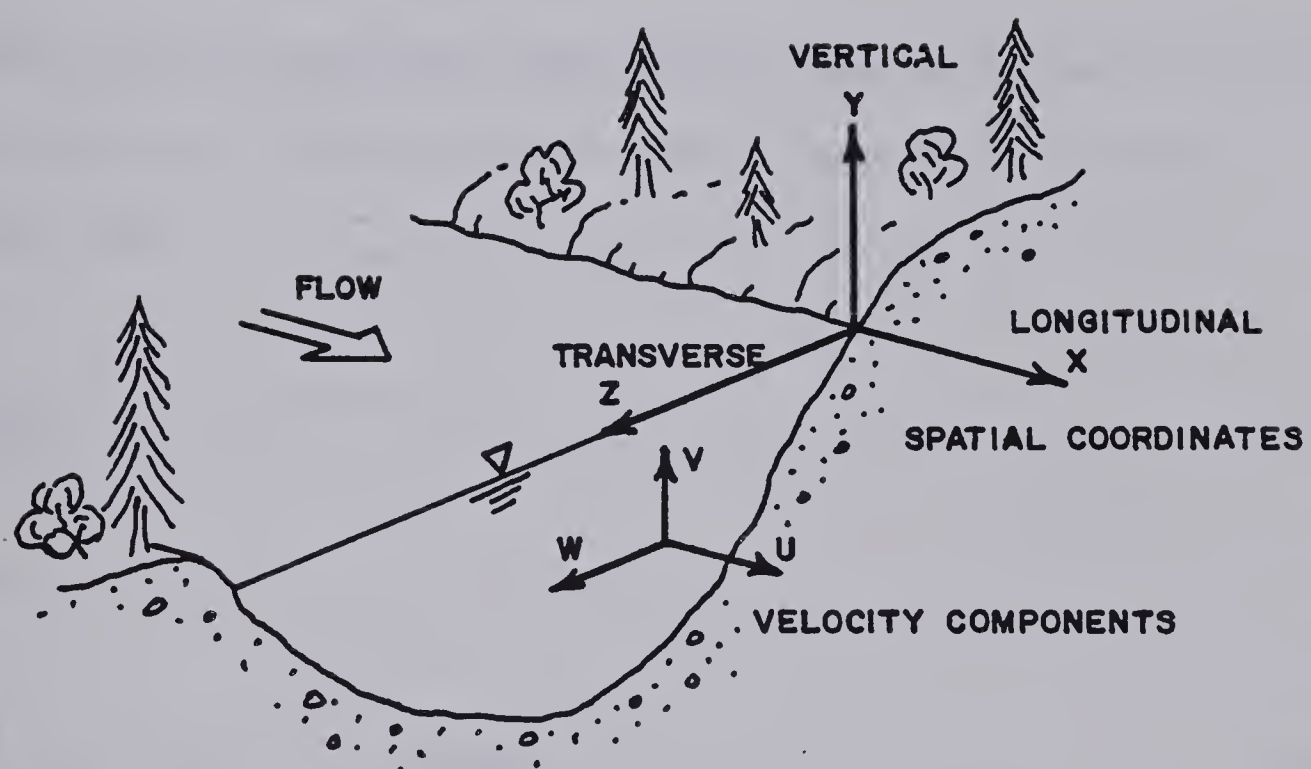


Figure II- 1 Coordinate System



Depth-averaging Equation I-7 gives:

$$\begin{aligned}
 & \frac{1}{h} \int_0^h \frac{\partial \bar{c}}{\partial t} dy + \frac{1}{h} \int_0^h \frac{\partial}{\partial x} (\bar{u} \bar{c}) dy + \frac{1}{h} \int_0^h \frac{\partial}{\partial y} (\bar{v} \bar{c}) dy \\
 & + \frac{1}{h} \int_0^h \frac{\partial}{\partial z} (\bar{w} \bar{c}) dy = \frac{1}{h} \int_0^h \frac{\partial}{\partial x} (\epsilon_x \frac{\partial \bar{c}}{\partial x}) dy \\
 & + \frac{1}{h} \int_0^h \frac{\partial}{\partial y} (\epsilon_y \frac{\partial \bar{c}}{\partial y}) dy + \frac{1}{h} \int_0^h \frac{\partial}{\partial z} (\epsilon_z \frac{\partial \bar{c}}{\partial z}) dy
 \end{aligned} \tag{II-2}$$

Considering the vertical diffusive flux and realizing there is no pollutant flux through the stream bed or water surface, ie.

$$\epsilon_y \frac{\partial \bar{c}}{\partial y} = 0 \quad \text{for } y=0 \text{ or } y=h \tag{II-3}$$

gives:

$$\frac{1}{h} \int_0^h \frac{\partial}{\partial y} (\epsilon_y \frac{\partial \bar{c}}{\partial y}) dy = \frac{1}{h} \left[ \epsilon_y \frac{\partial \bar{c}}{\partial y} \right]_0^h = 0 \tag{II-4}$$

Expanding the third term on the right side of Equation II-2 and using the Leibnitz Theorem gives

$$\frac{1}{h} \int_0^h \frac{\partial}{\partial z} (\epsilon_z \frac{\partial \bar{c}}{\partial z}) dy = \frac{1}{h} \frac{\partial}{\partial z} \left[ \epsilon_z \frac{\partial}{\partial z} \int_0^h (\bar{c} + c') dy \right] \tag{II-5}$$

but the depth-average of the fluctuating term is zero by definition, therefore:

$$\frac{1}{h} \int_0^h \frac{\partial}{\partial z} (\epsilon_z \frac{\partial \bar{c}}{\partial z}) dy = \frac{1}{h} \frac{\partial}{\partial z} (h \epsilon_z \frac{\partial \bar{c}}{\partial z}) \tag{II-6}$$







Similarly the first term on the right side of Equation II-2 reduces to

$$\frac{1}{h} \int_0^h \frac{\partial}{\partial x} (\epsilon_x \frac{\partial \bar{c}}{\partial x}) dy = \frac{1}{h} \frac{\partial}{\partial x} (h \epsilon_x \frac{\partial \bar{c}}{\partial x}) \quad (\text{II-7})$$

Expanding the first term on the left side of Equation II-2 and using the Leibnitz Theorem gives

$$\frac{1}{h} \int_0^h \frac{\partial \bar{c}}{\partial t} dy = \frac{1}{h} \frac{\partial}{\partial t} \int_0^h (\bar{c} + c'') dy = \frac{1}{h} \frac{\partial}{\partial t} (h \bar{c}) \quad (\text{II-8})$$

Similarly for the longitudinal and transverse advective terms

$$\begin{aligned} \frac{1}{h} \int_0^h \frac{\partial}{\partial x} (\bar{u} \bar{c}) dy &= \frac{1}{h} \frac{\partial}{\partial x} \int_0^h (\bar{u} \bar{c} + u'' c'' + \bar{u} c'' + u'' \bar{c}) dy \\ &= \frac{1}{h} \frac{\partial}{\partial x} \int_0^h (\bar{u} \bar{c} + u'' c'') dy \\ &= \frac{1}{h} \frac{\partial}{\partial x} (h \bar{u} \bar{c}) + \frac{1}{h} \frac{\partial}{\partial x} (h \overline{u'' c''}) \end{aligned} \quad (\text{II-9})$$

$$\frac{1}{h} \int_0^h \frac{\partial}{\partial z} (\bar{w} \bar{c}) dy = \frac{1}{h} \frac{\partial}{\partial z} (h \bar{w} \bar{c}) + \frac{1}{h} \frac{\partial}{\partial z} (h \overline{w'' c''}) \quad (\text{II-10})$$

where  $\overline{u'' c''}$  and  $\overline{w'' c''}$  represent depth-averaged transport due to differential convection in the x and z directions respectively;  $\overline{u'' c''}$  resulting from vertical shear and  $\overline{w'' c''}$  resulting from secondary circulation.

Considering the vertical advective flux and realizing the vertical velocity at the water surface and the stream bed



is zero gives

$$\frac{1}{h} \int_0^h \frac{\partial}{\partial y} (\bar{v}\bar{c}) dy = \frac{1}{h} [\bar{v}\bar{c}]_0^h = 0 \quad (\text{II-11})$$

Substituting Equations II-4, II-6, II-7, II-8, II-9, II-10 and II-11 into II-2 gives

$$\begin{aligned} \frac{\partial}{\partial t} (h\bar{c}) + \frac{\partial}{\partial x} (h\bar{u}\bar{c}) + \frac{\partial}{\partial z} (h\bar{w}\bar{c}) = \\ \frac{\partial}{\partial x} (h(\overline{u''c''} + \epsilon_x \frac{\partial \bar{c}}{\partial x})) + \frac{\partial}{\partial z} (h(\overline{w''c''} + \epsilon_z \frac{\partial \bar{c}}{\partial z})) \end{aligned} \quad (\text{II-12})$$

Generally the transport in the x and z directions due to turbulent fluctuations and differential convection are combined into single terms. This reduces Equation II-12 to

$$\frac{\partial}{\partial t} (h\bar{c}) + \frac{\partial}{\partial x} (h\bar{u}\bar{c}) + \frac{\partial}{\partial z} (h\bar{w}\bar{c}) = \frac{\partial}{\partial x} (hE_x \frac{\partial \bar{c}}{\partial x}) + \frac{\partial}{\partial z} (hE_z \frac{\partial \bar{c}}{\partial z}) \quad (\text{II-13})$$

where  $E_x$  and  $E_z$  are new parameters called mixing coefficients. The mixing coefficients approximately incorporate dispersional effects due to differential convection into Equation II-13 on the assumption they are dependent upon lateral concentration gradients. The overbars are generally omitted on the understanding that all values are time and depth averages.

### Transverse Mixing Zone

Observations of effluent plumes in streams have indicated that within the transverse mixing zone lateral



(transverse) spread of the plume is always very small in comparison to the length of the plume (the longitudinal extent of the plume). Establishing  $L$  as a longitudinal length scale (i.e.  $x \sim L$ ),  $\delta$  as a transverse length scale (i.e.  $z \sim \delta$ ), and  $C$  as a concentration scale the following order of magnitude analysis is possible.

$$\frac{\partial c}{\partial x} \sim \frac{C}{L}$$

$$\frac{\partial c}{\partial z} \sim \frac{C}{\delta} \quad (\text{II-14})$$

but  $L$  is much greater than  $\delta$ , therefore

$$\frac{\partial c}{\partial z} \gg \frac{\partial c}{\partial x} \quad (\text{II-15})$$

Applying this approximation to Equation II-13 and assuming the mean advective transport in the transverse direction is negligible compared to that in the streamwise direction gives

$$\frac{\partial}{\partial x} (huc) = \frac{\partial}{\partial z} (hE_z \frac{\partial c}{\partial z}) \quad (\text{II-16})$$

Considering only prismatic channels Equation II-16 may be further simplified to





$$hu \frac{\partial c}{\partial x} = \frac{\partial}{\partial z} (hE_z \frac{\partial c}{\partial z}) \quad (\text{II-17})$$

as  $\partial u / \partial x = 0$ . Equation II-17 describes two-dimensional mixing of a neutrally buoyant conservative tracer within the transverse mixing zone.

### Longitudinal Dispersion

Beyond the distance required to establish uniform lateral concentrations the transverse variation in concentration is negligible compared to that in the streamwise direction (ie.  $\partial c / \partial x$  is much greater than  $\partial c / \partial z$ ). Applying this approximation to Equation II-13 and again assuming negligible transverse advective transport compared to that in the streamwise direction gives

$$\frac{\partial}{\partial t} (hc) + \frac{\partial}{\partial x} (huc) = \frac{\partial}{\partial x} (E_x \frac{\partial c}{\partial x}) \quad (\text{II-18})$$

Again considering only prismatic channels Equation II-18 may be further simplified to

$$\frac{\partial c}{\partial t} + u \frac{\partial c}{\partial x} = \frac{\partial}{\partial x} (E_x \frac{\partial c}{\partial x}) \quad (\text{II-19})$$

which describes one-dimensional mixing of a neutrally buoyant conservative tracer beyond the mixing length.





## Mixing Regions

As mentioned earlier, downstream of an outfall, pollutant quickly becomes well mixed in the vertical in comparison to the longitudinal and transverse directions. Using analytical solutions to the classical diffusion equation (Equation 2.4) and the method of images it can be shown that a uniform concentration within the the vertical will be established within approximately 100 river depths downstream of an outfall. Beyond this point mixing is reduced to a two-dimensional problem until the plume reaches the stream boundaries and begins to reflect. Again using an analytical solution to the two-dimensional diffusion equation it can be shown the crossing distance for a bank discharge is in the order of 100 stream widths for natural streams of large aspect ratio. Using the method of images it can also be shown a distance of approximately 3 to 4 times greater is required to establish uniform lateral concentrations.

In general Equation II-17 would apply to the region between 100 stream depths and 300 to 400 stream widths downstream of a continuous bank discharge. Beyond 300 to 400 stream widths the mixing is essentially one-dimensional and Equation II-19 describes time-dependent mixing within this region. It must be recognized these distances represent approximations and will vary with channel geometry, roughness, and flow conditions.



## APPENDIX III Velocity Estimates and Flow Distributions

Depth-averaged velocity at any vertical may be estimated using a resistance equation if cross sectional geometry is known. Beltaos (1979) used the expression suggested by Sayre and Yeh

$$u/V \approx (h/H)^a \quad (\text{III-1})$$

where  $u$  is the depth-averaged streamwise velocity at a vertical,  $V$  is the mean section velocity,  $h$  is the total depth or depth below ice at a vertical,  $H$  is the mean section depth or depth below ice, and  $a$  is an exponent which depends upon the resistance equation from which Equation III-1 is derived. For example Equation III-1 can be derived from the Chezy resistance equation:

$$V = C_s \sqrt{gRS} \quad (\text{III-2})$$

where  $R$  is the section hydraulic radius,  $S$  is the slope of the water surface,  $C_s$  is the dimensionless Chezy roughness coefficient. In a wide channel the local depth-averaged velocity for a unit width of the stream is also given by

$$u = C_s \sqrt{gRS} \quad (\text{III-3})$$

where  $r$  is the hydraulic radius of the stream element. For open water conditions  $r \approx h$  at a vertical and  $R \approx H$ , whereas



under ice cover  $r \approx h/2$  and  $R \approx H/2$ . Dividing Equation III-3 by Equation III-2 and expressing  $r$  and  $R$  in terms of  $h$  and  $H$  gives

$$u/V \approx (h/H)^{0.5} \quad (\text{III-4})$$

or  $a = 0.5$  for the Chezy equation. A similar derivation using the Manning equation gives a value of  $a = 0.67$ .

Measured values of  $u/V$  plotted against  $h/H$  for all three field tests are shown in Figure III-1. Although the plot displays considerable scatter the Manning exponent appears to give the best estimate.

Cumulative flow distributions for the sampled sections were estimated using one of two procedures depending upon the survey data available:

- a. stream geometry only available, or
- b. stream geometry available and velocity measurements for part of the section.

For each section where only stream geometry was available velocities were estimated using Equation III-4 with  $a = 0.67$ . The dimensionless cumulative flow distribution was calculated using the algorithm

$$(q/Q)_i = \frac{1}{Q} \sum_{j=0}^i \frac{(h_{j-1} + h_j)(z_j - z_{j-1})(u_{j-1} + u_j)}{2} \quad (\text{III-5})$$

where  $i=0$  is the LB coordinate. A small error, indicated by  $q/Q$  not identically equal to 1.0 at the RB, generally





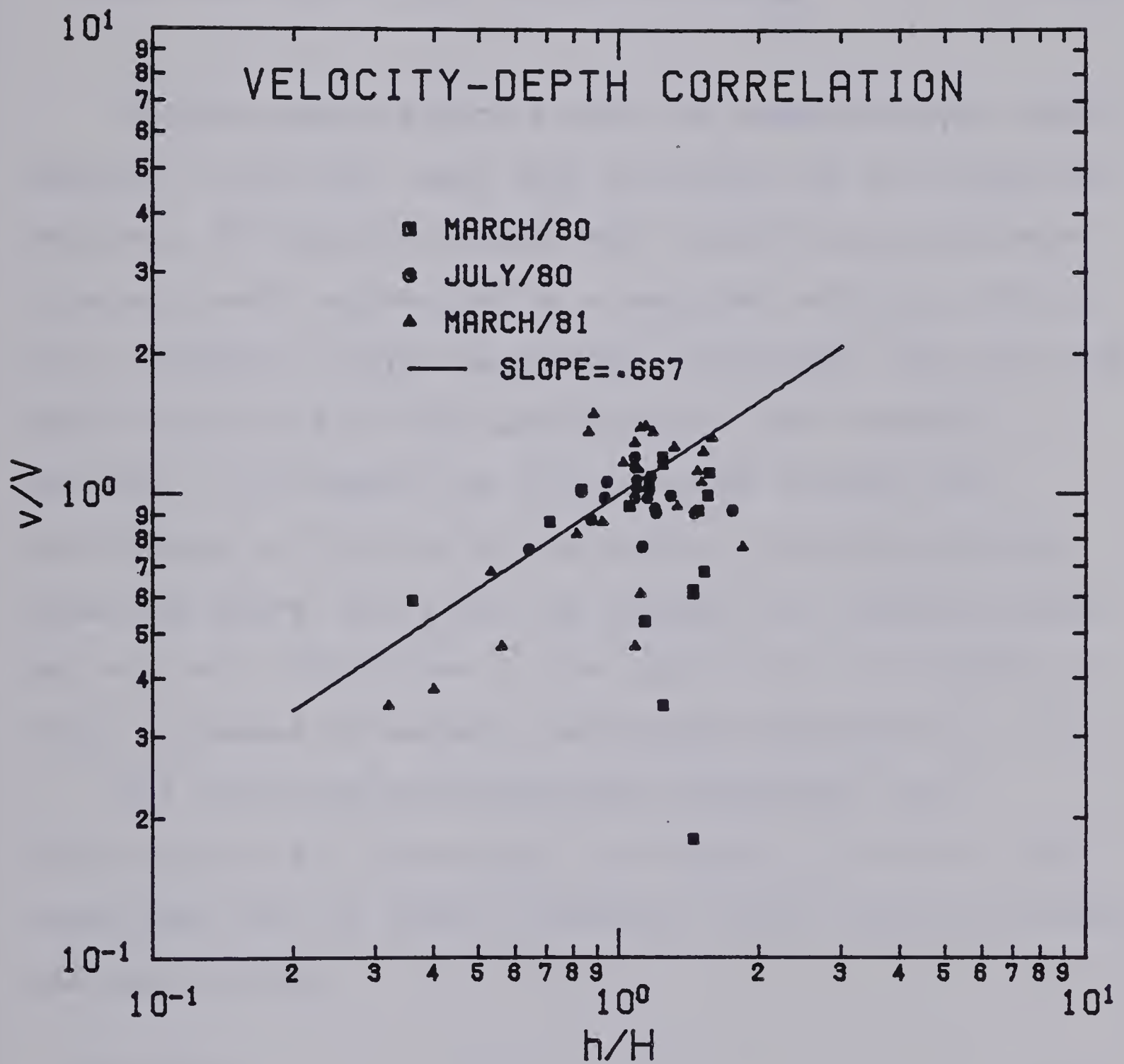


Figure III-1 Velocity-Depth Correlation





occurs because velocities are only estimated using Equation III-4. To correct this the error was distributed to normalize the distribution as follows

$$\text{normalized } (q/Q)_i = \text{calc. } (q/Q)_i / \text{calc. } (q/Q)_{RB} \quad (\text{III-6})$$

Velocity measurements within the expected plume region adjacent to the left bank were available for the remaining sections. The measured region was divided into transverse intervals each represented by a measured vertical and the flow increment within the interval calculated. The flow was then accumulated and  $q/Q$  calculated at each interval boundary. Flow beyond the last measured interval was distributed to the rest of the section using the method presented above. Any error was handled in a similar manner but was only distributed to the portion of the channel in which estimates of velocity were made using Equation III-4.

The resulting non-dimensional cumulative flow distributions are those shown in Figures 4.3 and 4.4. The curves may also be used to determine local velocities using the relationship

$$\begin{aligned} \Delta q &= uh\Delta z \\ \therefore u &= \Delta q / h\Delta z \end{aligned} \quad (\text{III-7})$$

where  $\Delta q$  is the change in flow between two transverse locations and  $h$  is the interval mean depth.



#### APPENDIX IV Dye Adsorption Studies

Incomplete recovery of the injected Rhodamine WT tracer mass at each of the measured sections may result due to:

- a. adsorption onto suspended solids,
- b. adsorption onto the stream boundaries,
- c. adsorption onto the surfaces of the sample container,
- d. photochemical decay, and
- e. chemical oxidation.

Feuerstein and Selleck (1963) have indicated the adsorption of Rhodamine B<sup>1</sup> upon predominantly inorganic suspended solids is not significant and the interference effects of turbidity may be largely eliminated if the solids are allowed to settle before analysis. Sediment load during ice cover conditions was extremely low and photochemical decay was eliminated by the ice sheet, yet a significant tracer loss was indicated by tracer mass balance calculations for the ice cover condition tests. The calculations for the summer test indicated an even lower tracer recovery. In an effort to roughly quantify adsorption losses due to suspended sediment and/or the sample containers a series of adsorption tests were conducted.

Plastic sample bottles identical to those used in the field and glass bottles were dosed with a volume of various

-----  
<sup>1</sup> Rhodamine B is a fluorescent dye similar in characteristics to Rhodamine WT



concentrations of Rhodamine WT solution to produce a series of samples of constant volume and different initial concentrations. A series using distilled water and Slave River water was prepared for each bottle type. The river water used was collected during the late spring and contained significant amounts of suspended sediment. The effects of photochemical decay were minimized by only exposing the samples to light during the initial dosing and when small volumes were withdrawn for measurement. The concentrations in excess of background were determined after 6 and 17 hours storage, allowing ample time for sediment to settle. The measured concentrations in excess of background are given in Table IV-1 and the averages plotted in Figure IV-1.

The results for the glass bottles indicate the sediment content has little effect upon the dye recovery, hence adsorption of Rhodamine WT upon the sediment is minimal as Feuerstein and Selleck suggested. However comparison of the results for the plastic and glass bottles indicates significant adsorption of dye onto the plastic bottles. The small losses of dye in the control sample (distilled water, glass bottle) are probably due to some photochemical decay and experimental error.

The adsorption of Rhodamine WT upon the plastic bottle surfaces was a major source of error in the original mass balance calculations and appears to be of sufficient magnitude, at least for the ice cover data, to account for







Table IV-1 Dye Adsorption Analysis

Init Conc (ppb)*	Sample	6 hr		17 hr		Avg ratio
		conc (ppb)*	ratio	conc (ppb)*	ratio	
2.0	DWG	1.9	.95	2.0	1.00	.98
	DWP	1.7	.85	1.6	.80	.83
	RWG	1.9	.95	2.0	1.00	.98
	RWP	1.6	.80	1.7	.85	.83
5.0	DWG	4.6	.92	4.7	.94	.93
	DWP	3.7	.74	3.5	.70	.72
	RWG	4.7	.94	4.8	.96	.95
	RWP	3.4	.68	3.8	.76	.72
19.8	DWG	18.9	.95	19.4	.98	.97
	DWP	15.8	.80	16.5	.83	.82
	RWG	19.1	.96	19.2	.97	.97
	RWP	14.8	.75	16.1	.81	.78
49.5	DWG	48.1	.97	49.5	1.00	.99
	DWP	40.8	.82	41.8	.84	.83
	RWG	46.5	.94	47.0	.95	.95
	RWP	40.7	.82	43.6	.88	.85

DWG - distilled water, glass bottle (control)

DWP - distilled water, plastic bottle

RWG - river water, glass bottle

RWP - river water, plastic bottle

\* - concentrations in excess of background



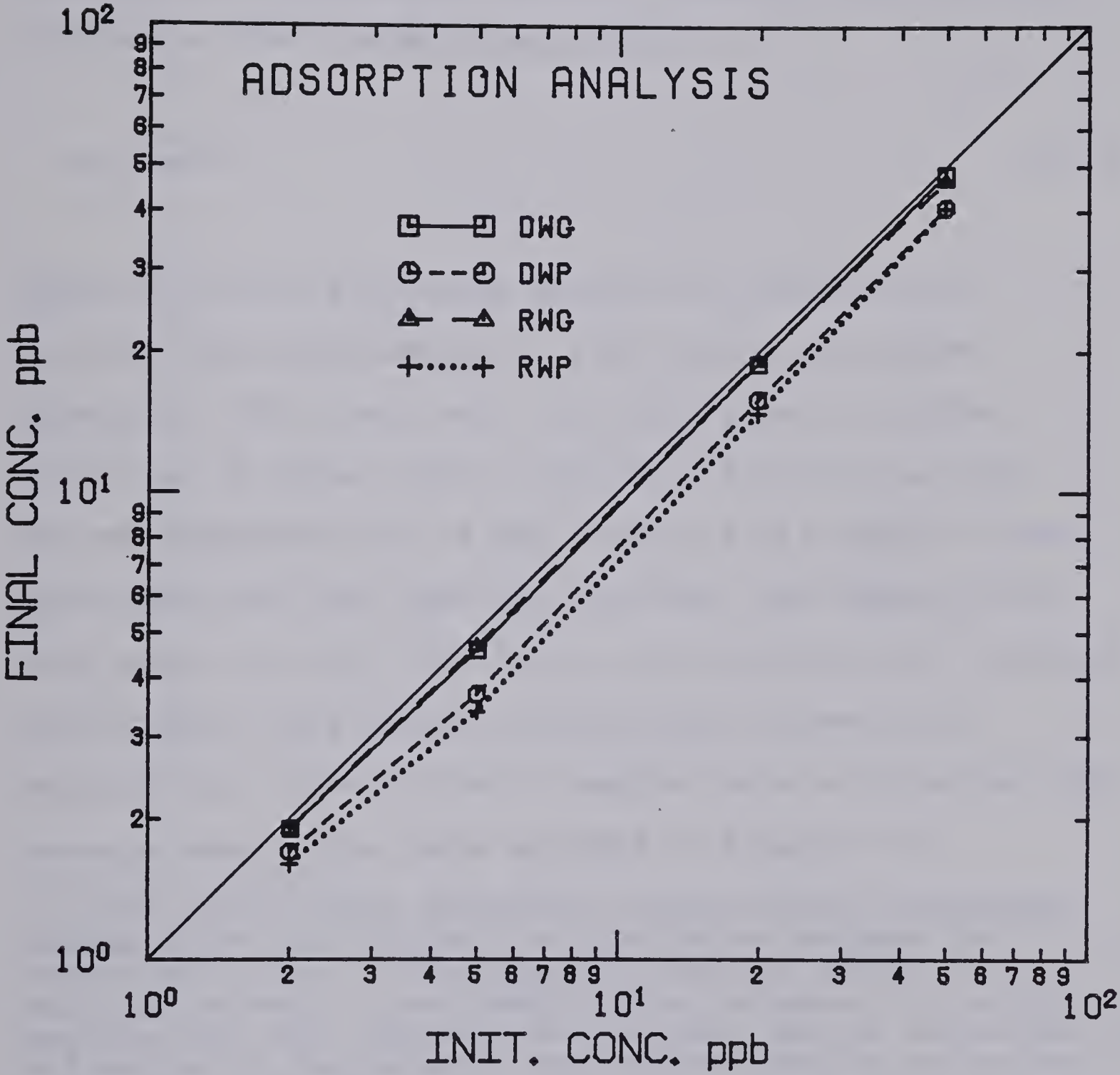


Figure IV-1 Dye Adsorption Analysis



most of the losses. A method of accurately calculating this loss would greatly improve the dye recoveries for the field data. A second series of adsorption tests were conducted over the range of field measured concentrations to determine an adsorption isotherm ' using a relationship similar to the Fruendlick equation

$$\Delta c = mc^{1/n} \quad (IV-1)$$

where  $\Delta c$  is the difference between the initial and equilibrium concentration  $c$ , and  $m$  and  $n$  are system constants.<sup>2</sup> The tests were run using plastic bottles identical to those used in the field filled to a total volume representative of the average field sample volume. Distilled water was used for dilution. The samples were once again isolated from light and analysed after a period sufficiently long enough to establish concentration equilibrium. Three series of samples were analysed and the average results are shown plotted in Figure IV-2.

-----  
 'In the solid-liquid adsorption system being considered Rhodamine WT, the solute, is distributed between the container surface, the absorbent, and the solution. At equilibrium and a fixed temperature the amount of solute absorbed per unit quantity of absorbent may be expressed as a function of the solution equilibrium concentration. An expresssion of this type is called an adsorption isotherm. For this system a relationship at room temperature is sufficiently accurate. A more detailed explanation of adsorption processes and equalibria is given by Weber (1972).

<sup>2</sup> In the classical Fruendlick equation  $\Delta c$  equals the total mass of material adsorbed divided by the mass of the adsorbing material at equilibrium conditions. In this modified form  $\Delta c$  represents the mass of tracer adsorbed at equilibrium by the surface area of plastic exposed.





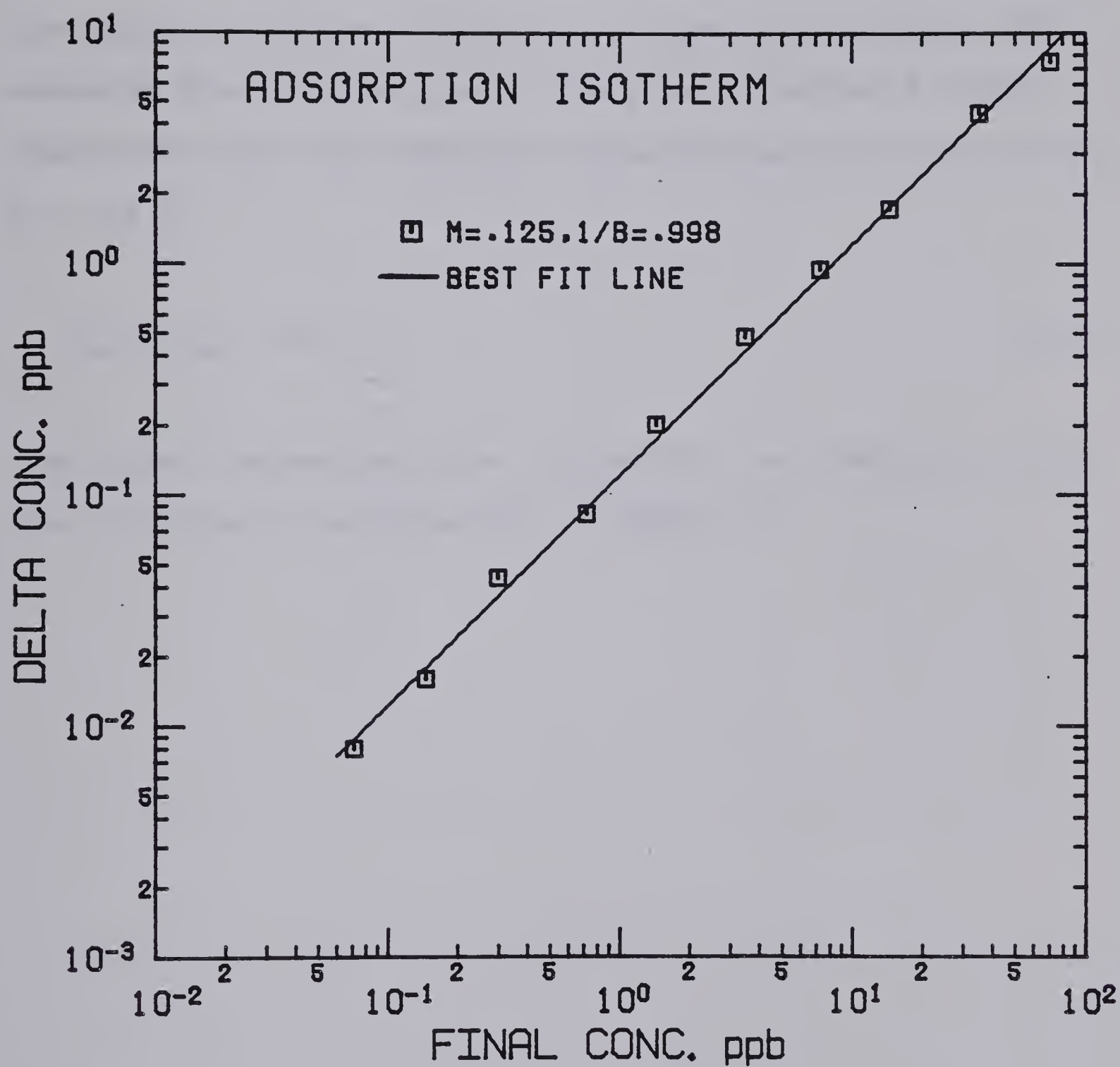


Figure IV-2 Adsorption Isotherm for Sample Containers





The results of the second adsorption test indicates a linear log-log relationship over the range of concentrations measured in the field. The constants  $m$  and  $n$  of Equation IV-1 were determined from a best fit line to the points of Figure IV-2 and are shown in the plot. The measured field concentration  $c$  may be corrected for dye adsorption onto the container by adding  $\Delta c$  calculated using  $m, n$  and  $c$

$$c_{\text{corrected}} = \Delta c + c \quad (\text{IV-2})$$

The tracer recoveries after correction for adsorption onto the containers are presented in Chapter IV.



## APPENDIX V Indicator Bacteria Data

The geometric averages of the measured total and fecal coliform concentrations in excess of background are shown in Table V-1, V-2 and V-3. The background concentration for the March 1980 test is given in Table V-1 and this single value was used to correct the measured data.

Difficulty was encountered in determining an accurate background reading for the July 1980 data. The range over which the background measurements were distributed was of the same order as the river concentrations in excess of background downstream of the outfall. To ensure satisfactory elimination of the background level the geometric mean plus one standard deviation was used to represent background rather than the actual geometric mean value. In this manner approximately an 84% confidence level in eliminating background from the samples is established. The estimated background concentration is given in Table V-2.

During the 1981 test the background readings fluctuated as shown in Figure V-1. These fluctuations were likely due to a thawing period which occurred during the initial portion of the field survey. The total coliforms were most significantly effected as would be expected since they do not represent indicators of exclusively fecal origin and would be subject to increases in numbers due to surface runoff. The background readings were made in the vicinity of the outfall and therefore the appropriate



Table V-1 Coliform Counts March 1980

Section (km)	Location metres to LB	No. of samples	TC* /100mL	FC* /100mL
Background	-	66	27	2
0.5	13.5	5	203	70
	20.8	5	143	55
	28.2	5	18	8
	37.4	5	0	0
	44.3	4	0	0
	50.4	3	0	0
	63.5	4	0	0
	77.7	3	0	4
	103.0	2	2	0
2.0	94.3	1	40	65
	165.1	2	133	91
	233.5	2	133	78
	302.1	2	83	82
	331.4	2	53	74
	371.4	1	66	64
	408.0	2	47	49
	448.2	1	16	9
	478.1	1	5	0
	583.0	1	0	0
	652.2	1	15	0
	718.6	1	2	0
	778.6	1	14	0
	855.5	1	51	0
	890.1	1	16	0
5.5	10.3	2	123	61
	90.0	2	103	54
	130.8	2	70	38
	171.1	2	17	11
	212.1	2	0	0
	256.1	1	0	1
	297.4	1	0	0
	378.4	1	0	0
	459.4	1	2	1
	537.6	1	20	0
	628.6	1	0	1
8.6 LC	19.2	2	83	61
	130.2	2	0	0
	219.2	2	0	0
	347.0	2	5	0
	452.0	1	7	0

\* geometric avg. in excess of background





Table V-1 cont. Coliform Counts March 1980

Section (km)	Location metres to LB	No. of samples	TC* /100mL	FC* /100mL
8.6 RC	91.7	1	10	1
	158.8	1	0	0
	230.3	1	0	0
	315.9	1	5	0
	454.3	1	2	0
	684.6	1	0	0
12.0 LC	40.0	2	83	50
	125.8	2	39	0
	182.3	2	9	0
	235.0	2	0	0
12.0 RC	20.0	1	0	0
	114.3	1	0	0
	186.8	1	11	0
	256.8	1	0	0
	365.8	1	0	0
	503.6	1	0	0
15.8 LC	20.0	2	93	40
	119.0	1	83	28
	207.6	2	37	12
	273.6	2	44	15
	407.2	2	-	14
15.8 RC	30.0	2	5	5
	123.0	2	0	0
	257.0	2	0	0
27.8	25.0	3	20	4
	77.5	3	4	1
	155.0	2	0	0
	232.0	3	2	0
	310.0	1	10	0
	465.0	1	15	0
	595.0	1	0	0
50.0	A	4	13	6
	B	4	11	7
	C	4	10	12
	D	2	5	2
	E	2	0	0
	F	2	15	0
Lagoon Effluent	-	8	$1.2 \times 10^6$	$3.6 \times 10^5$

\* geometric avg. in excess of background



Table V-2 Coliform Counts July 1980

Section (km)	Location metres to LB	No. of samples	TC* /100mL	FC* /100mL
Background**	-	142	54	13
0.5	0.9	3	0	0
	3.1	3	0	1
	4.6	3	0	0
	7.6	3	0	0
	15.4	3	0	0
	30.5	4	0	0
	45.7	3	0	1
2.0 LC	16.0	4	0	0
	31.7	3	0	0
	47.3	4	0	0
2.0 RC	61.0	3	0	0
	111.6	3	10	2
	185.2	3	0	0
	258.7	4	6	0
	283.6	3	0	0
	308.6	3	8	0
	333.3	3	3	0
	369.8	2	8	1
	406.3	2	0	5
	465.7	3	7	0
	525.2	2	4	0
	569.9	2	11	0
	614.5	2	18	0
	629.8	2	6	0
	645.0	10	0	0
5.5	19.0	3	1	2
	53.4	2	0	0
	87.8	2	0	5
	122.2	3	9	0
	148.6	2	0	0
	175.1	2	0	0
	201.5	3	5	0
	268.6	2	0	0
	335.6	3	0	2
	427.0	2	0	1
	475.8	3	0	0
	524.6	2	4	0

\* geometric avg. in excess of background

\*\* background set as the geometric mean plus one standard deviation



Table V-2 cont. Coliform Counts July 1980

Section (km)	Location metres to LB	No. of samples	TC* /100mL	FC* /100mL
8.6 LC	17.0	2	3	0
	49.6	1	0	0
	82.2	1	0	0
	114.8	1	6	0
	147.4	2	0	0
	177.6	1	0	0
	207.7	1	6	0
	237.9	2	0	6
	263.3	1	0	0
	288.6	1	0	0
	314.0	1	6	0
	367.9	2	0	0
	416.7	1	0	0
8.6 RC	161.3	2	0	0
	229.8	1	0	0
	303.3	2	0	0
	339.4	2	0	0
12.0 LC	12.0	1	0	0
	78.5	1	0	0
	150.0	1	0	0
	192.0	1	56	0
	235.0	1	6	0
	343.0	1	0	0
	465.1	2	6	0
12.0 RC	17.7	2	0	0
	73.7	1	0	0
	134.6	1	0	0
	220.0	2	0	0
	295.0	1	6	0
14.2	21.2	1	36	0
	54.8	1	36	0
	93.5	1	0	0
	132.1	1	0	0
	166.2	1	6	0
	200.2	1	0	0
	234.3	1	56	0
	273.9	1	0	0
	313.4	2	0	0
	405.8	2	0	0
	459.3	2	0	0
	512.7	1	0	0
	571.9	1	6	0
	631.0	1	6	0

\* geometric avg. in excess of background



Table V-2 cont. Coliform Counts July 1980

Section (km)	Location metres to LB	No. of samples	TC* /100mL	FC* /100mL
15.8 LC	44.7	1	0	0
	101.1	1	0	1
	134.9	1	0	0
15.8 CC	103.9	1	0	0
	210.3	1	0	0
	306.3	1	0	0
	370.5	1	0	0
	489.0	1	0	3
27.8	13.0	2	0	0
	63.0	2	0	0
	117.9	1	0	0
	176.5	1	0	0
	235.0	1	0	0
	285.0	1	16	0
	334.9	1	0	0
	390.7	1	0	0
	446.7	1	0	0
	553.1	1	0	0
56.8	145.1	1	0	0
	273.5	1	0	0
	381.2	1	0	0
	503.2	1	0	3
	622.2	1	0	0
Lagoon Effluent	-	15	5700	310

\* geometric avg. in excess of background





Table V-3 Coliform Counts March 1981

Section (km)	Location metres to LB	No. of samples	TC* /100mL	FC* /100mL
Background**				
Mar 16	-	22/26	17	8
17	-	17	18	5
18	-	8	26	4
19	-	3	107	2
20	-	12	73	4
0.5	1.1	3	183	82
	5.2	4	216	87
	12.7	3	156	93
	20.4	4	160	55
	28.3	3	16	11
	37.6	4	3	1
	51.1	2	0	1
	73.7	1	1	0
2.0	236.7	3	178	87
	278.1	5	204	69
	314.7	2	93	48
	355.5	4	18	13
	388.1	2	5	2
	414.9	4	5	1
	440.4	2	0	0
5.5	18.7	4	146	75
	30.0	4	115	48
	42.1	4	149	55
	59.0	3	156	52
	75.5	3	111	53
	93.1	4	122	52
	122.5	4	130	49
	150.9	5	47	15
	196.0	5	4	2
	238.8	1	0	2
12.0	0.0	3	73	38
	35.2	2	96	64
	46.0	3	112	33
	55.7	2	92	50
	62.4	3	75	36
	69.9	2	86	54
	79.8	2	49	37
	96.9	3	47	21
	127.6	2	20	11

\* geometric avg. in excess of background

\*\* background set as the geometric mean of samples on individual dates



Table V-3 cont. Coliform Counts March 1981

Section (km)	Location metres to LB	No. of samples	TC* /100mL	FC* /100mL
13.0	10.5	3	93	43
	19.0	3	73	39
	24.9	3	71	45
	34.5	2	83	38
	44.4	3	66	30
	68.6	3	57	26
	92.6	3	16	8
	114.0	1	9	4
	134.0	1	3	0
	211.0	1	0	6
	281.0	1	0	0
14.2	25.5	1	94	31
	45.0	1	94	29
	84.4	1	44	15
	123.8	1	24	5
15.8 LC	211.4	1	47	17
	298.9	1	34	15
	373.2	1	27	0
	482.7	1	1	3
22.9	0.0	1	30	17
	25.1	2	47	34
	70.0	2	62	41
	125.0	1	42	19
	166.9	2	49	10
	209.2	1	26	9
	270.0	1	12	5
	395.0	1	8	0
27.8	20.0	4	22	15
	37.0	2	43	28
	52.0	2	10	9
	79.0	1	13	7
	110.0	1/2	11	3
	141.0	2	5	7
	172.0	2	0	2
39.9	0.0	3/4	36	11
	35.5	2	25	9
	70.5	4/5	28	13
	102.4	2	30	8
	137.2	3/4	47	8
	166.0	2	25	0
	209.8	2	4	1
	261.6	2	2	0
	327.7	2	2	1
Lagoon Effluent	-	18	$8.7 \times 10^5$	$3.6 \times 10^5$

\* geometric avg. in excess of background



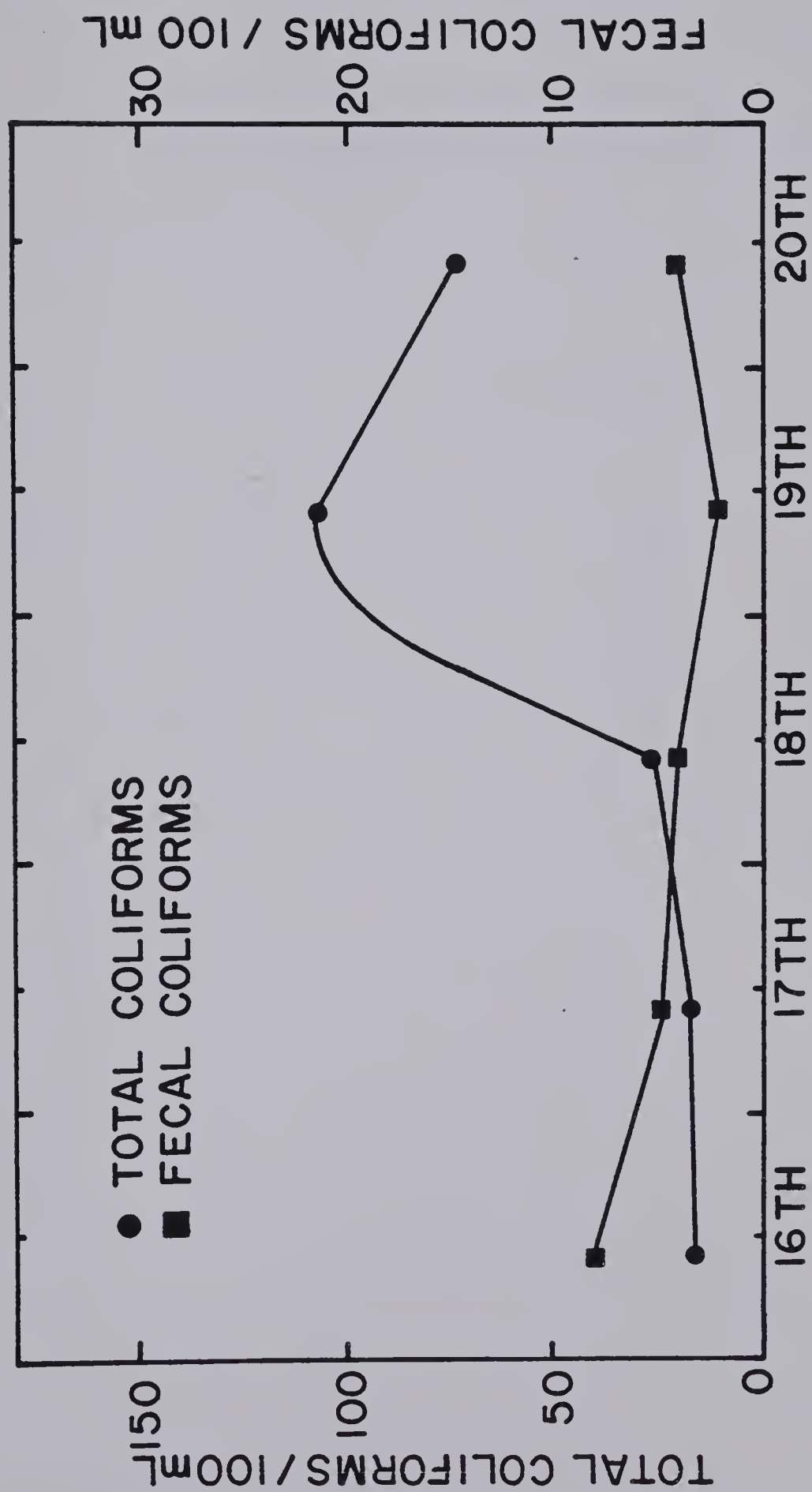


Figure V-1 Background Concentrations March 1981





correction for each section had to be determined for each day by considering the flow time to each section. The estimated flow times are shown in Table V-4.



Table V-4 Estimated Flow Times March 1981

Section (km)	Total Elapsed Time (hr)
0.5	0.23
2.0	1.30
5.5	4.83
8.6	7.50
12.0	9.67
13.0	10.47
14.2	11.23
15.8	12.31
22.9	18.95
27.8	23.00
39.9	28.86



## APPENDIX VI Numerical Solution Method, Conservative Tracers

The following differential equation describing steady-state mixing of a neutrally buoyant conservative tracer was derived in Chapter III.

$$\frac{\partial c'}{\partial x} = \frac{1}{Q^2} \frac{\partial}{\partial \eta} (u h^2 E_z \frac{\partial c'}{\partial \eta}) \quad (\text{VI-1})$$

Analytical solution to this equation assuming a constant reach-averaged value of the diffusion factor ( $u h^2 E_z$ ) proved unsatisfactory for the case of side discharge into a wide natural channel.<sup>1</sup> Therefore, numerical methods are required since analytical solutions are not available for a variable diffusion factor.

The equation may be solved numerically for the transverse mixing coefficient if field measurements from a steady-state mixing test are available. Solutions for trial values of  $E_z$  are compared to measured concentration distributions to select the best estimate of  $E_z$ . On the other hand when  $E_z$  is known or has been estimated the concentration distributions downstream may be computed.

Stone and Brian (1963) proposed an implicit finite-difference scheme to solve advection-diffusion equations of this type which reduced errors due to numerical dispersion and oscillations. Their solution

-----  
<sup>1</sup> This is the situation for discharge from the Fort Smith lagoon system to the Slave River.



method was for Equation VI-1 in expanded form:

$$\frac{\partial c'}{\partial x} = \frac{1}{Q^2} (uh^2 E_z) \frac{\partial^2 c'}{\partial \eta^2} + \frac{1}{Q^2} \left( \frac{\partial}{\partial \eta} (uh^2 E_z) \right) \frac{\partial c'}{\partial \eta} \quad (\text{VI-2})$$

Lau and Krishnappan (1981) used the method of Stone and Brian to analyse steady-state transverse diffusion in a natural channel and to investigate the sensitivity of the solution to various formulations of the diffusion factor  $uh^2 E_z$ .

The numerical method used in this study is essentially identical to that used by Lau and Krishnappan with only minor variations. The grid system for the numerical scheme is shown in Figure VI-1. Stone and Brian's discretization procedure for Equation VI-2 used weighting coefficients in the difference expressions used to approximate the first order derivatives  $\partial c'/\partial x$  and  $\partial c'/\partial \eta$ . The second order derivative  $\partial^2 c'/\partial \eta^2$  is approximated using a Crank-Nicolson expression. The Crank-Nicolson expression reduces the order of the error associated with the forward difference expression necessary to approximate  $\partial c'/\partial x$ . The resulting finite-difference expression is:

$$\begin{aligned} & \frac{1}{\Delta x} (g(c'_{i+1,j} - c'_{i,j}) + \frac{\theta}{2} (c'_{i+1,j-1} - c'_{i,j-1}) + m(c'_{i+1,j+1} - c'_{i,j+1})) \\ & = \frac{F_{i,j}}{\Delta \eta} (a(c'_{i,j+1} - c'_{i,j}) + \frac{\omega}{2} (c'_{i,j} - c'_{i,j-1}) + b(c'_{i+1,j+1} - c'_{i+1,j}) \\ & + d(c'_{i+1,j} - c'_{i+1,j-1})) + \frac{D_{i,j}}{2(\Delta \eta)^2} ((c'_{i,j+1} - 2c'_{i,j} + c'_{i,j-1}) \\ & + (c'_{i+1,j+1} - 2c'_{i+1,j} + c'_{i+1,j-1})) \end{aligned} \quad (\text{VI-3})$$





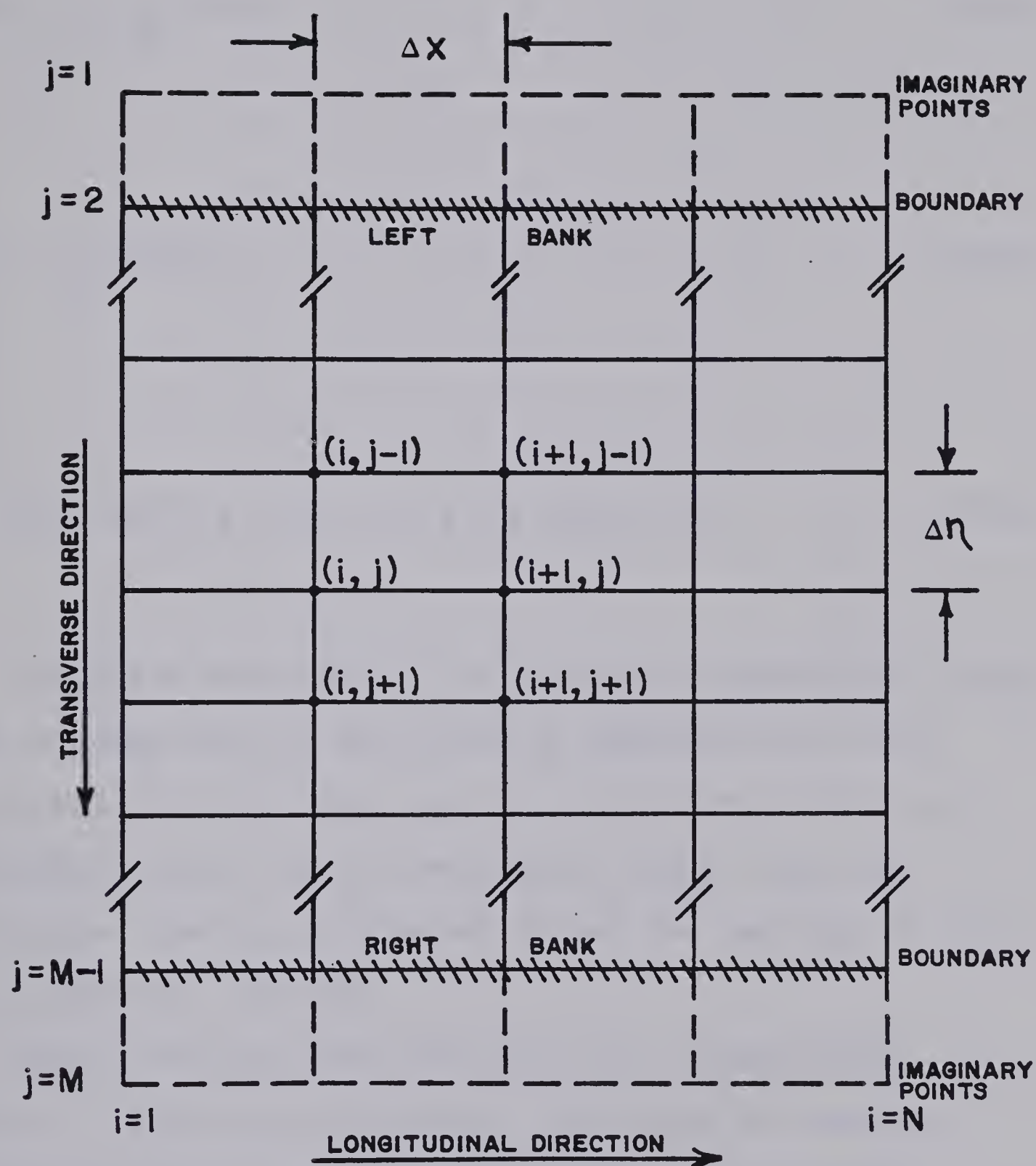


**Figure VI-1 Grid System Used in the Numerical Scheme**



where

$$F_{i,j} = \frac{1}{Q^2} \frac{\partial}{\partial \eta} (uh^2 E_z) \quad (\text{VI-4})$$

$$D_{i,j} = \frac{1}{Q^2} (uh^2 E_z) \quad (\text{VI-5})$$

$$g = 2/3 ; \theta/2 = m = 1/6 ; a = b = d = \omega/2 = 1/4 \quad (\text{VI-6})$$

Stone and Brian chose the weighting coefficient values after a comparison of solutions of Equation VI-3 with analytical solutions for constant values of  $F$  and  $D$  and recommended their use for variable  $F$  and  $D$ . Lau and Krishnappan used the suggested values for variable  $F$  and  $D$  with successful results.

When concentrations are known at a longitudinal location  $i$  Equation VI-3 may be rearranged to express concentrations at location  $i+1$  in terms of the known values. An individual equation may be written for each transverse grid point resulting in a system of linear equations. The boundary condition of no flux of tracer through the banks (i.e.  $\epsilon_z \partial c' / \partial z = 0$ ) may be simply handled



by establishing an imaginary point adjacent to the boundary (see Figure VI-1). The concentration of the imaginary point is set equal to the first real point adjacent to the boundary to satisfy the condition since

$$\frac{\partial c'}{\partial \eta} \approx \frac{c'_{i+1,j} - c'_{i-1,j}}{2\Delta\eta} \approx 0 \quad (\text{VI-7})$$

$$c'_{i+1,j} = c'_{i-1,j}$$

The system of equations expanded and written in matrix form is:

$$\begin{bmatrix} q_2 & r_2 \\ p_3 & q_3 & r_3 \\ & \ddots & \ddots & \ddots \\ & & p_{M-2} & q_{M-2} & r_{M-2} \\ & & & p_{M-2} & q_{M-2} \end{bmatrix} \begin{bmatrix} c'_{i+1,2} \\ c'_{i+1,3} \\ \vdots \\ c'_{i+1,M-2} \\ c'_{i+1,M-2} \end{bmatrix} = \begin{bmatrix} s_2 \\ s_3 \\ \vdots \\ s_{M-2} \\ s_{M-1} \end{bmatrix} \quad (\text{VI-8})$$

$$q_j = 2(g + \alpha) \quad (j = 2, 3, \dots, M-1) \quad (\text{VI-9})$$

$$p_j = \theta - \alpha + \gamma d \quad (j = 3, 4, \dots, M-2) \quad (\text{VI-10})$$

$$p_{M-1} = \theta + 2m - 2\alpha \quad (\text{VI-11})$$





$$r_j = 2m - \alpha - \gamma b \quad (j = 3, 4, \dots, M-2) \quad (\text{VI-12})$$

$$r_2 = \theta + 2m - 2\alpha \quad (\text{VI-13})$$

$$s_j = c'_{i,j-1} \left( \theta + \alpha - \frac{\gamma \omega}{2} \right) + c'_{i,j} (2(g - \alpha)) \\ + c'_{i,j+1} (2m + \alpha + \gamma a) \quad (j = 2, 3, 4, \dots, M-1) \quad (\text{VI-14})$$

$$\alpha = \frac{D_{i,j} \Delta x}{(\Delta \eta)^2} \quad (\text{VI-15})$$

$$\gamma = \frac{2F_{i,j} \Delta x}{\Delta \eta} \quad (\text{VI-16})$$

The values of  $D_{i,j}$  must be input for each equation. The average value of the term  $uh^2$  for each transverse interval (i.e. between position  $i-1$  and  $i+1$ ) may be derived from plots of  $\eta$  versus  $z$  prepared from hydrometric surveys. The value of  $E_z$  is assumed constant in the transverse direction (see Equation 6.1) but may be allowed to vary longitudinally. The term  $F_{i,j}$  can readily be determined by calculating the derivative of  $D_{i,j}$  with respect to  $\eta$  using



central difference approximations:

$$F_{i,j} = \frac{D_{i,j+1} - D_{i,j-1}}{2\Delta\eta} \quad (\text{VI-17})$$

At the boundaries local values of  $u$  and  $h$  are zero. This would create a singular point. However, since  $D$  represents an interval rather than a point, its boundary value must represent the mean between the imaginary and first real point adjacent to the boundary. The imaginary point has the same depth, velocity and concentration as the real point, therefore, the boundary  $D$  equals the mean between the boundary and first real point. The boundary value of  $F$  must be zero since the value of  $D$  at the real and imaginary points are equal.

The boundary conditions of geometry and concentration generate the individual expressions for  $p_{m-1}$  and  $r_2$  (Equation VI-11 and Equation VI-13).

The computer program developed evaluates the coefficients of the triadiagonal matrix and of the forcing vector  $S$  and then solves the system of equations for the downstream concentrations using the Gauss-Seidal method of successive substitutions.' A flow chart of the program is shown in Figure VI-2 followed by a program listing with explanatory notes.

---

' Explanation of the Gauss-Seidal method can be found in most elementary textbooks on numerical analysis, an example is Gerald, C. F. (1980).



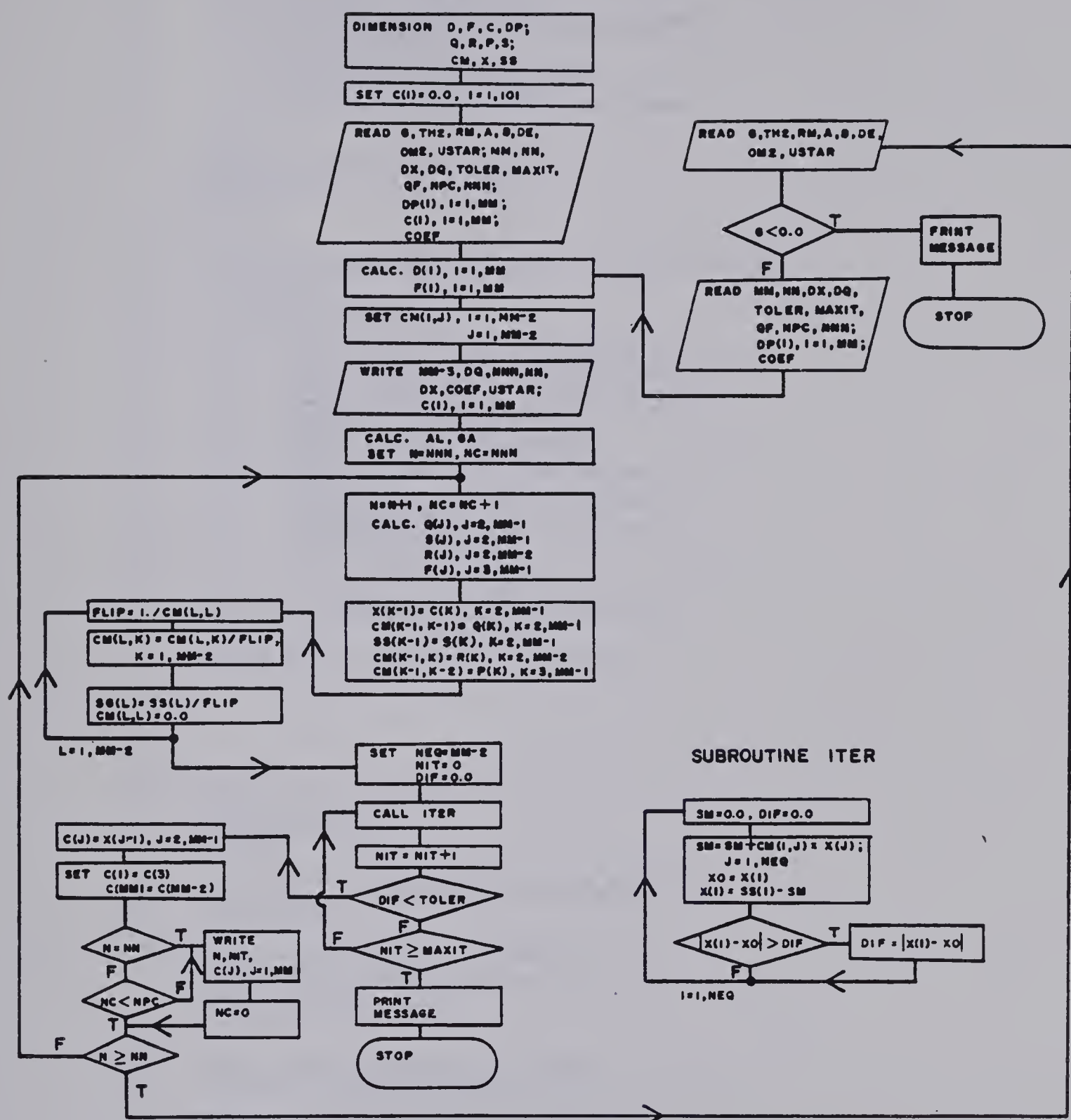


Figure VI-2 Program Flow Chart





```

C      FINITE DIFFERENCE PROGRAM TO NUMERICALLY SOLVE
C      STEADY STATE TRANSVERSE DIFFUSION PROBLEMS
C
C      DIMENSION ALL VECTORS AND ARRAYS TO BE USED IN CALCULATIONS
C      D - COEFFICIENTS GIVEN BY EQ. VI-5
C      F - COEFFICIENTS GIVEN BY EQ. VI-6
C      C - INPUT TRACER CONCENTRATIONS
C      DP - PRODUCT OF LOCAL DEPTH AND VELOCITY SQUARED
C      Q,R,P - TRIANGULAR MATRIX COEFFICIENTS GIVEN BY
C      EQ.VI-9 TO EQ.VI-13
C      S - FORCING VECTOR GIVEN BY EQ.VI-14
C      SS - FORCING VECTOR EXCLUDING IMAGINARY POINTS
C      X - SOLUTION CONCENTRATION VECTOR
C      CM - ARRAY OF SIMULTANEOUS EQUATION COEFFICIENTS
C
C      DIMENSION D(101),F(101),C(101),DP(101)
C      DIMENSION Q(101),R(101),P(101),S(101)
C      DIMENSION CM(101,101),X(101),SS(101)
C      DO 30 I=1,101
C      C(I)=0.0
30  CONTINUE
C
C      INPUT SOLUTION WEIGHTING COEFFICIENTS AND INITIAL PARAMETERS
C      THE WEIGHTING COEFFICIENTS ARE GIVEN BY EQ.VI-6
C      G= 0.666
C      TH2,RM =0.167
C      A,B,DE,DM2 = 0.25
C
C      USTAR - PLUME REGION SHEAR VELOCITY GIVEN BY EQ.III-5
C      USING THE PLUME REGION HYDRAULIC RADIUS
C      COEF - PRODUCT OF THE MIXING LENGTH SCALE AND A
C      CONSTANT COEFFICIENT, SEE EQ.VI-1
C      MM - NUMBER OF TRANSVERSE GRID POINTS INCLUDING
C      IMAGINARY AND BOUNDARY NODES
C      NN - FINAL LONGITUDINAL STEP
C      OX - LONGITUDINAL DISTANCE INCREMENT
C      DO - DIMENSIONLESS CUMULATIVE FLOW
C      TOLER - ACCURACY TO WHICH NUMERICAL SOLUTION WILL
C      PROCEED
C      MAXIT - MAXIMUM NUMBER OF ITERATIONS ALLOWED
C      QF - TOTAL STREAM DISCHARGE
C      NPC - LONGITUDINAL STEP AT WHICH PRINT OUT OF
C      CONCENTRATIONS REQUIRED
C      NNN - INITIAL LONGITUDINAL STEP
C
C      READ(5,1000)G,TH2,RM,A,B,DE,DM2,USTAR
C      READ(5,1100) MM,NN,OX,DO,TOLER,MAXIT,QF,NPC,NNN
C
C      VECTORS DP AND C ARE INPUT FOR THE INITIAL
C      RIVER PORTION
C
C
C
C
C      READ(5,1200) (DP(I),I=1,MM)
C      READ(5,1200) (C(I),I=1,MM)
C      READ(5,900) COEF
C      GO TO 803
C
C      FOR SUBSEQUENT RIVER PORTIONS INPUT THE WEIGHTING
C      COEFFICIENTS AND PARAMETERS LISTED ABOVE AND
C      VECTOR DP ONLY
C
C      802 READ(5,1000)G,TH2,RM,A,B,DE,DM2,USTAR
C      IF(G.LT.0.0) GO TO 800
C      READ(5,1100) MM,NN,OX,DO,TOLER,MAXIT,QF,NPC,NNN
C      READ(5,1200) (DP(I),I=1,MM)
C      READ(5,900) COEF
C      803 CONTINUE
C
C      SET UP TRANSVERSE COUNTERS AND CALCULATE
C      INDIVIDUAL COMPONENTS OF VECTORS D AND F
C
C      M1=MM-1
C      M2=MM-2
C      M3=MM-3
C      DO 10 I=1,MM
C      D(I)=DP(I)/QF**2*COEF*USTAR
C      10 CONTINUE
C      DO 20 I=4,M3
C      F(I)=(D(I+1)-D(I-1))/DO/2.
C      20 CONTINUE
C      F(2)=0.0
C      F(3)=D(3)/DO
C      F(M1)=0.0
C      F(M2)=D(M2)/DO
C      IF(D(4).EQ.D(2)) F(3)=0.0
C      IF(D(M1).EQ.D(M3)) F(M3)=0.0
C
C      ASSIGN INITIAL VALUE OF ZERO TO COMPONENTS
C      OF ARRAY CM
C
C      DO 100 L=1,M2
C      DO 101 LL=1,M2
C      CM(L,LL)=0.0
C      101 CONTINUE
C      100 CONTINUE
C
C      ECHO INPUT DATA FOR PRINTING

```





```
C
WRITE(6,2000) M3,DQ,NNN,NN,DX,CDEF,USTAR
WRITE(6,2100) (C(I),I=1,MM)

C C C
CALCULATE THE TRIODIAGONAL MATRIX COEFFICIENTS AND
FORCING VECTOR FOR THE SYSTEM OF FINITE DIFFERENCE
EQUATIONS
    ALPHA - GIVEN BY EQ.VI-15
    GAMMA - GIVEN BY EQ.VI-16
INITIALIZE LONGITUOINAL COUNTERS
    N - LONGITUOINAL COUNTER
    NC - LONGITUOINAL PRINT COUNTER

C C C
AL=OX/OQ**2
GA=OX/OQ**2.
N=NNN
NC=NNN
500 CONTINUE
N=N+1
NC=NC+1
DO 200 J=2,M1
ALPHA=AL*O(J)
GAMMA=GA*F(J)
Q(J)=(G+ALPHA)*2.
S(J)=C(J-1)*(ALPHA-GAMMA*OM2+2.*TH2)
&+C(J)*(2.*(G-ALPHA))
&+C(J+1)*(ALPHA+GAMMA*A+2.*RM)
200 CONTINUE
DO 201 J=2,M2
ALPHA=AL*O(J)
GAMMA=GA*F(J)
R(J)=(ALPHA+GAMMA*B-2.*RM)*(-1.)
IF(J.EQ.2) R(J)=(ALPHA+GAMMA*B-2.*RM)*(-2)
201 CONTINUE
DO 202 J=3,M1
ALPHA=AL*O(J)
GAMMA=GA*F(J)
P(J)=(ALPHA-GAMMA*OE-2.*TH2)*(-1.)
IF(J.EQ.M1) P(J)=(ALPHA-GAMMA*OE-2.*TH2)*(-2.)
202 CONTINUE

C C C
SET UP TRIODIAGONAL MATRIX,FORCING VECTOR,AND ASSUMED SOLUTION
VECTOR IN A FORM SUITABLE FOR SOLUTION BY GAUSS SEIOAL
ITERATION

C C C
DO 400 K=2,M1
X(K-1)=C(K)
CM(K-1,K-1)=Q(K)
SS(K-1)=S(K)

400 CONTINUE
DO 401 K=2,M2
CM(K-1,K)=R(K)
401 CONTINUE
DO 402 K=3,M1
CM(K-1,K-2)=P(K)
402 CONTINUE

C C C
GAUSS SEIOAL ROUTINE TO SOLVE THE TRIODIAGONAL SYSTEM
OF LINEAR EQUATIONS

C C C
DO 350 L=1,M2
FLIP=1./CM(L,L)
DO 340 K=1,M2
340 CM(L,K)=CM(L,K)*FLIP
SS(L)=SS(L)*FLIP
350 CM(L,L)=O.O
NEQ=M2

C C C
INITIALIZE ITERATION COUNTER NIT AND SET THE MAXIMUM
DIFFERENCE BETWEEN SUCCESSION SOLUTIONS OIF INITIALLY
TO ZERO

NIT=O
OIF=O.O

C C C
CALL SUBROUTINE ITER WHICH WILL CALCULATE A NEW ESTIMATE
OF THE CONCENTRATIONS AT EACH GRID POINT ONE LONGITUOINAL
STEP DOWNSTREAM AND DETERMINE THE MAXIMUM DIFFERENCE OIF
BETWEEN THE PREVIOUS AND THE NEW ESTIMATE

300 CALL ITER(CM,SS,X,NEQ,OIF)
NIT=NIT+1

C C C
COMPARE OIF TO THE ACCURACY REQUIRED
IF OIF>TOLER CONTINUE ITERATION
IF OIF<TOLER SOLUTION SOLUTION FOR ONE LONGITUOINAL
STEP IS COMPLETE
- IF OUTPUT REQUESTED PRINT CALCULATED CONC. PROFILE
- IF LAST INCREMENT IN THE RIVER PORTION COMPLETED
PRINT CALCULATED CONC. PROFILE, RETURN TO 802 AND
BEGIN NEW PORTION OR TERMINATE PROGRAM AND PRINT
MESSAGE
- IF LONGITUOINAL STEP IS LESS THAN THE FINAL STEP
INCREMENT N AND NC AND CONTINUE TO NEXT STEP
```



```

      IF(OIF.LT.TOLER) GO TO S02
C
C
C      IF NUMBER OF ITERATES NIT IS LESS THAN MAXIMUM ALLOWED
C      MAXIT CONTINUE SOLUTION
C      IF NIT EQUALS MAXIT TERMINATE THE RUN AND PRINT MESSAGE
C
      IF(NIT.GE.MAXIT) GO TO S01
      GO TO 300
S02   00 700 J=2,M1
700   C(J)=X(J-1)
      C(1)=C(3)
      C(MM)=C(M2)
      IF(N.EQ.NN) GO TO 1
      IF(NC.LT.NPC) GO TO S00
      1   WRITE(6,2200) N,NIT,(C(J),J=1,MM)
      NC=0
S00   IF(N.GE.NN) GO TO S02
      GO TO 600
S01   WRITE(6,2300) N
      GO TO S01
S00   WRITE(6,2400)
S01   STOP
C
C      FORMAT STATEMENTS
C
900   FORMAT(2F10.3)
1000  FORMAT(8F8.4)
1100  FORMAT(2I8,2F10.6,E10.4,I8,F10.6,2I8)
1200  FORMAT(8F8.4)
1201  FORMAT(4E10.3)
2000  FORMAT('1','      NUMERICAL SOLUTION TO STEADY STATE ',
*      'TRANSVERSE DIFUSION'/
*      '      NUMBER OF TRANSVERSE STEPS      = ',I5/
*      '      TRANSVERSE STEP SIZE           = ',F6.4/
*      '      INITIAL LONGITUDINAL STEP       = ',I5/
*      '      FINAL LONGITUDINAL STEP         = ',I5/
*      '      LONGITUDINAL STEP SIZE          = ',F6.1/
*      '      COEF                             = ',F6.2/
*      '      PLUME REGION SHEAR VELOCITY      = ',F6.4)
2100  FORMAT('0','      INITIAL CONC. VECTOR'/(8F8.2))
2200  FORMAT('0','      NUMBER OF LONGITUDINAL STEPS = ',I5/
*      '      NUMBER OF ITERATES              = ',I5/
*      '      CONC.VECTOR = '/(8F8.2))
2300  FORMAT('0','      NO.OF ALLOWABLE ITERATIONS EXCEEDED'/
*      '      LONGITUDINAL COUNTER = ',I5)
2400  FORMAT('0','      *** RUN COMPLETED ***')
      END
C
C      ITERATION ROUTINE USED FOR SUCCESSIVE SUBSTITUTION
C      IN GAUSS SEIDAL METHOD
C
C      ITER CALCULATES A NEW SOLUTION CONCENTRATION VALUE
C
C      AT EACH GRID POINT USING THE MOST RECENT ESTIMATE
C      OF THE CONCENTRATION AT ADJACENT TRANSVERSE GRID
C      POINTS
C
      SUBROUTINE ITER(CM,SS,X,NEQ,OIF)
      DIMENSION CM(101,101),SS(101),X(101)
      OIF=0.0
      00 310 I=1,NEQ
      SM=0.0
      00 320 J=1,NEQ
      SM=SM+CM(I,J)*X(J)
320   CONTINUE
      XO=X(I)
      X(I)=SS(I)-SM
      IF(ABS(X(I)-XO).GT.OIF) OIF=ABS(X(I)-XO)
C
C
C      THE VALUE OF OIF IS SET TO THE MAXIMUM DIFFERENCE
C      BETWEEN THE INITIAL ESTIMATE AND CALCULATED CONCENTRATION
C      AT A TRANSVERSE GRID POINT
C
310   CONTINUE
      RETURN
C
C      EXAMPLE DATA FILE WITH TWO RIVER PORTIONS
C
C      NOTE THE COMPONENTS OF VECTOR OP AND C ARE INPUT
C      8 PER LINE TO A TOTAL NUMBER MM INCLUDING
C      IMAGINARY AND BOUNDARY POINTS
C
      .666,.167,.167,.25,.25,.25,.25,.0218,
      (G,TH2,RM,A,B,OE,OM2,USTAR)
      23,230,10.0,.050,.0001,30,340.,200,85,
      (MM,NN,OX,OQ,TOLER,MAXIT,OF,NPC,NNN)
      .40,.20,.40,.76,1.15,1.66,2.26,2.95, (OP,.....,OP)
      3.66,3.62,3.59,3.56,3.59,3.62,3.66,2.95, (OP,.....,OP)
      2.26,1.66,1.15,0.76,0.40,0.20,0.40, (OP,.....,OP)
      25.27,25.44,25.27,24.80,22.87,18.14,11.15,5.11, (C,.....,C)
      2.11,1.18,0.85,0.58,0.31,0.11,0.02,0.00, (C,.....,C)
      0.00,0.0,0.0,0.0,0.0,0.0,0.0, (C,.....,C)
      2.90, (COEF)
      .666,.167,.167,.25,.25,.25,.25,.0280,
      23,78,100.,.050,.0005,30,340.,55,23,
      1.63,1.04,1.63,0.77,0.99,1.45,2.21,3.18,
      4.44,5.59,5.57,5.72,5.57,5.59,4.44,3.18,
      2.21,1.45,0.99,0.77,1.63,1.04,1.63,
      (NOTE C VECTOR NOT REQUIRED FOR SECOND PORTION)
      2.60,
      .666,.167,.167,.25,.25,.25,.25,.0280,
C
C      PROGRAM TERMINATED BY READING A NEGATIVE VALUE OF G
C
      END

```



Following the example of Lau and Krishnappan the numerical model accuracy was checked against that of an analytical solution when  $D$  is considered a constant. The solutions at various sections for  $D$  of  $0.1 \text{ m}^5/\text{sec}^2$ ,  $Q = 100 \text{ m}^3/\text{sec}$  and a line source between  $\eta = 0.0$  and  $\eta = 0.05$  are given in Table VI-1. The numerical solution can not accurately begin using a line source as an input distribution. Therefore, the line source was assumed to generate a triangular distribution one longitudinal step downstream of the source location with  $c' = 20.0$  at  $\eta = 0.00$  decreasing to  $c' = 0.00$  at  $\eta = 0.10$ . Comparison of the two solutions indicates excellent agreement.

Calculations in the accuracy check calculations were continued until the edge of the plume had reached the bank opposite the source at approximately 6000 m (the crossing distance). Simulation of the mixing in the Slave River was required for 40 km downstream of the source, however, the plume had only spread to approximately 50 percent of the channel width at this distance. Therefore the numerical solution technique, which has been verified within the crossing distance, can be used to simulate the mixing within the Slave River study reach.





Table VI- 1 Comparison of Analytical and Numerical Solutions for a constant *D*

q/Q	Dimensionless Concentration					
	2000 m		4000 m		6000m	
	anal.	num.	anal.	num.	anal.	num.
0.0	3.95	3.91	2.81	2.80	2.30	2.30
0.1	3.49	3.48	2.64	2.63	2.20	2.30
0.2	2.42	2.43	2.19	2.19	1.95	1.95
0.3	1.31	1.34	1.61	1.62	1.58	1.58
0.4	0.56	0.57	1.04	1.05	1.18	1.18
0.5	0.18	0.19	0.60	0.60	0.82	0.82
0.6	0.06	0.05	0.30	0.31	0.52	0.52
0.7	0.00	0.01	0.14	0.14	0.30	0.30
0.8	0.00	0.00	0.05	0.05	0.16	0.17
0.9	0.00	0.00	0.03	0.02	0.11	0.09
1.0	0.00	0.00	0.00	0.01	0.07	0.07



## APPENDIX VII Numerical Solution Method, Non-Conservative Pollutants

The differential equation describing steady-state mixing of a neutrally buoyant non-conservative (decaying) pollutant was derived in Chapter VII. The non-dimensional form of the equation is:

$$\frac{\partial N'}{\partial x} = \frac{1}{Q^2} \frac{\partial}{\partial \eta} (u h^2 E_z \frac{\partial N'}{\partial \eta}) - \frac{k N'}{u} \quad (\text{VII-1})$$

The form of Equation VII-1 is identical to Equation VI-1 with the addition of the decay term  $kN'/u$ . The decay term does not involve a differential therefore solution may proceed by the same method as used for Equation VI-1 (see Appendix VI) with only minor modifications.

The expanded form of Equation VII-1 is:

$$\frac{\partial N'}{\partial x} = \frac{1}{Q^2} (u h^2 E_z) \frac{\partial^2 N'}{\partial \eta^2} + \frac{1}{Q^2} \left( \frac{\partial}{\partial \eta} (u h^2 E_z) \right) \left( \frac{\partial N'}{\partial \eta} \right) - \frac{k N'}{u} \quad (\text{VII-2})$$

This expanded equation may be written in finite difference form using the same grid system, discretization procedure, and weighting coefficients described in Appendix VI. The microbial concentration in the decay term may be expressed as an average between longitudinal grid points, ie.

$$N' = \frac{N'_{i+1,j} + N'_{i,j}}{2} \quad (\text{VII-3})$$

Similar to the conservative tracer a system of linear



equations may be written describing the transverse microbial concentration distribution using the same boundary conditions. The equations written in matrix form are:

$$\begin{bmatrix} q_2 & r_2 \\ p_3 & q_3 & r_3 \\ & \ddots & \ddots & \ddots \\ & & p_{M-2} & q_{M-2} & r_{M-2} \\ & & & p_{M-1} & q_{M-1} \end{bmatrix} \begin{bmatrix} N'_{i+1,2} \\ N'_{i+1,3} \\ \vdots \\ N'_{i+1,M-2} \\ N'_{i+1,M-1} \end{bmatrix} = \begin{bmatrix} s_2 \\ s_3 \\ \vdots \\ s_{M-2} \\ s_{M-1} \end{bmatrix} \quad (\text{VII-4})$$

$$q_j = 2(g + \alpha) + \lambda \quad (j = 2, 3, \dots, M-1) \quad (\text{VII-5})$$

$$p_j = \theta - \alpha + \gamma d \quad (j = 3, 4, \dots, M-2) \quad (\text{VII-6})$$

$$p_{M-1} = \theta + 2m - 2\alpha \quad (\text{VII-7})$$

$$r_j = 2m - \alpha - \gamma b \quad (j = 3, 4, \dots, M-2) \quad (\text{VII-8})$$



$$r_2 = \theta + 2m - 2\alpha \quad (\text{VII-9})$$

$$S_j = N'_{i,j-1}(\theta + \alpha - \frac{\gamma\omega}{2}) + N'_{i,j}(2(g - \alpha) - \lambda) \quad (\text{VII-10})$$

$$+ N'_{i,j+1}(2m + \alpha + \gamma a) \quad (j = 2, 3, \dots, M-1)$$

$$\alpha = \frac{D_{i,j}\Delta x}{(\Delta\eta)^2} \quad (\text{VII-11})$$

$$\gamma = \frac{2F_{i,j}\Delta x}{\Delta\eta} \quad (\text{VII-12})$$

$$\lambda = \frac{k\Delta x}{u} \quad (\text{VII-13})$$

Values of  $D_{i,j}$  are input for each equation as for the conservative tracer, however a value of local velocity  $u$  is also required and input in a similar manner. The  $F_{i,j}$  terms are calculated within the program as described in Appendix VI. The transverse mixing coefficient  $E_z$  is input as for the conservative tracer and again is assumed constant transversely but may vary longitudinally. The value of  $k$  the decay coefficient must be input and is assumed constant for the reach.





The computer program developed solves the system of linear equation developed for the non-conservative pollutant by the same methods used for the conservative tracer. A listing of the program with explanatory notes follows.



```

C      FINITE DIFFERENCE PROGRAM TO NUMERICALLY SOLVE
C      STEADY STATE TRANSVERSE DIFFUSION PROBLEMS WITH
C      A TIME DEPENDENT DECAY COEFFICIENT
C
C      DIMENSION ALL VECTORS AND ARRAYS TO BE USED IN CALCULATIONS
C      D - COEFFICIENTS GIVEN BY EQ. VI-5
C      F - COEFFICIENTS GIVEN BY EQ. VI-6
C      C - INPUT CONCENTRATIONS
C      OP - PRODUCT OF LOCAL DEPTH AND VELOCITY SQUARED
C      VEL - DEPTH-AVERAGED VELOCITY
C      Q,R,P - TRIANGULAR MATRIX COEFFICIENTS GIVEN BY
C      EQ.VI-9 TO EQ.VI-13
C      S - FORCING VECTOR GIVEN BY EQ.VI-14
C      SS - FORCING VECTOR EXCLUDING IMAGINARY POINTS
C      X - SOLUTION CONCENTRATION VECTOR
C      CM - ARRAY OF SIMULTANEOUS EQUATION COEFFICIENTS
C
C      DIMENSION D(101),F(101),C(101),OP(101),VEL(101)
C      DIMENSION Q(101),R(101),P(101),S(101)
C      DIMENSION CM(101,101),X(101),SS(101)
C      DO 30 I=1,101
C      C(I)=0.0
30  CONTINUE
C
C      INPUT SOLUTION WEIGHTING COEFFICIENTS AND INITIAL PARAMETERS
C      THE WEIGHTING COEFFICIENTS ARE GIVEN BY EQ.VI-6
C      G= 0.666
C      TH2,RM =0.167
C      A,B,DE,DM2 = 0.25
C
C      USTAR - PLUME REGION SHEAR VELOCITY GIVEN BY EQ.III-5
C      USING THE PLUME REGION HYDRAULIC RADIUS
C      COEF - PRODUCT OF THE MIXING LENGTH SCALE AND A
C      CONSTANT COEFFICIENT, SEE EQ.VI-1
C      RK - DECAY COEFFICIENT(BASE E), UNITS OF /DAY
C      MM - NUMBER OF TRANSVERSE GRID POINTS INCLUDING
C      IMAGINARY AND BOUNDARY NODES
C      NN - FINAL LONGITUDINAL STEP
C      DX - LONGITUDINAL DISTANCE INCREMENT
C      QQ - DIMENSIONLESS CUMULATIVE FLOW
C      TOLER - ACCURACY TO WHICH NUMERICAL SOLUTION WILL
C      PROCEED
C      MAXIT - MAXIMUM NUMBER OF ITERATIONS ALLOWED
C      QF - TOTAL STREAM DISCHARGE
C      NPC - LONGITUDINAL STEP AT WHICH PRINT OUT OF
C      CONCENTRATIONS REQUIRED
C      NNN - INITIAL LONGITUDINAL STEP
C
C      READ(5,1000)G,TH2,RM,A,B,DE,DM2,USTAR,RK
C      READ(5,1100) MM,NN,DX,QQ,TOLER,MAXIT,QF,NPC,NNN
C
C
C      VECTORS DP, VEL AND C ARE INPUT FOR THE INITIAL
C      RIVER PORTION
C
C      READ(5,1200) (DP(I),I=1,MM)
C      IF(RK.EQ.0.0) GO TO 40
40  READ(5,1200) (VEL(I),I=1,MM)
C      READ(5,1200) (C(I),I=1,MM)
C      READ(5,900) COEF
C      GO TO 803
C
C      FOR SUBSEQUENT RIVER PORTIONS INPUT THE WEIGHTING
C      COEFFICIENTS AND PARAMETERS LISTED ABOVE AND
C      VECTORS DP AND VEL ONLY
C
C      802 READ(5,1000)G,TH2,RM,A,B,DE,DM2,USTAR,RK
C      IF(G.LT.0.0) GO TO 800
C      READ(5,1100) MM,NN,DX,QQ,TOLER,MAXIT,QF,NPC,NNN
C      READ(5,1200) (DP(I),I=1,MM)
C      IF(RK.EQ.0.0) GO TO 50
C      READ(5,1200) (VEL(I),I=1,MM)
C      50 READ(5,900) COEF
C      803 CONTINUE
C
C      SET UP TRANSVERSE COUNTERS AND CALCULATE
C      INDIVIDUAL COMPONENTS OF VECTORS D AND F
C
C      M1=MM-1
C      M2=MM-2
C      M3=MM-3
C      DO 10 I=1,MM
C      D(I)=DP(I)/QF**2*COEF*USTAR
C      10 CONTINUE
C      DO 20 I=4,M3
C      F(I)=(D(I+1)-D(I-1))/QQ/2.
C      20 CONTINUE
C      F(2)=0.0
C      F(3)=D(3)/QQ
C      F(M1)=0.0
C      F(M2)=D(M2)/QQ
C      IF(D(4).EQ.D(2)) F(3)=0.0
C      IF(D(M1).EQ.D(M3)) F(M3)=0.0
C
C      ASSIGN INITIAL VALUE OF ZERO TO COMPONENTS
C      OF ARRAY CM
C
C      DO 100 L=1,M2
C      DO 101 LL=1,M2
C      CM(L,LL)=0.0

```



```

101 CONTINUE
100 CONTINUE
C
C
C      ECHD INPUT DATA FOR PRINTING
C
C      WRITE(6,2000) M3,DQ,NNN,NN,DX,CDEF,USTAR,RK
C      WRITE(6,2100) (C(I),I=1,MM)
C
C
C      CALCULATE THE TRIDIAGONAL MATRIX COEFFICIENTS AND
C      FORCING VECTOR FOR THE SYSTEM OF FINITE DIFFERENCE
C      EQUATIONS
C      ALPHA - GIVEN BY EQ.VI-15
C      GAMMA - GIVEN BY EQ.VI-16
C      INITIALIZE LONGITUDINAL COUNTERS
C      N - LONGITUDINAL COUNTER
C      NC - LONGITUDINAL PRINT COUNTER
C
C      AL=DX/DQ**2
C      GA=DX/DQ**2.
C      N=NNN
C      NC=NNN
600 CONTINUE
N=N+1
NC=NC+1
DD 200 J=2,M1
ALPHA=AL*D(J)
GAMMA=GA*F(J)
Q(J)=(G+ALPHA)*2.
S(J)=C(J-1)*(ALPHA-GAMMA*DM2+2.*TH2)
&+C(J)*(2.*(G-ALPHA-RK/VEL(I)/172800.*DX))
&+C(J+1)*(ALPHA+GAMMA*A+2.*RM)
200 CONTINUE
DD 201 J=2,M2
ALPHA=AL*D(J)
GAMMA=GA*F(J)
R(J)=(ALPHA+GAMMA*B-2.*RM)*(-1.)
IF(J.EQ.2) R(J)=(ALPHA+GAMMA*B-2.*RM)*(-2.)
201 CONTINUE
DD 202 J=3,M1
ALPHA=AL*D(J)
GAMMA=GA*F(J)
P(J)=(ALPHA-GAMMA*DE-2.*TH2)*(-1.)
IF(J.EQ.M1) P(J)=(ALPHA-GAMMA*DE-2.*TH2)*(-2.)
202 CONTINUE
C
C
C      SET UP TRIDIAGONAL MATRIX, FORCING VECTOR, AND ASSUMED SOLUTION
C      VECTOR IN A FORM SUITABLE FOR SOLUTION BY GAUSS SEIDAL
C      ITERATION
C
C
C
C
C      DD 400 K=2,M1
C      X(K-1)=C(K)
C      CM(K-1,K-1)=Q(K)
C      SS(K-1)=S(K)
400 CONTINUE
DD 401 K=2,M2
CM(K-1,K)=R(K)
401 CONTINUE
DD 402 K=3,M1
CM(K-1,K-2)=P(K)
402 CONTINUE
C
C
C      GAUSS SEIDAL ROUTINE TO SOLVE THE TRIDIAGONAL SYSTEM
C      OF LINEAR EQUATIONS
C
C
C      DD 350 L=1,M2
C      FLIP=1./CM(L,L)
C      DD 340 K=1,M2
340 CM(L,K)=CM(L,K)*FLIP
SS(L)=SS(L)*FLIP
350 CM(L,L)=0.0
NEQ=M2
C
C
C      INITIALIZE ITERATION COUNTER NIT AND SET THE MAXIMUM
C      DIFFERENCE BETWEEN SUCCESSIVE SOLUTIONS DIF INITIALLY
C      TO ZERO
C
C
C      NIT=0
C      DIF=0.0
C
C
C      CALL SUBROUTINE ITER WHICH WILL CALCULATE A NEW ESTIMATE
C      OF THE CONCENTRATIONS AT EACH GRID POINT ONE LONGITUDINAL
C      STEP DOWNSTREAM AND DETERMINE THE MAXIMUM DIFFERENCE DIF
C      BETWEEN THE PREVIOUS AND THE NEW ESTIMATE
C
C
C      300 CALL ITER(CM,SS,X,NEQ,DIF)
C      NIT=NIT+1
C
C
C      COMPARE DIF TO THE ACCURACY REQUIRED
C      IF DIF>TDLER CONTINUE ITERATION
C      IF DIF<TDLER SOLUTION FOR ONE LONGITUDINAL
C      STEP IS COMPLETE
C      -IF OUTPUT REQUESTED PRINT CALCULATED CONC. PROFILE
C      -IF LAST INCREMENT IN THE RIVER PORTION COMPLETED
C      PRINT CALCULATED CONC. PROFILE, RETURN TO 802 AND
C      BEGIN NEW PORTION OR TERMINATE PROGRAM AND PRINT MESSAGE

```





```

C      -IF LONGITUDINAL STEP IS LESS THAN THE FINAL STEP
C      INCREMENT N AND NC AND CONTINUE TO NEXT STEP
C
C      IF(DIF.LT.TDLR) GO TO 502
C
C      IF NUMBER OF ITERATES NIT IS LESS THAN MAXIMUM ALLOWED
C      MAXIT CONTINUE SOLUTION
C      IF NIT EQUALS MAXIT TERMINATE THE RUN AND PRINT MESSAGE
C

```

```

C      IF(NIT.GE.MAXIT) GO TO 501
C      GO TO 300
502 DD 700 J=2,M1
700 C(J)=X(J-1)
C(1)=C(3)
C(MM)=C(M2)
IF(N.EQ.NN) GO TO 1
IF(NC.LT.NPC) GO TO 500
1 WRITE(6,2200) N,NIT,(C(J),J=1,MM)
NC=0
500 IF(N.GE.NN) GO TO 802
GO TO 600
501 WRITE(6,2300) N
GO TO 801
800 WRITE(6,2400)
801 STDP

```

```

C      FDRMAT STATEMENTS
C

```

```

900 FDRMAT(F10.3)
1000 FDRMAT(9F8.4)
1100 FDRMAT(2I8,2F10.6,E10.4,I8,F10.6,2I8)
1200 FDRMAT(8F8.4)
1201 FDRMAT(4E10.3)
2000 FDRMAT('1',' NUMERICAL SOLUTION TO STEADY STATE ',
* 'TRANSVERSE DIFFUSION'/
* ' NUMBER OF TRANSVERSE STEPS = ',I5/
* ' TRANSVERSE STEP SIZE = ',F6.4/
* ' INITIAL LONGITUDINAL STEP = ',I5/
* ' FINAL LONGITUDINAL STEP = ',I5/
* ' LONGITUDINAL STEP SIZE = ',F6.1/
* ' CDEF = ',F6.2/
* ' PLUME REGION SHEAR VELOCITY = ',F6.4/
* ' DECAY COEFFICIENT(BASE E) /DAY = ',F6.2)
2100 FDRMAT('0',' INITIAL CONC. VECTOR'/(8F8.2))
2200 FDRMAT('0',' NUMBER OF LONGITUDINAL STEPS = ',I5/
* ' NUMBER OF ITERATES = ',I5/
* ' CONC. VECTOR = '/(8F8.2))
2300 FDRMAT('0',' NO. OF ALLOWABLE ITERATIONS EXCEEDED'/
* ' LONGITUDINAL COUNTER = ',I5)
2400 FDRMAT('0',' **** RUN COMPLETED ****')
END

```

```

C      ITERATION ROUTINE USED FOR SUCCESSIVE SUBSTITUTION
C      IN GAUSS SEIDAL METHOD
C

```

```

C      ITER CALCULATES A NEW SOLUTION CONCENTRATION VALUE
C      AT EACH GRID POINT USING THE MOST RECENT ESTIMATE
C      OF THE CONCENTRATION AT ADJACENT TRANSVERSE GRID
C      POINTS
C

```

```

C      SUBROUTINE ITER(CM,SS,X,NEO,DIF)
C      DIMENSION CM(101,101),SS(101),X(101)
C      DIF=0.0
C      DD 310 I=1,NEO
C      SM=0.0
C      DD 320 J=1,NEO
C      SM=SM+CM(I,J)*X(J)
320 CONTINUE
XO=X(I)
X(I)=SS(I)-SM
IF(ABS(X(I)-XO).GT.DIF) DIF=ABS(X(I)-XO)

```

```

C      THE VALUE OF DIF IS SET TO THE MAXIMUM DIFFERENCE
C      BETWEEN THE INITIAL ESTIMATE AND CALCULATED CONCENTRATION
C      AT A TRANSVERSE GRID POINT
C

```

```

C      310 CONTINUE
C      RETURN
C

```

```

C      EXAMPLE DATA FILE WITH TWO RIVER PORTIONS
C

```

```

C      NOTE THE COMPONENTS OF VECTOR OP, VEL AND C ARE
C      INPUT 8 PER LINE TO A TOTAL NUMBER MM INCLUDING
C      IMAGINARY AND BOUNDARY POINTS
C

```

```

C      .666,.167,.167,.25,.25,.25,.25,0.0218,
C      (G,TH2,RM,A,B,OE,DM2,USTAR)
C      23,230,10.0,.050,.0001,30,340.,200,85,
C      (MM,NN,DX,DQ,TOLER,MAXIT,OF,NPC,NNN)
C      .40,.20,.40,.76,1.15,1.66,2.26,2.95, (DP,.....,OP)
C      3.66,3.62,3.59,3.56,3.59,3.62,3.66,2.95, (DP,.....,DP)
C      2.26,1.66,1.15,0.76,0.40,0.20,0.40, (DP,.....,DP)
C      .30,.19,.30,.34,.35,.35,.37,.37, (VEL,.....,VEL)
C      .37,.37,.37,.37,.37,.37,.37,.37, (VEL,.....,VEL)
C      .36,.35,.35,.34,.30,.19,.30, (VEL,.....,VEL)
C      25.27,25.44,25.27,24.80,22.87,18.14,11.15,5.11, (C,.....,C)
C      2.11,1.18,0.85,0.58,0.31,0.11,0.02,0.00, (C,.....,C)
C      0.00,0.0,0.0,0.0,0.0,0.0,0.0,0.0, (C,.....,C)
C      2.90,.40, (COEF,RK)

```



```

C .666, .167, .167, .25, .25, .25, .25, .0280,
C 23, 76, 100, .050, .0005, 30, 340, .55, 23,
C 1.63, 1.04, 1.63, 0.77, 0.99, 1.45, 2 21, 3.18,
C 4.44, 5.59, 5.57, 5.72, 5.57, 5.59, 4.44, 3.18,
C 2.21, 1.45, 0.99, 0.77, 1.63, 1.04, 1.63,
C .28, .18, .28, .22, .20, .25, .27, .27,
C .29, .33, .34, .33, .34, .33, .29, .27,
C .27, .25, .20, .22, .28, .18, .28,
C (NOTE C VECTOR NOT REQUIRED FOR SECOND PORTION)
C 2 60, 40,
C -.666, .167, .167, .25, .25, .25, .25, .0280,
C
C PROGRAM TERMINATED BY READING A NEGATIVE VALUE OF G
C
C      END

```





**B30368**